委託研究計劃

牛樟芝子實體在大鼠的90天亞慢性口服毒性試驗

參考文獻共 12 篇

GOLDEN DAPU BIOTECH CORP.

國立屏東科技大學 National Pingtung University of Science and Technology

鑫大埔生技實業股份有限公司與國立屏東科技大學 產學研究計畫

民國 105 年 4 月 15 日

Antrodia camphorata (niu-chang-chih), new combination of a medicinal fungus in Taiwan

Article *in* Botanical Bulletin- Academia Sinica Taipei · November 1996

Impact Factor: 1.11

3 authors, including:

Sheng-Hua Wu
National Museum of Natural Science
48 PUBLICATIONS **508** CITATIONS
SEE PROFILE

Leif Ryvarden
University of Oslo
80 PUBLICATIONS **1,758** CITATIONS
SEE PROFILE

Bot. Bull. Acad. Sin. (1997) **38:** 273–275

Antrodia camphorata ("niu-chang-chih"), new combination of a medicinal fungus in Taiwan

Sheng-Hua Wu[1], Leif Ryvarden[2] and Tun-Tschu Chang[3]

[1]*Division of Botany, National Museum of Natural Science, Taichung, Taiwan, Republic of China*

[2]*Department of Botany, Institute of Biology, University of Oslo, P.O. Box 1045, N-0316 Oslo, Norway*

[3]*Division of Forest Protection, Taiwan Forestry Research Institute, 53 Nan-hai Road, Taipei, Taiwan, Republic of China*

(Received February 5, 1997; Accepted May 2, 1997)

Abstract. A new combination, *Antrodia camphorata* (M. Zang & C.H. Su) Sheng H. Wu, Ryvarden & T.T. Chang, is proposed for *Ganoderma comphoratum* M. Zang & C.H. Su, a name originally based on a polypore with contaminating *Ganoderma* spores. *Antrodia cinnamomea* T.T. Chang & W.N. Chou is reduced to a taxonomic synonym of *A. camphorata*. The species is famous and highly valued in Taiwan as a medicine, and is restricted to a Taiwanese endemic tree species, *Cinnamomum kanehirai*.

Keywords: *Antrodia camphorata*; *A. cinnamomea*; *Ganoderma comphoratum*; Polypore; Taiwan.

Many polypores are used for medicinal purposes in Taiwan. One of the most valued is *Antrodia camphorata*, especially since it is said to have several medicinal uses including a curative effect on cancer. The species is known only from Taiwan and is restricted to *Cinnamomum kanehirai* Hay (Lauraceae), also endemic to Taiwan. The species is known in Taiwan as "niu-chang-chih"; "niu-chang" is the Chinese common name for *C. kanehirai* and "chih" means *Ganoderma*-like fungus. Many Taiwanese also call it "niu-chang-ku"; "ku" in Chinese means mushroom. It is also known simply as "chang-chih" or "chang-ku." In Taiwan, the wood of *C. kanehirai* has traditionally been regarded as high quality for manufacturing furniture. Nowadays this endemic tree species is becoming rare and has now been protected by the government. Consequently, it is also becoming difficult to find "niu-chang-chih" in the forest. "Niu-chang-chih" is very expensive in Taiwan. In recent years, basidiomes of good quality have sold for about US $ 15,000 per kg., a result of host specificity and rarity in nature, and the failure of artificial cultivation.

This species was first published by Zang and Su (1990). Dr. Su, a resident chemist, knew "niu-chang-chih" very well from his chemical studies of various medicinal fungi. However, he could not find any available name in the literature for this striking species. Thus, he sent a specimen of "niu-chang-chih" to Prof. Zang, a specialist in Chinese higher fungi. Later they jointly published the species as *Ganoderma comphoratum* M. Zang & C.H. Su. The generic name, however, was based on a mistake as the type (*HKAS 22294*, examined by us) was contaminated by spores of a *Ganoderma* species. After publication, Dr. Su told one of us (S.H. Wu) that the type specimen had been put in a bag together with a specimen of *Ganoderma*, the source of the foreign spores. In the original description, the host was also incorrectly given as *Cinnamomum comphora* (L.) Presl. (correct spelling: *C. camphora*), which explains the spelling of the specific epithet of the fungus.

Chang and Chou (1995) later described the species as *Antrodia cinnamomea* T.T. Chang & W.N. Chou (type = *TFRI 119*, examined by us). The specific epithet alludes to the host tree. They properly placed their species in *Antrodia* because of its dimitic hyphal system with clamped generative hyphae and brown rot causing ability.

After studying the types of both *Ganoderma comphoratum* and *Antrodia cinnamomea*, these fungi were found to be conspecific. Therefore a new combination is necessary, while *A. cinnamomea* is reduced to a taxonomic synonym.

Antrodia camphorata (M. Zang & C.H. Su) Sheng H. Wu, Ryvarden & T.T. Chang, comb. nov. (Figure 1)

Basionym: *Ganoderma comphoratum* M. Zang & C.H. Su, Acta Bot. Yunnanica 12: 395. 1990. Syn. nov.: *Antrodia cinnamomea* T.T. Chang & W.N. Chou, Mycol. Res. 99: 756. 1995.

Acknowledgments. The authors are indebted to Prof. Mu Zang for the loan of the holotype of *Ganoderma comphoratum* for this study.

[4]Corresponding author. Fax: +886-4-325-8684; E-mail: shwu@nmns1.nmns.edu.tw

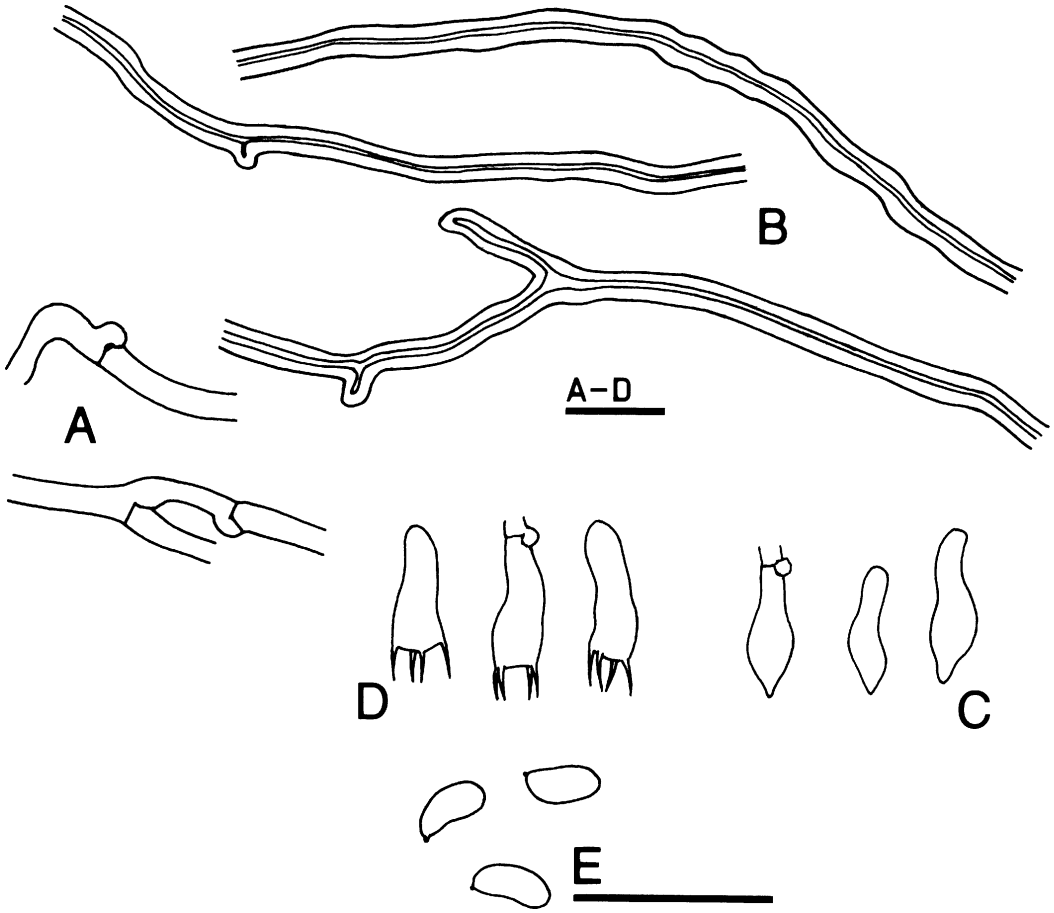

Figure 1. *Antrodia camphorata* (holotype). A, Contextual generative hyphae; B, Contextual skeletal hyphae; C, Cystidioles; D, Basidia; E, Basidiospores. Scale bars = 10 μm.

Literature Cited

Chang, T.T. and W.N. Chou. 1995. *Antrodia cinnamomea* sp. nov. on *Cinnamomum kanehirai* in Taiwan. Mycol. Res. **99:** 756–758.

Zang, M. and C.H. Su. 1990. *Ganoderma comphoratum*, a new taxon in genus *Ganoderma* from Taiwan, China. Acta Bot. Yunnanica **12:** 395–396.

Antrodia camphorata（牛樟芝），一種臺灣產醫用真菌的新組合名

吳聲華[1]　芮瓦頓[2]　張東柱[3]

[1]國立自然科學博物館蒐藏研究組
[2]挪威奧斯陸大學生物系
[3]臺灣省林業試驗所森林保護系

本文報導牛樟芝的新組合名：*Antrodia camphorata* (M. Zang & C.H. Su) Sheng H. Wu, Ryvarden & T.T. Chang。牛樟芝的基名是 *Ganoderma comphoratum* M. Zang & C.H. Su, 乃因模式標本沾染了靈芝孢子而被誤發表爲靈芝屬 (*Ganoderma*) 的成員。另本文將 *A. cinnamomea* T.T. Chang & W.N. Chou 處理爲 *A. camphorata* 的同義名。牛樟芝是臺灣著名且昂貴的醫用真菌，僅生長於臺灣特有的牛樟（*Cinnamomum kanehirai*）樹幹。

關鍵詞：牛樟芝；*A. cinnamomea*；*Ganoderma* comphoratum；多孔菌；臺灣。

Journal of Ethnopharmacology 121 (2009) 194–212

Contents lists available at ScienceDirect

Journal of Ethnopharmacology

journal homepage: www.elsevier.com/locate/jethpharm

Review

Niuchangchih (*Antrodia camphorata*) and its potential in treating liver diseases

Zong-Hua Ao[a], Zheng-Hong Xu[a,*], Zhen-Ming Lu[b], Hong-Yu Xu[a], Xiao-Mei Zhang[a], Wen-Fang Dou[a]

[a] *Laboratory of Pharmaceutical Engineering, School of Medicine and Pharmaceutics, Jiangnan University, No. 1800 Lihu Road, Wuxi 214122, PR China*
[b] *The Key Laboratory of Industrial Biotechnology, Ministry of Education, Jiangnan University, Wuxi 214122, PR China*

ARTICLE INFO

Article history:
Received 19 March 2008
Received in revised form 30 October 2008
Accepted 31 October 2008
Available online 17 November 2008

Keywords:
Niuchangchih
Antrodia camphorata
Fatty liver
Hepatitis
HBV
Liver fibrosis
Liver cancer

ABSTRACT

Niuchangchih (*Antrodia camphorata* (M. Zang & C.H. Su) Sheng H. Wu, Ryvarden & T.T. Chang) is a basidiomycete endemic to Taiwan. It is well known as a Traditional Chinese Medicine (TCM), and Taiwanese aborigines used this species to treat liver diseases and food and drug intoxication. The compounds identified in *Niuchangchih* are predominantly polysaccharides, triterpenoids, steroids, benzenoids and maleic/succinic acid derivatives. Recent research has revealed that *Niuchangchih* possesses extensive biological activity, such as hepatoprotective, antihypertensive, anti-hyperlipidemic, immuno-modulatory, anticancer, anti-inflammatory and antioxidant activities. The fruiting bodies and fermented products of *Niuchangchih* have been reported to exhibit activity when treating liver diseases, such as preventing ethanol-, CCl_4- and cytokine-induced liver injury, inhibiting the hepatitis B virus, ameliorating fatty liver and liver fibrosis, and inhibiting liver cancer cells. This review will address the protective effects of *Niuchangchih* on the pathological development of liver diseases, and the underlying mechanisms of action are also discussed.

Contents

* Corresponding author. Tel.: +86 510 85918206; fax: +86 510 85918206.
E-mail address: zhenghxu@jiangnan.edu.cn (Z.-H. Xu).

0378-8741/$ – see front matter © 2008 Elsevier Ireland Ltd. All rights reserved.
doi:10.1016/j.jep.2008.10.039

1. Introduction

The liver is the most important organ in terms of biochemical activity in the human body. The liver has great capacity to detoxify and synthesize useful substances, and therefore, damage to the liver inflicted by hepatotoxic agents has grave consequences (Achliya et al., 2004). Many risk factors, including hepatic viruses, alcohol consumption and chemical agents, have significant impact on the etiologies of liver diseases. Environmental pollution, bad dietary habits, and hepatic viruses have been considered to be the main factors that cause liver diseases (Day and Yeaman, 1994; Szabo, 2003). There are several characteristic pathologies in the livers of patients with liver disease, including fatty liver, hepatitis, liver fibrosis, hepatocirrhosis and liver cancer. Liver fibrosis is the common end stage of most chronic liver diseases regardless of the etiology (Bataller and Brenner, 2005), and its progression leads to liver cirrhosis and liver cancer. Currently, it is believed that the early stage of liver fibrosis can be reversed, while liver cirrhosis cannot. Therefore, preventing and eliminating the bad factors, and ameliorating fatty liver and liver fibrosis, are the most effective methods to prevent the liver from ultimately deteriorating (Freidman, 1993; Brenner et al., 2000). Much progress has been made in the understanding of the pathogenesis of liver diseases, resulting in improved prevention and therapy with promising prospects for even more effective treatments. In view of the severe undesirable side effects of synthetic agents, there is a growing focus on following systematic research methodology and evaluating the scientific basis of traditional herbal medicines that claim to possess hepatoprotective activity (Shahani, 1999; Achliya et al., 2004).

Niuchangchih, also named *Antrodia camphorata* (M. Zang & C.H. Su) Sheng H. Wu, Ryvarden & T.T. Chang, is a fungus that only grows on the brown heartwood of *Cinnamomum kanehirae* Hayata (Lauraceae) in Taiwan (Fig. 1) (Wu et al., 1997). *Niuchangchih* is also called "Niu-chang-ku", or "Chang-chih", in China. "Niu-chang" is the Chinese common name for *Cinnamomum kanehirae* (Bull camphor tree); "ku" in Chinese means mushroom; and "chih" means *Ganoderma*-like fungus. Being a local species, *Niuchangchih* was historically only used in Taiwan by the aborigines as a traditional prescription for the discomforts caused by alcohol drinking or exhaustion. The fruiting bodies of *Niuchangchih* are also used as a Chinese folk medicine for the treatment of liver diseases, food and drug intoxication, diarrhea, abdominal pain, hypertension, itchy skin and tumorigenic diseases (Tsai and Liaw, 1985; Chen et al., 2001a). However, in 1990, *Niuchangchih* was first reported as a new species. In the years since the initial report, *Niuchangchih* has received tremendous attention from the public. Primary investigations have revealed that *Niuchangchih* has extensive biological activities, such as hepatoprotective effects, anti-hepatitis B virus effects, anticancer activity, and antioxidant and anti-inflammation activities (Liu et al., 2007a; Rao et al., 2007).

Fig. 1. *Niuchangchih* fruiting bodies.

Niuchangchih grows at altitudes between 450 and 2000 m in the mountain ranges, and in the counties of Taoyuan, Miaoli, Nantou, Kaohsiung and Taitung. The trophophase of *Niuchangchih* occurs from June to October (Chen et al., 2001b). The fruiting bodies of *Niuchangchih* assume different shapes like the plate-type, the horse's hoof, or the tower shape, which is morphologically similar to *Antrodia salmonea* (vernacularly called Shiang-Shan-Chih), a brown heart rot basidiomata in the empty rotten trunk of *Cunninghamia konishii* Hayata (Lauraceae) (Chang and Chou, 2004). The red to light cinnamon fruiting bodies of *Niuchangchih* are bitter and have a mild camphor scent like the host woods (Chang and Chou, 1995). Chemical ingredients found in *Niuchangchih* include polysaccharides, triterpenoids, sesquiterpene lactones, steroids, phenol compounds, adenosine, cordycepin, ergosterol, etc. (Chang et al., 2005; Lu et al., 2006) The mycelia isolated from the fruiting bodies of *Niuchangchih* form orange red and orange brown to light cinnamon-colored colonies (Chang and Chou, 1995).

In the wild, the fruiting bodies of *Niuchangchih* grow slowly and are hardly noticeable until the host tree falls down. In order to harvest *Niuchangchih* more easily, some people illegally fall the host trees. This illegal felling has severely threatened *Cinnamomum kanehirae* (Chang et al., 2005), and the trees are currently protected by the Taiwan government. However, the wild fruiting bodies of *Niuchangchih* are in great demand and have been sold for about U.S. $15,000 per kg (Wang et al., 2005) due to the efficacies of this fungus. Thus, artificial cultivation was developed as a substitute. Currently, *Niuchangchih* is commercially available in Taiwan in the form of fermented wine or pure cultures in powdered, tablet and capsule form (Cheng et al., 2005b). The mycelia produced by liquid fermentation are innocuous (Lin et al., 2001).

In Chinese folk medicine, the fruiting bodies of *Niuchangchih* are considered to be a potent hepatoprotective remedy. The fruiting bodies and mycelia of *Niuchangchih* have been reported to exhibit the activities of preventing and ameliorating liver diseases, such as preventing ethanol- and CCl_4-induced liver injury, inhibiting the hepatitis B virus, ameliorating fatty liver and liver fibrosis, and inhibiting liver cancer cell growth. This review will address the protective effects of *Niuchangchih* on the pathological development of liver diseases. Most of the data presented here are from in vitro and animal studies, because the efficacy of *Niuchangchih* in preclinical liver diseases is not well documented.

2. Taxonomy

In past years, the taxonomy of *Niuchangchih* has been identified a few times, and several latin names have been suggested to stand as the correct name for the fungus. In 1990, *Niuchangchih* was first identified as a new *Ganoderma* species, *Ganoderma camphoratum*, due to their similar characteristics (Zang and Su, 1990). The generic name, however, was based on a mistake as the type was contaminated by spores of a *Ganoderma* species. Then, Chang and Chou (1995) described the species as *Antrodia cinnamomea* due to its dimitic hyphal system with clamped generative hyphae and ability to cause brown rot. After studying the both types of *Ganoderma comphoratum* and *Antrodia cinnamomea*, these fungi were found to be conspecific. Thus, a new combination, *Antrodia camphorata*, was thought to be more appropriate (Wu et al., 1997). However, given that the host tree of this latter species is *Cinnamomum kanehirae* rather than *Cinnamomum camphora* (L.) Presl., *Antrodia cinnamomea* was suggested again to stand as the correct name for the fungus associated with *Cinnamomum kanehirae* (Chang and Chou, 2004). In 2004, a phylogenetic analysis based on sequence data

derived from large ribosomal subunit (LSU) sequences of ribosomal RNA genes (rDNA) indicated that *Niuchangchih* is distantly related to other species in *Antrodia* and, consequently, the fungus was transferred to the new genus *Taiwanofungus* (Wu et al., 2004). However, using polymorphism analysis of internal transcribed spacer (ITS) regions of the ribosomal RNA gene, *Niuchangchih* was reconsidered as an *Antrodia* species (Chiu, 2007). The current taxonomic position of *Niuchangchih* is as follows (Hawksworth et al., 1995): Fungi, Basidiomycota, Homobasidiomycetes, Aphyllophorales, Polyporacea. Clearly, however, the nomenclature and exact taxonomy (genus and species) of *Niuchangchih* is still the subject of debate and needs further research. In this article, we have chosen to use the traditional name, *Niuchangchih*, to describe this unique Formosan fungus.

3. Ethnomedicine

Niuchangchih has a long history of medicinal use in Taiwan. It had been popularly used as a folkloric medicine long before 1773 (Su, 2002) for the treatment of twisted tendons and muscle damage, terrified mental state, influenza, cold, headache, fever and many internally affiliated diseases (Peng et al., 2007). In 1773, a famous doctor in the Traditional Chinese Medicine arena named Wu-Sha, who re-located to Taiwan from the Fujian province of China, found that Taiwan aborigines had discomfort caused by excess alcohol or exhaustion because of lifestyle (Su, 2002). The locals often chewed the fruiting bodies of *Niuchangchih* or took the decoction of the fruiting bodies, and noticed that this mushroom worked well for alcoholic hangover relief. Dr. Wu studied the effects of *Niuchangchih* based on the locals' experiences, and began to use it to treat diarrhea, abdominal pain, hypertension, itchy skin, viral infection, stomachitis, diabetes mellitus, nephritis, proteinuria, liver cirrhosis, hepatoma, influenza, car sickness, calenture and motion-sickness (Tsai and Liaw, 1985; Chiu and Zhang, 2001; Su, 2002; Chen, 2008). After being used for years, the mushroom is now believed to be one of the most potent liver-protecting herbs in Taiwan. However, little primary ethnomedical data describing its liver-protecting activity was recorded in the ancient literature. Recently, many studies have indicated that its medicinal applications go far beyond the original usage. It has been reported that many chemical components of *Niuchangchih* have functional properties like antioxidant, anticancer, antiviral, and antibiotic properties. Therefore, demand for the fruiting bodies of *Niuchangchih* has far exceeded the supply, and it is now considered among the most expensive herbal medicines on the market.

4. Chemical constituents

A series of publications have appeared on the structural characterization of the secondary metabolites of the fungus. Most of the investigators studied the fruiting bodies, though there are a few publications on the constituents of the mycelia of *Niuchangchih* in submerged cultures. The compounds identified from *Niuchangchih* are predominantly polysaccharides (Chen et al., 2005; Lin and Chen, 2007; Wu et al., 2007c), benzenoids, diterpenes, triterpenoids, steroids and maleic/succinic acid derivatives. These are summarized, with their structures and bioactivities, in Table 1.

5. Pharmacological studies

Several researchers have reported on the different biological activities of *Niuchangchih* in various in vitro and in vivo test models. As summarized in Table 2, different extracts and compounds of this species have been found to exhibit hepatoprotective, neuroprotective, antihypertensive, anti-hyperlipidemic, anti-genotoxic, anti-angiogenic, antimicrobial, depigment, immuno-modulatory, anticancer, anti-inflammatory, and antioxidant activities. The protective effects of *Niuchangchih* on the pathological development of liver diseases will be described in greater detail in the following sections.

5.1. Hepatoprotective activity of Niuchangchih

5.1.1. Effect on ethanol-induced acute liver injury

Bibulosity is one of the 10 factors leading to illness and death in the world. In western countries, the rate of death induced by alcohol toxicosis is similar to cancer and coronary heart disease. The major organ which metabolizes alcohol is the liver (Domschke et al., 1974). The liver disease induced by drinking is the alcohol liver diseases (ALD), which remains one of the most common causes of chronic liver diseases in the world. Alcohol consumption produces a spectrum of histologic abnormalities in the liver, including steatosis (fatty liver), steatohepatitis (alcoholic hepatitis) and cirrhosis. The three lesions of liver may occur alone, at the same time or sequentially (Day and Yeaman, 1994). Except abstinence and the treatment of the illness, there is a lack of effective drugs to cure alcohol addiction and interrupt the course of ALD.

There are three main pathways for the metabolism of ethanol, each located in a different subcellular compartment: the alcohol dehydrogenase (ADH) pathway in the cytosol, the microsomal ethanol-oxidizing system (MEOS) located in the endoplasmic reticula and catalase in the peroxisomes (Jiménéz-López et al., 2002). Among these pathways, the alcohol dehydrogenase pathway is the major metabolic pathway during the early stage of chronic alcohol liver injury. In the ADH-mediated oxidation of ethanol, hydrogen is transferred from the substrate to the cofactor nicotinamide adenine dinucleotide (NAD), resulting in excess conversion to its reduced form (NADH) with the production of acetaldehyde (Cronholm, 1985; Cronholm et al., 1988; French, 2000). The excess production of NADH alters the redox state in the liver and, in turn, leads to a variety of metabolic abnormalities. The elevated ratio of NADH to NAD increases the concentration of α-glycerophosphate and suppresses the citric acid cycle, which favors accumulation of hepatic triacylglycerols by trapping fatty acids.

Niuchangchih has been used to cure the discomfort caused by excess alcohol for many years. Recently, scientific research showed that both the fruiting bodies and mycelia of *Niuchangchih* possessed protective activity against liver hepatitis and fatty liver induced by acute hepatotoxicity of alcohol (Dai et al., 2003). Using acute ethanol-intoxicated rats as an experimental model, we compared the hepatoprotective effects of *Niuchangchih* and Liangjun (*Armillariella tabescens*), a traditional Chinese fungi drug for liver diseases, on liver injury induced by ethanol (Lu et al., 2007b). Treatment with *Niuchangchih* notably prevented the ethanol-induced elevation of levels of serum aspartate aminotransferase (AST), alanine aminotransferase (ALT), alkaline phosphatase (ALP) and bilirubin to an extent that was comparable to the standard drug silymarin. Meanwhile, the results from histological studies also supported the above parameters. Currently, the isolation and testing of constituents likely to be responsible for the hepatoprotective activities of *Niuchangchih* against alcoholic liver diseases is under investigation in our lab.

5.1.2. Effect on hepatitis induced by CCl_4

CCl_4-treated animals are frequently used to evaluate the hepatoprotective effect of tested samples. It is well established that hepatotoxicity by CCl_4 is due to enzymatic activation that releases CCl_3 radicals in the free state, which in turn disrupts the structure

Table 1
Compounds isolated from *Niuchangchih*.

No.	Chemical class	Compound name	Compound structure	Sources	Bioactivity	References
1	Fatty acids	Methyl oleate		F		Wu and Chiang (1995)
2	Benzenoids	Antrocamphin A	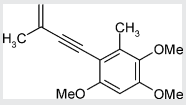	F	Anti-inflammatory activity, in vitro	Chen et al. (2007b)
3	Benzenoids	Antrocamphin B	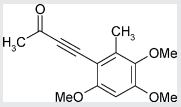	F		Chen et al. (2007b)
4	Benzenoids	2,3,4,5-Tetramethoxybenzoyl chloride	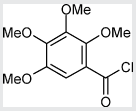	F		Chen et al. (2007b)
5	Benzenoids	Antrodioxolanone	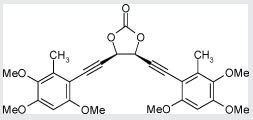	F		Chen et al. (2007b)
6	Benzenoids	Isobutylphenol	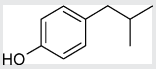	M		Wu et al. (2007b)
7	Benzoquinone	5-Methyl-benzo[1,3]dioxole-4,7-dione	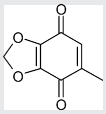	M		Wu et al. (2007b)
8	Benzoquinone derivative	2,3-Dimethoxy-5-methyl[1,4]benzoquinone	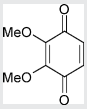	M		Wu et al. (2007b)
9	Benzoquinone derivative	2-Methoxy-5-methyl[1,4]benzoquinone	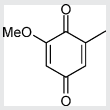	M	Antioxidant, in vitro	Wu et al. (2007b)
10	Phenyl methanoids	4,7-Dimethoxy-5-methyl-1,3-benzodioxole	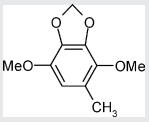	F		Chiang et al. (1995), Chen et al. (2007b)
11	Biphenyl methanoids	2,2′,5,5′-Tetramethoxy-3,4,3′,4′-dimethylenedioxy-6,6′-dimethyl biphenyl	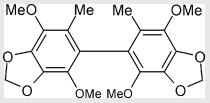	F	Anti-HBV, in vitro	Chiang et al. (1995), Shen et al. (2003a), Chen et al. (2007b)
12	Ubiquinone derivatives	Antroquinonol	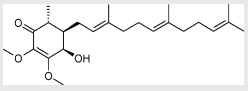	M, F	Antitumor, in vitro; anti-HBV, in vitro	Lee et al. (2007), Liu et al. (2008)
13	Tocopherols	α-Tocospiro B	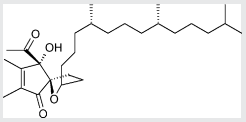	F		Chen et al. (2007b)
14	Maleic anhydrides	Camphorataanhydride A	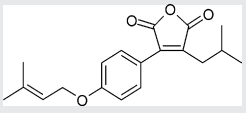	m		Nakamura et al. (2004), Cheng et al. (2008a,b)

Table 1 (*Continued*)

No.	Chemical class	Compound name	Compound structure	Sources	Bioactivity	References
15	Maleimides	Camphorataimide B	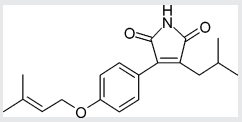	M, B	Anti-HBV, in vitro; cytotoxic effect, in vitro	Nakamura et al. (2004), Shen et al. (2005), Cheng et al. (2008a,b)
16	Maleimides	Camphorataimide C	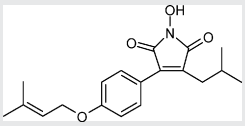	M	Cytotoxic effect, in vitro	Nakamura et al. (2004), Cheng et al. (2008a,b)
17	Succinic acid derivatives	Camphorataimide D	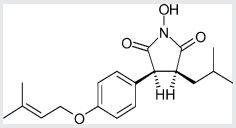	M		Nakamura et al. (2004), Cheng et al. (2008a,b)
18	Succinic acid derivatives	Camphorataimide E	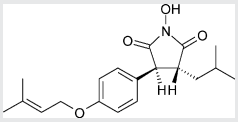	M		Nakamura et al. (2004), Cheng et al. (2008a,b)
19	Lignans	(+)-Sesamin	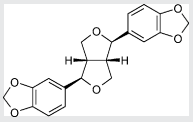	F		Wu and Chiang (1995)
20	Lignans	(−)-Sesamin	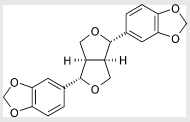	F		Chen et al. (2007b)
21	Lignans	4-Hydroxysesamin	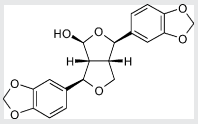	F		Wu and Chiang (1995)
22	Sesquiterpene lactones	Antrocin	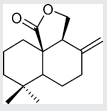	F		Chiang et al. (1995)
23	Diterpenes	19-Hydroxylabda-8(17)-en-16,15-olide	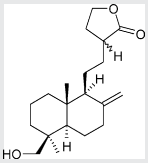	F		Chen et al. (2006)
24	Diterpenes	3β,19-Dihydroxylabda-8(17),11*E*-dien-16,15-olide	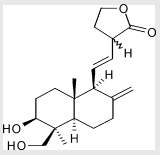	F		Chen et al. (2006)
25	Diterpenes	13-*epi*-3β,19-Dihydroxylabda-8(17),11*E*-dien-16,15-olide	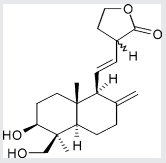	F		Chen et al. (2006)
26	Diterpenes	19-Hydroxylabda-8(17),13-dien-16,15-olide	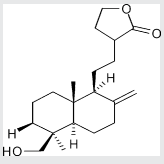	F		Chen et al. (2006)

Table 1 (*Continued*)

No.	Chemical class	Compound name	Compound structure	Sources	Bioactivity	References
27	Diterpenes	14-Deoxy-11,12-didehydroandrographolide	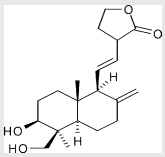	F		Chen et al. (2006)
28	Diterpenes	14-Deoxyandrographolide	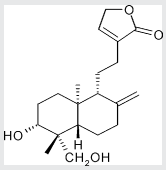	F		Chen et al. (2006)
29	Diterpenes	Pinusolidic acid	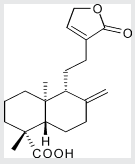	F		Chen et al. (2006)
30	Triterpenoids	Eburicoic acid	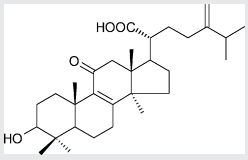	F		Shen et al. (2003a)
31	Triterpenoids	Dehydroeburicoic acid	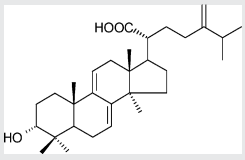	F	Anti-inflammatory activity, in vitro	Cherng et al. (1995), Yang et al. (1996), Shen et al. (2003a), Chen et al. (2007b)
32	Triterpenoids	Sulphurenic acid	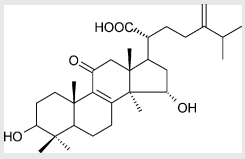	F		Shen et al. (2003a)
33	Triterpenoids	Dehydrosulphurenic acid	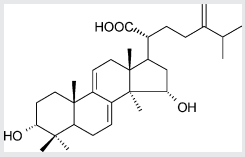	F		Yang et al. (1996), Shen et al. (2003a)
34	Triterpenoids	15α-Acetyl-dehydrosulphurenic acid	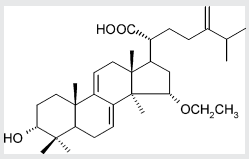	F		Yang et al. (1996), Shen et al. (2003a)
35	Triterpenoids	Versisponic acid D	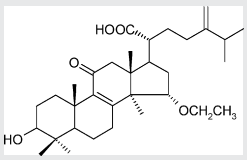	F		Shen et al. (2003a)
36	Triterpenoids	3β,15α-Dihydroxylanosta-7,9(11),24-trien-21-oic acid	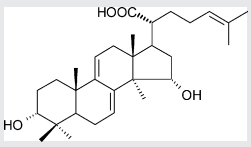	F		Shen et al. (2003a)

Table 1 (*Continued*)

No.	Chemical class	Compound name	Compound structure	Sources	Bioactivity	References
37	Triterpenoids	24-Methylenedihyd-rolanosterol	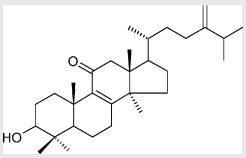	F		Cherng et al. (1995)
38	Triterpenoids	*epi*-Friedelinol	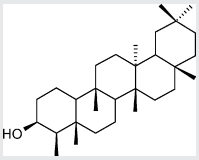	F		Chen et al. (2007b)
39	Steroids	Antcin A	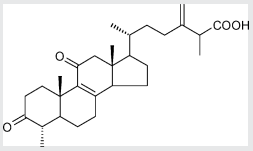	F	Anti-inflammatory activity, in vitro	Cherng et al. (1995), Chen et al. (2007b)
40	Steroids	Antcin C	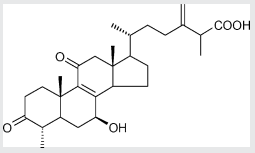	F		Cherng et al. (1995)
41	Steroids	Antcin E	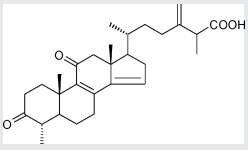	F		Cherng et al. (1996)
42	Steroids	Antcin F	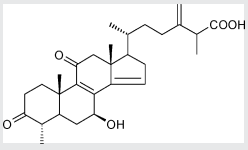	F		Cherng et al. (1996)
43	Steroids	Antcin K	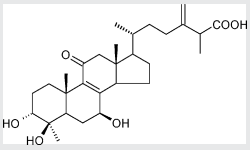	F		Shen et al. (2003a)
44	Steroids	Methyl antcinate B	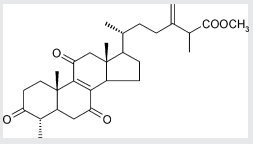	F		Shen et al. (2003a)
45	Steroids	Methyl antcinate G	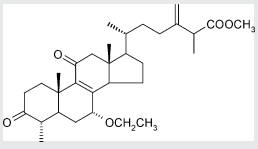	F		Cherng et al. (1996)
46	Steroids	Methyl antcinate H	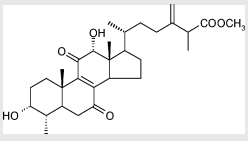	F		Cherng et al. (1996), Shen et al. (2003a)
47	Steroids	Zhankuic acid A (Antcin B)	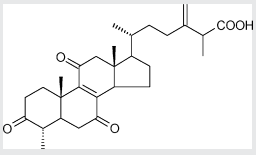	F	Cytotoxic effect, in vitro; anti-inflammatory activity, in vitro	Cherng et al. (1995), Chen et al. (1995, 2007b), Shen et al. (2003a)

Table 1 (*Continued*)

No.	Chemical class	Compound name	Compound structure	Sources	Bioactivity	References
48	Steroids	Zhankuic acid B	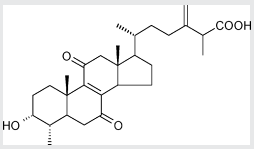	F	Anticholinergic and antiserotonergic activities, in vitro	Chen et al. (1995), Shen et al. (2003a)
49	Steroids	Zhankuic acid C (Antcin H)	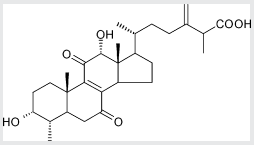	F	Cytotoxic effect, in vitro	Chen et al. (1995), Shen et al. (2003a)
50	Steroids	Zhankuic acid D	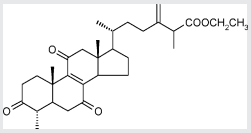	F		Yang et al. (1996)
51	Steroids	Zhankuic acid E	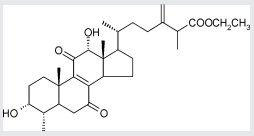	F		Yang et al. (1996)
52	Steroids	Zhankuic acid F (Antcin D)	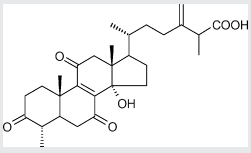	F		Shen et al. (1997), Cherng et al. (1996)
53	Steroids	β-Sitosterol	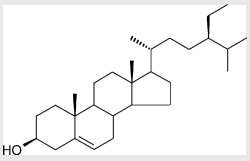	F		Wu and Chiang (1995), Chen et al. (2007b)
54	Steroids	β-Sitostenone	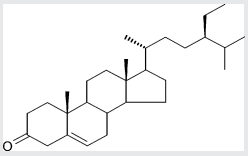	F		Chen et al. (2007b)
55	Steroids	Stigmasterol	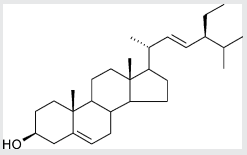	F		Chen et al. (2007b)
56	Steroids	Eburicol	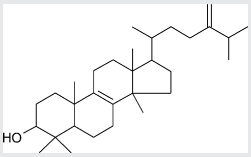	F		Wu and Chiang (1995), Chen et al. (2007b)
57	Steroids	Ergosta-4,6,8(14),22-tetraen-3-one	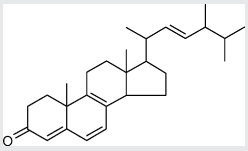	F		Chen et al. (2007b)

Table 1 (*Continued*)

No.	Chemical class	Compound name	Compound structure	Sources	Bioactivity	References
58	Steroids	Methyl-3,11-dioxo-4α-methylergost-8,24(28)-dien-26-oate	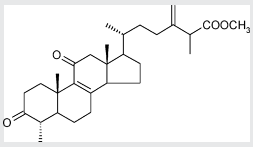	F		Wu and Chiang (1995)

Note: F: fruiting bodies; M: mycelia; B: culture broth; HBV: hepatic B virus

and function of lipids and protein macromolecules in the membrane of the cell organelles (Mujumdar et al., 1998).

The dry matter of fermented filtrate (DMF) from submerged cultures of *Niuchangchih* and aqueous extracts from *Niuchangchih* fruiting bodies have been reported to possess hepatoprotective activity against liver diseases induced by CCl_4 (Hsiao et al., 2003; Song and Yen, 2003). Both of them could reduce glutathione (GSH)-dependent enzymes (glutathione peroxidase, glutathione reductase, and glutathione S-transferase), and the GSH/GSSG ratio was significantly improved by the oral pretreatment of rats with DMF ($P < 0.01$). Histopathological evaluation of the rat liver revealed that the DMF reduced the incidence of liver lesions, including neutrophil infiltration, hydropic swelling and necrosis induced by CCl_4. Recently, Huang et al. (2006) reformulated the filtrate of *Niuchangchih* with extracts from some TCM, such as *Astragalus membranaceus*, as well as *Salvia miltiorrhiza* and *Lycimm chinense*, and found that the new formula showed significant inhibitory activity against the elevated ALT level in CCl_4-treated animals to an extent that was even better than when the filtrate was used alone.

5.1.3. Effect on Propionibacterium acnes- and lipopolysaccharide-induced hepatitis

The injection of *Propionibacterium acnes* (*P. acnes*) followed by a low dose of lipopolysaccharide (LPS) can induce fulminant hepatitis in mice, and this model has been used for the analysis of liver injury. Han et al. (2006) have separated and purified a neutral polysaccharide named *ACN2a* from the hot water extract of the mycelium of *Niuchangchih* that has hepatoprotective activity. The hepatoprotective effect of *ACN2a* was evaluated using the mouse model of liver injury that was induced by *Propionibacterium acnes*-LPS. The administration of *ACN2a* (0.4 or 0.8 g/(kg d)) significantly prevented an increase of the activities of AST and ALT in the serum of mice treated with *Propionibacterium acnes*-LPS, indicating hepatoprotective activity in vivo. Using the same cytokine-induced fulminant hepatitis animal model, Dr. Hattori isolated five maleic and succinic acid derivatives (Table 1; compound 14–18), namely Hepasim®, as the active compound(s) responsible for the anti-hepatitis activity of mycelia of *Niuchangchih* (Hattori and Sheu, 2006).

5.1.4. Possible mechanisms underlying the hepatoprotective effect of Niuchangchih

Currently available data show that *Niuchangchih* may exert its protective effects on liver injury though different mechanisms, such as scavenging free radicals responsible for cell damage, enhancing the enzymes responsible for antioxidant activity, inhibiting the inflammatory mediators and/or induction of the regeneration of the liver cells.

Chemical agents used in the in vivo research, including ethanol, CCl_4, and *Propionibacterium acnes*-LPS, not only induced liver injury, but also initiated oxidative stress and increased the level of reactive oxygen species (ROS), as manifested by an elevated level of MDA and an altered activity of SOD. Active oxygen molecules such as superoxide radicals ($O_2^{\bullet -}$) and hydroxyl radicals ($OH^{\bullet}$) have been shown to modify and damage proteins, carbohydrates, and DNA in both in vitro and in vivo models (Halliwell and Gutteridge, 1990). It is well known that free radicals derived from oxygen and other chemicals are important factors related to injury of the liver (Poli, 1993). Accumulating data have shown that *Niuchangchih* is a potent direct free radical scavenger (Huang et al., 1999; Song and Yen, 2002; Hsiao et al., 2003; Mau et al., 2004; Shu and Lung, 2008). It is therefore possible that prevention against liver injury by *Niuchangchih* is partially due to its antioxidant activity. The stable 1,1-diphenyl-2-picrylhydrazyl (DPPH) tests provided direct evidence that the *Niuchangchih* extract acted as a direct free radical scavenger (Huang et al., 1999; Hsiao et al., 2003; Mau et al., 2004). The antioxidant activities of the filtrate and mycelia extracts of *Niuchangchih* were correlated with the presence of total polyphenols, crude triterpenoids, and the protein/polysaccharide ratio of the crude polysaccharides (Song and Yen, 2002). Aqueous extracts of *Niuchangchih* inhibited nonenzymatic iron-induced lipid peroxidation in rat brain homogenates with an IC_{50} value of about 3.1 mg/ml (Hsiao et al., 2003). These results suggest that *Niuchangchih* exerts effective protection against chemical-induced hepatic injury in vivo by free radical scavenging activities.

Although the precise underlying mechanisms are not fully understood, *Niuchangchih* may act as an enzyme modulator in a way that is unrelated to its antioxidant properties. The DMF may play a role in preventing oxidative damage in living systems by upregulating hepatic GSH-dependent enzymes to preserve the normal GSH/GSSH ratio during CCl_4 metabolism (Song and Yen, 2003). The DMF showed the strongest inhibition of lipid peroxidation as a function of its concentration, and its effects were comparable to the antioxidant activity of BHA at the same concentration of 0.2 mg/ml (Song and Yen, 2002). When Hep G_2 cells were pretreated with the DMF at a concentration of 0.1 mg/ml for 4 h and then induced by 1 h of treatment with H_2O_2 (100 μM), lipid peroxidation was significantly ($P < 0.05$) decreased as measured by the formation of malondialdehyde. In another study, different solvent extracts (water, ethanol or ethyl acetate) from the fermented filtrate of *Niuchangchih* could increase hepatic SOD activity and the expression of CYP 1A1 in rat liver (Chen, 2003).

Based on our own studies and those by other groups, we believe that there are multiple potent mechanisms underlying the hepatoprotective effects of *Niuchangchih*. Further studies to fully elucidate the exact mechanism of the effects modulated by *Niuchangchih* are necessary.

5.2. Inhibition of hepatitis B virus (HBV) replication

HBV infection is known to cause acute and chronic hepatitis. Some chronic hepatitis patients subsequently suffer from cirrhosis and liver failure, and some may eventually develop hepatocellular carcinoma (HCC) (Szmuness, 1978; Beasley et al., 1981). Viral hepatitis is the most common cause of HCC worldwide, followed by alcoholic liver diseases (Lodato et al., 2006). Despite the availability of an effective preventive vaccine in recent years, about 300 million existing chronic carriers still urgently need therapy.

Table 2
A summary of the studies conducted on the pharmacological activities of *Niuchangchih*.

Study pertaining	Sample preparation, dosage and route	Model, study design	Observations	References
Hepatoprotective effect	Aqueous extract of *Niuchangchih* (250, 750, and 1250 mg/kg per day, respectively, p.o., 4 days per week)	Male ICR mice, in vivo	*Niuchangchih* showed protection against chronic CCl_4-induced hepatic injury by mediating antioxidative and free radical scavenging activities	Hsiao et al. (2003)
	Dry matter of fermented filtrate (DMF) from *Niuchangchih* (0.25 and 0.50 g/kg, p.o., daily)	Male Sprague–Dawley rats, in vivo	DMF inhibited CCl_4-induced hepatotoxicity by upregulating hepatic GSH-dependent enzymes to preserve the normal GSH/GSSH ratio and free radical scavenging effect	Song and Yen (2003)
	Mycelia or fruiting bodies of *Niuchangchih* (0.5 and 1.0 g/kg, p.o., daily)	Male Sprague-Dawley rats, in vivo	*Niuchangchih* showed protective effect on acute ethanol-induced liver injury due to its potent antioxidant ability	Dai et al. (2003)
	Mycelia of *Niuchangchih* (0.5 and 1.0 g/kg, i.g., daily)	Male Sprague-Dawley rats, in vivo	*Niuchangchih* prevented ethanol-induced elevation of serum levels of AST, ALT, ALP, and bilirubin comparable with silymarin	Lu et al. (2007b)
	Neutral polysaccharide isolated from the mycelia of *Niuchangchih* (0.4 and 0.8 g/kg, p.o., daily)	Male ICR mice, in vivo	*Niuchangchih* significantly prevented increases in AST and ALT enzyme activities in mice treated with *Propionibacterium acnes* and Lipopolysaccharide	Han et al. (2006)
	Filtrate of fermented mycelia from *Niuchangchih* (0.5 and 1.0 g/kg, p.o., daily)	Male Wistar rats, in vivo	*Niuchangchih* retarded the progression of liver fibrosis in CCl_4-treated rats possibly by scavenging free radicals formed in the liver	Lin et al. (2006)
	Fermented filtrate of *Niuchangchih*	CCl_4-induced hepatic injury in mouse, in vivo	Hepatoprotective effect of *Niuchangchih* on CCl_4-treated mouse was enhanced by extracts from Chinese traditional medicines, such as *Astragalus membranaceus*, *Salvia miltiorrhiza*, *Lycimm chinense*	Huang et al. (2006)
Anti-HBV activity	Polysaccharides from mycelia of five *Niuchangchih* strains (50 μg/ml)	HBV-producing cell line MS-G2, in vitro	All mycelia polysaccharide preparations exhibited anti-hepatitis B virus activity	Lee et al. (2002)
	Ten compounds isolated from fruiting bodies of *Niuchangchih* (5–50 μM)	Wild-type HBV producing cell line ES2, lamivudine-resistant HBV DNA integrated HCC cell line M33, in vitro	Bioassay-guided fractionation resulted in the isolation of an anti-HBV biphenyl	Huang et al. (2003)
	Culture broth of *Niuchangchih* (5–50 μM)	HBV-producing cell line MS-G2, in vitro	Bioassay-guided fractionation resulted in the isolation of an anti-HBV pyrroledione	Shen et al. (2005)
Neuroprotective effect	Extract of *Niuchangchih* mycelia (1–1000 μg/ml)	Neuronal-like rat PC12 cells, in vitro	Serum deprivation-induced PC12 cell apoptosis was prevented	Huang et al. (2005)
	Adenosine from the extract of *Niuchangchih* mycelia (1–1000 μg/ml)	Neuronal-like rat PC12 cells, in vitro	Adenosine prevented rat PC12 cells from serum deprivation-induced apoptosis through the activation of adenosine A2A receptors	Lu et al. (2006)
	Extract of *Niuchangchih* mycelia (1–1000 μg/ml)	Neuronal-like rat PC12 cells, in vitro	*Niuchangchih* prevented serum-deprived PC12 cell apoptosis through a PKA-dependent pathway and by suppression of JNK and p38 activities	Lu et al. (2008)
Antihypertensive effect	Mycelia extracts from five *Niuchangchih* strains (80–400 μg/ml)	Isolated aortic rings from Sprague-Dawley rats, in vitro	*Niuchangchih* induced an elevation in $[Ca^{2+}]_i$ mainly due to Ca^{2+} influx in endothelial cells, increased NO release and activated cGMP system activities which caused endothelium-dependent relaxation	Wang et al. (2003)

Table 2 (*Continued*)

Study pertaining	Sample preparation, dosage and route	Model, study design	Observations	References
	Methanolic extract from wild and solid-state cultures of *Niuchangchih* (10 mg/kg)	Spontaneously hypertensive rats (SHR) and Wistar Kyoto (WKY) rats, in vivo	The systolic blood pressure and diastolic blood pressure of SHR were lowered, but not of WKY rats	Liu et al. (2007b)
Anti-hyperlipidemic effect	Fruiting bodies of *Niuchangchih*	Sprague-Dawley rats, in vivo	*Niuchangchih* decreased the triglyceride and glucose levels, but could not affect the cholesterol level in rat fed with high cholesterol diet	Yen (2006)
Anti-genotoxic activity	Aqueous extracts from *Niuchangchih* mycelia (3 g/kg)	Human TK6 cells, in vitro; pregnant mice, in vivo	*Niuchangchih* possess the chemopreventive effects with no observable cytotoxicity in male mice, pregnant mice and their fetuses	Chiang et al. (2004)
Anti-angiogenic activity	Polysaccharide from mycelia of *Niuchangchih* (1 μg/ml)	Bovine aortic endothelial cells, in vitro	Polysaccharides inhibited cyclin D1 expression through inhibition of VEGF receptor signaling, leading to the suppression of angiogenesis	Cheng et al. (2005a)
Antimicrobial activity	Water and 95% ethanolic extract of mycelia of *Niuchangchih* in solid-state culture (5–10 mg)	*Bacillus cereus*, *Bacillus subtilis*, *Lactobacillus acidophilus*, *Lactobacillus lactis*, *Staphylococcus aureus*, *Staphylococcus faecalis*, *Enterobacter aerogenes*, *Escherichia coli*, *Proteus vulgaris*, *Pseudomonas aeruginosa*, *Pseudomonas fluorescens*, *Salmonella typhimurium*, *Shigella sonnei*, in vitro	Both water and ethanolic extract of *Niuchangchih* mycelia showed antimicrobial activity	Wu and Liang (2005)
Depigment effect	Water and ethanol extracts of *Niuchangchih* after fermented with *Scutellaria baicalensis*	B16-F10 cell, in vitro	Both water and ethanol extracts could protect cell from UV damage. However, ethanol extract had distinguished inhibition on tyrosinase in the cell after cell irradiation, but water extract did not	Chen (2007)
Immuno-modulatory activity	Compounds from fruiting bodies of *Niuchangchih* (50 μM)	Peripheral human neutrophils (PMN) and mononuclear cells (MNC), in vitro	Compounds from *Niuchangchih* exhibited leukocyte modulating activity by inhibiting ROS production in human PMN and MNC with no significant cytotoxic effect	Shen et al. (2003b)
	Polysaccharide from *Niuchangchih* mycelia (2.5 mg/d, i.g., 6 weeks)	Male BALB/c mice, *Schistosoma mansoni*, in vivo	*Niuchangchih* modulated the expression of CD8α and the MHC class II molecule I-A/I-E in splenic DCs and macrophages, the $CD4^+/CD8^+$ ratio of T cells and the number of B lymphocytes, also inhibited *Schistosoma mansoni* infection in vivo	Chen et al. (2008)
	Polysaccharide from *Niuchangchih* mycelia (1.0 and 2.5 mg/d, i.g., 6 weeks)	Male BALB/c or C57BL/6 mice, T1/T2 doubly transgenic mice, *Schistosoma mansoni*, in vivo	*Niuchangchih* modulated the expression of Type 1 cytokines on splenocytes as well as the percentages of $CD4^+$ T cells and B lymphocytes, induced these immune cells towards Type 1 differentiation, reduced the infection rate of *Schistosoma mansoni* in vivo	Cheng et al. (2008a,b)
Anticancer activity	Ethylacetate extract from fruiting bodies of *Niuchangchih* (10–100 μg/ml)	Human liver cancer cell lines Hep G2 and PLC/PRF/5, in vitro	Mechanisms of anticancer activity of *Niuchangchih* were involved to (1) induction of apoptosis, (2) initiation of Fas/Fas ligand pathway in Hep G2 cells, (3) trigger of mitochondrial pathway, (4) modulation of Bcl-2 family protein and (5) inhibition of NF-κB signaling pathway	Hsu et al. (2005)

Table 2 (*Continued*)

Study pertaining	Sample preparation, dosage and route	Model, study design	Observations	References
	Methanolic extracts of mycelia (MEM) from *Niuchangchih* (10–200 μg/ml)	Human hepatoma HepG2 cells, in vitro	MEM induced HepG2 apoptosis through inhibition of cell growth and up-regulation of Fas/FasL to activate the pathway of caspase-3 and -8 cascades	Song et al. (2005a)
	Methanolic extracts of mycelia (MEM) from *Niuchangchih* (10–50 μg/ml)	Chang liver cells, HepG2 and Hep3B cells, primary hepatocytes isolated from Sprague-Dawley rats, in vitro	MEM-induced apoptosis pathway in hepatoma cells were through activation of caspase-8 and -3 cascades and regulation of the cell cycle progression	Song et al. (2005b)
	Ethylacetate extract from fruiting bodies of *Niuchangchih* (30–120 μg/ml)	Human liver cancer cell line Hep 3B, in vitro	*Niuchangchih* induced apoptosis of Hep 3B cells through calcium and calpain-dependent pathways	Kuo et al. (2006)
	Ethylacetate extract from fruiting bodies of *Niuchangchih* (10–40 μg/ml)	Human liver cancer cell line PLC/PRF/5, in vitro	*Niuchangchih* inhibited invasion of cancer cells by down-regulation of invasion-related factors through NF-κB inhibition	Hsu et al. (2007)
	Extracts from *Niuchangchih* mycelia in liquid/solid-state culture	Human hepatoma cell lines C3A and PLC/PRF/5, in vitro; ICR nude mice inoculated with C3A or PLC/PRF/5, in vivo	*Niuchangchih* extract, when combined with anti-tumor agents, showed adjuvant antiproliferative effects on hepatoma cells (in vitro) and on xenografted cells in tumor-implanted nude mice (in vivo)	Chang et al. (2008)
	Fermented culture broth of *Niuchangchih* (25–150 μg/ml)	Human breast cancer cell line MCF-7, human healthy breast cell line HBL100, in vitro	*Niuchangchih* exhibited antiproliferative effect by induction of apoptosis that is associated with cytochrome c translocation, caspase 3 activation, PARP degradation, and dysregulation of Bcl-2 and Bax in MCF-7 cells	Yang et al. (2006a)
	Fermented culture broth of *Niuchangchih* (40–240 g/ml)	Human breast cancer cell line MDA-MB-231 and the MCF-7, in vitro	*Niuchangchih* exhibited antiproliferative effect by induction of apoptosis that is associated with COX-2 inhibition in MDA-MB-231 cells	Hseu et al. (2007)
	Fermented culture broth of *Niuchangchih* (40–240 g/ml)	Human breast cancer cells MDA-MB-231, in vitro; Nude mice inoculated with MDA-MB-231 cells, in vivo	*Niuchangchih* treatment induced cell cycle arrest and apoptosis of human breast cancer cells both in vitro and in vivo	Hseu et al. (2008a)
	Extract from fruiting bodies of *Niuchangchih* (10–150 μg/ml)	Human urinary bladder cancer cell line T24, in vitro	*Niuchangchih* was effective in inducing phase G_2M arrest, acting as an anti-proliferative, and an anti-metastatic agent against bladder cancer cell T24 cells	Peng et al. (2006)
	Extract from fruiting bodies of *Niuchangchih* (10–200 μg/ml)	Human urinary bladder cancer cell lines, RT4, T24 (HTB-4) and TSGH-8301, in vitro	*Niuchangchih* extract showed different significant inhibitory effects on the growth and proliferation of TCC cell lines through different mechanisms	Peng et al. (2007)
	Fermented culture broth of *Niuchangchih* (25–150 μg/ml)	Human premyelocytic leukemia HL-60, in vitro	*Niuchangchih* exerted antiproliferative action and growth inhibition through apoptosis induction	Hseu et al. (2004)
	Polysaccharide from *Niuchangchih* mycelia in submerged culture (200 μg/ml, in vitro; 100 and 200 mg/kg, in vivo)	Human leukemic U937 cells, in vitro; sarcoma 180-bearing mice, in vivo	Polysaccharides in *Niuchangchih* possessed antitumor effect through the activation of host immune response	Liu et al. (2004)
	Mycelia powder of *Niuchangchih* in submerged culture (100–200 μg/ml)	Human MG63 osteosarcoma cells, in vitro	*Niuchangchih* exerted multiple effects on viability and $[Ca^{2+}]_i$, and evoked apoptosis via inhibiting ERK and MAPK phosphorylation	Lu et al. (2007a)

Table 2 (*Continued*)

Study pertaining	Sample preparation, dosage and route	Model, study design	Observations	References
	Ethanolic extract of fruiting bodies of *Niuchangchih* (50–200 μg/ml)	Human prostate adenocarcinoma cell lines LNCaP and PC-3, in vitro	*Niuchangchih* showed anti-cancer activity against both PC-3 and LNCaP cells by modulating cell cycle regulatory proteins through different signaling pathways	Chen et al. (2007c)
	Ethanolic extract from mycelia of *Niuchangchih* in solid-state culture (0.2–2%)	Human non-small cell lung carcinoma A549 cell and primary human fetal lung fibroblast MRC-5, in vitro	Several tumor-associated genes that were changed in their expression by *Niuchangchih* were located, including human calpain small subunit, galectin-1, eukaryotic translation initiation factor 5A, annexin V and Rho GDP dissociation inhibitor α	Wu et al. (2006)
Anti-inflammatory activity	Methanolic extract from cultured mycelia of *Niuchangchih* (1–50 μg/ml)	Peripheral human neutrophils (PMN) or mononuclear cells (MNC), in vitro	The extracellular ROS production in PMN or MNC were prevented	Shen et al. (2004a)
	Zhankuic acids A, B, C, and antcin K from fruiting bodies of *Niuchangchih* (1–25 μM)	Peripheral human neutrophils, in vitro	Zhankuic acids and antcin K exhibited leukocytes modulating activity by inhibiting ROS production and firm adhesion by neutrophils with no significant cytotoxic effect	Shen et al. (2004b)
	Fermented culture broth of *Niuchangchih* (25–100 μg/ml)	Murine macrophage cell line RAW264.7, in vitro	*Niuchangchih* inhibited the production of cytokines and the degradation of IκB-α in LPS-stimulated macrophages, by down-regulation of iNOS and COX-2 expression via the suppression of NF-κB activation	Hseu et al. (2005)
	Lipopolysaccharide from mycelia of *Niuchangchih* (0.1–50 μg/ml)	Bovine aortic endothelial cells, in vitro	Bacterial LPS-induced intercellular adhersion molecule-1 and monocyte adhesion were reversed	Cheng et al. (2005b)
	Polysaccharide fractions from *Niuchangchih* mycelia (50–200 μg/ml)	Murine macrophage cell line RAW 264.7, in vitro	The lipopolysaccharide-induced NO production and the protein expression by the iNOS gene were inhibited	Chen et al. (2007a)
	Methanolic extracts from wild fruiting body, liquid-state fermentation, and solid-state culture of *Niuchangchih* (50 μg/ml)	Mouse microglia cell line EOC13.31, Female Balb/c mice, in vitro	*Niuchangchih* significantly inhibited iNOS, COX-2, and TNF-α expression in LPS/IFNγ- or β-amyloid-activated microglia	Liu et al. (2007a)
	$CHCl_3$ and methanolic extracts from fruiting bodies of *Niuchangchih* (3.125–50 μg/ml)	Mouse peritoneal excluded macrophages, in vitro	Anti-inflammatory effect of *Niuchangchih* is due to the inhibition of macrophage-mediated inflammatory mediators (NO, TNF-α and IL-12) and cell cycle arrest in G0/G1 phase in LPS/IFN-γ activated mouse peritoneal macrophages	Rao et al. (2007)
	Compounds isolated from fruiting bodies of *Niuchangchih* (100 μmol/L)	Neutrophils isolated from the venous blood of consenting healthy volunteers	Antrocamphin A, antcin A and antcin B exhibited potent inhibition against fMLP-induced superoxide production with IC_{50} values less than 10 μM	Chen et al. (2007b)
	Fractionated polysaccharides from mycelia powder of *Niuchangchih* (50–200 μg/ml)	Murine macrophage cell line RAW 264.7, in vitro	*Niuchangchih* inhibited the production of IL-6, IL-10, MPC-5, RANTES, and NO in LPS-stimulated mouse macrophages, by transcriptional down regulation of IL-6, IL-10, and iNOS genes	Wu et al. (2007c)
Antioxidant effect	Fresh and air-dried fruiting bodies and air-dried mycelia of *Niuchangchih* (2.5–10 mg/ml)	Antioxidant activity, reducing power, DPPH scavenging effect, chelating activity, in vitro	*Niuchangchih* acted as antioxidant and oxygen scavenger	Huang et al. (1999)

Table 2 (*Continued*)

Study pertaining	Sample preparation, dosage and route	Model, study design	Observations	References
	Dry matter of cultural medium, filtrate, and different solvent extracts of mycelia from *Niuchangchih* in submerged culture (0.2 mg/ml)	Antioxidant activities and free radical scavenging effects, in vitro	Dry matter of filtrate of *Niuchangchih* showed excellent antioxidant activities in different model systems	Song and Yen (2002)
	Aqueous extract from *Niuchangchih* mycelia (12.5–50 μl)	Normal human erythrocytes, HL-60 leukemic cells, in vitro	*Niuchangchih* reduced AAPH-induced erythrocyte hemolysis, lipid/protein peroxidation, and cell damage	Hseu et al. (2002)
	Methanolic extracts from red or white mycelia of *Niuchangchih* (0.5–10 mg/ml)	Antioxidant activity, reducing power, scavenging abilities on DPPH and hydroxyl radicals and chelating ability, in vitro	Antioxidants contents in mycelia were found in the order of total phenols > tocopherols > ascorbic acid > β-carotene. The antioxidant properties were good for mycelia at days 10–16	Mau et al. (2003)
	Methanolic extracts from red or white mycelia of *Niuchangchih* (0.5–10 mg/ml)	Antioxidant activity, reducing power, scavenging abilities on DPPH and hydroxyl radicals and chelating ability, in vitro	Both mycelia extracts showed potent antioxidant activities	Mau et al. (2004)
	Fermented culture broth of *Niuchangchih* (25–100 μg/ml) and aqueous extracts of mycelia from *Niuchangchih* (50–200 μg/ml)	Human low-density lipoproteins (LDL), human umbilical vein endothelial cells, in vitro	$CuSO_4$- or AAPH-induced oxidative modification of LDL was reduced; The endothelial cells were protected from the damaging effects of the $CuSO_4$-oxidized LDL	Yang et al. (2006b)
	Methanolic extract of mycelia of *Niuchangchih* irradiated with γ-rays (0.5–10 mg/ml)	Antioxidant activity, reducing power, scavenging abilities on DPPH and hydroxyl radicals and chelating ability, in vitro	γ-Irradiation enhanced the antioxidant properties of *Niuchangchih* mycelia	Huang and Mau (2007)
	Water-soluble polysaccharides from *Niuchangchih* in submerged culture (200 μg/ml)	Hydrogen peroxide-induced cytotoxicity and DNA damage in Chang liver cells, in vitro	Polysaccharides in *Niuchangchih* showed antioxidant properties by up-regulation of GST activity, maintenance of normal GSH/GSSG ratio, and scavenging of ROS	Tsai et al. (2007)
	Fermented culture broth of *Niuchangchih* (25–100 μg/ml) and aqueous extracts of mycelia from *Niuchangchih* (50–200 μg/ml)	Human umbilical vein endothelial cells, in vitro	The oxidative cell damage induced by AAPH was reduced, as evidence by reduced DNA fragmentation, cytochrome c release, caspase-3 activation, and dysregulation of Bcl-2 and Bax	Hseu et al. (2008b)

HBV is known to consist of 42-nm Dane particles and 22-nm subviral particles (containing both spherical and filamentous shells), both having the surface envelope. Serological markers are used routinely as diagnostic and prognostic indicators of acute and chronic HBV infections. The presence of hepatitis B surface antigen (HBsAg) is the most common marker of HBV infection, whereas hepatitis B e antigen (HBeAg) is used as an ancillary marker, primarily to indicate active HBV replication and associated progressive liver disease (Chisari, 2000).

Currently available data show that both fruiting bodies and liquid fermentation products (include mycelia and culture) of *Niuchangchih* possess anti-HBV activity. Polysaccharides, biphenyl, malaeimide and cyclohexenone are considered to be the bioactive components responsible for the anti-HBV activity of *Niuchangchih*.

It was reported that extracts from the mycelia of *Niuchangchih* have high inhibitory activities of HBV in a dose-dependent manner and show no cytotoxicity. In vivo HBV tests showed that mycelia of *Niuchangchih* had anti-HBV function and healing abilities for hepatitis (Chen et al., 2003). In another study, the anti-HBV effects of the polysaccharides from cultured mycelia of five *Niuchangchih* strains were evaluated in vitro. At a dosage of 50 μg/ml, polysaccharides from strain B86 showed the highest level of anti-HBsAg activity, which was higher than α-interferon at a dosage of 1000 U/ml. Furthermore, none of the polysaccharides exhibited cytotoxic effects (Lee et al., 2002).

Huang et al. also found that the ethanol extract of *Niuchangchih* displayed anti-HBV effects on both wild-type and lamivudine-resistant HBV mutants (Huang et al., 2003). Therefore, Huang's group further investigated the anti-viral activities of 10 pure compounds (Shen et al., 2003a) isolated from *Niuchangchih*, which included one biphenyl, four ergostane- and five lanostane derivatives. Among the 10 compounds, the biphenyl, namely 2,2′,5,5′-tetramethoxy-3,4,3′,4′-bis(methlylene-dioxy)-6,6′-dimethyl-biphenyl (Table 1; compound 11), was positively identified as the single active compound responsible for the anti-HBV effect of *Niuchangchih* on both wild-type and lamivudine-resistant HBV mutants. When compared to positive control interferon α-2a, the effect of compound 11 on wild-type HBV cell line ES2 was equal to that of interferon α-2a at a concentration of 1000 U/ml. When applied to lamivudine-resistant HBV cell line M33, the effect of compound 11 was less than that of α-2a at a concentration of 1000 U/ml, but equal to that of interferon α-2a at a concentration of 250 U/ml (Huang et al., 2003). More recently, bioassay-guided fractionation resulted in the isolation of an anti-HBV maleimide, namely Camphorataimide B (Table 1; compound 15), from the culture broth of *Niuchangchih*. Compound 15 suppressed both HBsAg and HBeAg expression with the

moderate inhibition percentages of 35.2 and 12.8%, respectively, at the non-cytotoxic concentration of 50 μM (Shen et al., 2005). Antroquinonol (Table 1; compound 12), a cyclohexenone isolated from mycelia and the fruiting bodies of *Niuchangchih*, was recently reported to be potent in inhibiting the synthesis of HBsAg and HBeAg to achieve the goal of HBV inhibition (Liu et al., 2008).

In conclusion, the ability of *Niuchangchih* to inhibit the replication of HBV in vivo and in vitro may be one additional reason for considering this fungus as a potential therapeutic for HBV infection. On the other hand, anti-HBV activity has not been reported for polysaccharides from any other mushroom (Lee et al., 2002). Thus, further studies on the relationship between specific polysaccharide fraction and their biological activities are also required.

5.3. Niuchangchih and liver fibrosis

Liver fibrosis is the common end stage of most chronic liver diseases, regardless of the etiology (Bataller and Brenner, 2005), and its progression leads to liver cirrhosis and liver cancer. Currently, it is regarded that the early phase of liver fibrosis can be reversed, while liver cirrhosis cannot. Thus, the key challenges in curing liver cirrhosis are how to diagnose the liver fibrosis at an early phase and developing new drugs against it (Freidman, 1993).

CCl_4-treated rats are frequently used as an experimental model to study liver fibrosis. Using this experimental model, Lin et al. (2006) have assayed the effectiveness of the filtrate of fermented mycelia from *Antrodia camphorata* (FMAC) in the preventive and curative treatment of liver fibrosis. Small fibrotic nodules were present in CCl_4-treated rats as evidenced from morphological analysis, and this was reversed when treated with FMAC. Post-treatment with FMAC to CCl_4-administered rats clearly accelerated the reversal of fibrosis and lowered the elevated mRNA levels of hepatic collagen I, transforming growth factor (TGF)-β1 and tissue inhibitors of matrix metalloproteinase (TIMP)-1.

Although the exact mechanisms of pathogenesis in liver cirrhosis are still obscure, the role of free radicals and lipid peroxides has attracted considerable attention (Gebhardt, 2002). It has been found that the metabolism of CCl_4 involves the production of free radicals through its activation by drug metabolizing enzymes located in the endoplasmic reticulum (Basu, 2003). CCl_4 is capable of causing liver lipid peroxidation, resulting in liver fibrosis (Comporti et al., 2005). Lin et al. (2006) confirmed that hepatic lipid peroxidation is increased during hepatic fibrogenesis. By treatment with FMAC, hepatic malondialdehyde (MDA) and hydroxyproline (HP) contents in curative groups were remarkably restored, indicating that *Niuchangchih* retards the progression of liver fibrosis, possibly by scavenging free radicals formed in the liver. Previous studies have reported that *Niuchangchih* plays a role in preventing oxidative damage in living systems by mediating the activities of hepatic antioxidative enzymes and scavenging free radicals formed during CCl_4 metabolism (Hsiao et al., 2003; Song and Yen, 2003). In another study, however, FMAC was effective in reversing liver fibrosis induced by dimethylnitrosamine (DMN), while the lowered activities of antioxidative enzymes (SOD, catalase and GSH-Px) in the liver were not restored by FMAC (Guo, 2002). Therefore, more in vivo studies and randomized controlled clinical studies should be performed to further elucidate the mechanisms of action of *Niuchangchih*.

5.4. Effect on liver cancer

Liver cancer is one of the most common malignancies in the world, and also one of the four most prevalent malignant diseases of adults in China, Korea and Sub-Sahara Africa (Marrero, 2006; Motola-Kuba et al., 2006). Ninety percent of liver cancers develop in the context of chronic liver diseases, and mainly in patients with cirrhosis. Although chemotherapeutic agents are the main approach for liver cancer, they are relatively ineffective. Accordingly, screening compounds for potential use as effective therapeutic agents for liver cancer is an important undertaking.

Both the fruiting bodies and mycelia of *Niuchangchih* have potent antiproliferative activity against liver cancer in vitro and in vivo. It was indicated that there were multiple potent mechanisms underlying the anticancerous effects of *Niuchangchih*.

Many studies have shown that the antiproliferative activity of *Niuchangchih* was related to cell cycle arrest and the induction of apoptosis. Song et al. (2005b) investigated the effect of the methanol extract of mycelia (MEM) from *Niuchangchih* on the inhibition of cell viability and the mechanism of MEM-induced cytotoxic in hepatoma cells. The IC_{50} of MEM on the cytotoxicity of Hep G2 (wild type p53) and Hep 3B (delete p53) was 49.5 and 62.7 μg/ml, respectively, after 48 h of incubation. Cell and nuclear morphological changes of the human hepatoma cells (Hep 3B and Hep G2) were suggestive of apoptosis. Cell cycle analysis revealed that MEM treatment induced apoptosis on Hep G2 via G_0/G_1 cell cycle arrest. The results also indicated that MEM-induced Hep G2 apoptosis through activation of the caspase-3 and -8 cascades, and regulation of the cell cycle progression to inhibit hepatoma cell proliferation. According to the results, Song and his colleagues hypothesized that the death receptor (DR)-regulated pathway may be the major mechanism of MEM-mediated apoptosis in Hep G2 cells. Thus, the involvement of the Fas/Fas ligand (FasL) death-receptor pathway in the MEM-induced apoptosis of Hep G2 cells was investigated. The results demonstrated that MEM-induced Hep G2 apoptosis through the inhibition of cell growth and the upregulation of Fas/FasL to activate the caspase-3 and -8 cascades (Song et al., 2005a). In another study, the inhibition of cell proliferation and the apoptosis induction resulting from *Niuchangchih* exposure was also confirmed (Hsu et al., 2005). The ethyl acetate extract from *Antrodia camphorata* (EAC) inhibited cell growth in two liver cancer cells, Hep G2 and PLC/PRF/5 cells, in a dose-dependent manner. In Fas/APO-1 positive-Hep G2 cells, EAC increased the expression level of Fas/APO-1 and its two forms of ligands, membrane-bound Fas ligand (mFasL) and soluble Fas ligand (sFasL), in a p53-independent manner. In addition, EAC also initiated the mitochondrial apoptotic pathway through regulation of Bcl-2 family protein expression, release of cytochrome c, and activation of caspase-9, both in Hep G2 and PLC/PRF/5 cells. Furthermore, EAC also inhibited cell survival signaling by enhancing the amount of IκBα in the cytoplasm and reducing the level and activity of NF-κB in the nucleus, which subsequently attenuated the expression of Bcl-X_L in Hep G2 and PLC/PRF/5 cells. Treatment with EAC also caused another human liver cancer cell line, Hep 3B, to undergo apoptotic cell death by way of the calcium–calpain–mitochondria signaling pathway (Kuo et al., 2006).

The activation of the immune response of the host was considered to be another mechanism by which *Niuchangchih* treated liver cancer (Meng, 2005). C57BL/6 mice bearing hepatic H22 tumors were used to investigate the anticancer and immuno-modulatory activity of the fruiting bodies of *Niuchangchih*. After 5 weeks, the inhibition rate of the high dose group (1000 mg/(kg d)) for H22 tumors was 74.24%. The macrophage phagocytic function of the high dose group was increased significantly compared with the other groups ($P < 0.01$). The proliferation activity of T cells and the ability to generate antibodies of B cells were improved significantly in the high dose group ($P < 0.01$), and the $CD4^+/CD8^+$ of mice bearing hepatic H22 tumors was recovered from inverted to normal. Compared with negative and normal control groups, the cell toxic activity of NK and LAK cells was improved significantly, and the serum concentration of interleukin-2 (IL-2), IL-12

and tumor necrosis factor-alpha (TNF-α) were increased significantly.

A recent study reported that EAC could inhibit the invasiveness and metastasis of liver cancer cells through the inhibition of angiogenesis (Hsu et al., 2007). Tumor growth inhibition was most evident in mice treated with EAC at 300 mg/(kg d), while about a 50% reduction in tumor size was observed compared to mice treated with the vehicle. EAC treatment inhibited the expression of VEGF, MMP-2 and MMP-9, and increased the expression of TIMP-1 and TIMP-2, thereby resulting in cancer invasion inhibition. Further analysis revealed that EAC suppressed constitutive and inducible NF-κB together with a reduction in MMP-9 and VEGF protein expression, MMP-9 activity and inducible cancer invasion.

In summary, the anticancer effects of *Niuchangchih* have been investigated in many studies, which have demonstrated the possibility of using *Niuchangchih* in the treatment of human liver cancer. However, as mentioned above, the anticancer activity of *Niuchangchih* is not the result of one mechanism of action only, but rather several mechanisms, including the induction of apoptosis, initiation of the calcium–calpain-dependent pathway, inhibition of angiogenesis and activation of the immune response. To further elucidate the mechanisms of action of *Niuchangchih*, more in vitro and in vivo studies should be carried out. On the other hand, *Niuchangchih* is an herbal medicine that possesses various types of active compounds, and the exact compounds responsible for the anticancer activity of *Niuchangchih* should also be further screened.

6. Effects of strains and culture conditions on its bioactivities

The fruiting bodies of *Niuchangchih* are in great demand in Taiwan due to host specificity, rarity in nature, and the difficulty of artificial cultivation. At present, solid-state culture and liquid fermentation of *Niuchangchih* have been used to obtain fruiting bodies and mycelia of *Niuchangchih*. However, it usually takes several months to cultivate the fruiting body of mushrooms, and it is difficult to control the product quality during soil cultivation (Chang and Wang, 2005; Zhong and Tang, 2004). It is generally recognized that growing mushroom mycelia in a defined medium by submerged fermentation is a rapid and alternative method to obtain fungal biomass of consistent quality (Yang and Liau, 1998). The large-scale production of the mycelia of *Niuchangchih* by submerged culture has been established, while the red color, aromatic smell and bitter taste of the harvested mycelia are similar to the fruiting bodies (Ao et al., 2003; Wu et al., 2007a).

On the other hand, marked effects have been observed on the relationship between the selected strains or culture conditions and the bioactivities of mycelia. Different culture medium and culture conditions could affect the formation of the red color in the fermented products, as the inhibitory activity against liver cancer cells was relative to the red color of the culture medium filtrate (Huang et al., 2002). Compositional analysis of polysaccharides and lipopolysaccharide showed differences in the gel profiles and carbohydrate components among different *Niuchangchih* strains (Lee et al., 2002; Cheng et al., 2005b). Polysaccharides from *Niuchangchih* strains (B71, B85, B86, BCRC35396 and BCRC35398) appeared to show varying levels of activity against the anti-HBV (Lee et al., 2002). In a study aimed at examining the effects of mycelial extracts from five different *Niuchangchih* strains on vascular tension, Wang et al. (2003) discovered that strain B85 produced the strongest vasorelaxation of the aorta among the five strains of *Niuchangchih* tested.

Aside from the strains, the pH values of the culture medium also affect the antioxidant properties and production and molecular weight distribution of exopolysaccharides from *Niuchangchih* in submerged cultures (Shu and Lung, 2004, 2008). While using the same strain, red or white mycelia of *Niuchangchih* were obtained due to different fermentation operations (Mau et al., 2004). Using the conjugated diene method, the antioxidant activity of the methanol extract of white mycelia was better than that of red mycelia (EC_{50} 3.11 vs. 19.8 mg/ml). Both mycelia were efficient in terms of the reducing power and scavenging effect on DPPH radicals, but white mycelia showed significantly lower EC_{50} values (1.56 and 1.70 mg/ml) (Mau et al., 2004). The difference was also observed in a few *Niuchangchih* mycelia cultured in different mediums on their scavenging activity against reactive oxygen species (Shen et al., 2004a).

As marked effects of different strains or culture conditions have been observed on the bioactivities of fermented products, the consensus strain should be selected and the optimum conditions for cultivating the mycelia and bioactive components warrants further investigation.

7. Conclusions

The Baisdomycete, *Niuchangchih*, has been shown to possess activity to prevent chemical and biological liver damage, avoid fatty liver and inhibit the hepatic B virus. Also, it ameliorates liver fibrosis and inhibits the growth of hepatoma cells. Thus, *Niuchangchih* is a useful substance to use in treating liver diseases due to its integrated bioactivities.

At present, solid-state culture and liquid fermentation are used to obtain fruiting bodies and mycelia of *Niuchangchih*, as well as useful metabolites for human requirements. However, very little data on the difference between the wild fruiting bodies and artificial products of *Niuchangchih* exists with regard to product components, biological function and medical effectiveness. Considering that many factors, such as the media and culture conditions, can affect the yield and bioactivity of *Niuchangchih* products, the metabolism of the fungus deserves to be extensively examined in order to obtain more metabolites possessing bioactive effects.

Niuchangchih is a medicinal fungus that possesses various types of active compounds (Table 1). Another traditional Chinese medicine, *Ganoderma lucidum*, has been considered as a therapeutic fungal biofactory, in that numerous compounds have been reported from the fungus (Paterson, 2006). Could *Niuchangchih* be the next one? Notably, the compounds isolated from the wild fruiting bodies are completely different from those isolated from the mycelia and culture broth (Table 1). The former are the majority because the previous research has focused on the isolation and identification of compounds from *Niuchangchih* fruiting bodies. Analysis of other compounds in the artificial products of *Niuchangchih* would be desirable, and it may be possible to isolate more novel compounds.

With regard to the potential of *Niuchangchih* for treating liver diseases, such as preventing chemical liver diseases, ameliorating liver fibrosis and inhibiting liver cancer, little information is available about the exact bioactive compounds of the fungus. Various extracts of *Niuchangchih* were applied in the literature to evaluate the bioactivities (Table 2). However, the significance of tests on extracts is reduced compared to those on pure compounds. Otherwise, the interaction between the different active compounds of *Niuchangchih*, whether they act synergistically or independently to elicit their protective activity against liver diseases, is not clear. Therefore, systematic research is needed to elucidate its bioactivities and to screen for the compounds responsible for such bioactivities. Furthermore, to further elucidate the mechanisms of action of *Niuchangchih*, more in vivo tests and randomized controlled clinical trials should be carried out, and the molecular mechanisms should be studied intensively.

Being the subject of debate, the nomenclature and taxonomy of *Niuchangchih* is still confusing. Different strains of *Niuchangchih* result in diverse bioactivities of the fermented cultures. Therefore, more molecular studies, such as amplified fragment length polymorphism (AFLP)-based DNA fingerprinting (Vos et al., 1995), should be used to establish the consensus strain, distinguish and select standardized stains for experiments, and determine the taxonomy of *Niuchangchih* and the geographic origins of the source material.

Acknowledgements

This work was supported by a grant from the National High-Tech Program of China (No. 2007AA021506) and the program for New Century Excellent Talents in the University of China (No. NCET-07-0380). The authors would like to thank Joanne Lim, Xiaodong Nie and Limin Chen for critically reading the manuscript.

References

Achliya, G.S., Wadodkar, S.G., Dorle, A.K., 2004. Evaluation of hepatoprotective effect of *Amalkadi Ghrita* against carbon tetrachloride-induced hepatic damage in rats. Journal of Ethnopharmacology 90, 229–232.

Ao, Z.H., Fu, H.Z., Zou, X.L., 2003. Large Scale Zhangzhi Fungus Deep Fermenting Process. CN 1456661-2003-11-19.

Basu, S., 2003. Carbon tetrachloride-induced lipid peroxidation: eicosanoid formation and their regulation by antioxidant nutrients. Toxicology 189, 113–127.

Bataller, R., Brenner, D.A., 2005. Liver fibrosis. Journal of Clinical Investigation 115, 209–218.

Beasley, R.P., Hwang, L.Y., Lin, C.C., Chien, C.S., 1981. Hepatocellular carcinoma and hepatitis B virus. A prospective study of 22707 men in Taiwan. Lancet 2, 1129–1133.

Brenner, D.A., Waterboer, T., Chio, S.K., Lindquist, J.N., Stefanovic, B., Burchardt, E., Yamauchi, M., Gillan, A., Rippe, R.A., 2000. New aspects of hepatic fibrosis. Journal of Hepatology 32 (Suppl. 1), 32–38.

Chang, T.T., Chou, W.W., 1995. *Antrodia cinnamomea* sp. nov. on *Cinnamomum kanehirai* in Taiwan. Mycological Research 99, 756–758.

Chang, T.T., Chou, W.W., 2004. *Antrodia cinnamomea* reconsidered and *A. salmonea* sp. nov. on *Cunninghamia konishii* in Taiwan. Botanical Bulletin of Academia Sinica 45, 347–352.

Chang, T.T., Wang, W.R., 2005. Basidiomatal formation of *Antrodia cinnamomea* on artificial agra media. Botanical Bulletin of Academia Sinica 46, 151–154.

Chang, C.Y., Lue, M.Y., Pan, T.M., 2005. Determination of adenosine, cordycepin and ergosterol contents in cultivated *Antrodia camphorata* by HPLC method. Journal of Food and Drug Analysis 13, 338–342.

Chang, C.Y., Huang, Z.N., Yu, H.H., Chang, L.H., Li, S.L., Chen, Y.P., Lee, K.Y., Chuu, J.J., 2008. The adjuvant effects of *Antrodia Camphorata* extracts combined with anti-tumor agents on multidrug resistant human hepatoma cells. Journal of Ethnopharmacology 118, 387–395.

Chen, X.H., 2003. Effects of the organic solvent extracts of the fermented mycelia extracts of *Antrodia camphorata* on the hepatic antioxidation and drug-metabolism systems of rats. Master Thesis. Chung Shan Medical University, Taiwan, China.

Chen, P.C., 2007. The depigment effect on B16-F10 melanoma cell by herb fermentation products with *Antrodia camphorata*. Master Thesis. Southern Taiwan University of Technology, Taiwan, China.

Chen, J.C., 2008. King of *Ganoderma*: *Antrodia camphorata* in Taiwan, 2nd ed. YuenChiJai Book Publishing Co., Taipei, Taiwan.

Chen, C.H., Yang, S.W., Shen, Y.C., 1995. New steroid acids from *Antrodia cinnamomea*, a fungal parasite of *Cinnamomum micranthum*. Journal of Natural Products 58, 1655–1661.

Chen, C.J., Su, C.H., Lan, M.H., 2001a. Study on solid cultivation and bioactivity of *Antrodia camphorata*. Fungal Sciences 16, 65–72.

Chen, J.C., Lin, W.H., Chen, C.N., Sheu, S.J., Huang, S.J., Chen, Y.L., 2001b. Development of *Antrodia camphorata* mycelium with submerged culture. Fungal Sciences 16, 7–22.

Chen, J.C., Chen, C.N., Sheu, S.J., Hu, M.L., Tsai, C.C., Dai, Y.Y., Sio, H.M., Chuang, C.H., 2003. Liver-caring medicine containing *Antrodia camphorata*, US 0113297-2003-6-19.

Chen, S.C., Lu, M.K., Cheng, J.J., Wang, D.L., 2005. Antiangiogenic activities of polysaccharides isolated from medicinal fungi. FEMS Microbiology Letters 249, 247–254.

Chen, C.C., Shiao, Y.J., Lin, R.D., Shao, Y.Y., Lai, M.N., Lin, C.C., Ng, L.T., Kuo, Y.H., 2006. Neuroprotective diterpenes from the fruiting body of *Antrodia camphorata*. Journal of Natural Products 69, 689–691.

Chen, C.C., Liu, Y.W., Ker, Y.B., Wu, Y.Y., Lai, E.Y., Chyau, C.C., Hseu, T.H., Peng, R.Y., 2007a. Chemical characterization and anti-inflammatory effect of polysaccharides fractionated from submerge-cultured *Antrodia camphorata* mycelia. Journal of Agricultural and Food Chemistry 55, 5007–5012.

Chen, J.J., Lin, W.J., Liao, C.H., Shieh, P.C., 2007b. Anti-inflammatory benzenoids from *Antrodia camphorata*. Journal of Natural Products 70, 989–992.

Chen, K.C., Peng, C.C., Peng, R.Y., Su, C.H., Chiang, H.S., Yan, J.H., Hsieh-Li, H.M., 2007c. Unique formosan mushroom *Antrodia camphorata* differentially inhibits androgen-responsive LNCaP and -independent PC-3 prostate cancer cells. Nutrition and Cancer—An International Journal 57, 111–121.

Chen, Y.J., Cheng, P.C., Lin, C.N., Liao, H.F., Chen, Y.Y., Chen, C.C., Lee, K.M., 2008. Polysaccharides from *Antrodia camphorata* mycelia extracts possess immunomodulatory activity and inhibits infection of *Schistosoma mansoni*. International Immunopharmacology 8, 458–467.

Cheng, J.J., Huang, N.K., Chang, T.T., Wang, D.L., Lu, M.K., 2005a. Study for anti-angiogenic activities of polysaccharides isolated from *Antrodia cinnamomea* in endothelial cells. Life Sciences 76, 3029–3042.

Cheng, J.J., Yang, C.J., Cheng, C.H., Wang, Y.T., Huang, N.K., Lu, M.K., 2005b. Characterization and functional study of *Antrodia camphorata* lipopolysaccharide. Journal of Agricultural and Food Chemistry 53, 469–474.

Cheng, C.F., Lai, Z.C., Lee, Y.J., 2008a. Total synthesis of (±)-camphorataimides and (±)-himanimides by $NaBH_4/Ni(OAc)_2$ or Zn/AcOH stereoselective reduction. Tetrahedron 64, 4347–4354.

Cheng, P.C., Hsu, C.Y., Chen, C.C., Lee, K.M., 2008b. In vivo immunomodulatory effects of *Antrodia camphorata* polysaccharides in a T1/T2 doubly transgenic mouse model for inhibiting infection of *Schistosoma mansoni*. Toxicology and Applied Pharmacology 227, 291–298.

Cherng, I.H., Chiang, H.C., Cheng, M.C., Wang, Y., 1995. Three new triterpenoids from *Antrodia cinnamomea*. Journal of Natural Products 58, 365–371.

Cherng, I.H., Wu, D.P., Chiang, H.C., 1996. Triterpenoids from *Antrodia cinnamomea*. Phytochemistry 41, 263–267.

Chiang, H.C., Wu, D.P., Cherng, I.W., Ueng, C.H., 1995. A sesquiterpene lactone, phenyl and biphenyl compounds from *Antrodia cinnamomea*. Phytochemistry 39, 613–616.

Chiang, S.Y., Hsieh, C.L., Chang, L.L., Pei, S.Y., Lin, M.Y., Kao, S.T., 2004. The safety and anti-genotoxic effects of *Antrodia camphorata* in vitro, in pregnant mice and their fetuses. Toxicology and Applied Pharmacology 197, 350–351.

Chisari, F.V., 2000. Viruses, immunity, and cancer: lessons from hepatitis B. American Journal of Pathology 156, 1118–1132.

Chiu, H.H., 2007. Phylogenetic analysis of *Antrodia* species and *Antrodia camphorata* inferred from internal transcribed spacer region. Antonie van Leeuwenhoek 91, 267–276.

Chiu, N.Y., Zhang, G.X., 2001. The Illustrated Medicinal Plant in Taiwan, vol. 6. SMC Publishing Inc., Taibei.

Comporti, M., Arezzini, B., Signorini, C., Sgherri, C., Monaco, B., Gardi, C., 2005. F2-isoprostanes stimulate collagen synthesis in activated hepatic stellate cells: a link with liver fibrosis? Laboratory Investigation 85, 1381–1391.

Cronholm, T., 1985. Hydrogen transfer between ethanol molecules during oxidoreduction in vivo. Biochemical Journal 229, 315–322.

Cronholm, T., Jones, A.W., Skagerberg, S., 1988. Mechanism and regulation of ethanol elimination in humans: intermolecular hydrogen transfer and oxidoreduction in vivo. Alcoholism, Clinical and Experimental Research 12, 683–686.

Dai, Y.Y., Chuang, C.H., Tsai, C.C., Sio, H.M., Huang, S.C., Chen, J.C., Hu, M.L., 2003. The protection of *Antrodia camphorata* against acute hepatotoxicity of alcohol in rats. Journal of Food and Drug Analysis 11, 177–185.

Day, C.P., Yeaman, S.J., 1994. The biochemistry of alcohol-induced fatty liver. Biochemica et Biophysica Acta 1215, 33–48.

Domschke, S., Domschke, W., Lieber, C.S., 1974. Hepatic redox state: attenuation of the acute effects of ethanol induced by chronic ethanol consumption. Life Sciences 15, 1327–1334.

Freidman, S., 1993. The cellular basis of hepatic fibrosis mechanism and treatment strategies. New England Journal of Medicine 328, 1828–1835.

French, S.W., 2000. Mechanisms of alcoholic liver injury. Canadian Journal of Gastroenterology 14, 327–332.

Gebhardt, R., 2002. Inhibition of cholesterol biosynthesis in HepG2 cells by artichoke extracts is reinforced by glucosidase pretreatment. Phytotherapy Research 16, 368–372.

Guo, S.Q., 2002. Ameliorative effects of *Antrodia camphorata* on liver fibrosis and gastrointestinal functions in rats. Master Thesis. China Medical College, Taiwan, China.

Halliwell, B., Gutteridge, J.M., 1990. Role of free radicals and catalytic metal ions in human disease: an overview. Methods in Enzymology 186, 1–85.

Han, H.F., Nakamura, N., Zuo, F., Hirakawa, A., Yokozawa, T., Hattori, M., 2006. Protective effects of a neutral polysaccharide isolated from the mycelium of *Antrodia cinnamomea* on *Propionibacterium acnes* and lipopolysaccharide induced hepatic injury in mice. Chemical & Pharmaceutical Bulletin 54, 496–500.

Hattori, M., Sheu, C.C., 2006. Compounds from *Antrodia camphorata* having anti-inflammatory and anti-tumor activity, US 7109232-2006-9-19.

Hawksworth, D.L., Kirk, P.M., Sutton, B.C., Pegler, D.N., 1995. Ainsworth and Bisby's Dictionary of the Fungi, 8th ed. International Mycological Institute, Egham, United Kingdom.

Hseu, Y.C., Chang, W.C., Hseu, Y.T., Lee, C.Y., Yech, Y.J., Chen, P.C., Chen, J.Y., Yang, H.L., 2002. Protection of oxidative damage by aqueous extract from *Antrodia camphorata* mycelia in normal human erythrocytes. Life Sciences 71, 469–482.

Hseu, Y.C., Yang, H.L., Lai, Y.C., Lin, J.G., Chen, G.W., Chang, Y.H., 2004. Induction of apoptosis by *Antrodia camphorata* in human premyelocytic leukemia HL-60 cells. Nutrition and Cancer-an International Journal 48, 189–197.

Hseu, Y.C., Wu, F.Y., Wu, J.J., Chen, J.Y., Chang, W.H., Lu, F.J., Lai, Y.C., Yang, H.L., 2005. Anti-inflammatory potential of *Antrodia camphorata* through inhibition of NOS,

COX-2 and cytokines via the NF-kappa B pathway. International Immunopharmacology 5, 1914–1925.
Hseu, Y.C., Chen, S.C., Tsai, P.C., Chen, C.S., Lu, F.J., Chang, N.W., Yang, H.L., 2007. Inhibition of cyclooxygenase-2 and induction of apoptosis in estrogen-nonresponsive breast cancer cells by *Antrodia camphorata*. Food and Chemical Toxicology 45, 1107–1115.
Hseu, Y.C., Chen, S.C., Chen, H.C., Liao, J.W., Yang, H.L., 2008a. *Antrodia camphorata* inhibits proliferation of human breast cancer cells in vitro and in vivo. Food and Chemical Toxicology 46, 2680–2688.
Hseu, Y.C., Chen, S.C., Yech, Y.J., Wang, L., Yang, H.L., 2008b. Antioxidant activity of *Antrodia camphorata* on free radical-induced endothelial cell damage. Journal of Ethnopharmacology 118, 237–245.
Hsiao, G., Shen, M.Y., Lin, K.H., Lan, M.H., Wu, L.Y., Chou, D.S., Lin, C.H., Su, C.H., Sheu, J.R., 2003. Antioxidant and hepatoprotective effective of *Antrodia camphorata* extract. Journal of Agricultural and Food Chemistry 51, 3302–3308.
Hsu, Y.L., Kuo, Y.C., Kuo, P.L., Ng, L.T., Kuo, Y.H., Lin, C.C., 2005. Apoptotic effects of extract from *Antrodia camphorata* fruiting bodies in human hepatocellular carcinoma cell lines. Cancer Letters 221, 77–89.
Hsu, Y.L., Kuo, P.L., Cho, C.Y., Ni, W.C., Tzeng, T.F., Ng, L.T., Kuo, Y.H., Lin, C.C., 2007. *Antrodia cinnamomea* fruiting bodies extract suppresses the invasive potential of human liver cancer cell line PLC/PRF/5 through inhibition of nuclear factor κB pathway. Food and Chemical Toxicology 45, 1249–1257.
Huang, S.J., Mau, J.L., 2007. Antioxidant properties of methanolic extracts from *Antrodia camphorata* with various doses of gamma-irradiation. Food Chemistry 105, 1702–1710.
Huang, L.C., Huang, S.J., Chen, C.C., Mau, J.L., 1999. Antioxidant properties of *Antrodia camphorata*. In: Proceedings of the 3rd International Conference on Mushroom Biology and Mushroom Products, Sydney, Australia, pp. 275–283.
Huang, R.C., Chen, J.C., Wang, B.C., 2002. Isolate of *Antrodia camphorata* process for producing a culture of the same and product obtained thereby. US 6391615-2002, 5–21.
Huang, R.L., Huang, Q., Chen, C.F., Chang, T.T., Chou, C.J., 2003. Anti-viral effects of active compounds from *Antrodia camphorata* on wild-type and lamivudine-resistant mutant HBV. The Chinese Pharmaceutical Journal 55, 371–379.
Huang, N.K., Cheng, J.J., Lai, W.L., Lu, M.K., 2005. *Antrodia camphorata* prevents rat pheochromo cells from serum deprivation-induced apoptosis. FEMS Microbiology Letters 244, 213–219.
Huang, J.S., Chang, H.C., Li, E.I.C., Huang, T.M., Su, Y.H., Wang, K.C., 2006. Enhancement of hepatoprotective efficacy of *Antrodia camphorata* by Chinese tradition medicine. Journal of Gastroenterology and Hepatology 21 (Suppl. 2), A234.
Jiménéz-López, J.M., Carrasco, M.P., Segovia, J.L., Marco, C., 2002. Resistance of HepG2 cells against the adverse effects of ethanol related to neutral lipid and phospholipid metabolism. Biochemical Pharmacology 63, 1485–1490.
Kuo, P.L., Hsu, Y.L., Cho, C.Y., Ng, L.T., Kuo, Y.H., Lin, C.C., 2006. Apoptotic effects of *Antrodia cinnamomea* fruiting bodies extract are mediated through calcium and calpain-dependent pathways in Hep 3B cells. Food and Chemical Toxicology 44, 1316–1326.
Lee, I.H., Huang, R.L., Chen, C.T., Chen, H.C., Hsu, W.C., Lu, M.K., 2002. *Antrodia camphorata* polysaccharides exhibit anti-hepatitis B virus effects. FEMS Microbiology Letters 209, 63–67.
Lee, T.H., Lee, C.K., Tsou, W.L., Liu, S.Y., Kuo, M.T., Wen, W.C., 2007. A new cytotoxic agent from solid-state fermented mycelium of *Antrodia camphorata*. Planta Medica 63, 86–88.
Lin, E.S., Chen, Y.H., 2007. Factors affecting mycelial biomass and exopolysaccharide production in submerged cultivation of *Antrodia cinnamomea* using complex media. Bioresource Technology 98, 2511–2517.
Lin, W.C., Kuo, S.C., Wu, Y.W., 2001. Effects of 28-days' repeated oral administration of the fermented extract of mycelia of *Antrodia comphorata* (CCRC 93032) on rats. Journal of Chinese Medicine 12, 293–303.
Lin, W.C., Kuo, S.C., Lin, W.L., Fang, H.L., Wang, B.C., 2006. Filtrate of fermented mycelia from *Antrodia camphorata* reduces liver fibrosis induced carbon tetrachloride in rats. World Journal of Gastroenterology 12, 2369–2374.
Liu, J.J., Huang, T.S., Hsu, M.L., Chen, C.C., Lin, W.S., Lu, F.J., Chang, W.H., 2004. Antitumor effects of the partially purified polysaccharides from *Antrodia camphorata* and the mechanism of its action. Toxicology and Applied Pharmacology 201, 186–193.
Liu, D.Z., Liang, H.J., Chen, C.H., Su, C.H., Lee, Z.H., Huang, C.T., Hou, W.C., Lin, S.Y., Zhong, W.B., Lin, P.J., Hung, L.F., Liang, Y.C., 2007a. Comparative anti-inflammatory characterization of wild fruiting body, liquid-state fermentation, and solid-state culture of *Taiwanofungus camphoratus* in microglia and the mechanism of its action. Journal of Ethnopharmacology 113, 45–53.
Liu, D.Z., Liang, Y.C., Lin, S.Y., Lin, Y.S., Wu, W.C., Hou, W.C., Su, C.H., 2007b. Antihypertensive activities of a solid-state culture of *Taiwanofungus camphoratus* (Chang-Chih) in spontaneously hypertensive rats. Bioscience Biotechnology and Biochemistry 71, 23–30.
Liu, S.Y., Kuo, M.T., Wen, W.C., 2008. Inhibition of hepatitis B virus by cyclohexenone compounds from *Antrodia camphorata*. US 7411003.
Lodato, F., Mazzella, G., Festi, D., Azzaroli, F., Colecchia, A., Roda, E., 2006. Hepatocellular carcinoma prevention: a worldwide emergence between the opulence of developed countries and the economic constraints of developing nations. World Journal of Gastroenterology 12, 7239–7249.
Lu, M.K., Cheng, J.J., Lai, W.L., Lin, Y.R., Huang, N.K., 2006. Adenosine as an active component of *Antrodia cinnamomea* that prevents rat PC12 cells from serum deprivation-induced apoptosis through the activation of adenosine A_{2A} receptors. Life Sciences 79, 252–258.
Lu, Y.C., Huang, C.C., Huang, C.J., Chu, S.T., Chi, C.C., Su, H.H., Hsu, S.S., Wang, J.L., Chen, I.S., Liu, S.I., Huang, J.K., Ho, C.M., Kuo, S.J., Jan, C.R., 2007a. Effects of *Antrodia camphorata* on viability, apoptosis, $[Ca^{2+}]_i$, and MAPKs phosphorylation in MG63 human osteosarcoma cells. Drug Development Research 68, 71–78.
Lu, Z.M., Tao, W.Y., Zou, X.L., Fu, H.Z., Ao, Z.H., 2007b. Protective effects of mycelia of *Antrodia camphorata* and *Armillariella tabescens* in submerged culture against ethanol-induced hepatic toxicity in rats. Journal of Ethnopharmcology 110, 160–164.
Lu, M.K., Cheng, J.J., Lai, W.L., Lin, Y.J., Huang, N.K., 2008. Fermented *Antrodia cinnamomea* extract protects rat PC12 cells from serum deprivation-induced apoptosis: the role of the MAPK family. Journal of Agricultural and Food Chemistry 56, 865–874.
Marrero, J.A., 2006. Hepatocellular carcinoma. Current Opinion in Gastroenterology 22, 248–253.
Mau, J.L., Huang, P.N., Huang, S.J., Chen, C.C., 2003. Time course for antioxidants production by *Antrodia camphorata* in submerged culture. Fungal Sciences 18, 59–71.
Mau, J.L., Huang, P.N., Huang, S.J., Chen, C.C., 2004. Antioxidant properties of methanol extracts from two kinds of *Antrodia camphorata* mycelia. Food Chemistry 86, 25–31.
Meng, F.Y., 2005. The antineoplastic property of *Antrodia camphorata* and its effect on the immune function of the tumor bearing mouse. Master Thesis. Harbin Medical University, China.
Motola-Kuba, D., Zamora-Valdes, D., Uribe, M., Mendez-Sanchez, N., 2006. Hepatocellular carcinoma. An overview. Annals of Hepatology 5, 16–24.
Mujumdar, A.M., Upadhye, A.S., Pradhan, A.M., 1998. Effect of *Azadirachta indica* leaf extract on CCl_4 induced hepatic damage in albino rats. Indian Journal of Pharmaceutical Sciences 60, 363–367.
Nakamura, N., Hirakawa, A., Gao, J.J., Kakuda, H., Shiro, M., Komatsu, Y., Sheu, C.C., Hattori, M., 2004. Five new maleic and succinic acid derivatives from the mycelium of *Antrodia camphorata* and their cytotoxic effects on LLC tumor cell line. Journal of Natural Products 67, 46–48.
Paterson, R.R.M., 2006. *Ganoderma*—a therapeutic fungal biofactory. Phytochemistry 67, 1985–2001.
Peng, C.C., Chen, K.C., Peng, R.Y., Su, C.H., Hsieh-Li, H.M., 2006. Human urinary bladder cancer T24 cells are susceptible to the *Antrodia camphorata* extracts. Cancer Letters 243, 109–119.
Peng, C.C., Chen, K.C., Peng, R.Y., Chyau, C.C., Su, C.H., Hsieh-Li, H.M., 2007. *Antrodia camphorata* extract induces replicative senescence in superficial TCC, and inhibits the absolute migration capability in invasive bladder carcinoma cells. Journal of Ethnopharmacology 109, 93–103.
Poli, G., 1993. Liver damage due to free radicals. British Medical Bulletin 49, 604–620.
Rao, Y.K., Fang, S.H., Tzeng, Y.M., 2007. Evaluation of the anti-inflammatory and anti-proliferation tumoral cells activities of *Antrodia camphorata*, *Cordyceps sinensis*, and *Cinnamomum osmophloeum* bark extracts. Journal of Ethnopharmacology 114, 78–85.
Shahani, S., 1999. Evaluation of hepatoprotective efficacy of APCL-A polyherbal formulation in vivo in rats. Indian Drugs 36, 628–631.
Shen, Y.C., Yang, S.W., Lin, C.S., Chen, C.H., Kuo, Y.H., Chen, C.F., 1997. Zhankuic acid F: a new metabolite from a Formosan fungus *Antrodia cinnamomea*. Planta Medica 73, 1412–1415.
Shen, C.C., Kuo, Y.C., Huang, R.L., Lin, L.C., Don, M.J., Chang, T.T., Chou, C.J., 2003a. New ergostane and lanostane from *Antrodia camphorata*. Journal of Chinese Medicine 14, 247–258.
Shen, Y.C., Chen, C.F., Wang, Y.H., Chang, T.T., Chou, C.J., 2003b. Evaluation of the immuno-modulating activity of some active principles isolated from the fruiting bodies of *Antrodia camphorata*. The Chinese Pharmaceutical Journal 55, 313–318.
Shen, Y.C., Chou, C.J., Wang, Y.H., Chen, C.F., Chou, Y.C., Lu, M.K., 2004a. Anti-inflammatory activity of the extracts from mycelia of *Antrodia camphorata* cultured with water-soluble fractions from five different *Cinnamomum* species. FEMS Microbiology Letters 231, 137–143.
Shen, Y.C., Wang, Y.H., Chou, Y.C., Chen, C.F., Lin, L.C., Chang, T.T., Tien, J.H., Chou, C.J., 2004b. Evaluation of the anti-inflammatory activity of zhankuic acids isolated from the fruiting bodies of *Antrodia camphorata*. Planta Medica 70, 310–314.
Shen, C.C., Yang, H.C., Huang, R.L., Chen, J.C., Chen, C.C., 2005. Anti-HBV principle from the culture broth of *Antrodia camphorata* (strain # CCRC-35396). Journal of Chinese Medicine 16, 57–61.
Shu, C.H., Lung, M.Y., 2004. Effect of pH on the production and molecular weight distribution of exopolysaccharide by *Antrodia camphorata* in batch cultures. Process Biochemistry 39, 931–937.
Shu, C.H., Lung, M.Y., 2008. Effect of culture pH on the antioxidant properties of *Antrodia camphorata* in submerged culture. Journal of the Chinese Institute of Chemical Engineers 39, 1–8.
Song, T.Y., Yen, G.C., 2002. Antioxidant properties of *Antrodia camphorata* in submerged culture. Journal of Agricultural and Food Chemistry 50, 3322–3327.
Song, T.Y., Yen, G.C., 2003. Protective effects of fermented filtrate from *Antrodia camphorata* in submerged culture against CCl_4-induced hepatic toxicity in rats. Journal of Agricultural and Food Chemistry 51, 1571–1577.
Song, T.Y., Hsu, S.L., Yeh, C.T., Yen, G.C., 2005a. Mycelia from *Antrodia camphorata* in submerged culture induced apoptosis of human heptoma HepG2 cells possibility through regulation of Fas pathway. Journal of Agricultural and Food Chemistry 53, 5559–5564.

Song, T.Y., Hsu, S.L., Yen, G.C., 2005b. Induction of apoptosis in human heptoma cells by mycelium of *Antrodia camphorata* in submerged culture. Journal of Ethnopharmacology 100, 158–167.

Su, C.H., 2002. Health Guardian Angel: *Antrodia camphorata*, 1st ed. EKS Book Publishing Co., Taipei, Taiwan.

Szabo, G., 2003. Pathogenic interactions between alcohol and hepatitis C. Current Gastroenterology Reports 5, 86–92.

Szmuness, W., 1978. Hepatocellular carcinoma and hepatitis B virus: evidence for a causal association. Progress in Medical Virology 24, 40–69.

Tsai, Z.T., Liaw, S.L., 1985. The Use and the Effect of Ganoderma. San Yun Press, Taiwan, pp. 116–117.

Tsai, M.C., Song, T.Y., Shih, P.H., Yen, G.C., 2007. Antioxidant properties of water-soluble polysaccharides from *Antrodia cinnamomea* in submerged culture. Food Chemistry 104, 1115–1122.

Vos, P., Hogers, R., Bleeker, M., Reijans, M., Van De Lee, T., Hornes, M., Frijters, A., Pot, J., Peleman, J., Kulper, M., Zabeau, M., 1995. AFLP: a new technique for DNA fingerprinting. Nucleic Acids Research 23, 4407–4414.

Wang, G.J., Tseng, H.W., Chou, C.J., Tsai, T.H., Chen, C.T., Lu, M.K., 2003. The vasorelaxation of *Antrodia camphorata* mycelia: involvement of endothelial Ca^{2+}-NO-cGMP pathway. Life Sciences 73, 2769–2783.

Wang, W.M., Wu, R.Y., Ko, W.H., 2005. Variation and segregation following nuclear transplantation in *Antrodia cinnamomea*. Botanical Bulletin of Academia Sinica 46, 217–222.

Wu, D.P., Chiang, H.C., 1995. Constituents of *Antrodia cinnamomea*. Journal of the Chinese Chemical Society 42, 797–800.

Wu, C.Y., Liang, Z.C., 2005. Antimicrobial activity of extract from *Antrodia camphorata* cultured on pearl barley by solid-state fermentation. Taiwanese Journal of Agricultural Chemistry and Food Science 43, 295–303.

Wu, S.H., Ryvarden, L., Chang, T.T., 1997. *Antrodia camphorata* ("niu-chang-chih"), new combination of a medicinal fungus in Taiwan. Botanical Bulletin of Academia Sinica 38, 273–275.

Wu, S.H., Yu, Z.H., Dai, Y.C., Chen, C.T., Su, C.H., Chen, L.C., Hsu, W.C., Hwang, G.Y., 2004. *Taiwanofungus*, a polypore new genus. Fungal Sciences 19, 109–116.

Wu, H., Pan, C.L., Yao, Y.C., Chang, S.S., Li, S.L., Wu, T.F., 2006. Proteomic analysis of the effect of *Antrodia camphorata* extract on human lung cancer A549 cell. Proteomics 6, 826–835.

Wu, M.C., Lin, S.J., Wang, B.C., 2007a. Process for producing a culture of *Antrodia camphorata* and product obtained thereby. US 7157090.

Wu, M.D., Cheng, M.J., Wang, B.C., Wang, W.Y., Lai, J.T., Yuan, G.F., 2007b. Chemical constituents from the mycelia of *Antrodia camphorata*. Journal of the Chilean Chemical Society 52, 1338–1340.

Wu, Y.Y., Chen, C.C., Chyau, C.C., Chung, S.Y., Liu, Y.W., 2007c. Modulation of inflammation-related genes of polysaccharides fractionated from mycelia of medicinal basidiomycete *Antrodia camphorata*. Acta Pharmacologica Sinica 28, 258–267.

Yang, F.C., Liau, C.B., 1998. Effects of cultivating conditions on the mycelial growth of *Ganoderma lucidum* in submerged flask cultures. Bioprocess Engineering 19, 233–236.

Yang, S.W., Shen, Y.C., Chen, C.H., 1996. Steroids and triterpenoids of *Antrodia cinnamomea*—a fungus parasitic on *Cinnamomum micranthum*. Phytochemistry 41, 1389–1392.

Yang, H.L., Chen, C.S., Chang, W.H., Lu, F.J., Lai, Y.C., Chen, C.C., Hseu, T.H., Kuo, C.T., Hseu, Y.C., 2006a. Growth inhibition and induction of apoptosis in MCF-7 breast cancer cells by *Antrodia camphorata*. Cancer Letters 231, 215–227.

Yang, H.L., Hseu, Y.C., Chen, J.Y., Yech, Y.J., Lu, F.J., Wang, H.H., Lint, P.S., Wang, B.C., 2006b. *Antrodia camphorata* in submerged culture protects low density lipoproteins against oxidative modification. American Journal of Chinese Medicine 34, 217–231.

Yen, S.J., 2006. Study on the hypotriglyceridemic effect of *Antrodia camphorata* in rats with high-cholesterol diet. Master Thesis. Taibei Medical University, Taiwan, China.

Zang, M., Su, Q.H., 1990. *Ganoderma comphoratum*, a new taxon in genus *Ganoderma* from Taiwan, China. Acta Botanica Yunnanica 12, 395–396.

Zhong, J.J., Tang, Y.J., 2004. Submerged cultivation of medicinal mushrooms for production of valuable bioactive metabolites. Advances in Biochemical Engineering, Biotechnology 87, 25–59.

ELSEVIER

FEMS Microbiology Letters 209 (2002) 63–67

FEMS MICROBIOLOGY Letters

www.fems-microbiology.org

Antrodia camphorata polysaccharides exhibit anti-hepatitis B virus effects

I.-Hung Lee [a], Ray-Ling Huang [b], Chi-Ting Chen [b], Hsiao-Chuan Chen [b], Wen-Chi Hsu [b], Mei-Kuang Lu [b,*]

[a] *China Medical College, 91 Hsueh-Shih Road, Taichung 40421, Taiwan*

[b] *National Research Institute of Chinese Medicine, No. 155-1, Sec. 2, Li-Nung St., Petto, Taipei 112, Taiwan*

Received 7 September 2001; received in revised form 11 January 2002; accepted 18 January 2002

First published online 26 February 2002

Abstract

Polysaccharides were extracted from fruiting bodies and cultured mycelia from five *Antrodia camphorata* strains. Polysaccharide profiles of the five strains, as determined by high-performance anion-exchange chromatography, showed varying yields and composition of neutral sugars. *A. camphorata* fruiting bodies also had different polysaccharide patterns compared to the cultured mycelium. Analysis of 26-day-old mycelia showed that the neutral sugars galactose, glucose, mannose, and galactosamine were predominant. All mycelia polysaccharide preparations exhibited anti-hepatitis B virus activity. Polysaccharides from strain B86 at a concentration of 50 μg ml^{-1} showed the highest level of anti-hepatitis B surface antigen effect, which was higher than α-interferon at a dosage of 1000 U ml^{-1}. Only strains B86 and 35398 had substantial anti-hepatitis B e antigen activities. None of the polysaccharides exhibited cytotoxic effects.

Keywords: Basidiomycetes; Mushroom; Water-soluble polysaccharides; Anti-hepatitis B virus; High-performance anion-exchange chromatography; *Antrodia camphorata*

1. Introduction

Antrodia camphorata (Chinese name, niu-chang-chih) is a medicinal fungus of the family Basidiomycetes that has been used as a folkdrug in Taiwan for the treatment of tumorigenic diseases. Chemical compounds found in *A. camphorata* include sesquiterpene lactone, steroids and triterpenoids [1–6]. The triterpenoids have anti-cholinergic and anti-serotonergic activities [6].

Polysaccharides are common structural and storage polymers in living organisms, representing more than 75% of the dry weight of plants [7]. Compositional analysis of glycoconjugates is important in structural studies of these compounds. Polysaccharides are potentially useful, biologically active ingredients for pharmaceutical uses due to a variety of biological activities, such as mitogenic activity, activation of alternative-pathway complement and plasma-clotting activity [8]. Tumor-inhibition activity has been documented in numerous mushroom polysaccharide fractions such as a glucan–protein complex from *Ganoderma tsugae* [9], lentinan (a 1→3-linked β-D-glucan) from *Lentinus edodes* [10], and schizophyllan from *Schizophyllum commune* [11]. We report here on the physiochemical properties of polysaccharides in *A. camphorata*. Quantification and profile analysis of the carbohydrates were carried out by anion-exchange chromatography with pulsed amperometric detection [12]. The effects of these polysaccharides on the hepatitis B virus (HBV) were also examined.

2. Materials and methods

2.1. A. camphorata strains

A. camphorata isolates, accessions 35396 and 35398, were obtained from the Culture Collection and Research Center (CCRC, Taiwan) [13]. Taiwan strains, B85 from

* Corresponding author. Tel: +886 (2) 28201999, ext.7391; Fax: +886 (2) 28264276.

E-mail address: mklu@cma23.nricm.edu.tw (M.-K. Lu).

0378-1097/02/$22.00
PII: S0378-1097(02)00487-1

Taitung, B86 from Hsinchu, and B71 from Alishan, were gifts from fungi specialist Dr. T.T. Chang. Fresh samples of fruiting bodies were collected from Ilan, in northern Taiwan.

2.2. Liquid culture of A. camphorata

A. camphorata was maintained on potato dextrose agar (PDA) slants and transferred to fresh medium at 3-week intervals. For each pasteurized Petri dish, 25 ml of PDA medium (39 g l^{-1}) was used. *A. camphorata* was inoculated at the center of Petri dishes which were then incubated at 28°C for 19 days. The fine mycelia of *A. camphorata* on the media surface were cut into pieces (approximately 1×1 cm) before transferring to 250-ml culture flasks containing 25 ml of potato dextrose broth (48 g l^{-1}) with 20 g l^{-1} glucose and pH 5.6. Polysaccharides were isolated from 26-day-old cultures. Following incubation, mycelia were rapidly washed with 1 l of 250 mM NaCl while aspirating to remove contaminating extracellular polysaccharides. Samples were then lyophilized and stored at 4°C. Growth media for solid and liquid cultures were purchased from Sigma Co. (St. Louis, MO, USA). LC grade organic solvents were purchased from E. Merck Co.

2.3. Isolation of polysaccharides

The lyophilized mycelia of *A. camphorata* were extracted with 80°C water in a 1:100 (w/w) ratio for 6 h. The extracts were cooled and 4 volumes of 95% ethanol were added, then allowed to precipitate overnight at 4°C. The precipitated polysaccharides were collected by centrifugation and lyophilized, resulting in a crude brownish polysaccharide sample.

2.4. High-performance anion-exchange chromatography (HPAEC) analysis of polysaccharides

Crude polysaccharides (200 μg) were separated by HPAEC (Dionex BioLC) equipped with a gradient pump, a pulsed amperometric detector (PAD-II) using a gold working electrode, and an anion-exchange column (Carbopac PA-100, 4.6×250 mm). Samples were applied using an autosampler (AS3500, SpectraSYSTEM®) via a microinjection valve with a 200-μl sample loop. Polysaccharide analysis was carried out in a linear gradient of 100–700 mM NaOAc in 90 mM NaOH for 90 min at ambient temperature. Data were collected and integrated on a PRIME DAK system (HPLC Technology, Ltd., UK).

2.5. Hydrolysis of polysaccharides

A series of experiments were conducted to determine the optimum acid concentration, i.e. a concentration sufficient to release the maximum amount of compounds but with minimal degradation and/or polycondensation. Comparable yields with 4 and 6 N HCl at 80°C were obtained. Hydrolysis was conducted on 1 mg of the crude polysaccharide sample with 6 N HCl in a heating block at 80°C for 6–8 h. The samples was cooled and the acid evaporated. The hydrolyzed polysaccharides were resuspended in Milli-Q water and filtered through a Millipore-GX nylon membrane prior to analysis.

2.6. General analytical methods

Total carbohydrate content was measured by the phenol-sulfuric acid method [14]. Total protein content was measured by the Bradford method [15]. Specific optical rotation was determined by an automated polarimeter (Jasco P1010) at 589 nm.

2.7. Compositional determination of the polysaccharides

The monosaccharide fractions of the polysaccharide hydrolysates were separated by HPAEC (Dionex BioLC) as mentioned above, with an anion-exchange column (Carbopac PA-10, 4.6×250 mm). The analysis of monosaccharides was carried out at an isocratic NaOH concentration of 18 mM at ambient temperature.

2.8. Anti-HBV test

Anti-viral analyses were performed as previously described [16]. Briefly, the HBV-producing cell line MS-G2 was plated onto 24-well flat-bottomed tissue culture plates at a density of 3×10^5 cells ml^{-1} well. After an overnight incubation to ensure that all cells were properly attached, the cells were challenged with the tested polysaccharides or with Interferon alfa-2a (Roche, Co., Mannheim, Germany) for comparison. Test samples were dissolved in autoclaved Milli-Q water at various concentrations (i.e. 10, 25, and 50 μg ml^{-1}). An additional set was treated with an equal volume of autoclaved Milli-Q water as a control. Subsequently, the cultures were collected at 3-day intervals and assayed for anti-viral activity. Anti-viral activities were assessed by analyses of anti-hepatitis B surface antigen (HBsAg) and anti-hepatitis B e antigen (HBeAg) values using an ELISA (enzyme-linked immunosorbent assay) kit (EverNew, Co., Taipei, Taiwan). The results were determined at 492 nm by a Power Wave× ELISA reader (Bio-Tek Instruments, Inc., USA). The inhibition percentage was calculated as $\%\text{inhibition} = (OD_{control} - OD_{sample})/OD_{control}$ and compared with the positive control group (α-interferon). The results from three replications were expressed as the mean ± standard error of the mean. Cell damage was tested using an AST (aspartate transaminase) kit (Fuji). AST values higher than 25 I.U. l^{-1} served as an indication of cell damage.

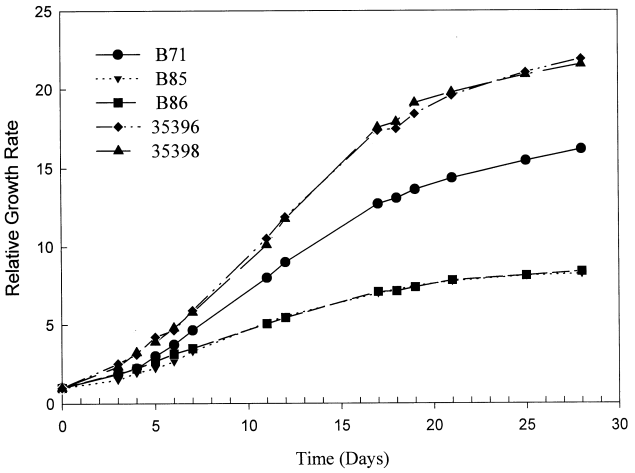

Fig. 1. Growth properties of five strains of *A. camphorata*.

3. Results and discussion

3.1. Growth-curve determination

The growth rate of *A. camphorata* mycelia was determined as the relative mass change (dry weight) over time (Fig. 1). Comparisons were made between five Taiwan strains. Strains 35396 and 35398 grew faster than the others. Generally, exponential phase was reached before 18 days of incubation.

3.2. Polysaccharide profiles of A. camphorata

Comparisons were made between polysaccharides isolated from the fruiting bodies of *A. camphorata* and cultured mycelium (Fig. 2). Polysaccharides were resolved in a linear gradient of 100–700 mM NaOAc in 90 mM NaOH for 90 min. The chromatograph was subdivided into three parts (I, II, III). Compounds located in part I were estimated to be small molecules. There were abundant polysaccharide species present in this range in strains B85, B86, and 35398. The intermediate-sized population of polysaccharides from the fruiting body (part II) contained numerous species. In the high molecular mass range (part III), several species of polysaccharides were present in the fruiting bodies but with low molarity. In cultured mycelia, two or three polysaccharide species were present in this range with greater amounts observed in strains B71 and 35398.

3.3. Physiochemical properties of polysaccharide of A. camphorata

Compositional analysis of the sugar moieties, and their

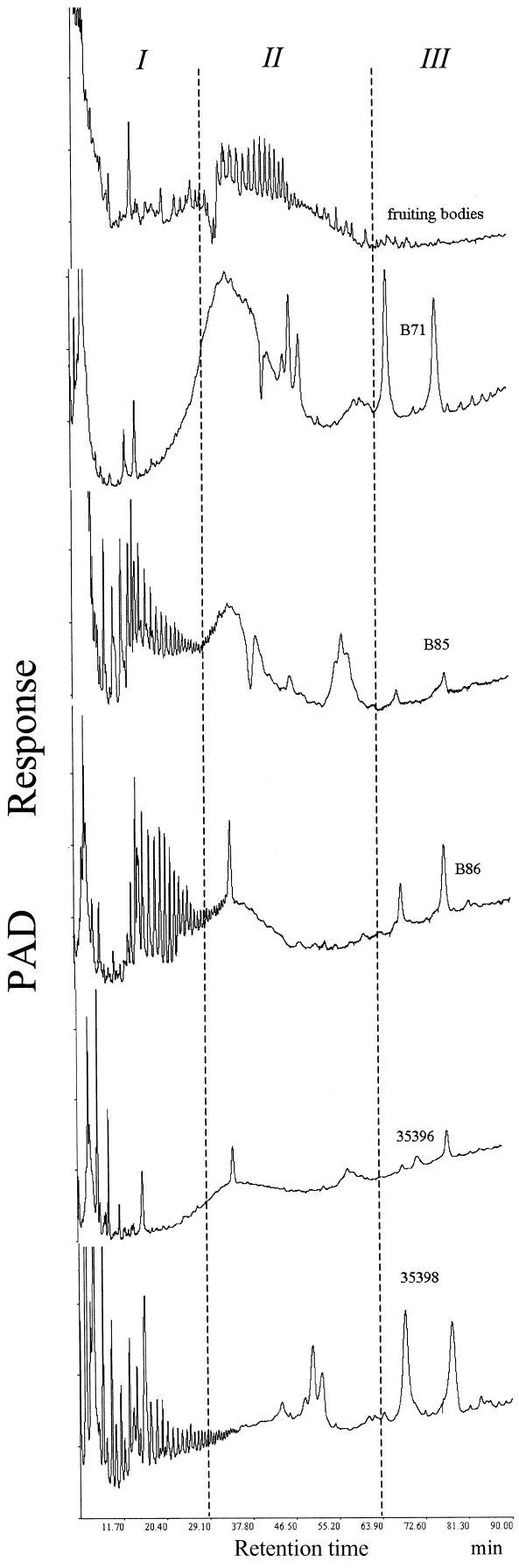

Fig. 2. Comparisons of polysaccharide profiles from fruiting bodies and from mycelium of different *A. camphorata* strains. The HPAEC analysis of polysaccharides was carried out in a linear gradient of 100–700 mM NaOAc in 90 mM NaOH for 90 min at ambient temperature.

Table 1
Characteristics of crude polysaccharide fractions isolated from *A. camphorata*

Strain	B71	B85	B86	35396	35398
Yield (%)	3.08	2.805	4.52	2.57	2.48
Total carbohydrate (mg g^{-1})	252	432	420	276	330
Protein (%)	49.8	33	44.4	42.6	45
Neutral sugars (μmol g^{-1})					
Myo-inositol	4.2	14.03	14.27	4.56	27.46
Sorbitol	0.68	4.66	5.1	1.08	10.47
Fucose	3.24	4.69	7.57	3.2	4.62
GalN	10.5	4.41	5.72	9.33	2.1
GlcN	26.64	0	0	21.23	28.545
Galactose	117.49	283.76	381.22	104	109.35
Glucose	146.74	35.6	63.9	137.32	209.56
Mannose	69.15	19.21	43.05	63.6	70.82
$[\alpha]_D$ (°)	30	151.8	67	29.2	19.2

A 26-day-old mycelium culture was harvested and used directly for polysaccharide extraction. The crude polysaccharide fractions were used for neutral sugar analysis. The amount of each neutral sugar is shown as μmol g^{-1}.

specific optical rotations are presented as means of at least two replicated extractions (Table 1). Yield and composition were species dependent. Of the five isolates, B85 and B86 had higher sugar contents than the others with total carbohydrate levels of 432 and 420 mg g^{-1} of crude polysaccharides respectively. Galactose, glucose, mannose, glucosamine and galactosamine were the major sugar components in the tested strains. However, glucosamine was absent in strains B85 and B86.

3.4. Anti-HBsAg and anti-HBeAg activities

The anti-HBV activities of polysaccharides from *A. camphorata* (B71, B85, B86, 35396, and 35398) were evaluated in MS-G2 cells. The anti-HBsAg inhibition percentage values for the treatments are presented in Fig. 3. Strains B71, B85, B86, 35396, and 35398 display different levels of anti-HBsAg effects. At 50 μg ml^{-1} the inhibition percentage was 42.6 ± 2.6, 34.7 ± 1.5, 51.6 ± 2.0, 32.2 ± 3.8, and 38.1 ± 4.1, respectively. B86 polysaccharides were the most effective with a slightly higher inhibition than that of α-interferon at a dosage of 1000 U ml^{-1} (50.4 ± 3.1). Polysaccharides from the other strains (B71, B85, 35396, and 35398) at 50 μg ml^{-1} were more effective than α-interferon at a dosage of 250 U ml^{-1}. Only B86 and 35398 showed substantial anti-HBeAg activities (Fig. 4). The anti-HBeAg inhibition percentage at 50 μg ml^{-1} concentration was 31.1 ± 6.0, and 31.6 ± 3.1 for B86 and 35398, respectively. Their effectiveness was lower than that of α-interferon at a dosage of 1000 U ml^{-1} (46.0 ± 2.9), but higher than that of α-interferon at a dosage of 250 U ml^{-1} (21.2 ± 2.3). No cytotoxic effects were observed for any of the treatments, as all AST values were lower than 25 I.U. l^{-1} even at the maximum dosage of 50 μg ml^{-1} (data not shown).

This study is the first report on the structural character-

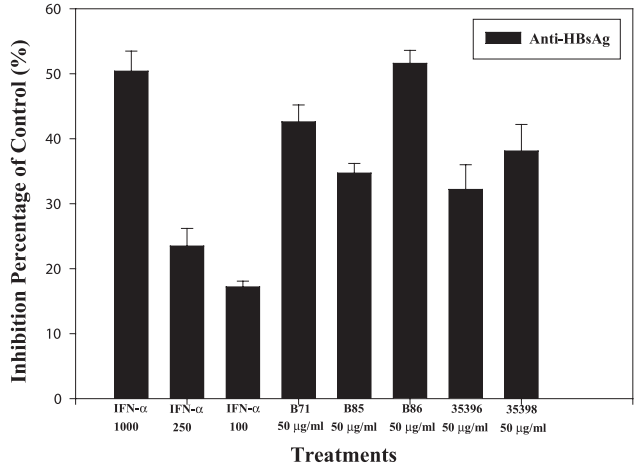

Fig. 3. Anti-HBsAg effect of α-interferon and polysaccharides isolated from cultured mycelia from five *A. camphorata* strains. Inhibition of viral multiplication as a percentage of the control was calculated as %inhibition = $(OD_{control} - OD_{sample})/OD_{control}$.

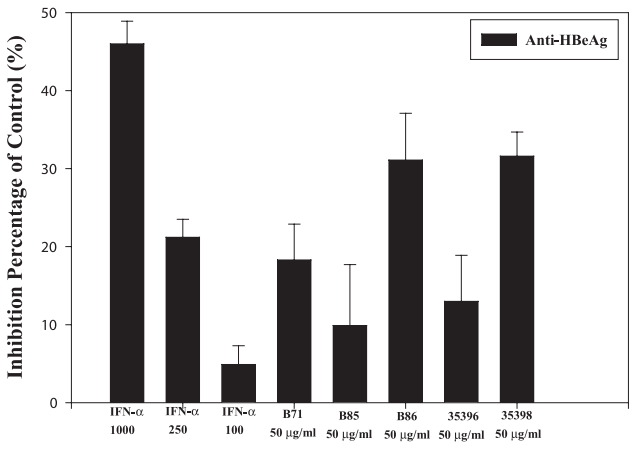

Fig. 4. Anti-HBeAg effect of α-interferon and polysaccharides isolated from cultured mycelia from five *A. camphorata* strains. %inhibition = $(OD_{control} - OD_{sample})/OD_{control}$.

ization of polysaccharides in the genus of *Antrodia*. Polysaccharide profiles obtained from different strains of *A. camphorata* were found to exhibit polymorphisms. Investigations on biologically active components of cultured *A. camphorata* mycelia have shown that the mushroom polysaccharides have anti-HBV activity. Anti-HBV activity has not been reported for polysaccharides from any other mushroom. Therefore, further studies on the relationship between specific polysaccharide fractions and their biological activities are necessary, and are in progress by our group.

Acknowledgements

The authors would like to thank Dr. Shui-Tein Chen, Institute of Biochemistry, Academia Sinica, Taiwan, and Dr. Chen-J. Chou, National Research Institute of Chinese Medicine, Taipei, for providing *A. camphorata* strains and the fruiting body collection. We also wish to thank Dr. Tsung-Che Tseng, Institute of Botany, Academia Sinica, for his constructive comment during the course of work. We thank Dr. Charles Papa, Institute of Botany, Academia Sinica, for critical reading of the manuscript.

References

[1] Wu, S.H., Ryvarden, L. and Chang, T.T. (1997) *Antrodia camphorata* ('niu-chang-chih'), new combination of a medicinal fungus in Taiwan. Bot. Bull. Acad. Sin. 38, 273–275.

[2] Cherng, I.W., Wu, D.P. and Chiang, H.C. (1996) Triterpenoids from *Antrodia cinnamomea*. Phytochemistry 41, 263–267.

[3] Yang, S.W., Shen, Y.C. and Chen, C.H. (1996) Steroids and triterpenoids of *Antrodia cinnamomea* – a fungus parasitic on *Cinnamomum micranthum*. Phytochemistry 41, 1389–1392.

[4] Chiang, H.C., Wu, D.P., Cherng, I.W. and Ueng, C.H. (1995) A sesquiterpene lactone, phenyl and biphenyl compounds from *Antrodia cinnamomea*. Phytochemistry 39, 613–616.

[5] Cherng, I.H. and Chiang, H.C. (1995) Three new triterpenoids from *Antrodia cinnamomea*. J. Nat. Prod. 58, 365–371.

[6] Chen, C.H. and Yang, S.W. (1995) New steroid acids from *Antrodia cinnamomea*, a fungal parasite of *Cinnamomum micranthum*. J. Nat. Prod. 58, 1655–1661.

[7] Moers, M.E.C., Jones, D.M., Eakin, P.A., Fallick, A.E., Grifths, H. and Larter, S.R. (1993) Carbohydrate diagenesis in hypersaline environments: application of GC-IRMS to the stable isotope analysis of derivatized saccharides from surficial and buried sediments. Org. Geochem. 20, 927–933.

[8] Dogasaki, C., Murakami, H., Nishijima, M., Ohno, N., Yadomae, T. and Miyazaki, T. (1994) Biological activity and structural characterization of alkaline-soluble polysaccharides from the kernels of *Prunus mume* Sieb. *et* Zacc. Biol. Pharm. Bull. 17, 386–390.

[9] Zhang, J., Wang, G., Li, H., Zhuang, C., Mizuno, T., Ito, H., Mayuzumi, H., Okamoto, H. and Li, J. (1994) Antitumor active protein-containing glycans from the chinese mushroom Songshan Lingzhi, *Ganoderma tsugae* mycelium. Biosci. Biotech. Biochem. 58, 1202–1205.

[10] Sasaki, T. and Takasuka, N. (1976) Further study of the structure of lentinan, an anti-tumor polysaccharide from *Lentinus edodes*. Carbohydr. Res. 47, 99–104.

[11] Tabata, K., Ito, W., Kojima, T., Kawabata, S. and Misaki, A. (1981) Ultrasonic degradation of schizophyllan, an antitumor polysaccharide produced by *Schizophyllum commune* Fries. Carbohydr. Res. 89, 121–135.

[12] Hardy, M.R., Townsend, R.R. and Lee, Y.C. (1998) Monosaccharide analysis of glycoconjugates by anion exchange chromatography with pulsed amperometric detection. Anal. Biochem. 170, 54–62.

[13] Chang, T.T. and Chou, W.N. (1995) *Antrodia cinnamomea* sp. nov. on *Cinnamomum kanehirai* in Taiwan. Mycol. Res. 99, 756–758.

[14] Dubois, M., Gilles, K., Hamilton, J., Rebers, P. and Smith, F. (1956) Colorimetric method for determination of sugars and related substances. Anal. Chem. 28, 350–356.

[15] Bradford, M. (1976) A rapid and sensitive method for the quantitation of microgram quantities of protein utilizing the principle of protein-dye binding. Anal. Biochem. 72, 248–254.

[16] Huang, R.L., Chen, C.C., Huang, H.L., Chang, C.G., Chen, C.F., Chang, C.M. and Hsieh, M.T. (2000) Anti-hepatitis B virus effects of wogonin isolated from *Scutellaria baicalensis*. Planta Med. 66, 687–784.

Journal of Ethnopharmacology 148 (2013) 254–265

Contents lists available at SciVerse ScienceDirect

Journal of Ethnopharmacology

journal homepage: www.elsevier.com/locate/jep

The anti-cancer activity of *Antrodia camphorata* against human ovarian carcinoma (SKOV-3) cells via modulation of HER-2/*neu* signaling pathway

Hsin-Ling Yang [a], Kai-Yuan Lin [b], Ying-Chen Juan [a], K.J. Senthil Kumar [e], Tzong-Der Way [c], Pei-Chun Shen [a], Ssu-Ching Chen [d], You-Cheng Hseu [e,*]

[a] Institute of Nutrition, China Medical University, Taichung, Taiwan
[b] Department of Medical Research, Chi-Mei Medical Center, Tainan, Taiwan
[c] Department of Life Sciences, China Medical University, Taichung, Taiwan
[d] Department of Life Sciences, National Central University, Chung Li, Taiwan
[e] Department of Cosmeceutics, College of Pharmacy, China Medical University, Taichung, Taiwan

ARTICLE INFO

Article history:
Received 21 December 2012
Received in revised form
9 March 2013
Accepted 8 April 2013
Available online 22 April 2013

Keywords:
Antrodia camphorate
HER-2/*neu*
Ovarian cancer
ROS
G_2/M arrest
Apoptosis

ABSTRACT

Ethnopharmacological relevance: *Antrodia camphorata* (AC) is well known in Taiwan as a traditional Chinese medicinal fungus. However, the anticancer activity of AC against human HER-2/*neu*-over-expressing ovarian cancers is poorly understood.

Materials and methods: The aim of this study is to investigate whether a submerged fermentation culture of AC can inhibit human ovarian carcinoma cell (SKOV-3) proliferation by suppressing the HER-2/*neu* signaling pathway. Cell viability, colony formation, DCFH-DA fluorescence microscopy, western blotting, HER-2/*neu* immunofluorescence imaging, flow cytometry, and TUNEL assays were carried out to determine the anti-cancer effects of AC.

Results: MTT and colony formation assays showed that AC induced a dose-dependent reduction in SKOV-3 cell growth. Immunoblot analysis demonstrated that HER-2/*neu* activity and tyrosine phosphorylation were significantly inhibited by AC. Furthermore, AC treatment significantly inhibited the activation of PI3K/Akt and their downstream effector β-catenin. We also observed that AC caused G_2/M arrest mediated by down-regulation of cyclin D1, cyclin A, cyclin B1, and Cdk1 and increased p27 expression. Notably, AC induced apoptosis, which was associated with DNA fragmentation, cytochrome *c* release, caspase-9/-3 activation, PARP degradation, and Bcl-2/Bax dysregulation. An increase in intracellular reactive oxygen species (ROS) was observed in AC-treated cells, whereas the antioxidant *N*-acetylcysteine (NAC) prevented AC-induced cell death, HER-2/*neu* depletion, PI3K/Akt inactivation, and Bcl-2/Bax dysregulation, indicating that AC-induced cell death was mediated by ROS generation.

Conclusions: These results suggest that AC may exert anti-tumor activity against human ovarian carcinoma by suppressing HER-2/*neu* signaling pathways.

1. Introduction

Ovarian cancer is the fifth most common cancer among women worldwide and is the leading cause of death among gynecologic malignancies (Gari et al., 2006). Ovarian cancer predominantly affects elderly and middle-aged women, and its greatest incidences are reported in North America and Northern Europe (Makar, 2000). However, ovarian cancer has a low incidence in Asia, Africa, and Latin America (Stewart, 2012). Ovarian Cancer (OC) incidence rates from 1984 to 2006 is due to development of better diagnostic techniques and equipment (Chiang et al., 2010). The incidence of ovarian cancer increases with age; it is relatively rare in women younger than 30 years, although with increased modernization and urbanization, the rates appear to be increasing (Makar, 2000). Although scientific advancements have increased ovarian cancer survival rates, much research is still needed. Approximately and 25–80% of ovarian cancers express estrogen receptor (ER). However, the expression pattern may vary with cell types (Kalli et al., 2004). The current treatment of ER-positive tumors primarily relies on surgery to remove gross tumors, followed by treatment with anti-cancer agents that target the hormone dependence of these tumors, including aromatase inhibitors and anti-estrogens such as tamoxifen (Ao et al., 2011). However, anti-hormonal therapy is rarely used to treat epithelial

* Corresponding author. Tel.: +886 4 22053366x5308; fax: +886 4 2207 808.
E-mail address: ychseu@mail.cmu.edu.tw (Y.-C. Hseu).

0378-8741/$ - see front matter © 2013 Elsevier Ireland Ltd. All rights reserved.
http://dx.doi.org/10.1016/j.jep.2013.04.023

ovarian cancers, but it is more often used to treat ovarian stromal tumors (Berek et al., 2000). Many women with ovarian cancer undergo anti-hormonal therapy that terminate ovarian function, resulting uncomfortable signs and symptoms, such as hot flashes, joint and muscular pain, bone thinning, and osteoporosis (Hervik and Mjaland, 2012). Therefore, the treatment of epithelial ovarian cancer still required non-side effect hormonal or chemotherapeutic agents.

Human epidermal growth factor receptor-2 (HER-2/*neu*) is one of the most widely studied putative biological prognostic factors in human epithelial ovarian cancers de Graeff et al. (2009). HER-2/*neu*, a proto-oncoprotein, belongs to the epidermal growth factor (EGFR) family, which consists of four receptors: EGFR (HER-1/ErbB1), HER-2 (ErbB2), HER-3 (ErbB3), and HER-4 (ErbB) (Jiang et al., 2012). Since HER-2/*neu* overexpression is limited to 20–30% of many human cancers, including ovarian, breast, lung and gastric cancers, conflicting epidemiological data may reflect differing proportion of HER-2/*neu* positive cancers in the various studies (Aigner et al., 2000; Howe et al., 2001). HER-2/*neu* expression is associated with increased metastatic potential and angiogenesis, suggesting that the enhanced tyrosine kinase activity of HER-2/*neu* may play a critical role in the initiation, progression, and outcome of human ovarian cancers (Hsieh et al., 2004). Therefore, targeting HER-2/*neu* has been the main focus of ovarian cancer treatment, and the inhibition of HER-2/*neu* has become an increasingly important therapeutic target for HER-2/*neu*-overexpressing ovarian cancers.

Antrodia camphorata (AC) is a native Taiwanese medicinal mushroom that is popularly known as “Niu Cheng Zhi” in Taiwan and grows in the inner sap of the tree *Cinnamomum kanehira* Hay (*Lauraceae*) (Hseu et al., 2002). AC has been used in traditional Chinese medicine for the treatment of food poisoning, drug intoxication, diarrhea, abdominal pain, hypertension, skin irritation and cancer (Yang et al., 2012). This medicinal mushroom is starting to attract interest because it possesses a number of bioactive components, including triterpenoids, polysaccharides, maleic/succinic acid derivatives, benzenoids and benzoquinone derivatives (Hseu et al., 2002; Ao et al., 2009; Yang et al., 2012). There is increasing evidence that AC possesses an extensive range of biological activities, including antioxidant, anti-inflammatory, hepatoprotective, anti-metastasis, anti-hypertensive, anti-hyperlipidemic, immunomodulatory and anti-cancer properties (Hseu et al., 2002; Ao et al., 2009; Lee et al., 2012; Yang et al., 2012). AC has low toxicity and is a non-mutagenic mushroom that efficiently reduces the tumorigenicity of various cancers in vitro and in vivo. However, the anticancer activity of AC against human HER-2/*neu*-overexpressing ovarian cancers is poorly understood.

In this study, we investigated the effectiveness of the fermented broth of AC harvested from submerged cultures against HER-2/*neu*-overexpressing human epithelial ovarian cancer (SKOV-3) cells. We demonstrated that AC induced growth inhibition, cell-cycle arrest, and apoptotic induction of HER-2/*neu*-overexpressing SKOV-3 cells through intracellular ROS generation, suppression of the HER-2/*neu* signaling cascade, and disruption of the PI3K/Akt signaling pathway.

2. Materials and methods

2.1. Reagents

Dulbecco's Modified Eagle's medium (DMEM), nutrient mixture F-12, fetal bovine serum (FBS), glutamine and penicillin/streptomycin were obtained from GIBCO BRL (Grand Island, NY). 3-(4,5-Dimethylthiazol-2-yl)-2,5-diphenyltetrazolium bromide (MTT), *N*-acetylcysteine (NAC), *p*-iodonitrotetrazolium violet, and fluorescein isothiocyanate (FITC) were purchased from Sigma-Aldrich Chemical Co. (St. Louis, MO). Antibodies against phospho-tyrosine, p27, Cdk1, Cdk2, cytochrome *c*, Bcl-2, Bax, PARP, cyclin A, cyclin B1, Cdc25C, and β-actin were purchased from Santa Cruz Biotechnology, Inc. (Heidelberg, Germany). Antibodies against HER-2/*neu*, phospho-PI3K, PI3K, phospho-Akt, Akt, β-catenin, caspase-9, caspase-3, cyclin D1, Cdk4, phospho-p38MAPK, p38MAPK, phospho-ERK, ERK, phospho-JNK, and JNK were obtained from Cell Signaling Technology, Inc. (Danvers, MA). Anti-phospho-HER-2/*neu* (Tyr1248) antibody was purchased from Millipore Corporation, Billerica, MA. 4′,6-Diamidino-2-phenylindole dihydrochloride (DAPI) was purchased from Calbiochem (La Jolla, CA). All other chemicals were reagent grade or HPLC grade and were supplied by either Merck & Co., Inc. (Darmstadt, Germany) or by Sigma-Aldrich.

2.2. Preparation of the fermented culture broth of AC from submerged cultures

The AC culture was inoculated onto potato dextrose agar and incubated at 30 °C for 15–20 days. The whole colony was subsequently added to a flask containing 50 mL sterile water. After homogenization, the fragmented mycelial suspension was used as an inoculum. The seed culture was prepared in a 20-L fermenter (BioTop Process & Eqipment, Taiwan) agitated at 150 rpm with an aeration rate of 0.2 vvm at 30 °C. A five-day culture of 15 L mycelium inoculum was inoculated into a 250 L agitated fermenter (BioTop). The fermentation conditions were the same as those used for the seed fermentation, but the aeration rate was 0.075 vvm. The fermentation product was harvested at hour 331 and poured through a non-woven fabric on a 20-mesh sieve to separate the deep-red fermented culture broth and the mycelia; the culture broth was then centrifuged at 3000*g* for 10 min followed by passage through a 0.22-μm filter. The culture broth was concentrated under vacuum and freeze-dried to a powder. The yield of dry matter from the culture broth was 18.4 g/L. The experiments were performed with 2–4 different batches of AC fermented culture (Hseu et al., 2010). To prepare the stock solution, the powder samples were solubilized with DMEM containing 1% FBS (pH 7.4). The stock solution (1.6 mg/mL) was stored at −20 °C before its anticancer properties were evaluated. We refer to the fermented culture broth of *Antrodia camphorata* as AC throughout the manuscript.

2.3. Cell culture and sample treatments

HER-2/*neu*-overexpressing human ovarian cancer cells (SKOV-3) were obtained from the American Type Culture Collection (ATCC, Manassas, VA) and human ovarian surface epithelial (IOSE) cells were kindly provided by Dr Michael Chan, National Chung Cheng University, Taiwan, and cultured in DMEM/F-12 supplemented with 10% heat-inactivated FBS, 2 mM glutamine and 1% penicillin-streptomycin-neomycin at 37 °C in a humidified incubator with 5% CO_2. Cultures were harvested and monitored for changes in cell number by counting cell suspensions using a hemocytometer with a phase contrast microscope. Cells were treated with 40–240 μg/mL of AC for 30 min-72 h, the incubation time varied depending on the assay. In additional experiments, cells were pretreated with 2.5 mM of NAC for 1 h followed by incubation with or without the indicated concentration of AC.

2.4. Cell viability assay

Cell viability was monitored by the colorimetric MTT assay. Briefly, SKOV-3 or IOSE cells (2.5×10^5 or 1×10^5 cells/well in a 24-well plate) were treated with AC (40–240 μg/mL) for 24 h. Then,

0.5 mg/mL MTT in phosphate-buffered saline (PBS, 400 μL) was added to each well and incubated at 37 °C for 4 h. The MTT-generated violet formazan crystals were dissolved in 10% SDS (400 μL/well), and the absorbance was measured at 570 nm (A_{570}). Cell viability was calculated as (A_{570} of treated cells/A_{570} of untreated cells) × 100%.

2.5. Colony formation assay

Anchorage-independent growth was determined by colony formation in soft agar (Koleske et al., 1995). The assay was performed in 6-well plates (1×10^4 cells/well) with a base layer containing 0.5% agar in DMEM containing 10% FBS, 1 mM glutamine, 100 units penicillin and 100 μg/mL streptomycin. This layer was overlaid with a second layer of 1 mL 0.35% agar (in DMEM containing 10% FBS, 1 mM glutamine, 100 units of penicillin and 100 μg of streptomycin) with a suspension of 1×10^4 cells/well. Fresh medium with AC (40–240 μg/mL) was then added to the plates every 72 h. The plates were incubated at 37 °C for 3 weeks, and the tumor colonies were analyzed with a microscope. Colonies with a diameter greater than 200 μm were counted.

2.6. Measurement of ROS generation

Intracellular ROS generation was detected by fluorescence microscopy with 2′,7′-dihydrofluorescein-diacetate (DCFH-DA) as described previously (Lee et al., 2012). Briefly, SKOV-3 cells at a density of 1×10^5 cells/12 wells were cultured in DMEM/F-12 supplemented with 10% FBS. To evaluate the generation of ROS over time, cells were treated with 160 μg/mL of AC for 0, 1, 5, 10 or 15 min. The cells were then incubated with 10 μM DCFH-DA in culture medium at 37 °C for 30 min. The acetate groups on DCFH-DA were removed by an intracellular esterase, trapping the probe inside the cells. After loading, the cells were washed with warm PBS buffer. The production of ROS was measured by the change in fluorescence due to the intracellular accumulation of dichlorofluorescein (DCF) caused by oxidation of DCFH. Intracellular ROS, as indicated by DCF fluorescence, was measured by fluorescence microscopy (Olympus 1 × 71 at 200 × magnification).

2.7. Fluorescence imaging of HER-2/neu

SKOV-3 cells at a density of 2×10^4 cells/well were cultured in DMEM/F-12 medium supplemented with 10% FBS in glass eight-well Tek chambers (Nunc, Denmark). After AC treatment for 24 h, the culture medium was removed, and the cells were washed with PBS, fixed in 2% paraformaldehyde for 15 min, permeabilized with 0.1% Triton X-100 for 10 min, washed, blocked with 10% FBS in PBS, and incubated for 2 h with an anti-HER-2/*neu* primary antibody in 1.5% FBS. The cells were subsequently incubated with a FITC-conjugated secondary antibody for 1 h in 6% bovine serum albumin (BSA) followed by nucleus staining with 1 μg/mL DAPI for 5 min. The stained cells were washed with PBS and visualized using a fluorescence microscope at 400 × magnification.

2.8. Cell-cycle analysis

Cellular DNA content was determined by flow cytometric analysis with propidium iodide (PI)-labeled cells as previously described (Hseu et al., 2012). Cells were seeded at a density of 1.5×10^6 cells/10 cm dish and incubated overnight. The synchronization of the cell cycle was achieved using a double thymidine block. Briefly, cells were treated with 3 mM thymidine in DMEM containing 10% FBS for 16 h. After treatment, the cells were washed twice with PBS and cultured in fresh medium for another 10 h. The cells were then blocked with DMEM containing 3 mM thymidine for 16 h. Cell-cycle-synchronized cells were washed with PBS and re-stimulated to enter the G_1 phase together by addition of fresh DMEM containing AC (160 μg/mL). The cells were harvested at 6, 12, or 18 h by trypsinization and then fixed in 3 mL of ice-cold 70% ethanol at −20 °C overnight. Cell pellets were collected by centrifugation, re-suspended in 500 μL of PI staining buffer (1% Triton X-100, 0.5 mg/mL RNase A and 4 μg/mL PI in PBS) and incubated at room temperature for 30 min. The cell-cycle progression was detected on a FACScan cytometer (BD Biosciences, San Jose, CA) equipped with a single argon ion laser (488 nm). The forward and right-angle light-scattering, which correlate with cell size and cytoplasmic complexity, respectively, were used to establish size gates and exclude cellular debris from the analysis. The DNA content of 1×10^4 cells/analysis was monitored using the BD FACSCalibur system. The cell-cycle profiles were analyzed with ModFit software (Verity Software House, Topsham, ME).

2.9. Quantification of apoptosis

Apoptotic cell death was measured using terminal deoxynucleotidyl transferase-mediated dUTP-fluorescein nick end labeling (TUNEL) with a fragmented DNA detection kit (Roche, Mannheim, Germany). SKOV-3 cells (2×10^4 cells/well) were seeded in DMEM/F-12 medium with 10% FBS in glass eight-well Tek chambers and treated with various concentrations of AC (40–240 μg/mL) for 24 h. After AC treatment, cells were washed with PBS twice, fixed in 2% paraformaldehyde for 30 min and permeabilized with 0.1% Triton X-100 for 30 min at room temperature. The cells were then incubated with TUNEL reaction buffer in a 37 °C humidified chamber for 1 h in the dark, rinsed twice with PBS and incubated with DAPI (1 mg/mL) at 37 °C for 5 min; stained cells were visualized by fluorescence microscopy (200 × magnification).

2.10. Western blot analysis

SKOV-3 cells at a density of 1.5×10^6 cells/10 cm dish were incubated with various concentrations of AC (40–240 μg/mL) for 24 h. After incubation, the cells were washed once in PBS, detached, pooled and centrifuged at 1500 × *g* for 5 min. The cell pellets were subsequently suspended in 100 μL lysis buffer containing 10 mM Tris-HCl, pH 8.0, 320 mM sucrose, 1% Triton X-100, 5 mM EDTA, 2 mM dithiothreitol and 1 mM phenylmethylsulfonyl fluoride. The suspensions were sonicated and kept on ice for 20 min, then centrifuged at 15,000*g* for 30 min at 4 °C. Total protein content was determined by Bio-Rad protein assay reagent (Bio-Rad, Hercules, CA) using BSA as a standard. Protein extracts were reconstituted in sample buffer (62 mM Tris–HCl, 2% SDS, 10% glycerol, 5% β-mercaptoethanol), and the mixture was boiled at 97 °C for 5 min. Equal amounts (50 μg) of denatured protein samples were loaded into each lane, separated by SDS-PAGE in an 8–15% polyacrylamide gel and transferred onto polyvinylidene difluoride (PVDF) membranes overnight. The membranes were blocked with 5% non-fat dried milk in PBS containing 1% Tween-20 for 1 h at room temperature, subsequently incubated with primary antibodies overnight, and further incubated with horseradish peroxidase-conjugated goat anti-rabbit or anti-mouse antibodies for 2 h. Blots were visualized on an ImageQuant™ LAS 4000 mini (Fujifilm) system with SuperSignal West Pico chemiluminescence substrate (Thermo Scientific, IL).

2.11. Statistical analysis

The results are presented as the mean ± standard deviation (mean ± SD). All data were analyzed using analysis of variance followed by Dunnett's test for pair-wise comparison. An asterisk

indicates that the experimental values were significantly different from those of the control (*$P < 0.05$).

3. Results

3.1. AC treatment inhibits proliferation and tumorigenic ability of ovarian cancer SKOV-3 cells

To evaluate the biological activity of AC in terms of cell viability and proliferation, cells were treated with various concentrations of AC (40–240 μg/mL) for 24 h. MTT assay detected a significant reduction in cell viability after exposure to AC for 24 h. The cell viability was reduced into 97%, 83%, 58%, and 42% by 40, 80, 160, and 240 μg/mL, respectively, as determined by MTT assay, with an IC_{50} value of 196 μg/mL (Fig. 1A). In addition, the normal human ovarian surface epithelial (IOSE) cells were exposed to AC (40–240 μg/mL) for 24 h, showed more than 80% of cell survival (Fig. 1B). These results confirm that AC treatment targets only the malignant calls. The level of colony formation ability of untreated ovarian cancer cells was directly proportional to the aggressive potential of the specific cell line (Nair et al., 2004). We next evaluated the ability of SKOV-3 cells to form colonies on 6-well culture plates in the presence or absence of AC for 3 weeks and observed their growth in soft agar. The aggressive human ovarian cancer SKOV-3 cells produced many colonies (Fig. 1C), whereas colony numbers were significantly ($P < 0.05$) suppressed to 82 ± 7%, 50 ± 4%, 27 ± 6%, and 7 ± 1% by 40, 80, 160, and 240 μg/mL, respectively (Fig. 1C). At the highest concentration of AC (240 μg/mL), colony formation was reduced by over 90% compared to the untreated control cells (Fig. 1C). Reductions in colony number were accompanied by reductions in colony size in SKOV-3 cells. These data suggest that the treatment of HER-2/*neu*-overexpressing ovarian cancer cells with AC decreases their rate of proliferation and tumorigenic ability.

3.2. AC-induced cell death is mediated by intracellular ROS generation in SKOV-3 cells

We have previously reported that AC treatment induces ROS generation in human breast cancer cells (MCF-7, MDA-MB-453, and BT474), which is proposed to be one of the early events in the activation of apoptotic signaling (Yang et al., 2006; Lee et al., 2012). In this study, we also examined the involvement of AC in ROS generation in SKOV-3 cells. Fluorescence microscopy with DCFH-DA as a fluorescent probe was performed to estimate the intracellular ROS accumulation in SKOV-3 cells. Incubation of cells with AC (160 μg/mL for 0, 1, 5, 10, or 15 min) caused a significant increase in fluorescence, and the maximum level of ROS accumulation ($p < 0.05$) was observed at 5 min after AC treatment (Fig. 2A). To further confirm that AC treatment induced ROS generation, SKOV-3 cells were pre-incubated with or without NAC (2.5 mM), a scavenger of ROS for 1 h and then treated with AC (160 μg/mL) for 5 min. As shown in Fig. 2B, exposure of SKOV-3 cells to AC (160 μg/mL) led to a 5.3-fold increase in the ROS generation compared with control cells, whereas NAC pretreatment significantly ($p < 0.05$) inhibited the increase in ROS generation, reducing ROS to the control level (Fig. 2B). To further demonstrate that AC-induced cell death is mediated by ROS generation, SKOV-3 cells were preincubated with NAC for 1 h and treated with or without AC (160 μg/mL) for 24 h. Cell viability was measured using MTT assay. As expected, NAC pretreatment significantly ($p < 0.05$) prevented AC-induced cell death in SKOV-3 cells (Fig. 2C), which was concomitant with the inhibition of AC-induced ROS generation in SKOV-3 cells.

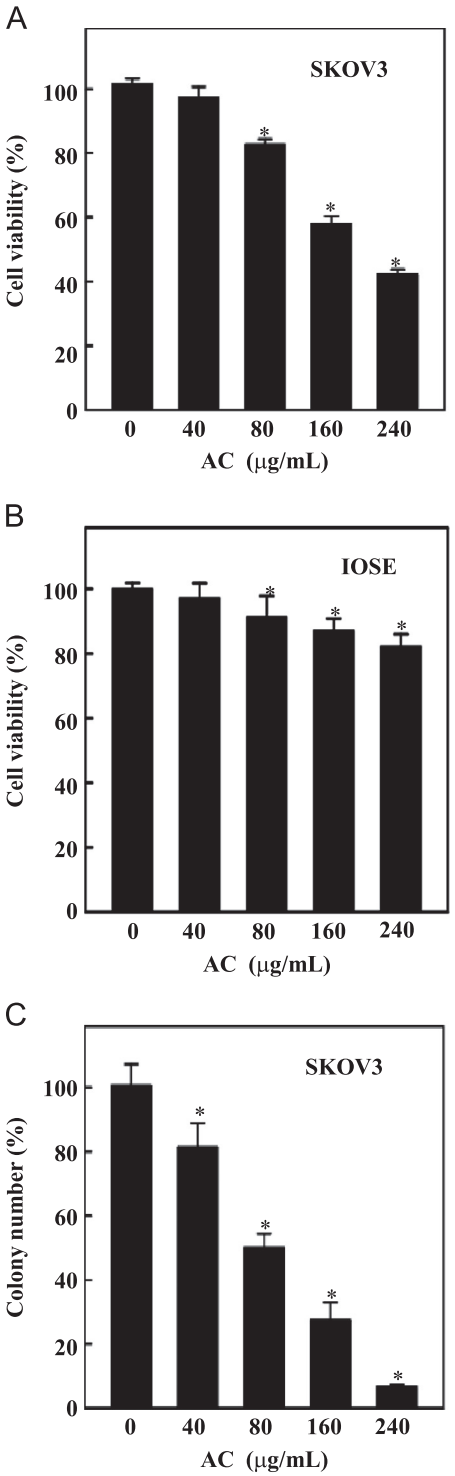

Fig. 1. AC inhibits cell proliferation and anchorage-independent growth of human ovarian cancer (SKOV-3) cell lines. After incubation with various concentrations of AC (40–240 μg/mL) for 24 h, cell viability of SKOV-3 (A) and Human ovarian surface epithelial (IOSE) cells (B) was examined by MTT assay. The number of viable cells after treatment is expressed as a percentage of the vehicle-only control, which was assigned as 100%. (C) Cells were assayed for their ability to proliferate and form colonies in soft agar. SKOV-3 cells were seeded onto 6-well plates in culture medium containing 0.35% low-melting agarose over a 0.7% agarose layer in the presence or absence of AC (40–240 μg/mL) or vehicle control (PBS) and incubated for 3 weeks at 37 °C. The numbers of colonies >200 μm in size were counted (at 40× magnification). Colonies were subsequently stained with *p*-iodonitrotetrazolium violet (1 mg/mL), and colonies larger than 200 μm were counted. The percentage of colony formation was calculated by defining the number of colonies in the absence of AC as 100%. The results are presented as the mean ± SD of three independent assays. * Significant difference in comparison to the control group ($p < 0.05$).

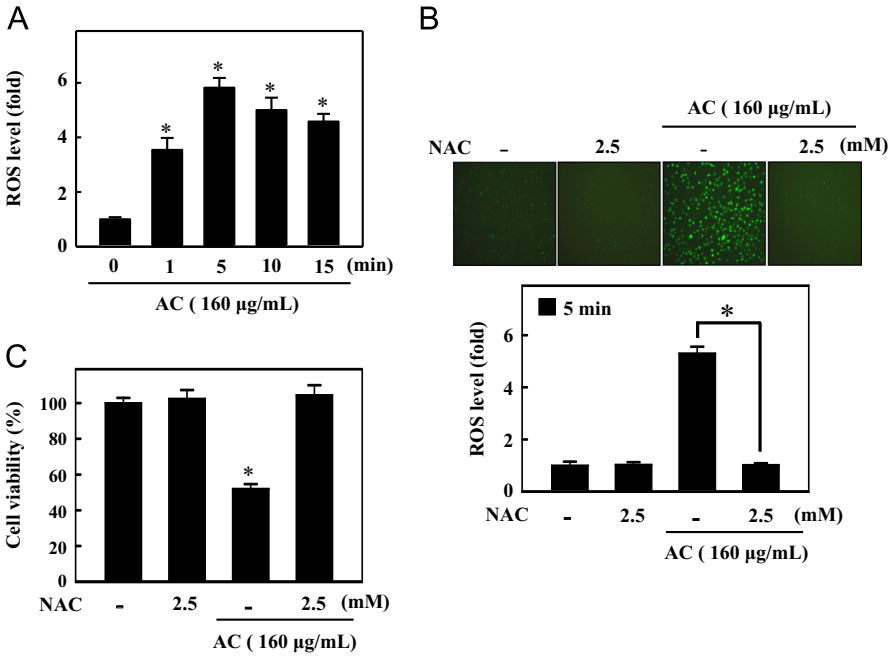

Fig. 2. AC-induced ROS generation and its involvement in cell death. (A) SKOV-3 cells were treated with AC (160 μg/mL) for 0, 1, 5, 10 or 15 min. The non-fluorescent, cell membrane-permeable probe DCFH-DA was added to the culture medium at a final concentration of 10 μM for 30 min before the end of each experiment. DCFH-DA penetrated the cells, reacted with cellular ROS and was metabolized into fluorescent DCF, as indicated by DCF fluorescence, which was measured by fluorescence microscopy (200 × magnification). The intracellular ROS level is expressed graphically as the relative fold increase over the control. (B) The antioxidant *N*-acetylcysteine (NAC) prevents AC-induced cell death in SKOV-3 cells. Cells were pretreated with 2.5 mM NAC for 1 h followed by treatment without or with AC (160 μg/mL) and quantification of ROS after 5 min. (C) NAC prevents AC-induced cell death in SKOV-3 cells. Cells were pretreated with 2.5 mM NAC for 1 h followed by treatment without or with AC (160 μg/mL) and quantification of cell viability after 24 h. The photomicrographs shown in this figure are from one representative experiment that was performed in triplicate. Each value is expressed as the mean ± SD ($n=3$). * Significant difference in comparison to the control group ($p < 0.05$).

3.3. AC treatment modulates HER-2/neu protein expression by inhibiting its tyrosine phosphorylation

Activation of the HER-2/*neu* leads to autophosphorylation of the C-terminal tyrosines of the receptor and the recruitment to these sites of cytoplasmic signal transducers that regulate cellular processes, such as proliferation, inhibition of apoptosis and transformation (Olayioye, 2001). We first examined whether AC treatment altered HER-2/*neu* tyrosine kinase activity in SKOV-3 cells. The active/inactive status of the main autophosphorylation site of HER-2/*neu* (Tyr1248) was semi-quantified by Western blot analysis using a specific anti-phospho HER-2/*neu* (Tyr1248) antibody. As shown in Fig. 3A, basal tyrosine kinase activity was observed in untreated control cells, whereas treatment of SKOV-3 cells with AC significantly decreased HER-2/*neu* tyrosine kinase activity in a dose- and time-dependent manner. We also observed that exposure of SKOV-3 cells to AC not only reduced HER-2/*neu* tyrosine kinase activity but further reduced the cellular content of HER-2/*neu* protein itself. The sustained reduction in HER-2/*neu* protein expression by AC was dose- and time-dependent (Fig. 3A). Taken together, these findings indicate that AC reduces the basal tyrosine kinase phosphorylation and the activation of HER-2/*neu* receptors in HER-2/*neu*-overexpressing ovarian cancer cells. To further confirm the reduction in HER-2/*neu* protein level by AC treatment, the immunofluorescence images of HER-2/*neu* expression were examined. Representative images of untreated SKOV-3 cells compared with cells treated with AC are shown in Fig. 3B. AC-treated cells exhibited lower levels of immunofluorescence at the plasma membrane, and fluorescence was replaced by diffuse cytoplasmic punctate staining. AC caused a significant reduction ($p < 0.05$) and localization of membrane-bound HER-2/*neu* in SKOV-3 cells in a dose-dependent manner (Fig. 3B).

To further delineate the link between AC-induced ROS generation and HER-2/*neu* activation, SKOV-3 cells were preincubated with NAC for 1 h and treated with or without AC (160 μg/mL) for 24 h. The levels of tyrosine kinase phosphorylation and total HER-2/*neu* expression were measured by Western blot analysis. As shown in Fig. 3C, AC treatment caused a significant decrease in tyrosine phosphorylation and HER-2/*neu* expression to 0.2-fold and 0.2-fold, respectively. However, pretreatment of SKOV-3 cells with NAC resulted in significant protection against the AC-induced reductions of tyrosine phosphorylation and HER-2/*neu* expression (Fig. 3C).

3.4. AC treatment inhibits the activation of PI3K/Akt in SKOV-3 cells

HER-2/*neu* regulates tumor cell growth, and HER-2/*neu* overexpression renders ovarian cancer cells chemo-resistant. This effect is mediated by the PI3K/Akt signaling pathway, and human ovarian cancer cells with overexpression and amplification of HER-2/*neu* make increased use of the PI3K/Akt signaling pathway (Chuang et al., 2011; Amler et al., 2012). We therefore sought to determine the involvement of HER-2/*neu* in the activation of the PI3K/Akt signaling pathway in SKOV-3 cells. Large amounts of PI3K and Akt phosphorylation were observed in control cells, whereas AC treatment significantly inhibited their phosphorylation in HER-2/*neu*-overexpressing SKOV-3 ovarian cancer cells in a dose-dependent manner (Fig. 4A). The levels of total PI3K and Akt were unaffected by AC treatment. These data demonstrate that AC-induced HER-2/*neu* depletion and growth inhibition may be mediated by the down-regulation of PI3K/Akt signaling in HER-2/*neu*-overexpressing ovarian cancer cells.

Next we sought to confirm whether AC-induced ROS generation has any functional role in PI3K/Akt activation or inhibition. SKOV-3 cells were pretreated with NAC for 1 h and treated with or without AC (160 μg/mL) for 24 h. The phosphorylation of PI3K and Akt was monitored by Western blot analysis. AC treatment significantly inhibited the phosphorylation of PI3K and Akt,

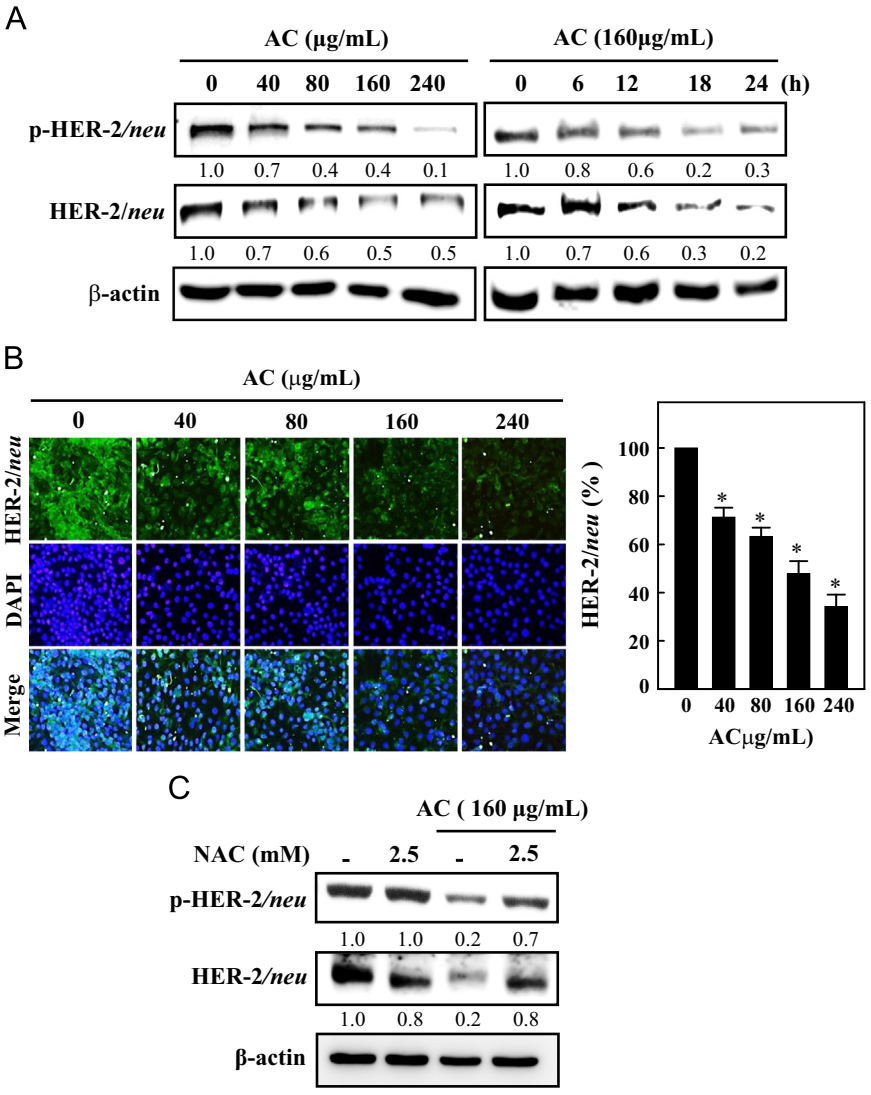

Fig. 3. Inhibitory effect of AC on phosphorylation of HER-2/*neu* (Tyr1248) and HER-2/*neu* expression in HER-2/*neu*-overexpressing human SKOV-3 cells. (A) Cells were incubated without or with AC (40–240 μg/mL) for 6–24 h. Immunoblotting was performed to measure total and tyrosine-phosphorylated HER-2/*neu*. Equal amounts of proteins (50 μg) were resolved by 8–15% SDS-PAGE, with β-actin serving as a control.. Relative changes in protein bands were measured using densitometric analysis; the control was 1.0-fold, as shown immediately below the gel data. (B) Changes in the subcellular distribution of HER-2/*neu* after a 24-h exposure to AC. Cells were grown on coverslips and treated without or with AC (40–240 μg/mL). Cells were fixed with 4% paraformaldehyde and stained with a HER-2/*neu* antibody followed by a fluorescein isothiocyanate-conjugated secondary antibody (green). The cells were photographed under fluorescence microscopy. (C) Cells were pretreated with 2.5 mM NAC for 1 h followed by treatment without or with AC (160 μg/mL) and quantification of p-tyrosine and total HER-2/*neu* protein levels after 24 h. Relative changes in protein bands were measured using densitometric analysis; the control was 1.0-fold, as shown immediately below the gel data. The results are presented as the mean ± SD of three independent experiments. * Significant difference in comparison to the control group ($p < 0.05$).

whereas the NAC pretreatment significantly protected the SKOV-3 cells against AC-induced inhibition of PI3K/Akt phosphorylation (Fig. 4B). In addition, the levels of total PI3K and Akt were unaffected by neither NAC nor AC. These data strongly suggest that AC-induced cell death is mediated by ROS generation.

3.5. AC treatment down-regulates the activation of β-catenin in SKOV-3 cells

Activated PI3K/Akt are critically involved in cell-cycle progression by phosphorylating and inactivating GSK-3β, thereby stabilizing nuclear translocation of β-catenin and increasing cyclin D1 transcription in human ovarian cancer cells (Rask et al., 2003). Therefore, to investigate the effect of AC on Wnt/β-catenin activity in human ovarian cancer cells, we treated SKOV-3 cells with AC for 24 h and measured the protein expression of β-catenin using cytoplasmic and nuclear extracts. As shown in Fig. 4C, strong β-catenin protein expression was observed in untreated cells. However, AC treatment caused a sustained decrease in β-catenin expression in both cytoplasmic and nuclear regions. Whereas, the loading controls β-catenin and histone levels were unaffected by AC. These data indicate that AC can inhibit Wnt/β-catenin signaling in human ovarian cancer cells.

3.6. AC treatment activates MAPK signaling pathways in SKOV-3 cells

MAP kinase family proteins, including p38, ERK, and JNK, play critical roles in cell fate. The p38 MAPK, ERK, and JNK modules are activated in response to cellular stress and seem to be exert both protective and pro-apoptotic functions (Boldt et al., 2002; Kim et al., 2008). To further examine whether AC treatment induces or inhibits the MAPK signaling pathways in human ovarian cancer cells, SKOV-3 cells were treated with AC (40–240 μg/mL) for 24 h, and the phosphorylation of p38, ERK, and JNK was assessed by Western blot analysis. As shown in Fig. 4D, AC treatment significantly induced the

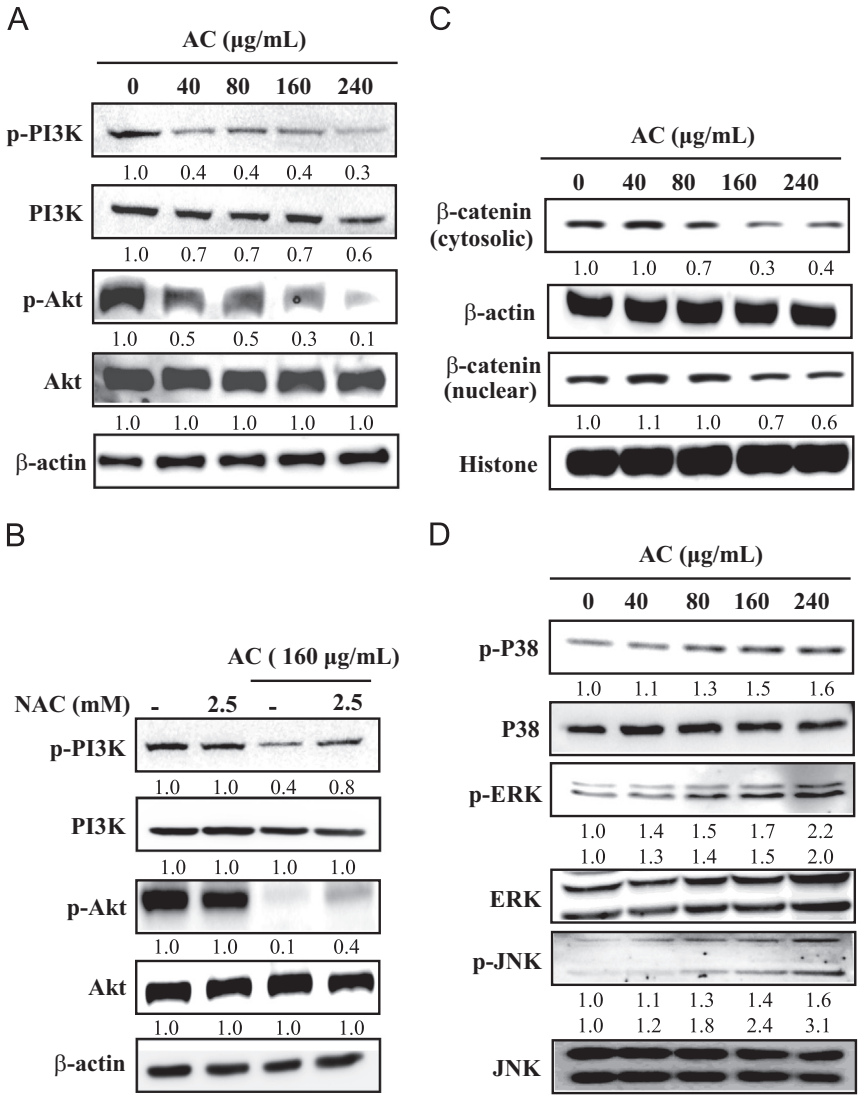

Fig. 4. (A) AC treatment suppressed the phosphorylation of PI3K/Akt in HER-2/*neu*-overexpressing SKOV-3 cells. Cells were treated with or without AC (40–240 μg/mL) for 24 h. The levels of phosphorylated PI3K (p-PI3K) and Akt (p-Akt, pSer 473) were evaluated using PI3K and Akt phosphorylation-specific antibodies. The total PI3K and Akt levels were assessed as controls. (B) SKOV-3 cells were pre-incubated with NAC (2.5 mM) and then treated with or without AC (40–240 μg/mL) for 24 h. The levels of phosphorylated and total PI3K and Akt were measured using Western blot analysis. (C) AC down-regulates β-catenin activity in SKOV-3 cells. Cells were incubated with control vehicle or AC (40–240 μg/mL) for 24 h. Western blots show the effects of AC on the total protein contents of β-catenin in both cytosol and the nucleus. (D) AC-induced activation of MAPK signaling pathways. SKOV-3 cells were treated with or without AC (40–240 μg/mL) for 24 h. The levels of phosphorylated p38 (p-p38), ERK1/2 (p-ERK1/2), and JNK1/2 (p-JNK1/2) were evaluated using phosphorylation-specific antibodies. The total p38, ERK1/2, and JNK1/2 levels were assessed as controls. The photomicrographs shown in this figure are from one representative experiment that was performed in triplicate. Relative changes in protein bands were measured using densitometric analysis; the control was 1.0-fold, as shown immediately below the gel data.

phosphorylation of p38 MAPK, ERK, and JNK in a dose-dependent manner, whereas total p38 MAPK, ERK, and JNK remained unaltered by AC treatment. These results suggest that AC treatment in SKOV-3 cells up-regulates p38 MAPK, ERK, and JNK protein activities, which may act as pro-apoptotic inducers.

3.7. AC treatment induces G_2/M cell-cycle arrest in SKOV-3 cells

We hypothesized that the reduction of cell viability in ovarian cancer cells by AC is due to cell-cycle arrest. To test this hypothesis, we determined the effect of AC on the distribution of cell-cycle phases. As shown in Fig. 5A, exposure of SKOV-3 cells to AC resulted in a dose-dependent, progressive and sustained accumulation of cells in the G_2/M phase. Furthermore, in response to AC treatment, the percentage of cells in the G_2/M phase gradually increased from 5% to 21% in SKOV-3 cells, whereas the percentage of those in the G_1 phase was significantly decreased (Fig. 5A).

To further examine the molecular mechanism(s) and underlying changes in cell-cycle patterns caused by AC treatment, we investigated the effects of AC on various cyclins and Cdks involved in cell-cycle regulation in SKOV-3 cells. AC treatment (40–240 μg/mL) for 24 h caused a dose-dependent reduction of cyclin D1 and cyclin A/B1 expression in HER-2/*neu*-overexpressing SKOV-3 cells (Fig. 5B). Cyclin D1 serves as the regulatory subunit of Cdk4 and contributes to its stability. Therefore, next we assessed the effects of AC on Cdk expression. Treatment of SKOV-3 cells with AC resulted in a dose-dependent decrease in Cdk1 expression (Fig. 5B). Nevertheless, there was no change in the Cdk4, Cdk2, and Cdc25C protein levels (Fig. 5B). These results imply that AC inhibits cell-cycle progression by reducing the levels of cyclin D1, cyclin A/B1, and Cdk1 in SKOV-3 cells. In addition, PI3K/Akt signaling may contribute to the induction of cell-cycle progression by regulating the Cdk inhibitor p27. Therefore, we examined whether AC treatment induced p27 expression in SKOV-3 cells. As expected,

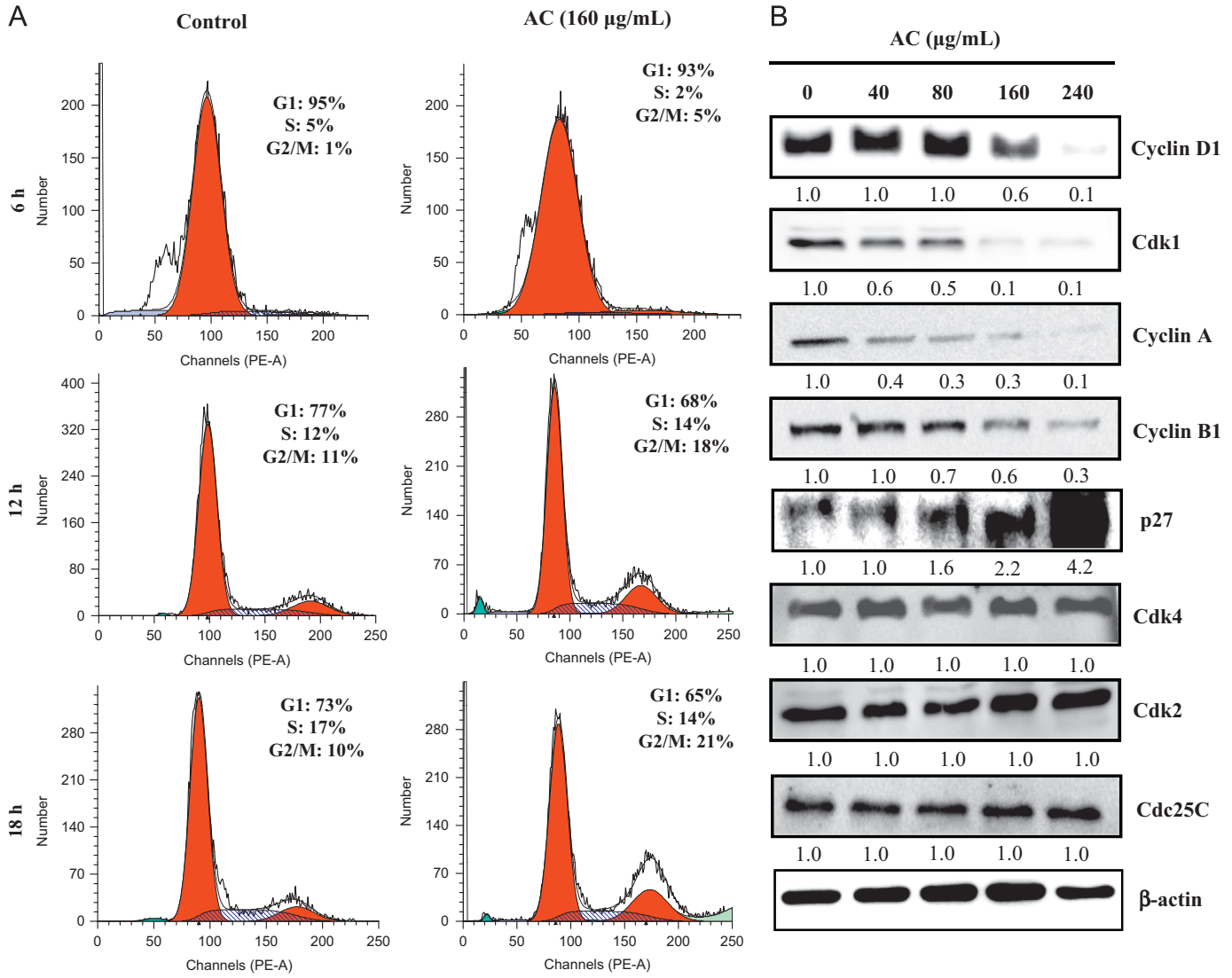

Fig. 5. AC induces G_2/M cell-cycle arrest in SKOV-3 cells. (A) Cells were treated with or without 160 μg/mL of AC for 6, 12 or 18 h, stained with PI and analyzed for cell-cycle phase by flow cytometry. Representative flow cytometry profiles are shown. (B) The effects of AC (40–240 μg/mL for 24 h) on cell-cycle regulatory protein levels were examined by immunoblotting. Equal amounts of protein (50 μg) were resolved by 8–15% SDS-PAGE with β-actin as a loading control. Relative changes in protein bands were measured by densitometric analysis in which the control was 1.0-fold, as shown immediately below the gel data. The photomicrographs shown in this figure are from one representative experiment that was performed in triplicate.

a significant increase in p27 protein level was observed in SKOV-3 cells after exposure to AC (Fig. 5B). Thus, it can be speculated that AC treatment induces G_2/M cell-cycle arrest by increasing the Cdk inhibitor p27 in SKOV-3 cells.

3.8. AC treatment promotes apoptotic cell death in SKOV-3 cells

The PI3K/Akt cell survival pathway plays an important role in inhibiting apoptosis in HER-2/*neu*-overexpressing ovarian cancer cells (Lee et al., 2012), which prompted us to examine whether this pathway plays a role in AC-induced apoptosis. We first assessed whether AC-induced cell death occurred through apoptotic induction. We used TUNEL staining to identify apoptotic cell death induced by AC. As shown in Fig. 6A, TUNEL-positive nuclei were found throughout the photomicrographs of the AC treatment group, whereas TUNEL-positive nuclei were undetectable in untreated control cells. Moreover, the number of TUNEL-positive nuclei significantly increased with AC concentration.

We further hypothesized that AC-induced apoptosis is mediated by mitochondrial pathways. Therefore, mitochondrial apoptosis was evaluated by directly measuring the release of mitochondrial cytochrome *c* into the cytosol by Western blot analysis. As shown in Fig. 6B, AC treatment caused a significant, dose-dependent increase in cytochrome *c* release from mitochondria, and the amount of cytochrome *c* in the cytoplasm was markedly increased, both of which show that AC caused mitochondrial membrane damage. Cytochrome *c* is involved in the activation of caspases that trigger apoptosis. Therefore, next we examined caspase-9 and caspase-3 cleavage by Western blot to evaluate caspase cascade activation in AC-induced apoptosis. Treatment of SKOV-3 cells with AC significantly induced the proteolytic cleavage of procaspase-9 and -3 into their active forms (Fig. 6B). In addition, PARP-specific proteolytic cleavage by caspase-3 is considered a biochemical characteristic of DNA damage. Our results demonstrate that AC treatment dose-dependently increased the cleavage of PARP (Fig. 6B). Moreover, the regulation of pro-apoptotic protein Bax and anti-apoptotic protein Bcl-2 plays a crucial role in cell homeostasis. Our results show that incubation of SKOV-3 cells with AC caused a dramatic reduction in the level of the anti-apoptotic protein Bcl-2 and

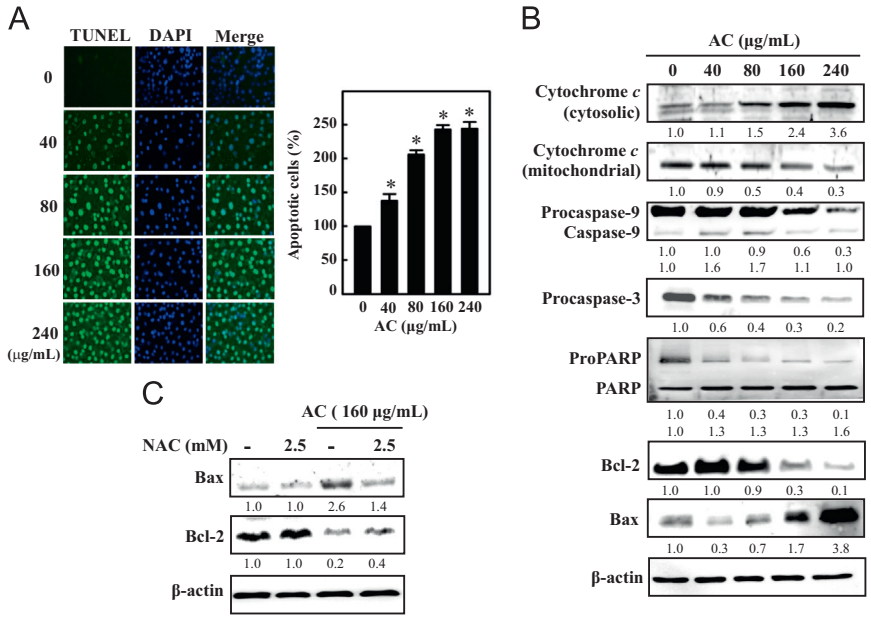

Fig. 6. AC induces apoptosis in ovarian cancer cells. (A) SKOV-3 cells were exposed to AC (40–240 μg/mL for 24 h), and the TUNEL assay was performed. The percentage of TUNEL positive cells were showed in the histogram. (B) Western blot analysis was performed to measure the protein levels of cytosolic and mitochondrial cytochrome *c*, procaspase-9 and -3, PARP, Bax, and Bcl-2 in SKOV-3 cells after exposure to AC (40–240 μg/mL for 24 h). (C) Cells were pretreated with 2.5 mM NAC for 1 h followed by treatment without or with AC (160 μg/mL) and quantification of Bax and Bcl-2 after 24 h using Western blot analysis. Relative changes in protein bands were measured by densitometric analysis in which the control was 1.0-fold, as shown immediately below the gel data. The photomicrographs shown here are from one representative experiment repeated two times.

increased the level of the pro-apoptotic Bax protein (Fig. 6B), which heterodimerizes with Bcl-2 to inhibit Bcl-2 activity. These results strongly indicate that AC-induced apoptosis is mediated by the dysregulation of Bcl-2/Bax expression. Therefore, we believe that the induction of apoptosis could be a major mechanism of AC-induced growth inhibition in SKOV-3 cells.

To determine whether there is a link between AC-induced ROS generation and Bcl-2/Bax dysregulation, SKOV-3 cells were pre-incubated with NAC for 1 h and treated with or without AC (160 μg/mL) for 24 h. The levels of Bcl-2 and Bax were measured by Western blot analysis. As shown in Fig. 6C, AC treatment caused a reduction in Bcl-2 protein and increased Bax protein. However, pretreatment of SKOV-3 cells with NAC resulted in significant protection against AC-induced up-regulation of Bax in SKOV-3 cells (Fig. 6C).

4. Discussion

Overexpression of HER-2/*neu*, a 185-kDa transmembrane kinase, is frequently observed in breast and ovarian cancer cells and implies a poor clinical diagnosis. HER-2/*neu* activates downstream signaling pathways, including the PI3K/Akt pathway, which mediates cell proliferation, survival and migration. The HER-2/*neu* oncogene encodes a receptor-like tyrosine kinase (p18) that has been extensively studied because of its role in several human carcinomas, including ovarian and breast carcinomas. In this study, AC-induced inhibition of cell proliferation, clonogenicity, and induction of apoptosis was observed in HER-2/*neu*-overexpressing human ovarian SKOV-3 cancer cells. We showed that AC treatment effectively inhibited the growth of SKOV-3 cells, with an IC_{50} value of 196 μg/mL. We also demonstrated that exposure of the HER-2/*neu*-overexpressing ovarian cancer cells to AC resulted in the induction of cell death mediated by ROS generation, HER-2/*neu* depletion, and down-regulation of PI3K/Akt signaling. Anti-HER-2/*neu* receptor therapy has been increasingly recognized as a potential treatment for HER-2/*neu*-overexpressing breast and ovarian cancer patients, as supported by recent advances in this direction. Several HER-2/*neu* tyrosine kinase inhibitors, including gefitinib and trastuzumab, are currently in pre-clinical and clinical development (Goyne and Cannon, 2012). However, phase II trials of gefitinib in refractory metastatic carcinomas yielded disappointing responses, and the course of treatment is expensive and requires multiple administrations of trastuzumab. The major observation reported in this study is that AC treatment effectively down-regulates HER-2/*neu* protein expression and tyrosine phosphorylation in HER-2/*neu*-overexpressing SKOV-3 cells. These data indicate that AC may be used as a chemo-preventive or chemotherapeutic agent against human ovarian cancers.

Naturally occurring phyto-compounds such as apigenin, rhein, sulforaphen, erucin, isothiocyanates, and anthocyanins, as well as several herbal products, potentially modulate the HER-2/*neu* signaling pathway in HER-2/*neu*-overexpressing human ovarian, breast, and bladder cancers in vitro and in vivo (Shiu et al., 2009; Hui et al., 2010; Abbaoui et al., 2012; Chang et al., 2012; Mafuvadze et al., 2012). In this study, we demonstrated that the fermented culture broth of AC exhibited significant growth inhibition by inhibiting HER-2/*neu* expression and tyrosine phosphorylation in HER-2/*neu*-overexpressing ovarian cancer cells. AC contains predominantly polysaccharides, triterpenoids, steroids, benzenoids, and maleic/succinic acid derivatives (Hseu et al., 2002; Ao et al., 2009; Yang et al., 2012). The reported yields of polysaccharides, crude triterpenoids, and total polyphenols in the fermented AC broth are 23.2 mg/g, 47 mg/g, and 67 mg/g, respectively, whereas no polysaccharides, crude triterpenoids, or polyphenols have been detected in the dry matter of the culture medium (Hseu et al., 2002). It is reasonable to suggest, therefore, that AC metabolizes the culture medium and releases active components during fermentation. Further bioassay-directed fractionations to identify and purify the compounds responsible for the anti-ovarian-cancer effect of AC are warranted.

Activation by phosphorylation of the HER-2/*neu* receptor tyrosine kinase activates PI3K and Akt signaling, which induce cell growth and inhibit apoptosis (Chuang et al., 2011; Amler et al.,

2012). In numerous tumor types, PI3K/Akt suppresses apoptosis and induces tumor cell survival by a variety of stimuli, including growth factor withdrawal and loss of cell adhesion (Datta et al., 1999). Overexpression of HER-2/*neu* activates the PI3K/Akt signaling pathway without exogenous ligand stimulation, and PI3K/Akt pathway activation also leads to delayed apoptosis (Zheng et al., 2004). In this study, AC treatment reduced the steady-state levels of total PI3K protein and phosphorylated Akt, indicating that the disruption of Akt activation plays a functional role in AC-induced apoptosis in HER-2/*neu*-overexpressing human ovarian cancer cells. The present study also suggests that AC-induced inhibition of cyclin A, cyclin B1, and cyclin D1 is directly proportional to the suppression of HER-2/*neu* and PI3K/Akt activation in human ovarian cancer cells. Taken together, these results suggest that HER-2/*neu* may regulate cellular cyclin A/B1/D1 *via* the PI3K/Akt pathway, implying that PI3K/Akt signaling predominantly contributes to cell-cycle progression in HER-2/*neu*-overexpressing ovarian cancer cells.

In the present study, we also demonstrated that AC treatment significantly inhibited β-catenin expression, which may contribute to its inhibitory effects on the Wnt/β-catenin pathway. Akt phosphorylates several downstream substrates, including GSK-3β, and phosphorylated GSK-3β undergoes proteasomal degradation to allow β-catenin to translocate to the nucleus and co-activate the transcription of several oncogenes and cell-cycle regulatory genes, such as cyclin D1, c-Myc, and matrix metalloproteinases (MMPs). These target genes up-regulate tumor cell migration and decrease cell-cell adhesion (Benton et al., 2009). The two most important proteins for ovarian cancer seem to be HER-2/*neu* and cyclin D1. Both proteins have prognostic significance because they are frequently overexpressed and implicated in experimental models of ovarian cancer (Meden and Kuhn, 1997; Hashimoto et al., 2011). The interaction between HER-2/*neu* and cyclin D1 appears to have therapeutic potential because several naturally occurring phytochemicals or synthetic drugs can reduce cyclin D1 expression through the down-regulation of HER-2/*neu* signaling, and the anti-HER-2/*neu* monoclonal antibody trastuzumab (Herceptin®) reduces cyclin D1 protein levels in human ovarian cancer cells (Abuharbeid et al., 2004; Menendez et al., 2005; Gianolio et al., 2012). Our results also demonstrate that AC treatment significantly inhibited SKOV-3 proliferation, which was associated with the inhibition of β-catenin activation and decreased expression of its transcriptional targets, including cyclin D1. Further studies are warranted to investigate the mechanisms underlying AC's effects on β-catenin and the possible application of AC for ovarian cancer chemotherapy.

The critical role of MAPK family proteins in cell proliferation and apoptosis is evidenced by the observation that dysregulation of MAP kinase cascades can result in cell transformation and cancer (Dhanasekaran and Johnson, 2007). p38 MAPK has recently gained attention as a tumor suppressor that is activated upon cellular stress and often engages pathways that can block proliferation or promote apoptosis (Dayem et al., 2010). The activation of ERK primarily involves a program of proliferation and survival, while the activation of JNK neither promotes nor inhibits proliferation or apoptosis. Transient activation of ERK and JNK leads to increased proliferation and survival of cancer cells, although inactivation of JNK in some instances may also promote tumorigenesis (Kennedy et al., 2007). Our results show that AC treatment increased the activation of p38 MAPK, ERK, and JNK. We believe p38 MAPK and JNK may be involved in AC-induced growth inhibition in SKOV-3 cells, whereas the role of ERK is unknown.

Eukaryotic cell-cycle progression is coordinated by the sequential activation of Cdks (cyclin-dependent kinases), the activation of which is dependent upon their association with cyclins (Johnson and Walker, 1999). Our study suggests that the marked reduction in cyclin A and B1 levels observed upon the inhibition of Cdk1 is involved in the transition from G_2 to M phase. Moreover, treatment of HER-2/*neu*-overexpressing ovarian cancer cells with AC down-regulated Cdk1 without altering Cdk2/4. Based on these results, we suggest that AC inhibits growth at the level of the G_2-M phase transition. In contrast with our results, a previous report showed that HER-2/*neu*-expressing human breast cancer MDA-MB-453 cells exposed to AC exhibited cell-cycle arrest at the G1-S transition through the down-regulation of cyclin D1, cyclin E1, and Cdk4, whereas Cdk1 and Cdk2 were unaffected (Boldt et al., 2002). These results indicate that the AC-induced cell-cycle arrest may vary from cell type to cell type, even among HER-2/*neu*-overexpressing cell lines. Cell-cycle progression is also coordinated by the balance between the cellular concentrations of Cdk inhibitors, including $p27^{Kip1/Cip1}$ and $p21^{WAF1}$ (Johnson and Walker, 1999). Loss of p27 protein activity is frequently observed in human cancers, including ovarian, prostate, gastric, colon, skin, lung and breast cancer, and is usually correlated with poor clinical outcome (Hsu et al., 2007). HER-2/*neu*-overexpression induces down-regulation of $p27^{Kip1}$ in a variety of cancer cell lines (Yang et al., 2000). The present study shows that p27 protein expression was dose-dependently increased by AC. Thus, we suggest that the inhibition of cyclin A, B1, and D activity may be due to the increase of p27 expression.

Apoptosis-inducing agents are being investigated as tools for the management of cancer treatment. Activation of caspases, induction of apoptosis-inducing factors, chromatin condensation, and DNA fragmentation are the major biomarkers of cellular apoptosis (Lee et al., 2012). In the present study, TUNEL assays and Western blot analyses demonstrated that treatment of SKOV-3 cells with AC markedly induced apoptotic cell death associated with internucleosomal DNA fragmentation and caspase-3 and capase-9 activation. Caspase activation induced an elevation of cytochrome *c* in the cytosol, with a corresponding decrease in its mitochondrial level. These results show that the AC-induced increase in cytoplasmic cytochrome *c* was due to the release of mitochondrial cytochrome *c* into the cytoplasm. In mammalian cells, apoptotic cell death is critically governed by the balance between anti-apoptotic proteins, such as Bcl-2 and Bcl-xL, and pro-apoptotic proteins, including Bax and Bak (Coultas and Strasser, 2003). The induction of apoptosis by AC is associated with down-regulation of Bcl-2 and up-regulation of Bax expression in human breast cancer cell lines (Hseu et al., 2002; Lee et al., 2012). Similarly, the present study also shows that AC treatment down-regulates the expression of Bcl-2 and up-regulates Bax in SKOV-3 cells. These data indicate that AC treatment disturbs the Bcl-2/Bax ratio and thereby leads to apoptosis of HER-2/*neu*-overexpressing ovarian cancer cells.

Several anti-cancer drugs have been proposed to induce ROS generation by causing oxidative stress, which further leads to apoptosis in a variety of cancer cell lines (Ozben, 2007). Those results are consistent with the hypothesis that AC-induced apoptotic cell death is driven by intracellular ROS generation because the anti-oxidant NAC prevents AC-induced cell death and Bcl-2/Bax dysregulation in SKOV-3 cells. By contrast, AC-induced ROS generation significantly inhibited HER-2/*neu* activity, as evidenced by inhibition of HER-2/*neu* tyrosine phosphorylation in SKOV-3 cells, whereas NAC treatment significantly prevented AC-induced HER-2/*neu* degradation and tyrosine phosphorylation, which strongly suggests that ROS could play a pivotal role in AC-induced growth inhibition in SKOV-3 cells.

In conclusion, AC-induced growth inhibition and apoptosis in SKOV-3 cells result from ROS generation, loss of HER-2/*neu* activation, and suppression of its downstream signaling, including the PI3K/Akt cascade. Our results also highlight the importance in ovarian cancer of HER-2/*neu* and PI3K/Akt signaling components,

including β-catenin, cyclin D1, and $p27^{KIP1}$, which may serve as future targets for the development of therapeutic strategies. Moreover, this is the first report that demonstrated the effects of *Antrodia camphorata* on HER-2/*neu*-overexpressing human ovarian cancer cells. However, further in vivo studies are warranted to confirm the chemotherapeutic efficacy and safety of *Antrodia camphorata*.

Acknowledgments

This work was supported by Grants NSC-99-2320-B-039-035-MY3, NSC-98-2320-B-039-037-MY3, CMU 98-C09, CMU 100-ASIA-13, and CMU 100-ASIA-14 from the National Science Council, China Medical University, and Asia University, Taiwan.

References

Abbaoui, B., Riedl, K.M., Ralston, R.A., Thomas-Ahner, J.M., Schwartz, S.J., Clinton, S. K., Mortazavi, A., 2012. Inhibition of bladder cancer by broccoli isothiocyanates sulforaphane and erucin: characterization, metabolism, and interconversion. Molecular Nutrition & Food Research 56, 1675–1687.

Abuharbeid, S., Apel, J., Sander, M., Fiedler, B., Langer, M., Zuzarte, M.L., Czubayko, F., Aigner, A., 2004. Cytotoxicity of the novel anti-cancer drug rViscumin depends on HER-2 levels in SKOV-3 cells. Biochemical and Biophysical Research Communications 321, 403–412.

Aigner, A., Hsieh, S.S., Malerczyk, C., Czubayko, F., 2000. Reversal of HER-2 overexpression renders human ovarian cancer cells highly resistant to taxol. Toxicology 144, 221–228.

Amler, L.C., Wang, Y., Hampton, G., 2012. HER2 as Therapeutic Target in Ovarian Cancer. Ovarian Cancers-Clinical and Therapeutic Perspectives. Intech Press, Rijeka, Croatia.

Ao, A., Morrison, B.J., Wang, H., Lopez, A., Reynolds, B.A., Lu, J., 2011. Response of estrogen receptor-positive ovarian cancer tumorspheres to antiestrogen treatments. PLoS One 6, e18810.

Ao, Z.H., Xu, Z.H., Lu, Z.M., Xu, H.Y., Zhang, X.M., Dou, W.F., 2009. Niuchangchih (*Antrodia camphorata*) and its potential in treating liver diseases. Journal of Ethnopharmacology 121, 194–212.

Benton, J.A., Kern, H.B., Leinwand, L.A., Mariner, P.D., Anseth, K.S., 2009. Statins block calcific nodule formation of valvular interstitial cells by inhibiting alpha-smooth muscle actin expression. Arteriosclerosis, Thrombosis, and Vascular Biology 29, 1950–1957.

Berek, J.S., Thomas, G.M., Ozols, R.F., 2000. Ovarian cancer. In: Bast Jr., R.C., Kufe, D. W., Pollock, R.E. (Eds.), Cancer Medicine, Fifth ed Decker Publishing Inc., Ontario, Canada.

Boldt, S., Weidle, U.H., Kolch, W., 2002. The role of MAPK pathways in the action of chemotherapeutic drugs. Carcinogenesis 23, 1831–1838.

Chang, C.Y., Chan, H.L., Lin, H.Y., Way, T.D., Kao, M.C., Song, M.Z., Lin, Y.J., Lin, C.W., 2012. Rhein induces apoptosis in human breast cancer cells. Evidence-Based Complementary and Alternative Medicine, 1–8, http://dx.doi.org/10.1155/2012/952504.

Chiang, C.J., Chen, Y.C., Chen, C.J., You, S.L., Lai, M.S., 2010. Cancer trends in Taiwan. Japanese Journal of Clinical Oncology 40, 897–904.

Chuang, T.C., Hsu, S.C., Cheng, Y.T., Shao, W.S., Wu, K., Fang, G.S., Ou, C.C., Wang, V., 2011. Magnolol down-regulates HER2 gene expression, leading to inhibition of HER2-mediated metastatic potential in ovarian cancer cells. Cancer Letters 311, 11–19.

Coultas, L., Strasser, A., 2003. The role of the Bcl-2 protein family in cancer. Seminars in Cancer Biology 13, 115–123.

Datta, S.R., Brunet, A., Greenberg, M.E., 1999. Cellular survival: a play in three Akts. Genes and Development 13, 2905–2927.

Dayem, A.A., Choi, H.Y., Kim, J.H., Cho, S.G., 2010. Role of oxidative stress in stem, cancer, and cancer stem cells. Cancers 2, 859–884.

Dhanasekaran, D.N., Johnson, G.L., 2007. MAPKs: function, regulation, role in cancer and therapeutic targeting. Oncogene 26, 3097–3099.

Gari, A., Souhami, L., Arseneau, J., Stanimir, G., 2006. Primary malignant mesodermal ovarian sarcomas. International Journal of Gynecological Cancer 16, 106–109.

Gianolio, D.A., Rouleau, C., Bauta, W.E., Lovett, D., Cantrell Jr., W.R., Recio 3rd., A., Wolstenholme-Hogg, P., Busch, M., Pan, P., Stefano, J.E., Kramer, H.M., Goebel, J., Krumbholz, R.D., Roth, S., Schmid, S.M., Teicher, B.A., 2012. Targeting HER2-positive cancer with dolastatin 15 derivatives conjugated to trastuzumab, novel antibody-drug conjugates. Cancer Chemotherapy and Pharmacology 70, 439–449.

Goyne, H.E., Cannon, M.J., 2012. The case for HER2/neu as a therapeutic target for gynecologic malignancies. Immunotherapy 4, 781–784.

de Graeff, P., Crijns, A.P., de Jong, S., Boezen, M., Post, W.J., de Vries, E.G., van der Zee, A.G., de Bock, G.H., 2009. Modest effect of p53, EGFR and HER-2/neu on prognosis in epithelial ovarian cancer: a meta-analysis. British Journal of Cancer 101, 149–159.

Hashimoto, T., Yanaihara, N., Okamoto, A., Nikaido, T., Saito, M., Takakura, S., Yasuda, M., Sasaki, H., Ochiai, K., Tanaka, T., 2011. Cyclin D1 predicts the prognosis of advanced serous ovarian cancer. Experimental and Therapeutic Medicine 2, 213–219.

Hervik, J., Mjaland, O., 2012. Examining the relationship between traditional Chinese medicine and conventional medicine in breast cancer patients medicated with estrogen antagonists. Alternative Medicine Studies 2, e11.

Howe, L.R., Subbaramaiah, K., Brown, A.M., Dannenberg, A.J., 2001. Cyclooxygenase-2: a target for the prevention and treatment of breast cancer. Endocrine-Related Cancer 8, 97–114.

Hseu, Y.C., Chang, W.C., Hseu, Y.T., Lee, C.Y., Yech, Y.J., Chen, P.C., Chen, J.Y., Yang, H.L., 2002. Protection of oxidative damage by water extract from *Antrodia camphorata* mycelia in normal human red blood cells. Life Sciences 71, 469–482.

Hseu, Y.C., Huang, H.C., Hsiang, C.Y., 2010. *Antrodia camphorata* suppresses lipopolysaccharide-induced nuclear factor-kappaB activation in transgenic mice evaluated by bioluminescence imaging. Food and Chemical Toxicology 48, 2319–2325.

Hseu, Y.C., Lee, M.S., Wu, C.R., Cho, H.J., Lin, K.Y., Lai, G.H., Wang, S.Y., Kuo, Y.H., Kumar, K.J., Yang, H.L., 2012. The chalcone flavokawain B induces G2/M cell-cycle arrest and apoptosis in human oral carcinoma HSC-3 cells through the intracellular ROS generation and downregulation of the Akt/p38 MAPK signaling pathway. Journal of Agricultural and Food Chemistry 60, 2385–2397.

Hsieh, C.Y., Chen, C.A., Chou, C.H., Lai, K.P., Jeng, Y.M., Kuo, M.L., Wei, L.H., 2004. Overexpression of Her-2/NEU in epithelial ovarian carcinoma induces vascular endothelial growth factor C by activating NF-kappa B: implications for malignant ascites formation and tumor lymphangiogenesis. Journal of Biomedical Science 11, 249–259.

Hsu, M.C., Chang, H.C., Hung, W.C., 2007. HER-2/neu transcriptionally activates Jab1 expression via the AKT/beta-catenin pathway in breast cancer cells. Endocrine-Related Cancer 14, 655–667.

Hui, C., Bin, Y., Xiaoping, Y., Long, Y., Chunye, C., Mantian, M., Wenhua, L., 2010. Anticancer activities of an anthocyanin-rich extract from black rice against breast cancer cells in vitro and in vivo. Nutrition and Cancer 62, 1128–1136.

Jiang, N., Saba, N.F., Chen, Z.G., 2012. Advances in targeting HER3 as an anti-cancer therapy. Chemotherapy Research and Practice, 2012, http://dx.doi.org/10.1155/2012/817304.

Johnson, D.G., Walker, C.L., 1999. Cyclins and cell cycle checkpoints. Annual Review of Pharmacology and Toxicology 39, 295–312.

Kalli, K.R., Bradley, S.V., Fuchshuber, S., Conover, C.A., 2004. Estrogen receptor-positive human epithelial ovarian carcinoma cells respond to the antitumor drug suramin with increased proliferation: possible insight into ER and epidermal growth factor signaling interactions in ovarian cancer. Gynecologic Oncology 94, 705–712.

Kennedy, N.J., Cellurale, C., Davis, R.J., 2007. A radical role for p38 MAPK in tumor initiation. Cancer Cell 11, 101–103.

Kim, B.W., Lee, E.R., Min, H.M., Jeong, H.S., Ahn, J.Y., Kim, J.H., Choi, H.Y., Choi, H., Kim, E.Y., Park, S.P., Cho, S.G., 2008. Sustained ERK activation is involved in the kaempferol-induced apoptosis of breast cancer cells and is more evident under 3-D culture condition. Cancer Biology & Therapy 7, 1080–1089.

Koleske, A.J., Baltimore, D., Lisanti, M.P., 1995. Reduction of caveolin and caveolae in oncogenically transformed cells. Proceedings of the National Academy of Science of the United States of America 92, 1381-1385.

Lee, C.C., Yang, H.L., Way, T.D., Kumar, K.J.S., Juan, Y.C., Cho, H.J., Lin, K.Y., Hsu, L.S., Chen, S.C., Hseu, Y.C., 2012. Inhibition of cell growth and induction of apoptosis by *Antrodia camphorata* in HER-2/neu-overexpressing breast cancer cells through the induction of ROS, depletion of HER-2/neu, and disruption of the PI3K/Akt signaling pathway. Evidence-Based Complementary and Alternative Medicine 2012, 1–15, http://dx.doi.org/10.1155/2012/702857.

Mafuvadze, B., Liang, Y., Besch-Williford, C., Zhang, X., Hyder, S.M., 2012. Apigenin induces apoptosis and blocks growth of medroxyprogesterone acetate-dependent BT-474 xenograft tumors. Hormones and Cancer 3, 160–171.

Makar, A.P., 2000. Hormone therapy in epithelial ovarian cancer. Endocrine-Related Cancer 7, 85–93.

Meden, H., Kuhn, W., 1997. Overexpression of the oncogene c-erbB-2 (HER2/neu) in ovarian cancer: a new prognostic factor. European Journal of Obstetrics, Gynecology, and Reproductive Biology 71, 173–179.

Menendez, J.A., Vellon, L., Colomer, R., Lupu, R., 2005. Effect of gamma-linolenic acid on the transcriptional activity of the Her-2/neu (erbB-2) oncogene. Journal of the National Cancer Institute 97, 1611–1615.

Nair, H.K., Rao, K.V.K., Aalinkeel, R., Mahajan, S., Chawda, R., Schwartz, S.A., 2004. Inhibition of prostate cancer cell colony formation by the flavonoid quercetin correlates with modulation of specific regulatory genes. Clinical and Diagnostic Laboratory Immunology 11, 63–69.

Olayioye, M.A., 2001. Update on HER-2 as a target for cancer therapy: intracellular signaling pathways of ErbB2/HER-2 and family members. Breast Cancer Research 3, 385–389.

Ozben, T., 2007. Oxidative Stress and apoptosis: impact on cancer therapy. Journal of Pharmaceutical Sciences 96, 2181–2196.

Rask, K., Nilsson, A., Brannstrom, M., Carlsson, P., Hellberg, P., Janson, P.O., Hedin, L., Sundfeldt, K., 2003. Wnt-signalling pathway in ovarian epithelial tumors: increased expression of beta-catenin and GSK3beta. British Journal of Cancer 89, 1298–1304.

Shiu, L.Y., Liang, C.H., Chang, L.C., Sheu, H.M., Tsai, E.M., Kuo, K.W., 2009. Solamargine induces apoptosis and enhances susceptibility to trastuzumab and epirubicin in breast cancer cells with low or high expression levels of HER2/neu. Bioscience Reports 29, 35–45.

Stewart, S.L., 2012. Ovarian Cancer Incidence: Current and Comprehensive Statistics. Ovarian Cancers-Clinical and Therapeutic Perspectives. Intech Press, Rijeka, Croatia.

Yang, H.Y., Zhou, B.P., Hung, M.C., Lee, M.H., 2000. Oncogenic signals of HER-2/neu in regulating the stability of the cyclin-dependent kinase inhibitor p27. The Journal of Biological Chemistry 275, 24735–24739.

Yang, H.L., Chen, C.S., Chang, W.H., Lu, F.J., Lai, Y.C., Chen, C.C., Hseu, T.H., Kuo, C.T., Hseu, Y.C., 2006. Growth inhibition and induction of apoptosis in MCF-7 breast cancer cells by *Antrodia camphorata*. Cancer Letters 231, 215–227.

Yang, H.L., Kumar, K.J.S., Hseu, Y.C., 2012. Multiple Molecular Targets of *Antrodia camphorata*: A Suitable Candidate for Ovarian Cancer Chemoprevention. Breast Cancer Cells-2. Intech Press, Rijeka, Croatia.

Zheng, L., Ren, J.Q., Li, H., Kong, Z.L., Zhu, H.G., 2004. Downregulation of wild-type p53 protein by HER-2/neu mediated PI3K pathway activation in human breast cancer cells: its effect on cell proliferation and implication for therapy. Cell Research 14, 497–506.

Pergamon

0031-9422(95)00025-9

Phytochemistry, Vol. 39, No. 3, pp. 613–616, 1995

0031-9422/95 $9.50 + 0.00

A SESQUITERPENE LACTONE, PHENYL AND BIPHENYL COMPOUNDS FROM *ANTRODIA CINNAMOMEA*

HUNG-CHEN CHIANG,* DE-PENG WU, I-WHA CHERNG and CHUEN-HER UENG

Institute of Chemistry, National Taiwan Normal University, Taipei 117, Taiwan, Republic of China

(*Received* 24 *October* 1994)

Key Word Index—*Antrodia cinnamomea*; sesquiterpene; antrocin; *Cinnamomum kanehirai*.

Abstract—Three novel compounds, a sesquiterpene, phenyl and biphenyl derivatives, have been isolated from the crude methanol extract of the fungus *Antrodia cinnamomea*, a new genus of *Antrodia* species. Their structures were all determined by spectroscopic data and confirmed by X-ray analysis.

INTRODUCTION

Antrodia cinnamomea Chang & Chou, sp. nov. growing rarely on the inner cavity wall of *Cinnamomum kanehirai* Hay. was identified as a new species of *Antrodia* in 1995 [1]. It was early identified as a new *Ganoderma* species, *Ganoderma camphoratum* in 1990 [2] because there were several similar characteristics. *A. cinnamomea* is well known in Taiwan under the name "niu chang ku" or "Jang-Jy" and is also popular and very expensive as medicinal material. It is used traditionally as an antidote, anticancer and antichromic material, but no biological activity tests have been reported. We report now the isolation and identification of three novel compounds, a sesquiterpene lactone (**1**) (antrocin), and the phenyl and biphenyl derivatives **2a** (4,7-dimethoxy-5-methyl-1,3-benzodioxole) and **3** (2,2′,5,5′-tetramethoxy-3,4,3′4′-bimethylenedioxy-6,6′-dimethylbiphenyl), respectively.

RESULTS AND DISCUSSION

The structure of antrocin (**1**) was elucidated by NMR spectroscopy, mass spectrometry and X-ray crystallography studies. The EI-mass spectrum of **1** indicated a molecular formula of $C_{15}H_{22}O_2$. Its IR absorption band at 1763 cm^{-1} indicates a γ-lactone system [3, 4], and a terminal methylene at 893 cm^{-1}. The above data were indicative of a three-membered ring system.

The ^{13}C NMR and DEPT spectra of **1** showed signals of 15 carbon atoms corresponding to Me (×2), CH_2 (×7), CH (×2), three quaternary carbons and one carbonyl carbon. Irradiation of the methyl group at δ0.93 (H-13) gave NOE enhancement of δ1.36 *dd* (H-5), 1.18 *s* (H-14) and 1.21 *m*, δ1.55 *m* (H-3). Irradiation of the terminal methylene group (H-12) at δ4.83 and 4.80 gave NOE enhancement of δ2.25 *m*, 2.35 *m* (H-7) and 2.66 (H-9). Two protons on the lactone's γ-position (H-11) at δ4.14 (*d*, J = 9.1 Hz) and 4.48 (*dd*, J = 6.8, 9.1 Hz) coupled to the methine proton (H-9) at δ2.66 (*d*, J = 6.8 Hz).

The ^1H and ^{13}C NMR spectral chemical shifts of **1** were assigned on the basis of 2 D NMR (^1H–^1H COSY, ^{13}C–^1H COSY) and difference NOE techniques (Table 1). A single crystal X-ray diffraction study further confirmed the molecular structure of **1**.

The molecular formula of **2a** was assigned as $C_{10}H_{12}O_4$ by HR-mass spectrometry. In the IR spectrum, bands at 1584 and 1612 cm^{-1} showed that the compound was a benzenoid [5]. The ^1H NMR spectrum showed signals for two methoxy (δ3.84, 3,88), one methylenedioxy (δ5.93), one methyl group (δ2.18) and a single aromatic proton (δ6.30) [5, 6]. Considering all the spectral evidence, six possible forms (**2a**–**2f**) were possible for

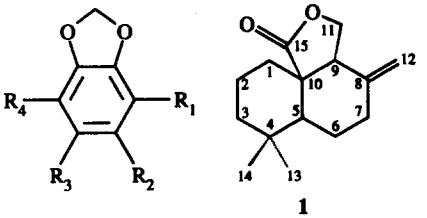

1

	R_1	R_2	R_3	R_4
2a	OMe	H	Me	OMe
2b	H	Me	OMe	OMe
2c	Me	H	OMe	OMe
2d	H	OMe	Me	OMe
2e	Me	OMe	H	OMe
2f	H	OMe	OMe	Me

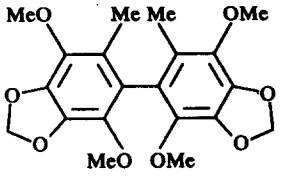

3

Table 1 ^1H and ^{13}C NMR spectral data of **1** ($CDCl_3$ solution, δ value in ppm, J value in Hz)

Atom	^1H	^{13}C
1	1.35 *m*, 2,15 *m*	36.8
2	1.50 *m*, 1.80 *m*	18.6
3	1.21 *m*, 1.55 *m*	41.9
4	—	33.2
5	1.36 *m*	46.6
6	1.53 *m*, 1.80 *m*	22.1
7	2.25 *m*, 2.35 *m*	30.3
8	—	146.7
9	2.66 *d* (J = 6.8)	54.1
10	—	48.4
11	4.48 *dd* (J = 6.8, 9.1) 4.14 *d* (J = 9.1)	69.3
12	4.83 *s*, 4.80 *s*	111.1
13	0.93 *s*	33.1
14	1.18 *s*	22.3
15	—	178.3

2a. The proposed structure (**2a**) was confirmed by a difference NOE experiment.

Irradiation of the methyl group led to enhancements of the aromatic proton and one methoxy group at δ(3.88), and thus (**2c-2f**) can be ruled out. Further, irradiation of the single aromatic proton gave NOE enhancements of the methyl group and the other methoxy group (δ3.84). The above experiment indicated the structure of **2a** to be 4,7-dimethoxy-5-methyl-1,3-benzodioxole.

Compound **3** gave a molecular ion peak in the HR-mass spectrum at m/z 390.1306 corresponding to a molecular formula $C_{20}H_{22}O_8$. In the IR spectrum, it showed the absorption of a benzene ring at 1616 and 1506 cm^{-1}. In the ^1H NMR spectrum, one signal of a methylenedioxy at δ5.95, two methoxy groups at δ3.92 and δ3.73 and one methyl group at δ1.78 were observed but there was no aromatic proton. The ^{13}C NMR spectrum also indicated the functional group mentioned above. Comparison of the spectral data of **3** with those of **2** showed similarities. In particular, **3** was a biphenyl of the phenyl of **2**. On the basis of the above data, **3** is proposed to have a structure similar to that of **2**. However, the spectral data alone could not provide a precise structure. Therefore an X-ray analysis was carried out and the structure was determined unequivocally. ORTEP diagrams [7] for the molecular structure are shown in Figs 1 and 2.

The skeleton of **1** consists of two six-membered cyclohexanes, with one ring [C(1), C(5) to C(10)] being chair form and the other being twist–boat form and a five-membered lactone which are fused together with C(5)–C(10) and C(9)–C(10) as the sharing edges. Except the C(15) = O(2) and C(8) = C(12), all bonds in **1** are single bonds. The range of the C–C single bond lengths [1.499(8) to 1.560(8) Å] and the two double bonds [1.196(7) and 1.325(7) Å] are reasonable. The bond length of C(15)–O(1) is significantly smaller than that of C(11)–O(1). This is expected since the bond strength of C^2_{sp}–O is stronger than that of C^3_{sp}–O. Compound **3** is a biphenyl derivative with each phenyl group fused by a heterocyclic five-membered ring and substituted by two

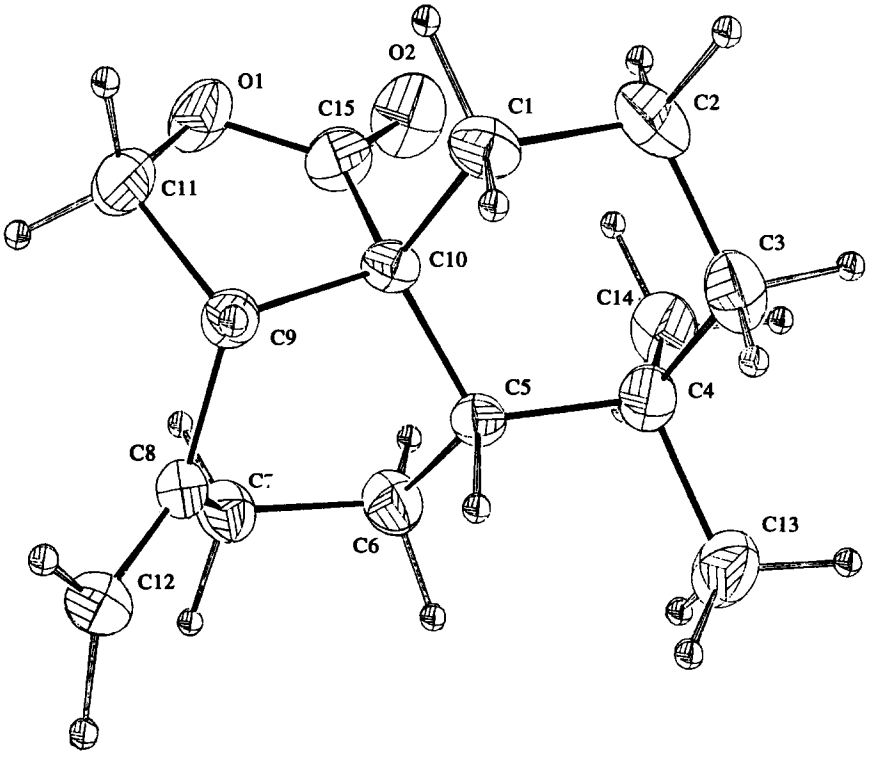

Fig. 1. Molecular structure of **1**.

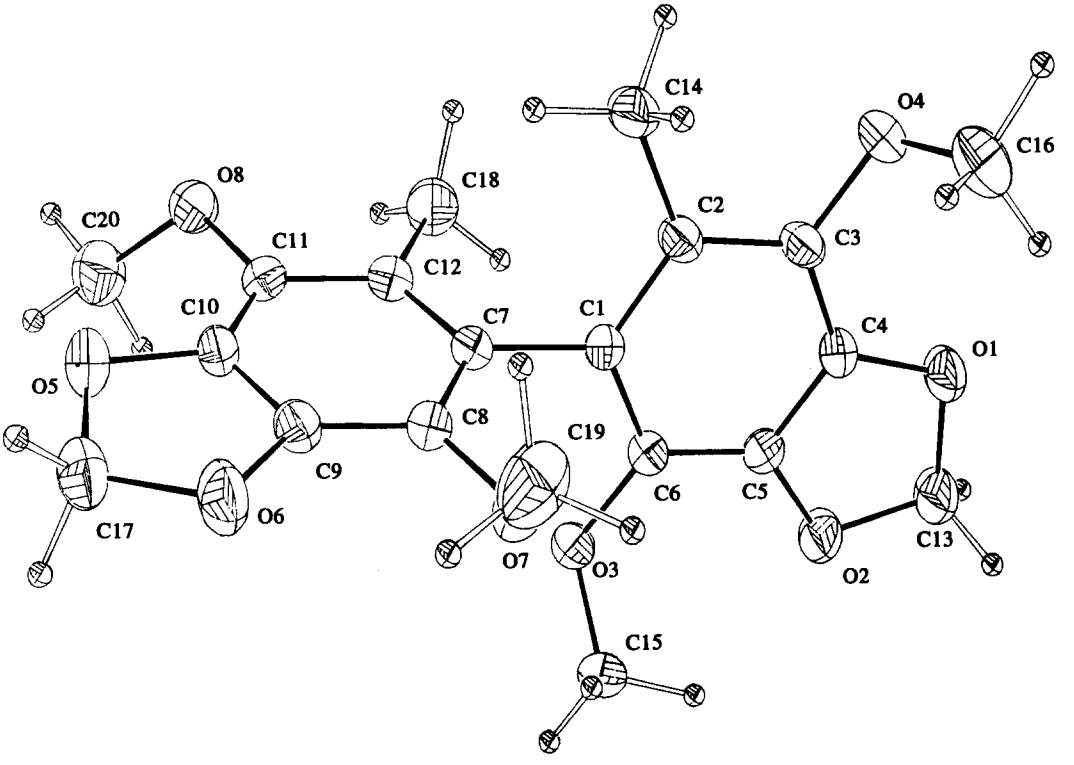

Fig. 2. Molecular structure of **3**.

methoxyl groups and a methyl group. The large dihedral angle between the two phenyl groups [81.8(1)°] is indicative of no possible π-interaction between them and the C(1)–C(7) bond is a typical single bond. The nonequality of the C–O bonds in each methoxyl group and in each heterocyclic ring is also due to the different bond strength between C^2_{sp}–O and C^3_{sp}–O bonding. The bond lengths and bond angles of the two phenyl groups are reasonable. No intermolecular contact of structural significance was observed for either compound.

EXPERIMENTAL

General. Mps are uncorr.; IR: KBr disk. ^{1}H and ^{13}C NMR were 400 and 100 MHz, respectively, in $CDCl_3$ soln, with TMS as int. standard. EIMS: 30 eV. HPLC was performed with *n*-hexane–EtOAc on a Si60 (Waters, 6 μm, 7.8 × 300 nm) column employing a refractive index detector at a flow rate of 2.0 ml min^{-1}.

Extraction and sepn. The dry fruit bodies were obtained from *A. cinnamomea* (300 g), growing in Taiwan. They were collected by Ju-Chen Wang, Ling-Chih Co., Taipei, in 1987 and identified by Prof. Chiu-yuan Chien, Institute of Biological Science, National Taiwan Normal University. The fruit bodies were cut into small pieces and refluxed (× 6) with MeOH (2 l) for 5 hr. The conc MeOH extract was partitioned between H_2O and $CHCl_3$. The $CHCl_3$ fr. (70 g) was then chromatographed on a silica gel column (800 g) by stepwise elution with *n*-hexane–EtOAc (7:3), *n*-hexane–EtOAc (1:1), and *n*-hexane–EtOAc (2:3). The *n*-hexane (7:3) elution was chromatographed on a silica gel column repeatedly (*n*-hexane–EtOAc, 10:1) and then sepd by HPLC (*n*-hexane–EtOAc, 15:1) to afford **1** (15 mg), **2a** (40 mg). Compound **3** (30 mg) was crystallized in crude *n*-hexane–EtOAc (7:3) fr.

Antrocin (**1**), (1 β, 4a α, 8a β)-*decahydro*-5,5-*dimethyl*-8-*methylene naphthol*[1,8a-c] *furan*-1(3H)-*one*. Crystallized from MeOH as needles, mp 96–98°, $[\alpha]_D^{25}$ − 112° (c = 1.0 $CHCl_3$). IR ν_{max}^{KBr} cm^{-1} : 2957, 1763, 1445, 1366, 1125, 1053, 986, 893; EIMS (30 eV) *m/z* (rel. int.): 234 $[M]^+$ (6), 219 $[M - Me]^+$ (8), 204 $[M - CH_2O]^+$ (100), 189 $[M - CH_2O - Me]^+$ (7), 175.2 (8), 161 (29), 151 $[M - C_4H_3O_2]^+$ (57), 131 (12), 105 (13), 89 (21). ^{1}H and ^{13}C NMR: see Table 1.

The crystal data of **1** were as follows: a crystal of dimension 0.2 × 0.3 × 0.5 mm^3 was mounted on a Nonius CAD4 diffractometer equipped with Mo radiation (λ = 0.711 Å) and a graphite monochromater. Crystal data: $C_{15}H_{22}O_2$, M_r = 234.34, monoclinic, $P2_1$, a = 6.221(3), b = 16.102(4), c = 7.196(2) Å, β = 113.92(3), V = 659.0(4) Å^3, z = 2, D_c1.181 mg·m^{-3}, F(000) = 255.97. Data collections: $3 \leqq 2\theta \leqq 50$, using the $\theta/2$ θ scan mode; 1301 total reflections, 1207 unique and 1030 reflections with $I > 2.5\,\sigma(I)$. Besides, absorption corrections were made, and the structure was solved by direct method. The final residual: R = 0.051, R_w = 0.046, GoF = 4.27 for 154 parameters and 1030 reflections. The largest residual electron density was 0.180 eÅ^{-3}. All data reduction and structural refinement were performed by using NRCVAX package [8]. The X-ray data are deposited at the Cambridge Crystallographic Data centre.

Compound **2a**: (*4,7-dimethoxy-5-methyl-1,3-benzodioxole*). Yellow liquid, IR ν_{max}^{KBr} cm^{-1}: 2952, 2855, 1612, 1584, 1458, 1427, 1346, 1256, 1138, 1065, 1055, 949; HRMS *m/z* 196.0737 $[M]^+$ ($C_{10}H_{12}O_4$ requires: 196.0735); EIMS (20 eV) *m/z* (rel. int.): 196 $[M]^+$ (100), 181 $[M - Me]^+$ (16), 123 (2), 95 (1). ^{1}H NMR ($CDCl_3$): δ6.3 (1H, *s*), 5.93 (2H, *s*), 3.88 (3H, *s*), 3.84 (3H, *s*), 2.18 (3H, *s*). ^{13}C NMR ($CDCl_3$): δ138.8 (C); 138.6 (C); 136.5 (C); 134.6 (C); 134.6 (C); 123.6 (C); 108.8 (CH); 101.4 (CH_2); 59.9 (Me); 56.8; 15.9 (Me).

Compound **3**: (*2,2',5,5'-tetramethoxy-3,4,3'4'-bi-methylenedioxy-6,6'-dimethylbiphenyl*). Recrystallized from EtOAc as prism, mp 145–147°; $[\alpha]_D^{25}$ 0° ($CHCl_3$, $c = 0.2$). IR ν_{max}^{KBr} cm^{-1}: 3003, 2937, 2095, 2079, 1616, 1456, 1446, 1419, 1271, 1224, 1122, 1051, 979, 950; EIMS (30 eV) *m/z* (rel. int.): 390 $[M]^+$ 375 $[M - Me]^+$(15), 360 $[M - 2Me]^+$ (8), 345 $[M - 3Me]^+$ (18), 329 $[M - 2Me\ OMe]^+$ (18), 302 (10), 195 $[M - 1/2M]^+$ (15). ^{1}H NMR ($CDCl_3$): δ5.95 (4H, *s*), 3.92 (6H, *s*), 3.73 (6H, *s*), 1.78 (6H, *s*). ^{13}C NMR ($CDCl_3$): δ137.8 (C); 137.2 (C); 136.8 (C); 136.5 (C); 123.0 (C); 101.0 (CH_2); 59.8 (Me); 59.8 (Me); 12.6 (Me).

Compound **3** crystallized in the monoclinic crystal system ($P2_{1/C}$) with $a = 11.226(6)$, $b = 10.823(2)$, $c = 15.702(2)$ and $\beta = 99.58(3)$. A prismatic crystal ($0.6 \times 0.6 \times 0.7$ mm^3) was selected and mounted on a Nonius CAD4 diffractometer. Reflections (3438 total) were measured in the range of $3 \leqq \theta \leqq 50°$, using the $\theta/2\ \theta$ scan mode. 3305 unique and 2470 of which were assumed as observed applying the condition $1 > 2.5\sigma$ (1). The final residual: $R = 0.056$, $R_w = 0.58$, GoF = 6.41 for 254 parameters and 2470 reflections. The largest residual electron density was 0.200 $eÅ^{-3}$.

Acknowledgements—The authors thank the National Science Council of the Republic of China for financial support (NSC84-2113-M-003-002).

REFERENCES

1. Chang, T.-T. and Chou, W.-N. (1995) *Mycol. Res.*, in press.
2. Mu, Z. and Su, Q. (1990) *Acta Botanica Yunnanco* **12**, 395.
3. Lopes, L. M. S., Yoshida, M. and Gottlieb, O. R. (1983) *Phytochemistry* **22**, 1516.
4. Kioy, D., Gray, A. I. and Waterman, P. G. (1990) *Phytochemistry* **29**, 3535.
5. Atal, C. K., Moza, P. N. and Pelter, A. (1968) *Tetrahedron Letters* **11**, 1397.
6. Burke, B. and Nair, M. (1986) *Phytochemistry* **25**, 1427.
7. Johnson, C. K. (1965) *ORTEP*, Report ORNL-3794, Oak Ridge National Laboratory, TN, U.S.A.
8. Larson, A. C., Lee, F. L., Le Page, Y., Webster, M., Charland, J.-P. and Gabe, E. J. (1990) *NRCVAX Crystal Structure System*, Chemistry Division, NRC, Ottawa, Canada.

Hindawi Publishing Corporation
Evidence-Based Complementary and Alternative Medicine
Volume 2012, Article ID 364741, 8 pages
doi:10.1155/2012/364741

Research Article

Triterpenoid-Rich Extract from *Antrodia camphorata* Improves Physical Fatigue and Exercise Performance in Mice

Chi-Chang Huang,[1] Mei-Chich Hsu,[1,2] Wen-Ching Huang,[3,4] Huei-Ru Yang,[1] and Chia-Chung Hou[3]

[1] *Graduate Institute of Sports Science, National Taiwan Sport University, Taoyuan 33301, Taiwan*
[2] *Department of Sports Medicine, Kaohsiung Medical University, Kaohsiung 80708, Taiwan*
[3] *Dong Jyu Biotechnology Corporation, Taipei 10683, Taiwan, Taiwan*
[4] *Graduate Institute of Athletics and Coaching Science, National Taiwan Sport University, Taoyuan 33301, Taiwan*

Correspondence should be addressed to Chi-Chang Huang, john5523@mail.ntsu.edu.tw
and Chia-Chung Hou, d8501002@tmu.edu.tw

Received 14 March 2012; Accepted 30 May 2012

Academic Editor: Cheorl-Ho Kim

Antrodia camphorata (AC) is an endemic mushroom that grows in Taiwan. We investigated the fatigue-alleviating effects of AC on endurance capacity in swim-exercised and weight-loading mice. Male Institute of Cancer Research (ICR) strain mice from 3 groups ($n = 10$ per group in each test) were orally administered AC fruiting body extract for 7 days at 0, 50, and 200 mg/kg/day, designated vehicle, AC-50, and AC-200, respectively. Trend analysis revealed that AC treatments increased grip strength. AC dose-dependently increased swim time, blood glucose, and muscular and hepatic glycogen levels and dose-dependently decreased plasma lactate and ammonia levels and creatine kinase activity. The increase in swimming endurance with AC administration was caused by an increase in liver and muscle glycogen deposition. *A. camphorata* may have potential for use in ergogenic and antifatigue activities.

1. Introduction

Fatigue is characterized as physical and/or mental weariness resulting in negative impacts on work performance and exercise intensity, family life, and social relationships [1]. Fatigue can be classified as secondary, physiologic, or chronic. Secondary fatigue results from disturbed sleep, depression, excess exertion, and medication side effects. Physiological fatigue is caused by inadequate rest, physical effort or mental strain [2]. Chronic fatigue syndrome involves a persistent unexplainable fatigue lasting for more than 6 months, but the etiology remains unclear [3]. Long-term physical and mental fatigue leads to health damage and chronic fatigue [4]. Physical fatigue is also called peripheral fatigue and may be accompanied by deterioration in performance [5]. Two mechanisms, oxidative stress and exhaustion, play an important role in physical fatigue [6]. Hard work or intense exercise can lead to the production and accumulation of excess reactive free radicals, which results in oxidation stress injury to the body. Exhaustion theory suggests that energy source depletion and excess metabolite accumulation lead to fatigue [7]. However, several studies have shown that exogenous antioxidants can reduce exercise-induced oxidative stress [8]. Research in specific nutrients or herbal supplements is needed to find agents that reduce metabolite production and/or improve energy utilization.

The fungus *Antrodia camphorata* is a traditional Chinese remedy used by the Taiwan aboriginal community for discomforts caused by alcohol drinking or exhaustion. It grows only on the unique, local, large, evergreen broad-leaved tree *Cinnamomum kanehirae* Hayata (Lauraceae). The fruiting bodies of *A. camphorata* are well-known but expensive medicinal material that are used in Asian countries to treat several diseases such as liver disease, tumors, intoxication, and abdominal pain [9]. The chemical and pharmacological properties of *A. camphorata* extracts from its mycelium, cultivation filtrate, and fruiting bodies have been investigated. These studies demonstrated that *A. camphorata* has extensive

bioactivities including anticancer [10], anti-inflammation [11], immunomodulation [12], and hepatoprotection [13] activities.

Herbal medicines and natural compounds have been investigated as an important resource for postponing fatigue, accelerating the elimination of fatigue-related metabolites, and improving athletic ability. For a long time *A. camphorata* has been considered a potent remedy for regulating the body balance, with few adverse effects. Although more detailed studies are needed to confirm the traditional effects in light of rational bioactivity function, *A. camphorata* may be an antifatigue herbal supplement candidate. We examined the antifatigue activities of ethanol extracts of AC fruiting bodies in mice. We further examined the possible mechanism and the active components to determine a scientific basis for use of this natural species for fatigue.

2. Materials and Methods

2.1. Plant Material. Fresh *A. camphorata* fruiting bodies were cultivated on *Cinnamonum Kanehirai* Hayata and provided by Dong Jyu Biotechnology Corp. (Taipei). All materials were identified by the Food Industry Research and Development Institute (Hsinchu, Taiwan). A voucher specimen was deposited in the Graduate Institute of Sports Science, National Taiwan Sport University (Taoyuan, Taiwan).

2.2. Extract Preparation and Identification of Index Compounds. Fresh *A. camphorata* fruiting bodies were freeze-dried and ground into powder. The dried powder (45 g) was extracted 3 times with ethanol under reflux. After filtration, the solvent was concentrated by use of a rotary evaporator to obtain the ethanol extract (15 g). Total extract was partitioned with ethyl acetate to yield an ethyl acetate fraction (14.8 g), which was chromatographed on an MCI CHP 20P column eluted with H_2O-MeOH gradient to yield 1–7 fractions. After recrystallization with acetone, antcin K (1) was isolated from fraction 2. Fraction 3 was subsequently separated on silica gel column eluted with CH_2Cl_2/MeOH gradient to give antcin C (2), antcin H (3), and dehydrosulphurenic acid (4). Fraction 4 was purified by ODS gel (H_2O-MeOH gradient) to obtain antcin I (5). Chromatography of fraction 5 over a Sephadex LH-20 column with H_2O-MeOH yielded antcin B (6) and 15α-acetyl-dehydro-sulphureic acid (7). All chemical structures were identified by nuclear magnetic resonance and mass spectral analyses and were in agreement with published data [14].

2.3. Animals and Experiment Design. Specific pathogen-free male ICR mice (5 weeks old) were purchased from BioLASCO (A Charles River Licensee Corp., Yi-Lan, Taiwan). All animals were given a standard laboratory diet (no. 5001; PMI Nutrition International, Brentwood, MO, USA) and distilled water *ad libitum* and housed at room temperature (23 ± 1°C) with a 12 h light/12 h dark cycle (lights on from 6:00 AM to 6:00 PM). All animal experiments adhered to the guidelines of the Institutional Animal Care and Use Committee (IACUC) of National Taiwan Sport University (NTSU). The IACUC ethics committee approved this study under the protocol IACUC-9903.

Mice were divided into 3 groups ($n = 10$ per group in each test) for treatment: (1) vehicle, (2) 50 mg/kg ethanol extract of AC fruiting body (AC-50), and (3) 200 mg/kg ethanol extract of AC fruiting body (AC-200). Vehicle or AC extract was given once by oral gavage for 7 days each. The control group received the same dose of vehicle.

2.4. Forelimb Grip Strength. A low-force testing system (Model-RX-5, Aikoh Engineering, Nagoya, Japan) was used to measure forelimb grip strength in mice. The force transducer equipped with a metal bar (2 mm in diameter and 7.5 cm in length) was used to measure the amount of tensile force from each mouse. As described in [15], we grasped the mouse at the base of the tail and lowered it vertically toward the bar. The mouse was pulled slightly backwards by the tail while the 2 paws (forelimbs) grasped the bar, which triggered a "counter pull." This grip strength meter recorded the grasping force in grams. Before AC administration, all mice were trained to perform this procedure for 3 days. The 3 groups did not differ in performing the activity. Grip strength was measured 1 h after the last treatment administration. The maximal force (grams) exerted by the mouse counter pull was used as forelimb grip strength.

2.5. Forced Swimming Test. The protocol was adapted from a previous study with some modifications [16]. Mice were pretreated with vehicle, AC-50, or AC-200 for 7 days and 1 h after the last treatment administration and underwent an exhaustive swimming test. The mice were placed individually in a columnar swimming pool (length 65 cm and radius 20 cm) with 40 cm water depth maintained at 37 ± 1°C. A weight equivalent to 5% of body weight was attached to the root of mouse tail, and endurance for each mouse was measured as swimming times recorded from the beginning of the time in the pool to exhaustion. The swimming period was considered the time spent floating, struggling, and making necessary movements until exhaustion and possible drowning. When the mice were unable to remain on the water surface, they were considered exhausted.

2.6. Determination of Blood Biochemical Variables. We evaluated the effects of AC on plasma lactate, ammonia, and glucose levels and creatine kinase (CK) activity after exercise. A 15 min swimming test was performed 1 h after the last treatment administration. Blood samples were collected from the submandibular duct of pretreated mice after the 15 min swimming test. The plasma was prepared by centrifugation at 1500 ×g, 4°C for 10 min. Lactate, ammonia, and glucose levels and CK activity were determining by use of an autoanalyzer (Hitachi 7060, Hitachi, Japan).

2.7. Tissue Glycogen Determination. To investigate whether AC increases glycogen deposition in target tissues, mice were pretreated with vehicle, AC-50, and AC-200 for 7 days and

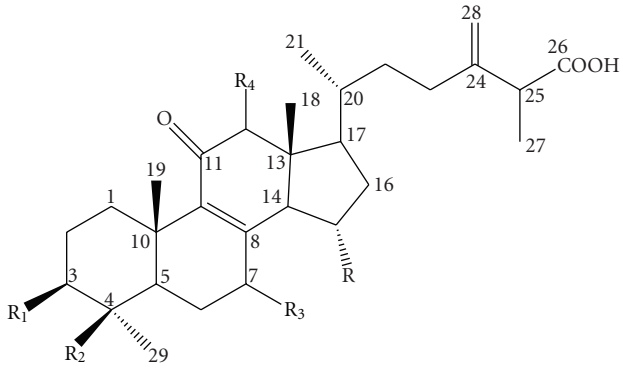

	R_1	R_2	R_3	R_4
Antcin B	=O	H	=O	H
Antcin I	α−OH	H	=O	H
Antcin H	α−OH	H	=O	α−OH
Antcin C	=O	β−H	β−OH	H
Antcin K	α−OH	β−OH	β−OH	H

(a)

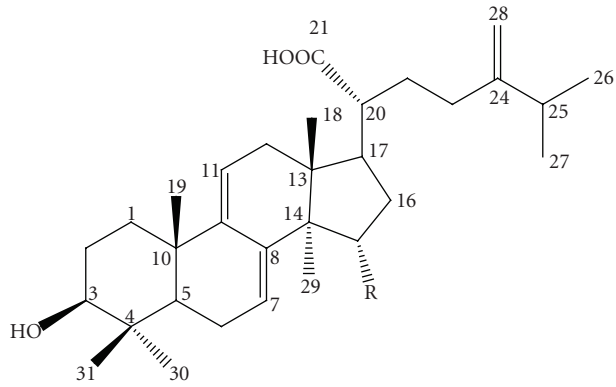

	R
Dehydrosulphurenic acid	OH
15α-Acetyl-dehydrosulphurenic acid	OAc

(b)

Figure 1: Chemical structure of identified triterpenoids from *Antrodia camphorata.*

1 h after the last treatment administration and the liver and muscle were excised and weighed for tissue glycogen level analysis. The muscular and hepatic glycogen levels were measured as described in [17]. For each mouse, 100 mg of liver and muscle was finely cut, weighed, and homogenized in 0.5 ml cold perchloric acid. The homogenate was centrifuged for 15 min at 15000 ×g at 4°C. The supernatant was carefully decanted and kept on ice. A standard glycogen (Sigma) or tissue extract, 30 μL, was added to 96-well microplates, and iodine-potassium iodide reagent, 200 μL, was added to each well for binding iodine to glycogen. An amber-brown compound developed immediately after the reaction. Absorbance was measured at wavelength 460 nm with use of an ELISA reader (Tecan Infinite M200, Tecan Austria, Austria) after the material rested for 10 min.

2.8. Histopathology of Liver Tissues. Fresh liver tissues were embedded in OCT compound (Tissue-Tek 4583, Sakura Finetek, Torrance, CA, USA), then sectioned at 4 μm by use of a cryostat microtome (Leica CM3050S, Leica Microsystems, Nussloch GmbH, Nussloch, Germany), and stained with periodic acid Schiff (PAS) as we described [18]. Specimens were photographed using a SPOT Idea 3MP camera on an Olympus CKX41 inverted microscope.

2.9. Statistical Analysis. Data are expressed as mean ± SEM and analyzed by one-way AVOVA with SAS version 9.0 (SAS Inst., Cary, NC). $P < 0.05$ was considered statistically significant. A Cochran-Armitage test was used for dose-effect trend analysis.

3. Results

3.1. Identification of Chemical Constituents of A. camphorata. Repeated-column chromatography of EtOH extracts of the fruiting body of *A. camphorata* on highly porous polymer gel and silica gel revealed 7 compounds. The structures were elucidated by spectroscopic analysis and compared with the literature [14]. Figure 1 shows the predominant constituents, identified as antcin B, C, H, I, K (ergostane-type triterpenoids) and dehydrosulphurenic acid, 15α-acetyl-dehydrosulphurenic acid (lanostane-type triterpenoids).

3.2. Effect of A. camphorata on Mouse Forelimb Grip Strength. The grip strength of mice in the vehicle, AC-50, and AC-200 groups was 125 ± 5, 142 ± 1, and 142 ± 4 g, respectively (Figure 2), which was significantly higher, by 1.13-fold ($P = 0.005$), with AC than vehicle treatment. Grip strength was increased dose dependently with AC but not significantly ($P = 0.066$).

3.3. Effect of A. camphorata on Mouse Exercise Capacity by Forced Swim Test. The endurance of mice administered vehicle, AC-50, and AC-200 was 70.9 ± 15.7, 113.6 ± 12.1, and 152.8 ± 9.8 min, respectively (Figure 3). The swimming time was significantly longer by 1.60- ($P = 0.016$) and 2.15-fold ($P < 0.0001$) with AC-50 and AC-200, respectively, than vehicle treatment. Endurance was greater with AC-200 than AC-50 treatment ($P < 0.05$). Trend analysis revealed a significant dose-dependent effect with vehicle, AC-50, and AC-200 on swimming time ($P < 0.0001$).

3.4. Effect of A. camphorata on Mouse Plasma Lactate, Ammonia, and Glucose Levels and CK Activity with Exercise. Lactate levels in the vehicle, AC-50 and AC-200 groups

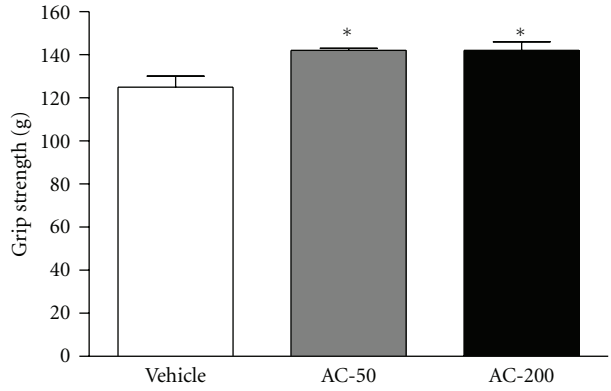

Figure 2: Effect of *A. camphorata* (AC) supplementation on forelimb grip strength in mice. Male ICR mice were pretreated with vehicle or 50 or 200 mg/kg ethanol extract of AC fruiting body (AC-50 or AC-200) for 7 days and then 1 h later underwent a low-force grip-strength test. Data are mean ± SEM ($n = 10$ mice). $^*P < 0.01$ compared to vehicle control.

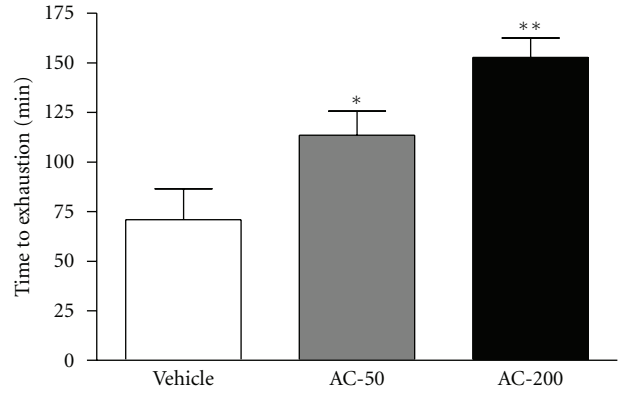

Figure 3: Effect of AC on swim exercise performance in mice. Mice were pretreated with vehicle, AC-50, or AC-200 for 7 days and then 1 h later underwent an exhaustive swimming test with a 5% body-weight load attached to the mouse tail. Data are mean ± SEM ($n = 10$ mice). $^*P < 0.05$, $^{**}P < 0.001$ compared to vehicle control.

were 7.5 ± 0.4, 5.9 ± 0.4, and 5.2 ± 0.3 mmol/L, respectively (Figure 4(a)), and were significantly lower, by 21% ($P = 0.0046$) and 31% ($P < 0.0001$), with AC-50, and AC-200, respectively, than vehicle treatment.

Plasma ammonia levels in the vehicle, AC-50, and AC-200 groups were 438 ± 18, 283 ± 20, and 257 ± 15 μmol/L, respectively (Figure 4(b)), and were significantly lower, by 35% and 41%, with AC-50 and AC-200, respectively, than vehicle treatment ($P < 0.0001$).

Plasma glucose content in the vehicle, AC-50, and AC-200 groups was 164 ± 9, 183 ± 8, and 213 ± 14 mg/dL, respectively (Figure 4(c)), and was significantly higher, by 1.3-fold ($P = 0.0035$), with AC-200 than vehicle treatment.

Plasma CK activity, a muscular damage marker, in the vehicle, AC-50, and AC-200 groups was 56 ± 8, 133 ± 3 and 26 ± 2 U/L, respectively (Figure 4(d)), and was significantly lower, by 41% ($P = 0.0038$) and 54% ($P = 0.0003$), with AC-50 and AC-200, respectively, than vehicle treatment. Trend analysis revealed that AC treatment had a significant dose-dependent effect on increasing blood glucose ($P = 0.0003$) content and decreasing plasma lactate and ammonia levels and CK activity (all $P < 0.0001$).

3.5. Effect of A. camphorata on Mouse Muscular and Hepatic Glycogen Levels. Muscular glycogen levels in the vehicle, AC-50, and AC-200 groups were 1.72 ± 0.05, 2.07 ± 0.08, and 2.20 ± 0.21 mg/g skeletal muscle, respectively (Figure 5(a)), and were significantly higher, by 1.20- ($P = 0.0010$) and 1.28-fold ($P < 0.0001$), with AC-50 and AC-200, respectively, than vehicle treatment.

Hepatic glycogen levels in the vehicle, AC-50, and AC-200 groups were 14.28 ± 2.26, 20.70 ± 1.64, and 20.70 ± 1.64 mg/g liver, respectively (Figure 5(b)), and were significantly higher, by 1.45- ($P = 0.0213$) and 1.51-fold ($P = 0.0098$), with AC-50 and AC-200, respectively, than vehicle treatment. Trend analysis revealed that AC treatment had a significant dose-dependent effect on increasing muscular ($P < 0.0001$) and hepatic glycogen levels ($P = 0.0034$).

PAS staining is used to detect glycogen in tissues. Liver sections with AC-50 and AC-200 treatment showed a significantly greater number of PAS-positive hepatocytes than those with vehicle treatment, which suggests glycogen accumulation in AC-50 and AC-200 hepatocytes (Figure 5(c)). Thus, AC treatment significantly increased glycogen deposition in liver tissues.

4. Discussion

Many natural sources have been studied as supplements to improve fatigue symptoms. These studies focused on plant extracts and emphasized the importance of phytocompounds such as polysaccharides [19], flavonoids [20], and peptides [7]. In this study, we compared the fatigue-alleviating effects of 2 doses of *A. camphorata* and vehicle on endurance in exercised and weight-loading mice. Ethanol extract of *A. camphorata* fruiting bodies dose-dependently enhanced exercise performance and reduced muscle fatigue physiological indexes; so *A. camphorata* may have ergogenic and antifatigue functions.

The energy metabolism of muscular activity determines the level of physiological fatigue [21]. Exercise endurance is an important variable in evaluating antifatigue treatment. In our mice, forelimb grip strength was significantly elevated, by 1.13-fold with both AC doses. Regulatory training programs are needed for grip strength elevation, so we observed no difference between the doses. However, in the exhaustive physical-exercise swim test, maximal swimming time was increased dose-dependently with the AC doses (Figure 2). Both results show an elevation in exercise endurance in mice, which suggests that *A. camphorate* ethanol extract has antifatigue effects.

Biochemical variables, including lactate, ammonia (NH_3), glucose, and CK, are important indicators of muscle fatigue after exercise [22]. The muscle produces a great quantity of lactate when it obtains enough energy from anaerobic glycolysis during high-intensity exercise.

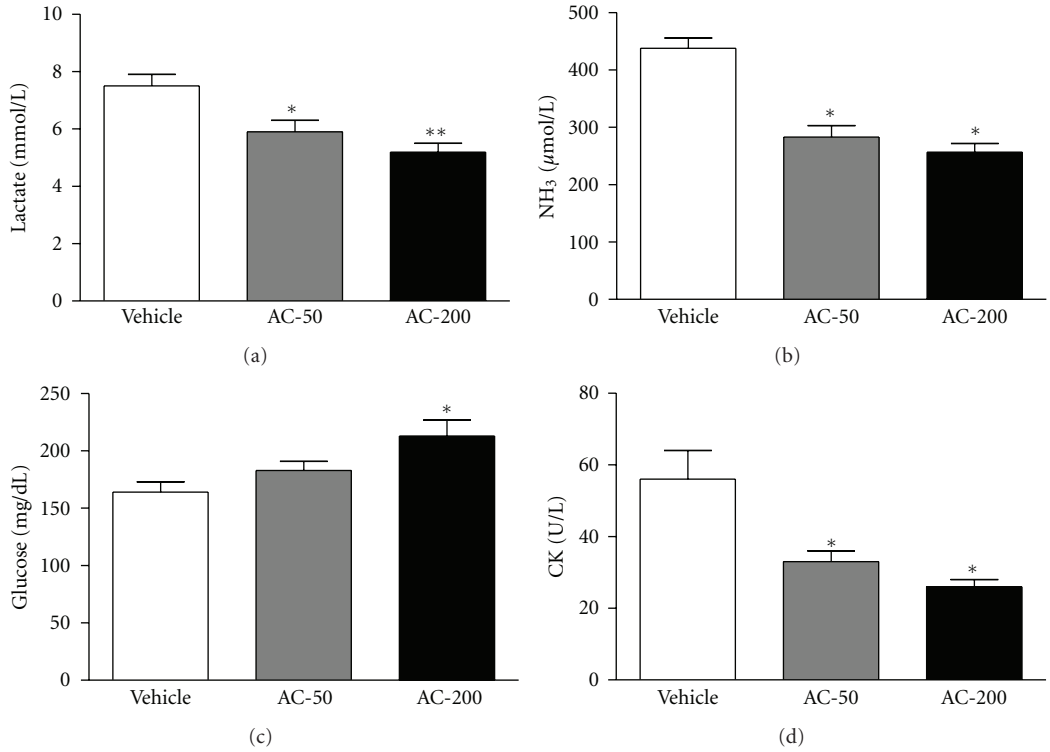

Figure 4: Effect of AC on plasma lactate, ammonia, and glucose levels and creatine kinase (CK) activity after exercise. Mice were pretreated with vehicle, AC-50, or AC-200 for 7 days and then 1 h later underwent a 15 min swim test. Data are mean ± SEM ($n = 10$ mice). (a) Lactate: $^*P < 0.005$, $^{**}P < 0.0001$ compared to vehicle control. (b) Ammonia: $^*P < 0.0001$ compared to vehicle control. (c) Glucose: $^*P < 0.05$ compared to vehicle control. (d) CK: $^*P < 0.005$ compared to vehicle control.

The increased lactate level further reduces pH value, which could induce various biochemical and physiological side effects, including glycolysis and phosphofructokinase and calcium ion release, through muscular contraction [23]. Ammonia, the metabolite of protein and amino acid, was linked to fatigue as early as 1922 [24]. The increase in ammonia in response to exercise can be managed by the use of amino acids or carbohydrates that interfere with ammonia metabolism [25]. The increase in ammonia level is related to both peripheral and central fatigue during exercise. Energy storage and supply is another important factor related to exercise performance. In terms of energy expenditure with exercise, rapid ATP consumption and energy deficiency is a critical cause of physical fatigue [26]. Skeletal muscle mainly catabolizes fat and carbohydrates as sources of energy during exercise. Glycogen is the predominant source of glycolysis for ATP production. Therefore, glycogen storage directly affects exercise ability [27]. After we administered AC or vehicle to mice for 7 days, serum lactate and ammonia levels were notably lower with AC than vehicle treatment after the swim test. Therefore, AC should enhance lactate and ammonia elimination. Additionally, both hepatic and muscular glycogen levels were increased in response to AC treatments. These results illuminate the release of glucose from tissue glycogen for energy recovery with AC and the statistical significance on trend analysis after exercise.

CK, a muscular damage index, was significantly ameliorated dose-dependently with AC treatment on trend analysis. High-intensity exercise challenge could physically or chemically cause tissue damage. It can cause sacromeric damage and muscular cell necrosis [28]. The cells release specific proteins such as CK and myoglobin into the blood as muscular damage indexes. Clinically, CK is assayed in blood tests as a marker of myocardial infarction, rhabdomyolysis (severe muscle breakdown), muscular dystrophy, autoimmune myositides, and acute renal failure [28].

To clarify the components contributing to the AC antifatigue function, we separated AC extracts to identify the index compounds and found a great proportion of triterpenoid compounds. We identified about 78 compounds, including polysaccharides, benzenoids, diterpenes, triterpenoids, steroids, and maleic/succinic acid derivatives [9]. Previous studies demonstrated triterpenoids as the predominant constituents in fruiting bodies of *A. camphorata*, with its bioactivity widely studied in antitumor research [10]. Triterpenoids are an important bioactive class of natural products with diverse structures. They are synthesized from isopentenyl pyrophosphate through the 30-carbon intermediate squalene; the major skeleton types include oleananes, ursanes, lupanes, protostanes, lanostanes, and dammaranes [29]. More than 20,000 compounds have been reported. Although their functions and promising biological properties have received considerable attention, studies of the relationship of triterpenoids and antifatigue activity are still limited. Pentacyclic triterpenoid-enriched extracts from Chinese bamboo shavings were

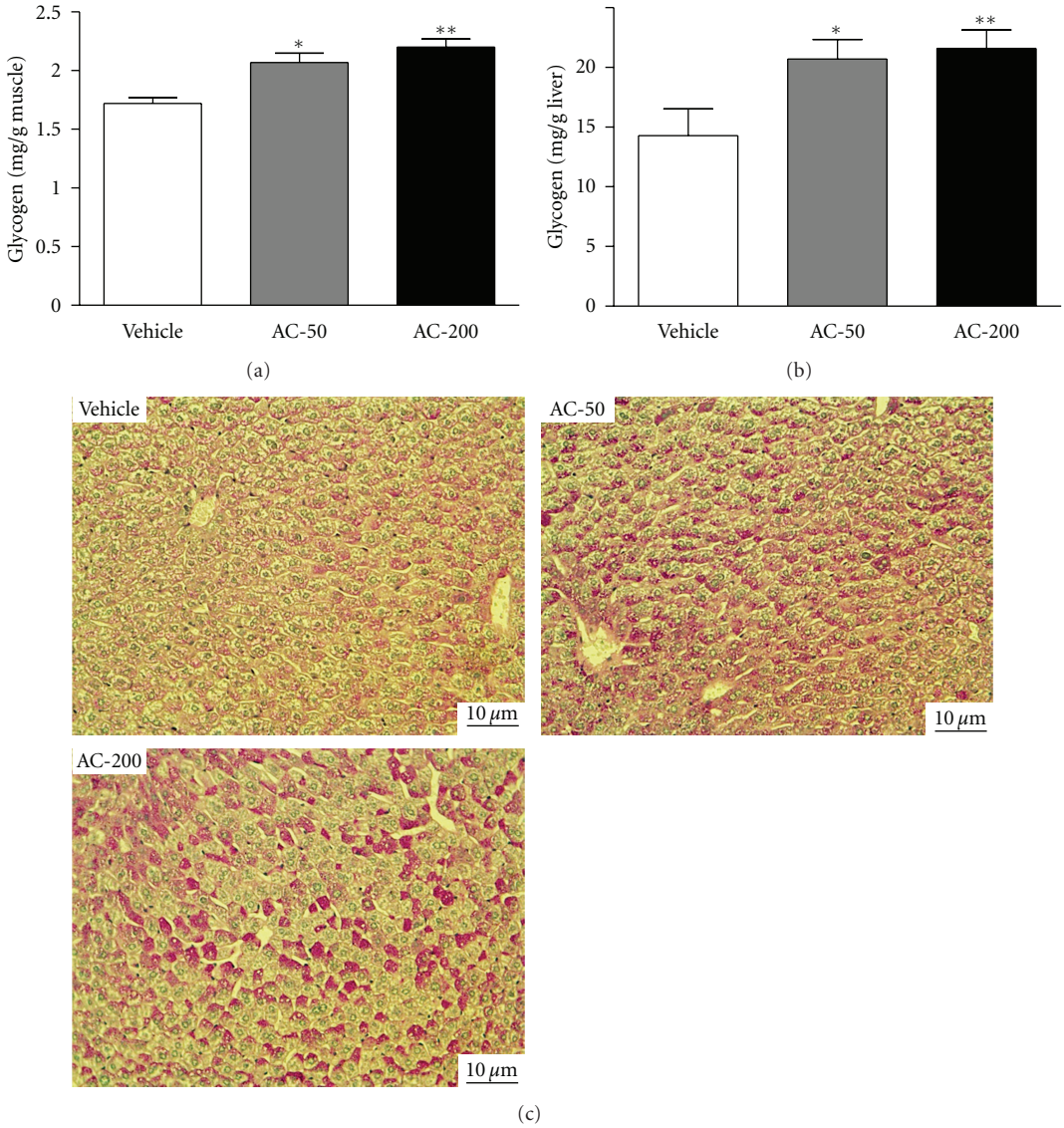

Figure 5: Effect of AC on muscular and hepatic glycogen levels. Mice were pretreated with vehicle, AC-50, or AC-200 for 7 days and then killed 1 h later. Glycogen levels in muscle and liver tissues were determined. Data are mean ± SEM ($n = 10$ mice). (a) Skeletal muscle glycogen: $^{*}P < 0.005$, $^{**}P < 0.0001$ compared to vehicle control. (b) Liver glycogen: $^{*}P < 0.05$, $^{**}P < 0.005$ compared to vehicle control. (c) Light micrographs of liver tissue hepatocytes stained with periodic acid-Schiff (PAS) (magnification ×200; scale bar, 10 μm).

recently shown to have antifatigue activities [30]. We found ergostane and lanostane skeleton triterpenoids in the bioactive *A. camphorata* extract. Ergostane-type triterpenoids are specific to the fruiting body of *A. camphorata*. These ergostane and lanostane triterpenoids may therefore be important antifatigue active components in *A. camphorata*.

In conclusion, ethanol extracts of the fruiting body of *A. camphorata* have antifatigue activity by decreasing plasma lactate and ammonia levels and increasing blood glucose concentration and liver and muscle glycogen deposition, thereby elevating exercise performance in mice. We identified putative bioactive components in these extracts. Although the detailed antifatigue mechanisms of *A. camphorata* remain to be elucidated, this study provides science-based evidence to support traditional claims of antifatigue results with *A. camphorata* treatment and suggests a use for *A. camphorata* as an ergogenic and antifatigue agent.

Conflict of Interests

All authors have no conflicts of interests with respect to the data collected and procedures used within this study.

Authors' Contribution

M.-C. Hsu and W.-C. Huang contributed equally to this work.

Acknowledgments

The authors are grateful to Dr. Hsiao-Li Chuang, National Laboratory Animal Center, National Applied Research Laboratories, for technical assistance in histological examination. They thank their colleague, Dr. Chin-Shan Ho, for technical assistance in measuring forelimb grip strength. The authers also thank Laura Smales for editing the manuscript. The present study was funded by the University-Industry Cooperation Fund no. 991035 (National Taiwan Sport University, Taoyuan, Taiwan).

References

[1] R. K. Mehta and M. J. Agnew, "Influence of mental workload on muscle endurance, fatigue, and recovery during intermittent static work," *European Journal of Applied Physiology*. In press.

[2] R. F. Brown and N. S. Schutte, "Direct and indirect relationships between emotional intelligence and subjective fatigue in university students," *Journal of Psychosomatic Research*, vol. 60, no. 6, pp. 585–593, 2006.

[3] K. Fukuda, S. E. Straus, I. Hickie, M. C. Sharpe, J. G. Dobbins, and A. Komaroff, "The chronic fatigue syndrome: a comprehensive approach to its definition and study," *Annals of Internal Medicine*, vol. 121, no. 12, pp. 953–959, 1994.

[4] T. J. Lowry and K. I. Pakenham, "Health-related quality of life in chronic fatigue syndrome: predictors of physical functioning and psychological distress," *Psychology, Health and Medicine*, vol. 13, no. 2, pp. 222–238, 2008.

[5] R. H. Fitts, "Cellular mechanisms of muscle fatigue," *Physiological Reviews*, vol. 74, no. 1, pp. 49–94, 1994.

[6] J. S. Coombes, B. Rowell, S. L. Dodd et al., "Effects of vitamin E deficiency on fatigue and muscle contractile properties," *European Journal of Applied Physiology*, vol. 87, no. 3, pp. 272–277, 2002.

[7] L. You, M. Zhao, J. M. Regenstein, and J. Ren, "In vitro antioxidant activity and in vivo anti-fatigue effect of loach (*Misgurnus anguillicaudatus*) peptides prepared by papain digestion," *Food Chemistry*, vol. 124, no. 1, pp. 188–194, 2011.

[8] X. Zheng, W. Long, G. Liu, X. Zhang, and X. Yang, "Effect of seabuckthorn (*Hippophae rhamnoides* ssp. sinensis) leaf extract on the swimming endurance and exhaustive exercise-induced oxidative stress of rats," *Journal of the Science of Food and Agriculture*, vol. 92, no. 4, pp. 736–742, 2012.

[9] Y. M. Tzeng and M. Geethangili, "Review of pharmacological effects of *Antrodia camphorata* and its bioactive compounds," *Evidence-Based Complementary and Alternative Medicine*, vol. 2011, Article ID 212641, 2011.

[10] Y. C. Hsieh, Y. K. Rao, J. Whang-Peng et al., "Antcin B and its ester derivative from *Antrodia camphorata* induce apoptosis in hepatocellular carcinoma cells involves enhancing oxidative stress coincident with activation of intrinsic and extrinsic apoptotic pathway," *Journal of Agricultural and Food Chemistry*, vol. 59, no. 20, pp. 10943–10954, 2011.

[11] G. J. Huang, S. S. Huang, S. S. Lin et al., "Analgesic effects and the mechanisms of anti-inflammation of ergostatrien-3β-ol from *Antrodia camphorata* submerged whole broth in mice," *Journal of Agricultural and Food Chemistry*, vol. 58, no. 12, pp. 7445–7452, 2010.

[12] J. M. Chang, Y. R. Lee, L. M. Hung et al., "An extract of *Antrodia camphorata* mycelia attenuates the progression of nephritis in systemic lupus erythematosus-prone NZB/W F1 mice," *Evidence-Based Complementary and Alternative Medicine*, vol. 2011, Article ID 465894, 2011.

[13] G. J. Huang, J. S. Deng, S. S. Huang, Y. Y. Shao, C. C. Chen, and Y. H. Kuo, "Protective effect of antrosterol from *Antrodia camphorata* submerged whole broth against carbon tetrachloride-induced acute liver injury in mice," *Food Chemistry*, vol. 132, no. 2, pp. 709–716, 2012.

[14] S. W. Yang, Y. C. Shen, and C. H. Chen, "Steroids and triterpenoids of *Antrodia cinnamomea*—a fungus parasitic on *Cinnamomum micranthum*," *Phytochemistry*, vol. 41, no. 5, pp. 1389–1392, 1996.

[15] X. Li, S. Mohan, W. Gu, J. Wergedal, and D. J. Baylink, "Quantitative assessment of forearm muscle size, forelimb grip strength, forearm bone mineral density, and forearm bone size in determining humerus breaking strength in 10 inbred strains of mice," *Calcified Tissue International*, vol. 68, no. 6, pp. 365–369, 2001.

[16] R. D. Porsolt, M. Le Pichon, and M. Jalfre, "Depression: a new animal model sensitive to antidepressant treatments," *Nature*, vol. 266, no. 5604, pp. 730–732, 1977.

[17] V. Chamberland and P. Rioux, "Not only students can express alcohol dehydrogenase: goldfish can too!," *Advances in Physiology Education*, vol. 34, no. 4, pp. 222–227, 2010.

[18] H. L. Chuang, Y. T. Huang, C. C. Chiu et al., "Metabolomics characterization of energy metabolism reveals glycogen accumulation in gut-microbiota-lacking mice," *Journal of Nutritional Biochemistry*, vol. 23, no. 7, pp. 752–758, 2012.

[19] J. Wang, S. Li, Y. Fan et al., "Anti-fatigue activity of the water-soluble polysaccharides isolated from *Panax ginseng* C. A. Meyer," *Journal of Ethnopharmacology*, vol. 130, no. 2, pp. 421–423, 2010.

[20] F. R. Yu, Y. Liu, Y. Z. Cui et al., "Effects of a flavonoid extract from *Cynomorium songaricum* on the swimming endurance of rats," *American Journal of Chinese Medicine*, vol. 38, no. 1, pp. 65–73, 2010.

[21] N. Belluardo, H. Westerblad, G. Mudó et al., "Neuromuscular junction disassembly and muscle fatigue in mice lacking neurotrophin-4," *Molecular and Cellular Neuroscience*, vol. 18, no. 1, pp. 56–67, 2001.

[22] P. Brancaccio, N. Maffulli, and F. M. Limongelli, "Creatine kinase monitoring in sport medicine," *British Medical Bulletin*, vol. 81-82, no. 1, pp. 209–230, 2007.

[23] S. P. Cairns, "Lactic acid and exercise performance: culprit or friend?" *Sports Medicine*, vol. 36, no. 4, pp. 279–291, 2006.

[24] S. Tashiro, "Studies on alkaligenesis in tissues: I. Ammonia production in the nerve fiber during excitation," *American Journal of Physiology*, vol. 60, no. 3, pp. 519–543, 1922.

[25] E. S. Prado, J. M. de Rezende Neto, R. D. de Almeida, M. G. Dória de Melo, and L. C. Cameron, "Keto analogue and amino acid supplementation affects the ammonaemia response during exercise under ketogenic conditions," *British Journal of Nutrition*, vol. 105, no. 12, pp. 1729–1733, 2011.

[26] K. Sahlin, M. Tonkonogi, and K. Söderlund, "Energy supply and muscle fatigue in humans," *Acta Physiologica Scandinavica*, vol. 162, no. 3, pp. 261–266, 1998.

[27] A. J. Young and J. W. Castellani, "Exertion-induced fatigue and thermoregulation in the cold," *Comparative Biochemistry and Physiology*, vol. 128, no. 4, pp. 769–776, 2001.

[28] G. L. Warren, C. P. Ingalls, D. A. Lowe, and R. B. Armstrong, "Excitation-contraction uncoupling: major role in contraction-induced muscle injury," *Exercise and Sport Sciences Reviews*, vol. 29, no. 2, pp. 82–87, 2001.

[29] A. Petronellia, G. Pannitterib, and U. Testaa, "Triterpenoids as new promising anticancer drugs," *Anti-Cancer Drugs*, vol. 20, no. 10, pp. 880–892, 2009.

[30] Y. Zhang, X. Yao, B. Bao, and Y. Zhang, "Anti-fatigue activity of a triterpenoid-rich extract from chinese bamboo shavings (*Caulis bamfusae* in taeniam)," *Phytotherapy Research*, vol. 20, no. 10, pp. 872–876, 2006.

Pergamon

0031-9422(95)00767-9

Phytochemistry, Vol. 41, No. 5, pp. 1389 1392, 1996

0031-9422/96 $15.00 + 0.00

STEROIDS AND TRITERPENOIDS OF *ANTRODIA CINNAMOMEA*—A FUNGUS PARASITIC ON *CINNAMOMUM MICRANTHUM*

SHU-WEI YANG,* YA-CHING SHEN†‡ and CHUNG-HSIUNG CHEN*‡

*School of Pharmacy, National Taiwan University, Taipei, Taiwan, Republic of China; †Institute of Marine Resources, National Sun Yat-sen University, 70 Lien-Hai Rd, Kaohsiung, Taiwan, Republic of China

(*Received* 15 *June* 1995)

Key Word Index—*Antrodia cinnamomea*; Polyporaceae; steroids; zhankuic acids D, E; triterpenoids; 15α-acetyl-dehydrosulphurenic acid; dehydroeburicoic acid; dehydrosulphurenic acid.

Abstract—Two ergostane related steroids, zhankuic acids D and E together with three lanosta related triterpenes, 15α-acetyl-dehydrosulphurenic acid, dehydroeburicoic acid, dehydrosulphurenic acid were isolated from the fruit body of the fungus *Antrodia cinnamomea*. Their structures were determined by spectral analyses and comparison with known compounds.

INTRODUCTION

Antrodia cinnamomea Chang & Chou, sp. nov. (Zhan-Ku, family Polyporaceae, Aphyllophorales) is a new and exclusive fungus parasitic on the inner wall of the endemic species *Cinnamomum micranthum* (Hayata) Hayata [1]. It has been used for the treatment of food, alcohol and drug intoxication, diarrhoea, abdominal pain, hypertension, skin itches and liver cancer in Chinese folk medicine [2]. Preliminary pharmacological studies revealed that the ethanolic extract of this fungus possessed significant anti-serotonin and anticholinergic activities. In addition, the crude extract of the fruit bodies showed cytotoxicity against P 388 murine leukaemia cells at 4 $\mu g\,ml^{-1}$. Chemical investigation revealed that *Antrodia cinnamomea* was rich in steroids and triterpene acids. The pharmacological activities and the chemical constituents of crude extract of Zhan-Ku are quite different from those reported for *Ganoderma lucidum* [3, 4]. Recently, three new ergosteroids named antcins, A, B and C were isolated and structures elucidated [5]. Among them, antcin A was confirmed by X-ray crystallographic analysis. In a previous communication we have isolated and elucidated three new ergosteroids, zhankuic acids, A (**1**), B (**3**) and C (**4**) from the fruit body of *Antrodia cinnamomea* [6]. Herein, we wish to report the isolation and structural elucidation of five additional compounds, zhankuic acids D (**2**) and E (**5**), 15α-acetyl-dehydrosulphurenic acid (**6**) dehydroeburicoic acid (**7**) and dehydrosulphurenic acid (**8**) from this fungus.

‡Authors to whom correspondence should be addressed.

RESULTS AND DISCUSSION

As reported in our previous paper, the ethyl acetate-soluble material of the ethanol extract of *Antrodia cinnamomea* was chromatographed on Sephadex LH-20 and silica gel columns. Four new compounds designated zhankuic acid D (**2**), zhankuic acid E (**5**), dehydrosulphurenic acid (**8**) and 15α-acetyl-dehydrosulphurenic acid (**6**) were isolated and characterized in addition to three previously isolated steroid acids, zhankuic acids, A (**1**), B (**3**) and C (**4**). One more known compound was identified as dehydroeburicoic acid (**7**) by spectral comparison with authentic sample.

The molecular formulas of zhankuic acid D (**2**) ($C_{31}H_{45}O_5$) and E (**5**) ($C_{31}H_{47}O_6$) were established by ^{13}C NMR and DEPT as well as EI-mass spectra of **2** and **5**, respectively. The ^1H NMR spectra of Zhankuic acid D (**2**) and E (**5**) were very closely related to those of zhankuic acid A (**1**) and C (**4**), respectively. Studies of the mass fragmentation indicated that compound **2** was an analogue of **1** and compound **5** was an analogue of **4**. The molecular ion peaks at *m/z* 496 and *m/z* 514, respectively in the EI-mass spectra of **2** and **5** suggested that both compounds contained an ethyl moiety in the side chain. The ^1H NMR spectra of both **2** and **5** exhibited a quartet (2H, δ4.1, $J = 7.1$) and a triplet (3H, δ1.20, $J = 7.1$) indicating that **2** and **5** were 2,6-ethyl ester derivatives of **1** and **4**, respectively. These findings were supported by ^{13}C NMR spectra of **2** and **5**, which showed corresponding carbon signals of ester groups at δ14.2 (*q*), δ60.5 (*t*) and δ174.5 (*s*). Both **2** and **5** might be the artefacts from the esterification products of **1** and **4** in the procedure of fractionation.

Compounds **6**–**8** showed identical UV absorption pattern (250, 243, 237 nm) indicating that these compounds

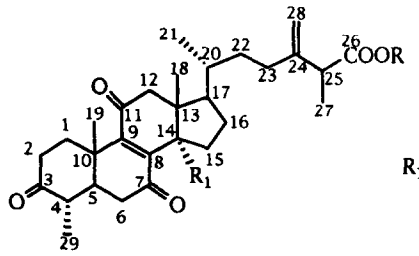

1 R= R_1= H

2 R= CH_2CH_3 R_1= H

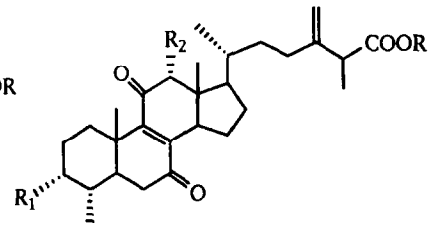

3 R= H R_1= OH R_2= H

4 R= H R_1= R_2= OH

5 R= CH_2CH_3 R_1= R_2= OH

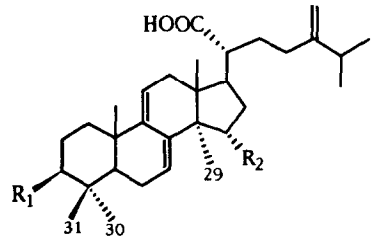

6 R_1= OH R_2= OAc

7 R_1= OH R_2= H

8 R_1= R_2= OH

9 R_1= OAc R_2= H

shared a common hetero-annular conjugated diene chromophore in the skeleton [7]. The molecular formulas of **6–8** ($C_{33}H_{50}O_5$, $C_{31}H_{48}O_3$, $C_{31}H_{48}O_4$) were established by high resolution EI-mass spectra, which showed molecular ions at *m/z* 526, 468 and 484, respectively. In addition, compounds **6–8** shared a common side chain fragment ($C_9H_{15}O_2$). This fragmentation pattern is quite similar to those reported for 24-methylene-containing triterpenoids [8, 9]. The ^{1}H NMR, ^{13}C NMR and DEPT spectra of **7** indicated the presence of four olefinic protons (δ5.49, 5.32, 4.51, 4.59) and carbons (δ121.3 *d*, 142.9 *s*, 146.7 *s*, 116.7 *d*), two secondary methyls (δ0.96 *d*, 0.95 *d*), five tertiary methyls (δ0.47 *s*, 0.83 *s*, 0.70 *s*, 0.73 *s*, 0.80 *s*), and an oxymethine proton (δ3.04) and carbon (δ78.1 *d*). It was suggested that the data of compound 7 was closely related to those reported for 24-methylenelanosta-7, 9(11)-diene-3β-ol [9]. However, the absence of a C-21 methyl doublet in **7** and the presence of a carboxylic acid carbon (δ 178.3) as well as formation of a monoacetate (**9**) suggested that compound **7** was dehydroeburicoic acid, which is a known compound reported in 1951 [10]. The assignment of ^{1}H NMR data was completed by the application of a COSY experiment on compound **9**. The ^{1}H and ^{13}C NMR data are listed in the Experimental section. The ^{1}H and ^{13}C NMR spectra of **8** exhibited signals similar to those of compound **7** suggesting a close analogue. The only difference between **8** and **7** is that compound **8** contained two oxymethine carbons (δ 78.1 *d*, 73.8 *d*) and protons (δ 3.44, 4.80) instead of one in **7**. The location of the second hydroxyl was determined at C-15 due to the down-field shifts of C-14 and C-16. The configuration of the C-15 hydroxyl was determined as α due to the γ-effect of C-29 (upfield shift $\Delta\delta = -7.7$ compared with the corresponding signal in **7**). Thus, compound **8** was identified as dehydrosulphurenic acid, a new compound from natural source [11].

Compound **6** is a new analogue of compound **8**. The fragment ion peak at *m/z* 466 in the EI-mass spectrum of **6** indicated the presence of an acetoxyl group in **6**. The ^{1}H and ^{13}C NMR spectra of **6** were superimposable on those of **8**. The location of the acetoxy group was determined as the C-15 position due to the downfield shift

(+ 2.9 ppm) of C-15 and upfield shift (− 1.5 and − 3.8 ppm, respectively) of C-14 and C-16 when compared with those of compound **8**. Based on spectral evidence, compound **6** was established as 15α-acetoxy-24-methylene-lanosta-7,9(11)-dien-3β-ol-21-oic acid.

EXPERIMENTAL

General. Mps uncorr. and were determined on a Fisher–Johns melting point apparatus. Optical rotations were measured on a JASCO DIP-360 polarimeter. UV and IR spectra were taken with a Hitachi 150-120 and a JASCO A-100 IR spectrometers, respectively. The HREI-MS data were recorded on MAT 112S-JMS D300 and JEOL JMS-HX 110 spectrometers. ^{1}H- and ^{13}C NMR spectra were taken on a Bruker 300 AM spectrometer using TMS as internal standard.

Plant material. The fruit bodies of *Antrodia cinnamomea* were purchased from Ti-hua street in Taipei, 1987. A voucher specimen was preserved in the Institute of Marine Resources, National Sun Yat-sen University.

Extraction and isolation. The fourth fr. (3.3 g) obtained from LH-20 Sephadex column as reported previously [5] was chromatographed on a silica gel column with the solvent mixt. of MeOH and $CHCl_3$ (1%, 2%, 4%, and 8%) to give fr. *d* (53 mg). Purification of fr. *d* by prep. TLC provided 15-acetyl dehydroeburicoic acid (**6**, 13 mg). The third fr. (19 g) was chromatographed on a silica gel column using the same solvent system of increasing polarity to give 14 frs. Zhankuic acid D (**2**, 50 mg), E (**5**, 15 mg) and dehyrdrosulphurenic acid (**8**, 20 mg) were obtained from frs 1, 5 and 6, respectively, by using prep. TLC plates. Dehydroeburicoic acid (**7**, 50 mg) was furnished from fr. 3 by trituating the residue with Me_2CO followed by recrystallization.

Zhankuic acid D (**2**). Pale yellow needle crystals, UV λ_{max}^{MeOH}: 244 nm (log ε 3.6); IR ν_{max}^{KBr} cm^{-1}: 2976, 2938, 1733, 1712, 1650, 1459, 1378, 1375, 1239, 1189, 1183, 903; ^{1}H NMR (300 MHz, $CDCl_3$): δ 1.40 (1H, H-1α), 3.04 (1H, H-1β), 2.42 (1H, H-2), 2.50 (1H, H-2), 2.43 (1H, H-4), 1.86 (1H, H-5), 2.4 (1H, H-6α), 2.5 (1H, H-6β), 2.38 (1H, *brd*, J = 14 Hz, H-12α), 2.91 (1H, *d*, J = 14 Hz, H-12β), 2.62 (1H, *dd*, J = 11.9, 7.3 Hz, H-14), 1.4 (1H, H-15), 2.46 (1H, H-15), 1.2 (1H, H-16), 1.95 (1H, H-16), 1.4 (1H, H-17), 0.67 (3H, *s*, H-18), 1.50 (3H, *s*, H-19), 1.4 (1H, H-20), 0.91 (3H, *d*, J = 5.3 Hz, H-21), 1.19 (1H, *m*, H-22), 1.55 (1H, H-22), 1.92 (1H, H-23), 2.13 (1H, *m*, H-23), 3.08 (1H, *q*, J = 7.0 Hz, H-25), 1.23 (3H, *d*, J = 7.0 Hz, H-27), 4.84 (1H, *brs*, H-28a), 4.89 (1H, *d*, J = 4.0 Hz, H-28b), 1.01 (3H, *d*, J = 6.6 Hz, H-29), 4.10 (2H, *q*, J = 7.1 Hz, $OC\underline{H}_2CH_3$), 1.21 (3H, *t*, J = 7.1 Hz, $OCH_2C\underline{H}_3$); ^{13}C NMR (75 MHz, $CDCl_3$): δ 34.7 (*t*, C-1), 37.5 (*t*, C-2), 210.8 (*s*, C-3), 43.9 (*d*, C-4), 48.9 (*d*, C-5), 38.9 (*t*, C-6), 200.7 (*s*, C-7), 145.5 (*s*, C-8), 151.9 (*s*, C-9), 38.3 (*s*, C-10), 202.5 (*s*, C-11), 57.3 (*t*, C-12), 47.1 (*s*, C-13), 49.3 (*d*, C-14), 24.8 (*t*, C-15), 27.8 (*t*, C-16), 54.0 (*d*, C-17), 11.9 (*q*, C-18), 16.2 (*q*, C-19), 35.6 (*d*, C-20), 18.5 (*q*, C-21), 33.8 (*t*, C-22), 31.2 (*t*, C-23), 148.5 (*s*, C-24), 45.6 (*d*, C-25), 174.5 (*s*, C-26), 16.2 (*q*, C-27), 110.8 (*t*, C-28), 11.4 (*q*, C-29), 60.5 (*t*, $O\underline{C}H_2CH_3$), 14.2 (*q*, $OCH_2\underline{C}H_3$); EI-MS *m/z* (rel. int.): 496 (69), 482 (33), 468 (4), 450 (5), 422 (5), 354 (27), 341 (10), 326 (7), 313 (29), 311 (100), 286 (23), 273 (15), 260 (29), 246 (10), 220 (24), 205 (11), 189 (10), 175 (6), 142 (11), 123 (9), 109 (22), 102 (6), 95 (35), 82 (13), 68 (30).

Zhankuic acid E (**5**). Pale yellow needle crystals, UV λ_{max}^{MeOH}: 268 nm (log ε 3.7); IR ν_{max}^{KBr} cm^{-1}: 3387, 2955, 2926, 2869, 1730, 1668, 1460, 1377, 1329, 1186, 990, 973, 904; ^{1}H NMR (300 MHz, $CDCl_3$): δ 3.77 (1H, *br s*, H-3), 4.04 (1H, *s*, H-12β), 2.99 (1H, *dd*, J = 12.4, 7.4 Hz, H-14), 0.62 (3H, *s*, H-18), 1.29 (3H, *s*, H-19), 0.95 (3H, *d*, J = 5.5 Hz, H-21), 3.09 (1H, *q*, J = 7.0 Hz, H-25), 1.28 (3H, *d*, J = 7.0 Hz, H-27), 4.84 (1H, *d*, J = 3.9 Hz, H-28a), 4.89 (1H, *d*, J = 3.9 Hz, H-28b), 0.93 (3H, *d*, J = 6.3 Hz, H-29), 4.11 (2H, *q*, J = 7.1 Hz, $OC\underline{H}_2CH_3$), 1.21 (3H, *t*, J = 7.1 Hz, $OCH_2C\underline{H}_3$); ^{13}C NMR (75 MHz, $CDCl_3$): δ 27.8 (*t*, C-1), 28.9 (*t*, C-2), 70.4 (*d*, C-3), 34.5 (*d*, C-4), 40.7 (*d*, C-5), 38.1 (*t*, C-6), 201.6 (*s*, C-7), 144.9 (*s*, C-8), 152.4 (*s*, C-9), 38.3 (*s*, C-10), 202.7 (*s*, C-11), 80.8 (*t*, C-12), 49.5 (*s*, C-13), 41.8 (*d*, C-14), 23.9 (*t*, C-15), 26.9 (*t*, C-16), 45.6 (*d*, C-17), 11.5 (*q*, C-18), 16.1 (*q*, C-19), 35.4 (*d*, C-20), 17.9 (*q*, C-21), 33.9 (*t*, C-22), 31.2, (*t*, C-23), 148.5 (*s*, C-24), 45.6 (*d*, C-25), 174.5 (*s*, C-26), 16.3 (*q*, C-27), 110.7 (*t*, C-28), 15.6 (*q*, C-29), 60.5 (*t*, $O\underline{C}H_2CH_3$), 14.2 (*q*, $OCH_2\underline{C}H_3$); EIMS *m/z* (rel. int.): 514 (100), 486 (3), 372 (3), 357 (4), 341 (10), 331 (9), 329 (18), 313 (16), 303 (24), 291 (29), 275 (21), 261 (21), 248 (17), 229 (8), 215 (7), 201 (10), 189 (11), 175 (17), 161 (13), 149 (19), 137 (22), 123 (10), 121 (25), 109 (45), 95 (13), 81 (13), 69 (11), 57 (7).

Dehydroeburicoic acid (**7**). White powder, $[\alpha]_D^{25}$ + 75 (c = 0.11, $CHCl_3$); UV λ_{max}^{MeOH}: 243 nm (log ε 4.12), 250 nm (log ε 3.98), 237 nm (log ε 4.04); IR ν_{max}^{KBr} cm^{-1}: 3435, 2961, 2875, 1719, 1703, 1655, 1459, 1377, 1225, 1194, 1076, 1031, 890; ^{1}H NMR (300 MHz, pyridine-d_5): δ 1.90 (2H, H-2), 3.44 (1H, *t*, J = 7.5 Hz, H-3), 1.28 (1H, H-5), 2.18 (2H, H-6), 5.63 (1H, *br s*, H-7), 5.39 (1H, *d*, J = 5.4 Hz, H-11), 2.5 (1H, H-12α), 2.34 (1H, H-12β), 1.00 (3H, *s*, H-18), 1.12 (3H, *s*, H-19), 2.30 (1H, H-25), 1.06 (3H, H-26), 1.06 (3H, H-27), 1.06 (3H, *s*, H-29), 1.04 (3H, *s*, H-30), 1.03 (3H, *s*, H-31); (300 MHz, $CDCl_3/CD_3OD$): δ 3.04 (1H, *t*, J = 7.9 Hz, H-3), 5.49 (1H, *br s*, H-7), 5.32 (1H, *d*, J = 6.0 Hz, H-11), 2.08 (1H, H-12α), 1.62 (1H, *dd*, J = 17.5, 6.0 Hz, H-12β), 0.47 (3H, *s*, H-18), 0.83 (3H, *s*, H-19), 0.96 (3H, *d*, J = 6.8 Hz, H-26), 0.95 (3H, *d*, J = 6.9 Hz, H-27), 4.51 (1H, *s*, H-28a), 4.59 (1H, *s*, H-28b), 0.70 (3H, *s*, H-29), 0.73 (3H, *s*, H-30), 0.80 (3H, *s*, H-31); ^{13}C NMR (75 MHz, $CDCl_3$): δ 36.5 (*t*, C-1), 28.5 (*t*, C-2), 78.1 (*d*, C-3), 39.4 (*s*, C-4), 49.1 (*d*, C-5), 23.6 (*t*, C-6), 121.3 (*d*, C-7), 142.9 (*s*, C-8), 146.7 (*s*, C-9), 37.9 (*s*, C-10), 116.7 (*d*, C-11), 36.1 (*t*, C-12), 44.4 (*s*, C-13), 50.6 (*s*, C-14), 31.9 (*t*, C-15), 27.3 (*t*, C-16), 48.2 (*d*, C-17), 16.3 (*q*, C-18), 23.4 (*q*, C-19), 49.9 (*d*, C-20), 178.3 (*s*, C-21), 32.8 (*t*, C-22), 31.7 (*t*, C-23), 156.0 (*s*, C-24), 34.3 (*d*, C-25), 22.0 (*q*, C-26), 22.1 (*q*, C-27), 107.1 (*t*, C-28), 26.0 (*q*, C-29), 28.7 (*q*, C-30), 16.6 (*q*, C-31); HREI-MS: 468.3596 ($C_{31}H_{48}O_3$, calcd 468.3603); EI-MS *m/z* (rel. int.): 468 (100), 455 (40), 437 (42), 372 (7), 341 (11), 311 (59), 297 (22), 281 (18), 271 (41), 253 (30), 240 (21), 225 (19), 213 (11), 201 (11), 187 (19), 173 (17), 159 (18), 135 (23), 121 (11), 109 (16), 97 (16), 83 (9), 71 (9), 57 (9), 43 (20), 44 (19).

Dehydroeburicoic acid monoacetate (**9**). Acetylation (Ac_2O–Py; 1:1; room temp. of **7** (30 mg) gave after work-up and column chromatogrpahy (silica gel) **9** (25 mg) as a solid, UV λ_{max}^{MeOH}: 243 nm (log ε 4.02), 250 nm (log ε 3.91), 237 nm (log ε 3.96); IR ν_{max}^{KBr} cm^{-1}: 3449, 2960, 1767, 1717, 1678, 1655, 1648, 1459, 1377, 1249, 1034, 893, 815; ^1H NMR (300 MHz, $CDCl_3$): δ1.69 (2H, H-2), 4.48 (1H, *dd*, J = 8.9, 6.4 Hz, H-3), 1.20 (1H, H-5), 2.05 (2H, H-6), 5.46 (1H, *brs*, H-7), 5.27 (H, *d*, J = 6.1 Hz, H-11), 2.16 (1H, H-12α), 1.82 (1H, *dd*, J = 16.1, 6.1 Hz, H-12β), 0.62 (3H, *s*, H-18), 0.97 (3H, *s*, H-19), 2.20 (1H, H-25), 1.00 (3H, *d*, J = 6.8 Hz, H-26), 0.99 (3H, *d*, J = 6.9 Hz, H-27), 4.67 (1H, *s*, H-28a), 4.74 (1H, *s*, H-28b), 0.86 (3H, *s*, H-29), 0.88 (3H, *s*, H-30), 0.93 (3H, *s*, H-31), 2.03 (3H, *s*, $COCH_3$); ^{13}C NMR δ (75 MHz, $CDCl_3$): 35.4 (*t*, C-1), 24.3 (*t*, C-2), 80.6 (*d*, C-3), 37.3 (*s*, C-4), 49.3 (*d*, C-5), 22.8 (*t*, C-6), 120.5 (*d*, C-7), 142.3 (*s*, C-8), 145.8 (*s*, C-9), 37.6 (*s*, C-10), 116.3 (*d*, C-11), 35.6 (*t*, C-12), 43.6 (*s*, C-13), 50.1 (*s*, C-14), 31.0 (*t*, C-15), 26.9 (*t*, C-16), 47.5 (*d*, C-17), 15.8 (*q*, C-18), 22.7 (*q*, C-19), 47.6 (*d*, C-20), 181.6 (*s*, C-21), 30.9 (*t*, C-22), 32.0 (*t*, C-23), 155.2 (*s*, C-24), 33.8 (*d*, C-25), 21.8 (*q*, C-26), 21.8 (*q*, C-27), 106.9 (*t*, C-28), 25.6 (*q*, C-29), 28.1 (*q*, C-30), 16.9 (*q*, C-31), 170.9 (*s*, O<u>C</u>OCH$_3$), 21.3 (*q*, OCO<u>C</u>H$_3$); EIMS *m/z*: (rel. int.): 510 (48), 497 (16), 450 (10), 437 (57), 407 (3), 381 (4), 367 (5), 353 (85), 339 (18), 331 (6), 313 (25), 301 (14), 295 (34), 288 (21), 281 (27), 271 (10), 253 (100), 240 (44), 225 (42), 213 (22), 201 (17), 187 (36), 169 (35), 159 (31), 145 (19), 135 (29), 121 (21), 109 (33), 97 (39), 91 (5), 84 (20), 71 (11), 57 (12), 43 (20).

Dehydrosulphurenic acid (**8**). White powder, mp 240–247°, $[\alpha]_D^{25}$ + 55 (*c* =0.1, $CHCl_3$); UV λ_{max}^{MeOH} 243 nm (log ε 4.07), 250 nm (log ε 3.95), and 237 nm (log ε 3.99); IR ν_{max}^{KBr} cm^{-1}: 3400, 2962, 2932, 1773, 1699, 1686, 1458, 1377, 1273, 1048, 889; ^1H NMR δ (300 MHz, pyridine-d_5): 1.90 (2H, H-2), 3.44 (1H, *m*, H-3), 1.30 (1H, H-5), 2.16 (2H, H-6), 5.50 (1H, *br s*, H-7), 5.38 (1H, *d*, J = 5.3 Hz, H-11), 2.70 (1H, H-12α), 2.37 (1H, H-12β), 4.80 (1H, *m*, H-15), 1.70 (1H, H-16), 2.37 (1H, H-16), 1.08 (3H, *s*, H-18), 1.10 (3H, *s*, H-19), 2.22 (1H, H-25), 0.99 (3H, *d*, J = 7.0 Hz, H-26), 0.98 (3H, *d*, J = 6.9 Hz, H-27), 4.84 (1H, *s*, H-28a), 4.88 (1H, *s*, H-28b), 1.44 (3H, *s*, H-29), 1.17 (3H, *s*, H-30), 1.13 (3H, *s*, H-31); ^{13}C NMR (75 MHz, pyridine-d_5): δ 36.9 (*t*, C-1), 28.9 (*t*, C-2), 78.1 (*d*, C-3), 39.4 (*s*, C-4), 49.7 (*d*, C-5), 23.6 (*t*, C-6), 122.3 (*d*, C-7), 142.0 (*s*, C-8), 147, 1 (*s*, C-9), 38.0 (*s*, C-10), 116.3 (*d*, C-11), 36.4 (*t*, C-12), 44.9 (*s*, C-13), 52.5 (*s*, C-14), 73.8 (*t*, C-15), 39.6 (*t*, C-16), 46.5 (*d*, C-17), 16.9 (*q*, C-18), 23.1 (*q*, C-19), 48.9 (*d*, C-20), 178.7 (*s*, C-21), 32.7 (*t*, C-22), 31.9 (*t*, C-23), 155.8 (*s*, C-24), 34.2 (*d*, C-25), 21.9 (*q*, C-26), 22.0 (*q*, C-27), 107.1 (*t*, C-28), 18.3 (*q*, C-29), 28.7 (*q*, C-30), 16.7 (*q*, C-31); HREI-MS: 484.3520 ($C_{31}H_{48}O_4$, calcd 484.3553); EI-MS *m/z* (rel. int.): 484 (100), 470 (13), 468 (10), 451 (22), 433 (10), 423 (12), 400 (9), 383 (6), 367 (6), 351 (18), 339 (9), 327 (24), 311 (25), 295 (10), 285 (10), 273 (16), 261 (10), 239 (9), 227 (13), 221 (21), 211 (8), 199 (7), 179 (10), 159 (11), 147 (8), 135 (9), 123 (11), 107 (11), 97 (11), 83 (8), 69 (5), 44 (8).

15α-*Acetyl-dehydrosulphurenic acid* (**6**). White powder, mp 243–248°, $[\alpha]_D^{25}$ + 177 (*c* = 0.1, $CHCl_3$); UV λ_{max}^{MeOH}: 243 nm (log ε 4.13), 250 nm (log ε 3.98), 237 nm (log ε 4.04); IR ν_{max}^{KBr} cm^{-1}: 3435, 2961, 2932, 1735, 1718, 1655, 1459, 1378, 1249, 1039, 993, 889; ^1H NMR (300 MHz, $CDCl_3$). δ 1.66 (2H, H-2), 3.22 (1H, *dd*, J = 11, 4.6 Hz, H-3), 1.06 (1H, H-5), 2.06 (2H, H-6), 5.50 (1H, *d*, J = 6.1 Hz, H-7), 5.26 (1H, *d*, J = 6.2 Hz, H-11), 2.20 (1H, H-12α), 1.80 (1H, *dd*, J = 17, 6.2 Hz, H-12β), 5.04 (1H, *dd*, J = 9.6, 5.5 Hz, H-15), 1.72 (1H, H-16), 2.10 (1H, H-16), 1.08 (3H, *s*, H-18), 1.10 (3H, *s*, H-19), 2.14 (1H, H-25), 0.99 (3H, *d*, J = 7.0 Hz, H-26), 0.98 (3H, *d*, J = 6.9 Hz, H-27), 4.74 (1H, *s*, H-28a), 4.64 (1H, *s*, H-28b), 0.93 (3H, *s*, H-29), 0.85 (3H, *s*, H-30), 1.00 (3H, *s*, H-31), 2.08 (3H, *s*, OAc); ^{13}C NMR (75 MHz, $CDCl_3$): δ35.6 (*t*, C-1), 27.8 (*t*, C-2), 78.8 (*d*, C-3), 38.6 (*s*, C-4), 48.8 (*d*, C-5), 23.0 (*t*, C-6), 121.8 (*d*, C-7), 139.9 (*s*, C-8), 146.0 (*s*, C-9), 37.4 (*s*, C-10), 115.6 (*d*, C-11), 29.7 (*t*, C-12), 43.9 (*s*, C-13), 51.0 (*s*, C-14), 76.7 (*t*, C-15), 35.8 (*t*, C-16), 45.6 (*d*, C-17), 16.2 (*q*, C-18), 22.7 (*q*, C-19), 47.2 (*d*, C-20), 181.5 (*s*, C-21), 35.9 (*t*, C-22), 31.9 (*t*, C-23), 154.8 (*s*, C-24), 33.7 (*d*, C-25), 21.7 (*q*, C-26), 21.8 (*q*, C-27), 107.0 (*t*, C-28), 18.5 (*q*, C-29), 28.2 (*q*, C-30), 15.8 (*q*, C-31), 21.4 (*q*, CO<u>C</u>H$_3$), 171.2 (*s*, <u>C</u>OCH$_3$); HREI-MS: 526.3668 ($C_{33}H_{51}O_5$, calcd 526.3658); EIMS *m/z* (rel. int.): 526 (98), 513 (12), 469 (28), 453 (39), 435 (48), 372 (20), 353 (17), 339 (14), 326 (15), 313 (46), 311 (100), 295 (48), 259 (53), 241 (38), 225 (32), 211 (22), 199 (22), 187 (28), 171 (29), 159 (22), 145 (16), 133 (13), 121 (15), 111 (15), 97 (21), 83 (10), 44 (10).

Acknowledgements—This investigation was supported by grants from the National Science Council (NSC 80-0420-B002-153 and NSC 83-0208-M110-041). We thank Dr Shoei-sheng Lee, School of Pharmacy, National Taiwan University and Ms Siew-Leng Ng of NSC northern NMR Instrument Centre for assistance and measurements of NMR spectral data.

REFERENCES

1. Chang, T. T. and Chou, W. N. (1995) *Mycol. Res.*, **99**, 756.
2. Tsai, Z. T. and Liaw, S. L. (1985) *The Use And The Effect of Ganoderma*, Taichung, pp. 116.
3. Lin, L. J. and Shiao, M. S. (1989) *J. Nat. Prod.* **52**, 595.
4. Kohda, H., Tokumoto, W., Sakamoto, K., Fujii, M., Hirai, Y., Yamasaki, K., Komoda, Y., Nakamura, H., Ishinara, S. and Uchida, M., (1985) *Chem. Pharm. Bull.* **33**, 1367.
5. Cherng, I. H., Chiang, H. C., Cheng, M. C. and Wang, Y. (1995) *J. Nat. Prod.* **58**, 365.
6. Chen, C. H., Yang, S. W. and Shen, Y. C. (1995) *J. Nat. Prod.*, in press.
7. Arisawa, M., Fujita, A., Saga, M., Fukumura, H., Hayashi, T., Shimizu, M. and Morita, N. (1986) *J. Nat. Prod.* **49**, 621.
8. Kobayashi, M., Kanda, F., Damarla, S. R., Rao, D. V. and Rao, C. B. (1990) *Chem. Pharm. Bull.* **38**, 2400.
9. Hasan, C. M., Shahnaz, S., Muhammad, I., Gray, A. I. and Waterman, P. G. (1987) *J. Nat. Prod.* **50**, 762.
10. Gascoigne, R. M., Robertson, A. and Hsimes, J. J. (1951) *J. Chem. Soc.* 1830.
11. Anderson, C. G., Epstein, W. W. and van Lear, G. (1972) *Phytochem.* **11**, 2847.

Phytomedicine 19 (2012) 788–796

Contents lists available at SciVerse ScienceDirect

Phytomedicine

journal homepage: www.elsevier.de/phymed

Antileukemia component, dehydroeburicoic acid from *Antrodia camphorata* induces DNA damage and apoptosis *in vitro* and *in vivo* models

Ying-Chi Du[a,1], Fang-Rong Chang[a,b,c,d,1], Tung-Ying Wu[a], Yu-Ming Hsu[a], Mohamed El-Shazly[a,e], Chieh-Fu Chen[f], Ping-Jyun Sung[g,h], Yan-Yu Lin[a], Yi-Hsin Lin[a], Yang-Chang Wu[a,i,j,k,**], Mei-Chin Lu[a,g,h,*]

[a] *Graduate Institute of Natural Products, College of Pharmacy, Kaohsiung Medical University, Kaohsiung 807, Taiwan*
[b] *Cancer Center, Kaohsiung Medical University Hospital, Kaohsiung 807, Taiwan*
[c] *Research and Development Center of Chinese Herbal Medicines and New Drugs, College of Pharmacy, Kaohsiung Medical University, Kaohsiung 807, Taiwan*
[d] *Department of Marine Biotechnology and Resources, National Sun Yat-sen University, Kaohsiung 804, Taiwan*
[e] *Department of Pharmacognosy and Natural Products Chemistry, Faculty of Pharmacy, Ain-Shams University, Organization of African Unity Street 11566, Abassia, Cairo, Egypt*
[f] *Chih-Ying Plant Research and Development Foundation, Taipei City 100, Taiwan*
[g] *Graduate Institute of Marine Biotechnology, National Dong Hwa University, Pingtung 944, Taiwan*
[h] *National Museum of Marine Biology & Aquarium, Pingtung 944, Taiwan*
[i] *School of Chinese Medicine, College of Chinese Medicine, China Medical University, Taichung 404, Taiwan*
[j] *Natural Medicinal Products Research Center, China Medical University Hospital, Taichung 404, Taiwan*
[k] *Center for Molecular Medicine, China Medical University Hospital, Taichung 404, Taiwan*

ARTICLE INFO

Keywords:
Antrodia camphorata
Dehydroeburicoic acid (DeEA)
DNA damage
Apoptosis
Topoisomerase II inhibitor

ABSTRACT

Antrodia camphorata (AC) is a native Taiwanese mushroom which is used in Asian folk medicine as a chemopreventive agent. The triterpenoid-rich fraction (FEA) was obtained from the ethanolic extract of AC and characterized by high performance liquid chromatography (HPLC). FEA caused DNA damage in leukemia HL 60 cells which was characterized by phosphorylation of H2A.X and Chk2. It also exhibited apoptotic effect which was correlated to the enhancement of PARP cleavage and to the activation of caspase 3. Five major triterpenoids, antcin K (**1**), antcin C (**2**), zhankuic acid C (**3**), zhankuic acid A (**4**), and dehydroeburicoic acid (**5**) were isolated from FEA. The cytotoxicity of FEA major components (**1**–**5**) was investigated showing that dehydroeburicoic acid (DeEA) was the most potent cytotoxic component. DeEA activated DNA damage and apoptosis biomarkers similar to FEA and also inhibited topoisomerase II. In HL 60 cells xenograft animal model, DeEA treatment resulted in a marked decrease of tumor weight and size without any significant decrease in mice body weights. Taken together, our results provided the first evidence that pure AC component inhibited tumor growth *in vivo* model backing the traditional anticancer use of AC in Asian countries.

Introduction

Antrodia camphorata (AC), also known as *Antrodia cinnamomea* or *Taiwanofungus camphoratus*, is an endemic fungus in Taiwan which only parasitizes in the internal heartwood or the dark humid wood surface of *Cinnamomum kanehirai* (Bull camphor tree) (Ao et al. 2009; Lu et al. 2009a). Mature AC fruiting bodies are regarded as the colored gems of the forests, ruby in Taiwanese forest, due to their colorful orange to brown-red appearance. It takes one year for AC fruiting bodies to grow to the size of one Euro forcing the price of one kilogram to reach 10,000–28,000 €. Due to the slow growth rate and the high price of wild fruiting bodies, AC is widely cultured.

AC, which is known in folk medicine as "chang-chih" has a long history in the prevention and treatment of several life threatening diseases including cancer, inflammatory disorders, and hepatitis (Geethangili and Tzeng 2009; Huang et al. 2010; Lu et al. 2009b; Shen et al. 2003; Yeh et al. 2009). Currently, AC is used as food dietary supplement for cancer prevention and hepatoprotection in several Asian and European countries. Its products are commercially available in China, Japan, Korea, Malaysia, and Singapore. It is also marketed in the United Kingdom under the name *Antrodia camphorata*.

* Corresponding author at: Graduate Institute of Marine Biotechnology, National Dong Hwa University, Pingtung 944, Taiwan. Tel.: +886 8 8825038; fax: +886 8 8825087.
** Corresponding author at: School of Chinese Medicine, College of Chinese Medicine, China Medical University, Taichung 404, Taiwan. Tel.: +886 4 22057153; fax: +886 4 22060248.
E-mail addresses: yachwu@mail.cmu.edu.tw (Y.-C. Wu), jinx6609@yahoo.com.tw (M.-C. Lu).
[1] The first two authors contributed equally to this study.

0944-7113/$ – see front matter © 2012 Elsevier GmbH. All rights reserved.
doi:10.1016/j.phymed.2012.03.014

Our group has been devoted to the anticancer research of AC for many years. In our previous report, we demonstrated that the water extract of AC wild fruiting bodies (ACW) promoted the functional maturation of dendritic cells in the expression of phenotypic characteristics, IL-12 production and chemotaxic activity (Lu et al. 2009b). Moreover, according to ^{1}H NMR analysis, it was suggested that the polysaccharides of ACW could act as a potent adjuvant for cancer immunotherapy through promoting Th1 immune response. We also reported that the ethanolic extract from the wild fruiting bodies of AC (EEAC) could induce HL 60 cell apoptosis and potentiate the anticancer effect of trichostatin A (Lu et al. 2009a). Fractionation of EEAC using different solvents provided three fractions, among them the ethyl acetate fraction (FEA) was the primary contributor to EEAC cytotoxicity. The aforementioned results encouraged us to identify FEA major components and study their cytotoxic activity. We believe that a thorough understanding of the cytotoxic molecular mechanism induced by FEA major components will shed light on the potential utilization of these components as future anticancer agents.

Materials and methods

Assessment of apoptosis

The accumulation of the sub G_1 population in cancer cells was determined by flow cytometry. Cells were seeded onto 6 cm dishes and treated with or without the indicated concentration of the tested samples for 24 h. Cells were then washed twice with PBS and collected by centrifugation at 200 × *g* for 5 min at 4 °C. Cells were fixed in 70% (v/v) ethanol at 4 °C for 30 min. After fixation, cells were treated with 0.2 ml of DNA extraction buffer (0.2 M Na_2HPO_4 and 0.1 M citric acid buffer, pH 7.8) for 30 min, centrifuged, and resuspended in 1 ml of propidium iodide staining buffer (0.1% TritonX-100, 100 μg/ml RNase A, 500 μg/ml of propidium iodide in PBS) at 37 °C for 30 min. Cytometric analyses were performed using a flow cytometer FACS-Calibur (Becton-Dickinson, San Jose, CA, USA) and CellQuest software. Approximately 10,000 cells were counted for each determination.

The externalization of phosphatidylserine (PS) and membrane integrity was quantified using an Annexin V-FLOUS staining kit (Roche Diagnostics GmbH, Mannheim, Germany). In short, 10^6 cells were grown in 35 mm diameter plates and labeled with Annexin V-FLOUS (10 μg/ml) and propidium iodide (PI) (Sigma–Aldrich Corp., St. Louis, MO, USA) (20 μg/ml) prior to harvesting. After labeling, all plates were washed with binding buffer and harvested by scraping. Cells were resuspended in binding buffer at a concentration of 2×10^5 cells/ml before analysis by flow cytometry.

Neutral comet assay for the detection of DNA double-strand breaks (DSBs)

The assay was carried out using a CometAssay™ Kit (Trevigen Inc., Gaithersburg, MD, USA) following the manufacturer's protocol for the neutral comet assay. Briefly, cancer cells (2×10^5 cells/ml) were treated with the tested samples for 18 h. Cells were combined with 1% low melting point agarose at a ratio of 1:10 (v/v). From the mixture, 75 μl were pipetted onto CometSlide™ and allowed to stand at 4 °C in the dark. The slides were immersed in ice-cold lysis solution for 30–60 min. The slides were placed in a horizontal electrophoresis apparatus and electrophoresed in 1× TBE (90 mM Tris–HCl, 90 mM boric acid, and 2 mM EDTA, pH 8.0) at 20 V for 10 min. The samples were then fixed in 70% ethanol and dried before being stained with 1:10,000 SYBR Green I to visualize cellular DNA. The fluorescence images were analyzed using the TriTek Comet Image program to circumscribe the 'head' and the 'tail' regions of each comet and the integrated fluorescence values of each defined area were recorded. The comet length was measured from the trailing edge of the nucleus to the leading edge of the tail. This length was indicative to the extent of DNA damage. Calculations were averaged per replicate.

Western blotting analysis

Cell lysates were prepared as described previously (Yang et al. 2006), by treating the cells for 30 min in RIPA lysis buffer [1× PBS, 1% Nonidet P-40, 0.5% sodium deoxycholate, 0.1% sodium dodecyl sulfate (SDS), 1 mM sodium orthovanadate, 100 μg/ml phenylmethylsulfonyl fluoride and 30 μg/ml aprotinin, all chemicals were obtained from Sigma–Aldrich Corp.]. The lysates were centrifuged at 20,000 × *g* for 30 min, and the protein concentration in the supernatant was determined using a BCA protein assay kit (Pierce, Rockford, IL, USA). Equal amounts of proteins were respectively separated by 7.5%, 10% or 12% of SDS-polyacrylamide gel electrophoresis and then electro-transferred to a PVDF membrane. The membrane was blocked with a solution containing 5% fat free dry milk TBST buffer (20 mM Tris–HCl, pH 7.4, 150 mM NaCl and 0.1% Tween 20) for 1 h and washed with TBST buffer. Protein expression was monitored by immunoblotting using specific antibodies: Bcl-2 and Bcl-x (Santa-Cruz Biotechnology, Santa Cruz, CA, USA); caspases 3, 7, 8 and 9; Bax, Bid, Bad, p-H2AX, and PARP (Cell Signaling Technologies, Beverly, MA, USA). Caspases 3, 8, and 9 inhibitors (Z-DEVD-FMK, Z-IETD-FMK, and Z-LEHD-KMK) were purchased from R&D Systems Inc. (Minneapolis, MN, USA). Anti-mouse and rabbit 1gG peroxidase-conjugated secondary antibodies were purchased from Pierce. These proteins were detected by an enhanced chemiluminescence kit (Pierce, Rockford, IL, USA).

Assay of topoisomerase II inhibitors and poisons

The assay was performed as described previously with minor modifications (Giri et al. 2010). Standard relaxation reaction mixtures (20 μl) containing 50 mM Tris–HCl (pH 8.0), 10 mM $MgCl_2$, 200 mM potassium glutamate, 10 mM dithiothreitol, 50 μg/ml bovine serum albumin, 1 mM ATP, 0.3 μg of pHOT1 plasmid DNA, two units of human topoisomerase II (Topogen, Columbus, OH, USA) and the indicated concentrations of etoposide and DeEA were incubated at 37 °C for 30 min. Reactions were terminated by adding 2 μl of 10% SDS to facilitate trapping the enzyme in a cleavage complex, followed by the addition of 2.5 μl of proteinase K (50 μg/ml) to digest the bound protein (incubated 37 °C for 15 min) and finally by adding 0.1 vol of the sample loading dye. The DNA products were analyzed by electrophoresis through vertical 2% agarose gels at 2 V/cm in 0.5× TAE buffer. Gels were stained with ethidium bromide and photographed using an Eagle Eye II system (Stratagene, La Jolla, CA, USA).

Human leukemia HL-60 cells xenograft animal model

Establishment of nude mice with xenografts was performed as described previously (Dowdy et al. 2006). Six-week-old female immunodeficient athymic mice were purchased from the National Laboratory Animal and Research Center (Taipei, Taiwan). All the animals were maintained under standard laboratory conditions (temperature 24–26 °C, 12–12 h dark–light circle) and fed with laboratory diet and water. The protocols of animal experiments were conformed to the Guide for the Care and Use of Laboratory Animals, published by the US National Institute of Health (NIH publication no. 85-23, revised in 1996).

HL 60 cells (1×10^7) resuspended in 0.2 ml PBS were injected s.c. into the right flank of each mouse, and tumor growth was monitored every day. Fourteen days after tumor cell injection, mice with confirmed tumor growth were randomly divided into two groups.

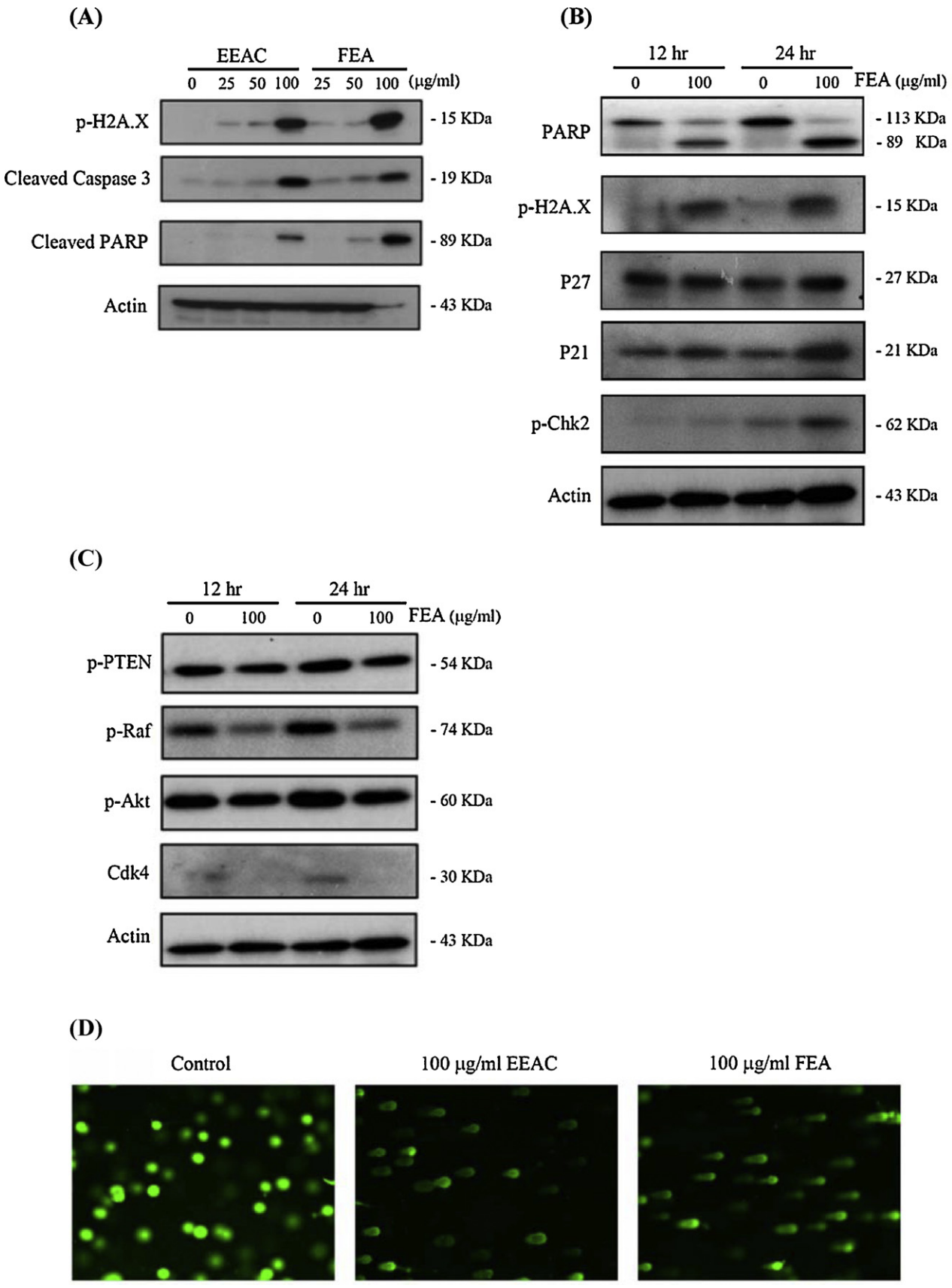

Fig. 1. Western plotting and alkaline comet assays. (A) Effect of EEAC and FEA on apoptotic and DNA damaged-related proteins in HL 60 cells (24 h). (B) Effect of FEA on tumor suppressor genes, apoptotic and DNA damaged-related proteins in HL 60 cells (12 h and 24 h). (C) Effect of FEA on the expression of survival-related proteins and Cdk4 (12 h and 24 h). (D) Assessment of DNA damage by comet assay. HL 60 cells were treated with EEAC or FEA for 18 h and then subjected to the alkaline comet assay to detect the broken DNA (comet tails).

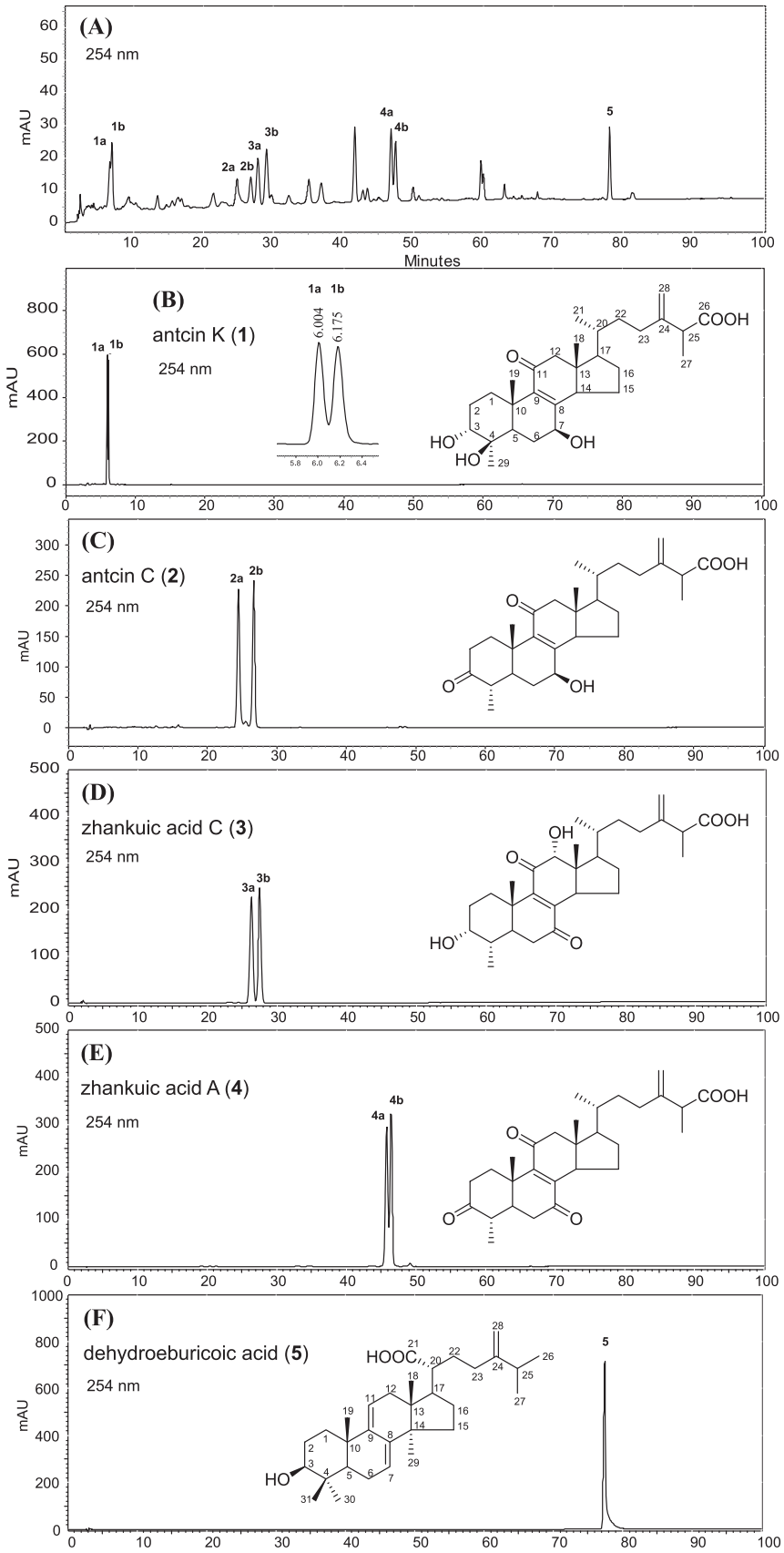

Fig. 2. HPLC chromatogram of the ethyl acetate fraction (FEA, an active triterpenoid-rich fraction) from the ethanolic extract of wild AC. Standard isolates (compounds **1**–**5**) are shown for comparison.

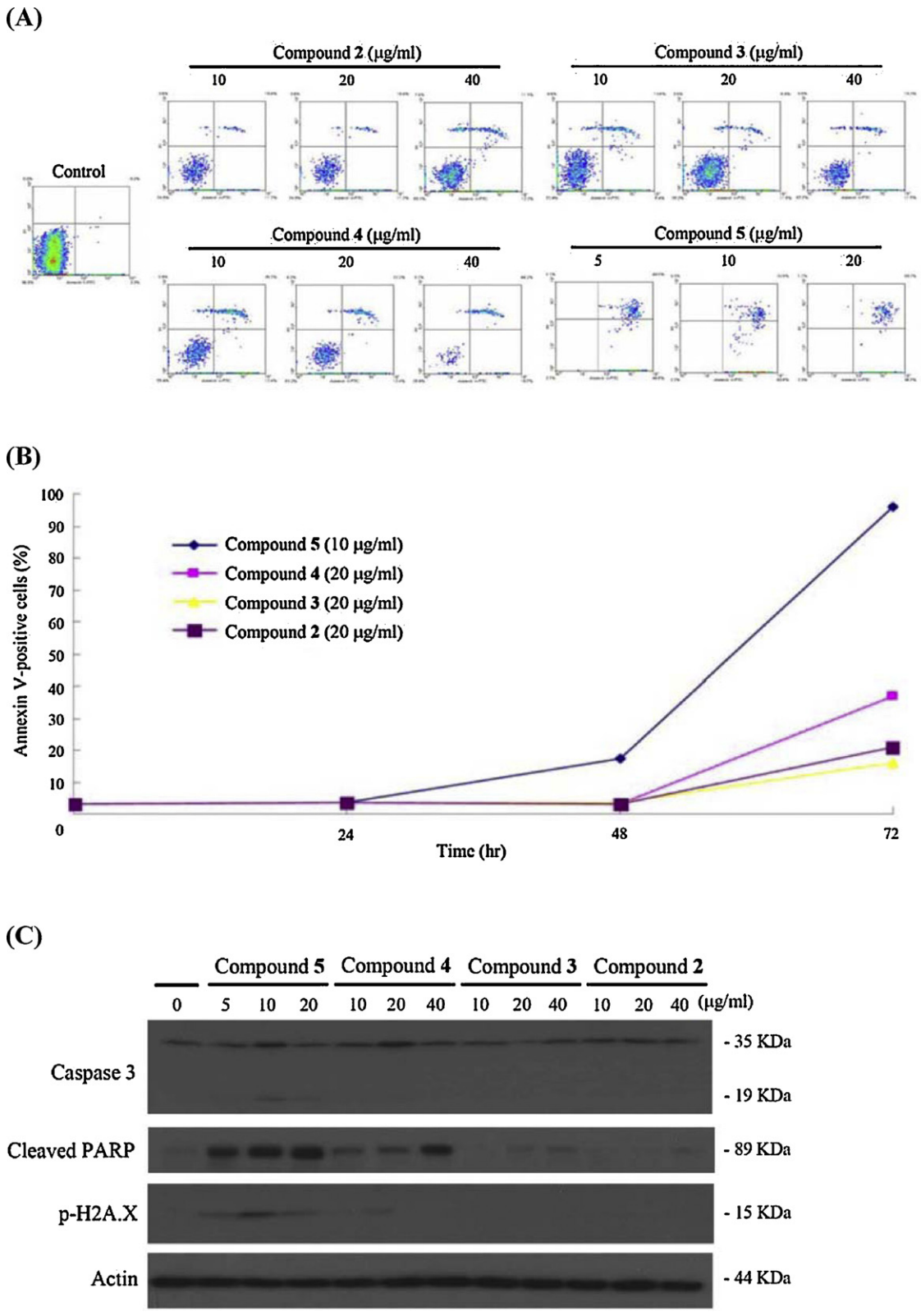

Fig. 3. The effect of FEA compounds **2**–**5** on apoptosis induction and DNA damage in HL 60 cells. (A) FACS dot plots representing HL 60 cells stained with Annexin V and PI after treatment with **2**–**5** (72 h). (B) Effect of **2**–**5** on the percentage of Annexin V-positive cells at different treatment times (24, 48, and 72 h). (C) Western blotting detecting the expression of apoptotic and DNA damaged-related proteins caused by **2**–**5**.

DeEA (10 μg/g) was orally administered to the treatment group and the control group received solvent only. DeEA was administrated every other day for five weeks. Animals were sacrificed by carbon dioxide. The tumors were carefully dissected from each mouse, and tumor weights were measured. Half of the tumor tissue was fixed with formalin and used for immunohistochemical studies, whereas the other half was snap frozen in liquid nitrogen and stored at −80 °C. These tissues were used to extract proteins for

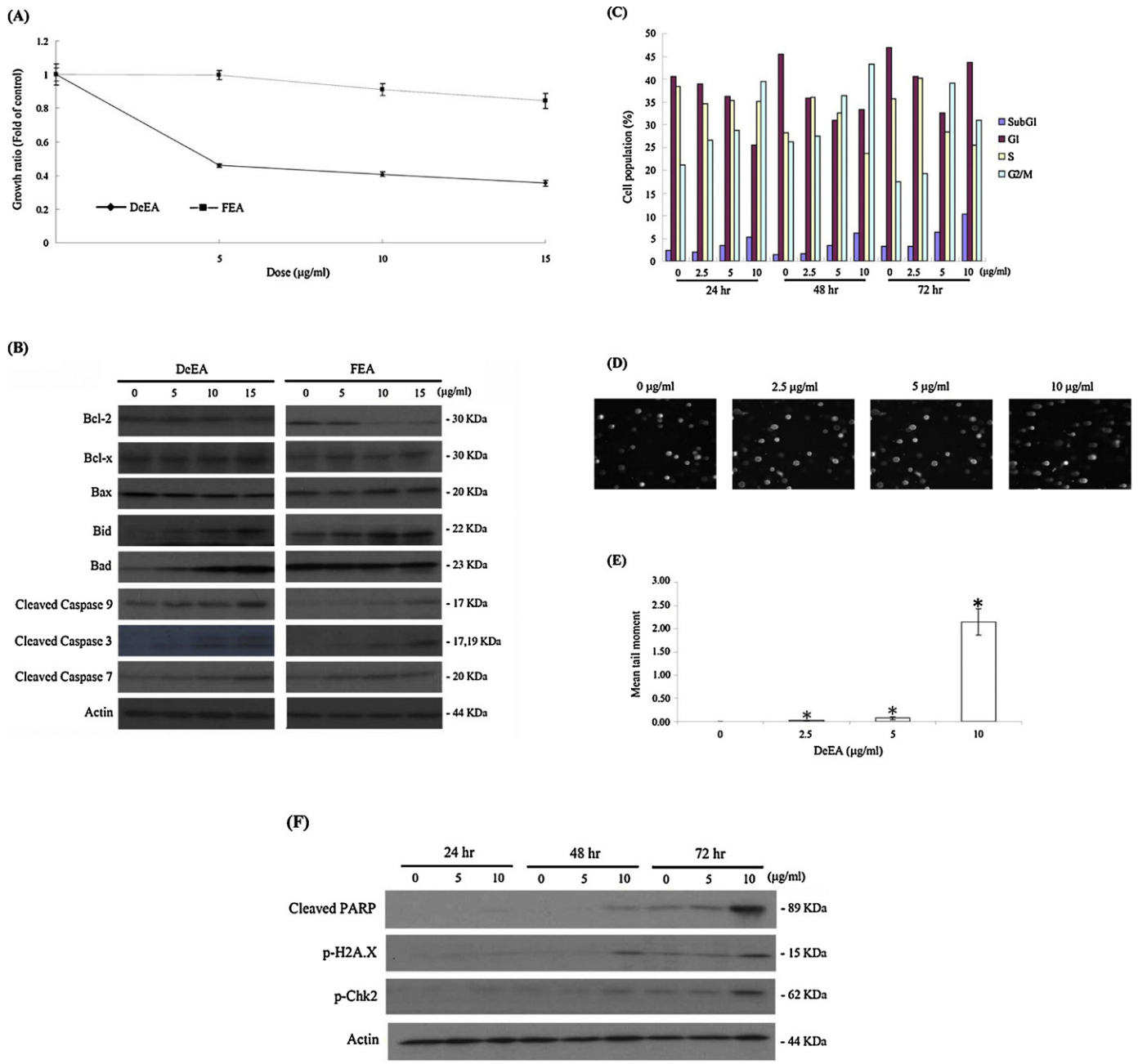

Fig. 4. The cytotoxic effect of DeEA on HL 60 cells. (A) DeEA and FEA cytotoxic activity at various concentrations (72 h) in MTT assay. (B) Effect of DeEA and FEA on anti-apoptotic and pro-apoptotic proteins and caspases 3, 7, and 9 (72 h). (C) Graphical representation of the percentages of cells at SubG$_1$, G$_1$, S and G$_2$/M phases in DeEA-treated cells. (D) Representative images of comet assay showing abnormal comet tails caused by chromosomal DNA double strand breaks in DeEA (2.5, 5 and 10 μg/ml) treated HL 60 cells. (E) DeEA effect on tail movement in HL 60 cells. Histogram was generated by TriTek Comet Image program. Values are expressed as mean ± SEM. *Significantly different from control groups at $p < 0.05$. (F) Effect of DeEA on the cleavage of PARP and on the phosphorylation of H2A.X and Chk2.

western blotting assay. Tumor size was measured three times a week using calipers and tumor volumes were calculated according to the standard formula: width^2 × length/2.

Statistics

The results were expressed as mean ± standard deviation (SD). Comparison in each experiment was performed using an unpaired Student's *t*-test, and a *p* value of less than 0.05 was considered statistically significant.

Results and discussion

The apoptotic and the DNA damaging activities of EEAC and FEA

Our previous study revealed that the ethanolic extract of wild AC (EEAC) and its active fraction (FEA, the ethyl acetate fraction from EEAC) possessed cytotoxicity against leukemia HL 60 cells with IC$_{50}$ values measured after 24 h of 104.82 and 80.53 μg/ml, respectively (Lu et al. 2009a). In the current study, EEAC and FEA were prepared as previously reported (see supplementary data, sections *S2* and *S3*). HL 60 cells were treated for 24 h with 0, 25, 50

Table 1
Comparisons of peak area and height for the respective components in FEA with HPLC at 254 nm.

Compound	Peak number	Retention time (min)	Area (%)	Height (%)
Antcin K	1a	6.004	4.96	7.08
	1b	6.175	6.23	9.40
Antcin C	2a	24.805	7.34	4.20
	2b	26.733	5.36	4.36
Zhankuic acid C	3a	27.778	6.91	6.59
	3b	28.981	8.07	7.59
Zhankuic acid A	4a	46.825	7.17	9.24
	4b	47.453	6.37	7.68
Dehydroeburicoic acid	5	78.058	4.58	8.79
Others			43.01	35.07
Total			100.00	100.00

and 100 μg/ml of EEAC or FEA and subsequently cell lysates were analyzed by western blotting. FEA or EEAC induced phosphorylation of H2A.X at Ser-139 (γH2A.X) (Fig. 1A) which is considered as a biomarker for DNA double-strand breaks (Kuo and Yang 2008; Mah et al. 2010). Additionally, the use of FEA or EEAC enhanced the cleavage of PARP and the activation of caspase 3, which are both regarded as markers of apoptosis (Fig. 1A). These results implied that FEA is the active apoptotic fraction of EEAC and thus selected for further investigation.

The effect of using FEA (100 μg/ml) on protein expression was also determined. FEA led to a marked increase in the amount of tumor suppressor genes, p21 and p27, enhancement of H2A.X and Chk2 phosphorylation, as well as induction of PARP cleavage (Fig. 1B). On the other hand, phosphorylation levels in each of the survival proteins (Akt, Raf, and PTEN) as well as the expression of Cdk4 decreased following treatment with FEA in a time dependent manner (Fig. 1C). The DNA damaging effect of FEA was further confirmed using alkaline comet assay resulting in comets with abnormal tails sizes (Fig. 1D). The aforementioned results confirmed the DNA damaging and the apoptotic activities of FEA implying its importance as a potential cytotoxic agent (Kim et al. 2011).

The apoptotic and the DNA damaging activities of FEA major components

FEA major components were separated by normal phase chromatography and purified by reverse phase high performance liquid chromatography (HPLC) yielding five major constituents (see supplementary data, section *S4*). The isolated compounds were four ergostanes, antcin K (**1**), antcin C (**2**), zhankuic acid C (**3**), and zhankuic acid A (**4**) as well as one lanostane, dehydroeburicoic acid (**5**) (Chen et al. 1995; Shen et al. 2003). The isolation of these major triterpenes as standards led to the establishment of HPLC fingerprint of FEA (Fig. 2) (see supplementary data for detailed HPLC condition, section *S5*). According to the published report (Chen et al. 1995), each AC ergostane triterpene (compounds **1**–**4**) exists as a pair of stereo isomers due to the presence of chiral center at C-25. Two peaks representing an isomeric pair of each ergostane can be observed in the HPLC fingerprint. For example, peak pairs 1a and 1b, 2a and 2b, 3a and 3b, as well as 4a and 4b corresponding to antcin K (**1**), antcin C (**2**), zhankuic acid C (**3**), and zhankuic acid A (**4**), respectively were observed (Fig. 2B–E). On the other hand, dehydroeburicoic acid with no chiral center at C-25 existed only as a single isomer, peak 5 (Fig. 2F). Peak areas and heights of FEA major components (**1**–**5**) at 254 nm were calculated and compared as shown in Table 1. The areas of the labeled peaks (**1**–**5**) accounted for 56.99% of the total peak areas observed in the HPLC fingerprint.

Regarding the antiproliferative activity of **1**–**5** against leukemia HL 60 cells, **1** showed no activity even at a high concentration (100 μg/ml). Compounds **2**–**5** exhibited antiproliferative activity against HL 60 cells and were further investigated using Annexin V and PI double staining technique. HL 60 cells were treated by different concentrations of antcin C (**2**), zhankuic acid C (**3**), zhankuic acid A (**4**), and dehydroeburicoic acid (**5**) for 24, 48, and 72 h. Cells were stained with Annexin V/PI and examined with flow cytometry. FACS dot plots representing Annexin V and PI staining after the treatment with **2**–**5** are shown in Fig. 3A. The quantification of Annexin V/PI experiment revealed that **4** and **5** increased the apoptotic population of HL 60 cells in a dose dependent manner. On the other hand, only **5** (10 μg/ml) induced apoptosis in a time dependent manner (Fig. 3B).

Compounds **4** and **5** induced cleavage of PARP in a dose dependent manner (Fig. 3C). The treatment of HL 60 cells with **4** (20 μg/ml) and **5** (10 μg/ml) induced the activation of caspase 3 and the phosphorylation of H2A.X. The analytical and the biological assays clearly implied that **5** (DeEA) is FEA major component with the most potent apoptotic and DNA damaging activities.

The apoptotic and the DNA damaging activities of DeEA

To further confirm the fact that DeEA is the lead active compound of FEA (triterpenoid-rich fraction) the cytotoxicity of DeEA and FEA against HL 60 cells was compared (Fig. 4A). DeEA exhibited more potent cytotoxicity compared to FEA with IC_{50} 3.39 and 22.4 μg/ml, respectively, after 72 h as indicated by MTT assay. The effect of DeEA and FEA on the expression of anti-apoptotic (Bcl-2 and Bcl-x) and pro-apoptotic (Bax, Bid, and Bad) proteins as well as the activation of caspases 3, 7, and 9 was also investigated (Fig. 4B). DeEA was more potent compared to FEA in enhancing the expression of pro-apoptotic proteins Bid and Bad. Also DeEA induced the activation of caspases 3, 7, and 9 and similar results were observed upon the treatment of FEA. To analyze whether the apoptotic induction of DeEA and FEA involves intrinsic or extrinsic apoptotic pathways, specific inhibitors for caspases 3, 8, and 9 were tested. Pretreatment of cells with caspase inhibitors did not inhibit the apoptotic effect of DeEA and FEA, suggesting that the apoptotic effect of DeEA and FEA is independent on caspase activation (data not shown).

Treatment of HL 60 cells with increasing doses of DeEA (0, 2.5, 5 and 10 μg/ml) resulted in G2/M distribution rates of 21.1%, 26.6%, 28.7% and 39.5%, respectively after 24 h (Fig. 4**C**). Similar results were observed after 48 and 72 h. Thus DeEA treatment appeared to induce G2/M phase arrest in a dose dependent manner.

To clarify the role of DeEA as DNA damaging agent, we treated HL 60 cells with various concentrations of DeEA for 18 h and analyzed

the level of tail movement with the alkaline comet assay. DeEA at 10 μg/ml caused severe DNA damage in HL 60 cells as indicated by abnormal tail size in comet assay (Fig. 4D and E).

To examine the extent of DNA damage which can lead to the activation of cell cycle checkpoints in HL 60 cells, the effect of DeEA on PARP, p-H2A.X and p-Chk2 was studied (Fig. 4F). DeEA at 10 μg/ml significantly increased the phosphorylation of Chk2 and H2A.X, but did not change the phosphorylation of Chk1 (data not shown). Additionally, DeEA induced PARP cleavage. These findings confirmed the apoptotic and the DNA damaging activities of DeEA on HL 60 cells.

The inhibitory activity of DeEA on topoisomerase II

Topoisomerases are essential enzymes for DNA metabolism and their inhibitors are emerging as potential cytotoxic agents. Exposure of cells to DNA topoisomerase I (topo I) or topoisomerase II (topo II) inhibitors leads to DNA damage that often involves

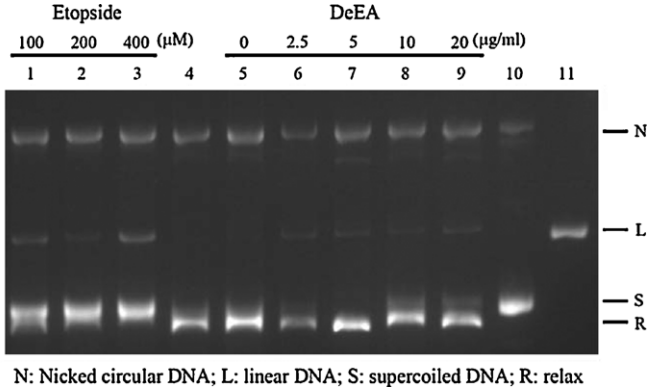

Fig. 5. Effect of DeEA on topoisomerase II mediated supercoiled pHOT1 plasmid DNA relaxation. Lane 1–3: positive control, etoposide (100, 200 and 400 μM); Lane 4: negative control plasmid DNA; Lane 5–9: DeEA (0, 2.5, 5, 10, and 20 μg/ml); Lane 10: plasmid DNA + topoisomerase II; Lane 11: linear DNA.

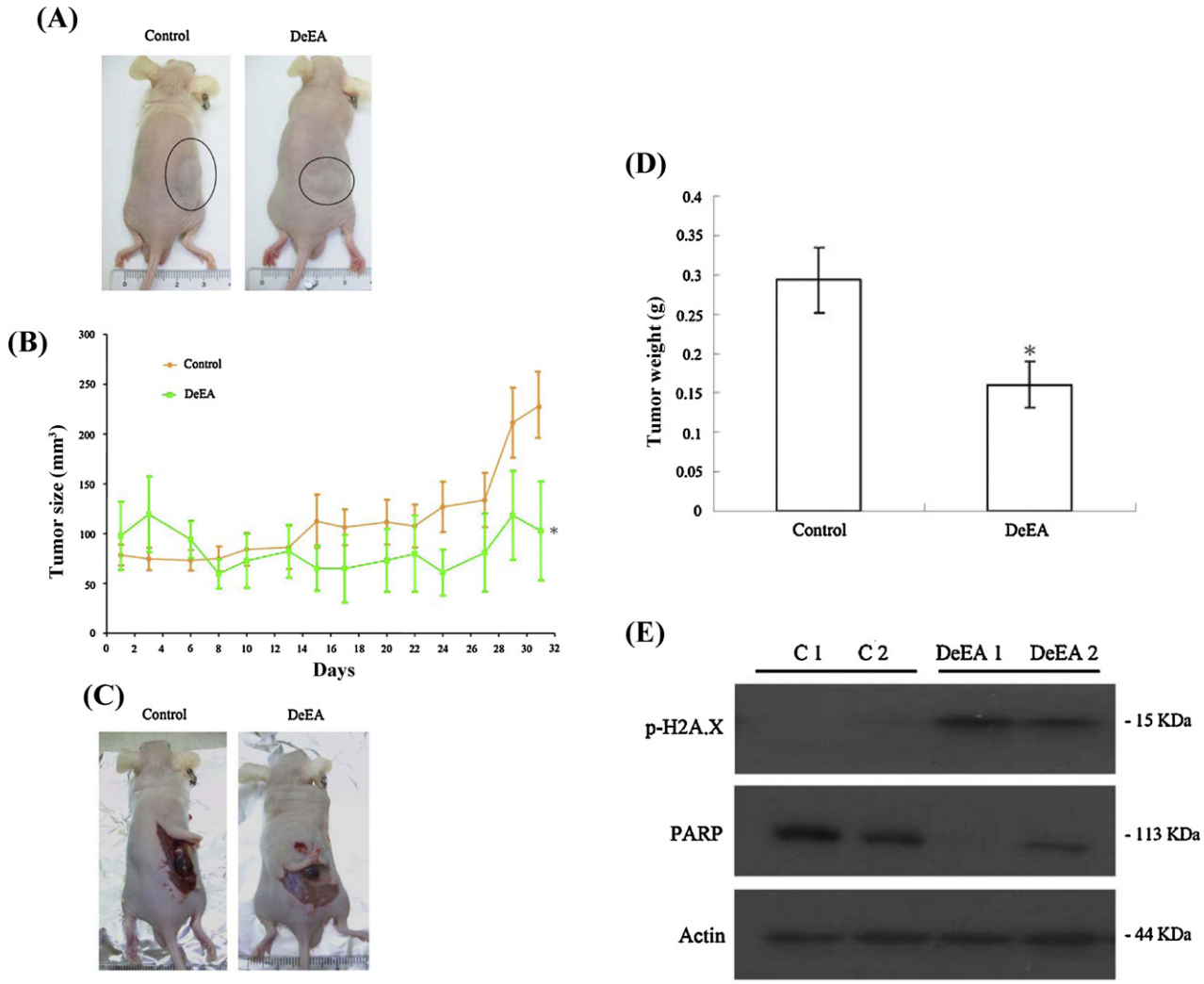

Fig. 6. Effect of DeEA on HL 60 cells tumor growth in xenograft animal model. Female nude mice bearing leukemia HL 60 tumors were treated with the solvent (negative control) or DeEA (10 μg/g) for 5 weeks. (A) A representative picture of tumor growth in xenograft nude mice administrated solvent only (left) and DeEA (right). (B) Tumor volumes were measured every other day, and results are expressed as mean ± SEM. *Significantly different from control groups at $p < 0.05$. (C) A representative picture of tumor tissue as it appears in the right flank of the mouse. (D) Histogram of the tumor weight from the control group and DeEA treated group. Values are expressed as mean ± SEM. *Significantly different from control groups at $p < 0.05$. (E) Effect of DeEA on PARP and on H2A.X in tumor samples. Two mice were picked randomly from each group. C1 and C2 represent two mice from the control group. DeEA1 and DeEA2 represent two mice from the DeEA treated group chosen randomly.

the formation of DNA double-strand breaks (Darzynkiewicz et al. 2009; Deng et al. 2009). Mizushina et al. (2004) revealed that dehydroebriconic acid, from the sclerotium of *Poris cocos* inhibited DNA topo II with no activity on DNA topo I. The structure of dehydroebriconic acid is similar to DeEA except the hydroxyl group at C-3 in DeEA is replaced by a carbonyl group in dehydroebriconic acid.

The inhibitory activity of dehydroebriconic acid on DNA topo II encouraged us to examine whether DeEA treatment can induce DNA damage in leukemia cells through inhibition of topo II or not. For this purpose, a cell-free DNA cleavage assay was performed using enzyme-mediated negatively supercoiled pHOT1 plasmid DNA. It was found that DeEA induced DNA cleavage in the presence of topo II (Lanes 6–9) (Fig. 5), as indicated by the appearance of linear DNA (marked by L). The results were similar to those obtained upon utilizing etoposide, a standard topo II inhibitor (Lanes 1–3) (Das et al. 2007).

The inhibitory effect of DeEA on tumor growth in xenograft animal model

HL 60 cells were inoculated subcutaneously at the right flank of female immunodeficient athymic mice. After 5 weeks of treatment, the tumor growth of HL 60 cells was significantly suppressed by oral administration of DeEA (10 μg/g) (Fig. 6A). The average tumor size on day 31 in the control group was 229.46 mm^3, whereas the average tumor size in the DeEA-treated group was 102.75 mm^3 (Fig. 6B). The tumor size was significantly lower in the DeEA-treated group as compared to the control group ($p < 0.05$) with no significant difference in the mice body weights. At the end of the treatment, the tumor tissue was isolated and weighed (Fig. 6C). The mean of tumor weights was obviously less in the DeEA-treated group compared to the control group ($p < 0.05$) (Fig. 6D). The western blotting analysis of tumor tissue indicated that the level of PARP was decreased and the phosphorylation of H2A.X was increased in DeEA-treated group compared to the control group (Fig. 6E).

Conclusion

In this study, we illustrated the apoptotic and the DNA damaging activities of the triterpenoid-rich fraction (FEA) and its major components obtained from the ethanolic extract of *A. camphorata*. FEA induced PARP cleavage and caspase 3 activation indicating its apoptotic activity. It also induced the phosphorylation of H2A.X as a marker of DNA double strand break. From the active FEA fraction, dehydroeburicoic acid (DeEA) was isolated as the lead most active component. DeEA induced G2/M phase arrest in a dose dependent manner in HL 60 cells. It also induced apoptotic and DNA damaging markers revealing its role as the potent cytotoxic constituent of FEA. Additionally it inhibited topo II suggesting the possible role of this enzyme in the cytotoxic activity of DeEA. The antitumor effect of DeEA was further demonstrated in reducing tumor weight and size in xenograft animal model. The present findings not only support the ethnopharmacological use of *A. camphorata* but also divulge the antitumor activity of dehydroeburicoic acid as the major lead compound of this treasured mushroom.

Conflict of interest

The authors declare that they have no conflicts of interest.

Acknowledgments

This work was supported by the National Science Council grants (NSC 98-2324-B-037-001 and 98-2321-B-037-060) and the Department of Health, Executive Yuan, Taiwan (DOH99-TD-C-111-002). This work was also supported by the Academic-Industrial Collaborative Project of Kaohsiung Medical University and Yung Peng Biotechnology Co., Ltd., Kaohsiung (S099009 and 100A502).

Appendix A. Supplementary data

Supplementary data associated with this article can be found, in the online version, at doi:10.1016/j.phymed.2012.03.014.

References

Ao, Z.H., Xu, Z.H., Lu, Z.M., Xu, H.Y., Zhang, X.M., Dou, W.F., 2009. Niuchangchih (*Antrodia camphorata*) and its potential in treating liver diseases. Journal of Ethnopharmacology 121, 194–212.

Chen, C.H., Yang, S.W., Shen, Y.C., 1995. New steroid acids from *Antrodia cinnamomea*, a fungal parasite of *Cinnamomum micranthum*. Journal of Natural Products 58, 1655–1661.

Darzynkiewicz, Z., Halicka, D.H., Tanaka, T., 2009. Cytometric assessment of DNA damage induced by DNA topoisomerase inhibitors. Methods in Molecular Biology 582, 145–153.

Das, C.M., Aguilera, D., Vasquez, H., Prasad, P., Zhang, M., Wolff, J.E., Gopalakrishnan, V., 2007. Valproic acid induces p21 and topoisomerase-II (alpha/beta) expression and synergistically enhances etoposide cytotoxicity in human glioblastoma cell lines. Journal of Neuro-Oncology 85, 159–170.

Deng, J.Y., Chen, S.J., Jow, G.M., Hsueh, C.W., Jeng, C.J., 2009. Dehydroeburicoic acid induces calcium- and calpain-dependent necrosis in human U87MG glioblastomas. Chemical Research in Toxicology 22, 1817–1826.

Dowdy, S.C., Jiang, S., Zhou, X.C., Hou, X., Jin, F., Podratz, K.C., Jiang, S.W., 2006. Histone deacetylase inhibitors and paclitaxel cause synergistic effects on apoptosis and microtubule stabilization in papillary serous endometrial cancer cells. Molecular Cancer Therapeutics 5, 2767–2776.

Geethangili, M., Tzeng, Y.M., 2009. Review of pharmacological effects of *Antrodia camphorata* and its bioactive compounds. Evidence Based Complementary and Alternative Medicine 2011, 1–17.

Giri, R., Goodell, J.R., Xing, C., Benoit, A., Kaur, H., Hiasa, H., Ferguson, D.M., 2010. Synthesis and cancer cell cytotoxicity of substituted xanthenes. Bioorganic and Medicinal Chemistry 18, 1456–1463.

Huang, C.H., Chang, Y.Y., Liu, C.W., Kang, W.Y., Lin, Y.L., Chang, H.C., Chen, Y.C., 2010. Fruiting body of Niuchangchih (*Antrodia camphorata*) protects livers against chronic alcohol consumption damage. Journal of Agricultural and Food Chemistry 58, 3859–3866.

Kim, S., Jun, D.H., Kim, H.J., Jeong, K.C., Lee, C.H., 2011. Development of a high-content screening method for chemicals modulating DNA damage response. Journal of Biomolecular Screening 16, 259–265.

Kuo, L.J., Yang, L.X., 2008. Gamma-H2AX—a novel biomarker for DNA double-strand breaks. In Vivo 22, 305–309.

Lu, M.C., Du, Y.C., Chuu, J.J., Hwang, S.L., Hsieh, P.C., Hung, C.S., Chang, F.R., Wu, Y.C., 2009a. Active extracts of wild fruiting bodies of *Antrodia camphorata* (EEAC) induce leukemia HL 60 cells apoptosis partially through histone hypoacetylation and synergistically promote anticancer effect of trichostatin A. Archives of Toxicology 83, 121–129.

Lu, M.C., Hwang, S.L., Chang, F.R., Chen, Y.H., Chang, T.T., Hung, C.S., Wang, C.L., Chu, Y.H., Pan, S.H., Wu, Y.C., 2009b. Immunostimulatory effect of *Antrodia camphorata* extract on functional maturation of dendritic cells. Food Chemistry 113, 1049–1057.

Mah, L.J., El-Osta, A., Karagiannis, T.C., 2010. γH2AX: a sensitive molecular marker of DNA damage and repair. Leukemia 24, 679–686.

Mizushina, Y., Akihisa, T., Ukiya, M., Murakami, C., Kuriyama, I., Xu, X., Yoshida, H., Sakaguchi, K., 2004. A novel DNA topoisomerase inhibitor: dehydroebriconic acid, one of the lanostane-type triterpene acids from *Poria cocos*. Cancer Science 95, 354–360.

Shen, C.C., Kuo, Y.C., Huang, R.L., Lin, L.C., Don, M.J., Chang, T.T., Chou, C.J., 2003. New ergostane and lanostane from *Antrodia camphorata*. Journal of Chinese Medicine 14, 247–258.

Yang, H.L., Hseu, Y.C., Chen, J.Y., Yech, Y.J., Lu, F.J., Wang, H.H., Lin, P.S., Wang, B.C., 2006. *Antrodia camphorata* in submerged culture protects low density lipoproteins against oxidative modification. American Journal of Chinese Medicine 34, 217–231.

Yeh, C.T., Rao, Y.K., Yao, C.J., Yeh, C.F., Li, C.H., Chuang, S.E., Luong, J.H., Lai, G.M., Tzeng, Y.M., 2009. Cytotoxic triterpenes from *Antrodia camphorata* and their mode of action in HT-29 human colon cancer cells. Cancer Letters 285, 73–79.

Journal of Pharmaceutical and Biomedical Analysis 58 (2012) 182–192

Contents lists available at SciVerse ScienceDirect

Journal of Pharmaceutical and Biomedical Analysis

journal homepage: www.elsevier.com/locate/jpba

Chemical profiling of the cytotoxic triterpenoid-concentrating fraction and characterization of ergostane stereo-isomer ingredients from *Antrodia camphorata*

Ying-Chi Du[a,1], Tung-Ying Wu[a,1], Fang-Rong Chang[a,b,c,d], Wan-Yu Lin[a], Yu-Ming Hsu[a], Fu-Ting Cheng[a], Chi-Yu Lu[e], Ming-Hong Yen[a], Ya-Ting Tsui[a], Hsuan-Lun Chen[a], Ming-Feng Hou[c], Mei-Chin Lu[a,f,g,*], Yang-Chang Wu[a,h,i,**]

[a] *Graduate Institute of Natural Products, College of Pharmacy, Kaohsiung Medical University, Kaohsiung 807, Taiwan*
[b] *Research and Development Center of Chinese Herbal Medicines and New Drugs, College of Pharmacy, Kaohsiung Medical University, Kaohsiung 807, Taiwan*
[c] *Cancer Center, Kaohsiung Medical University Hospital, Kaohsiung 807, Taiwan*
[d] *Department of Marine Biotechnology and Resources, National Sun Yat-sen University, Kaohsiung 804, Taiwan*
[e] *Department of Biochemistry, College of Medicine, Kaohsiung Medical University, Kaohsiung 807, Taiwan*
[f] *Graduate Institute of Marine Biotechnology, National Dong Hwa University, Pingtung 944, Taiwan*
[g] *National Museum of Marine Biology & Aquarium, Pingtung 944, Taiwan*
[h] *Graduate Institute of Integrated Medicine, College of Chinese Medicine, China Medical University, Taichung 404, Taiwan*
[i] *Natural Medicinal Products Research Center, and Center for Molecular Medicine, China Medical University Hospital, Taichung 404, Taiwan*

ARTICLE INFO

Article history:
Received 28 June 2011
Received in revised form 9 September 2011
Accepted 12 September 2011
Available online 16 September 2011

Keywords:
Antrodia camphorate
Triterpenoid
Zhankuic acid
HPLC-PDA/MS
Cytotoxicity

ABSTRACT

Antrodia camphorata (AC), also known as *Antrodia cinnamomea*, an endemic species in Taiwan, is one of the treasured medicinal mushrooms. AC is traditionally used for its chemopreventive biofunctions. In this investigation, we report a convenient method for concentrating the antiproliferative active triterpenoid-rich fraction (FEA), from ethanolic extract of AC (EEAC). A series of stereo-isomers of zhankuic acids (**1**–**8**) from the FEA was purified by HPLC using an efficient acidic solvent system. The structures of compounds **1**–**8** were elucidated based on spectroscopic data analysis, and the absolute configuration of α-chiral carboxylic acid at C-25 in the structures was assigned based on reaction with (*R*)- and (*S*)-1-(9-anthryl)-2,2,2-trifluoroethanol. Major ingredients of FEA (eight ergostanes **1**–**8** and two lanostanes **9**–**10**) were further characterised by high-performance liquid chromatography-photodiode array detection/mass spectrometry (HPLC-PDA/MS). Compounds **1**–**8** and their pair mixture forms (antcin K, antcin C, zhankuic acid C, and zhankuic acid A) were subjected to anti-proliferative assay against three human leukemia cell lines. Among them, the derivatives with carbonyl group at C-3 showed cytotoxicity with IC_{50} values ranging from 16.44 to 77.04 μg/ml.

1. Introduction

Antrodia camphorata (AC, also known as *Antrodia cinnamomea*), by name Chang-Chih, is an endemic fungus in Taiwan. Hundreds years before, the Taiwanese aborigines found that the wild AC had a special effect to relief hangover syndrome. It was also used in folk medicine for the treatment of food and drug detoxication, diarrhea, abdominal pain, hypertension, skin itching, and cancer [1,2]. Because of the potential pharmaceutical value of its biologically active ingredients, the fruiting bodies of AC are regarded as one of the health treasure troves of Taiwan [3]. Due to scarcity in nature and the difficulty in its artificial cultivation, the average price of AC is higher than the Truffle (*Tuber magnatum*), which is considered as one of the most expensive mushrooms worldwide. Several research groups have studied the phytochemical constituents of AC fruiting bodies and their pharmacological activities [4]. However, few studies have focused on analyzing the active components of AC fruiting bodies and their pharmacological mechanism of action [5–8].

In our previous study, we reported that the ethanolic extract from wild fruiting bodies of *A. camphorata* (EEAC) could induce HL 60 cell apoptosis via histone hypoacetylation, up-regulation of histone deacetyltransferase 1, and down-regulation of histone

* Corresponding author at: Graduate Institute of Marine Biotechnology, National Dong Hwa University, Pingtung 944, Taiwan. Tel.: +886 8 8825038; fax: +886 8 8825087.
** Corresponding author at: Graduate Institute of Integrated Medicine, College of Chinese Medicine, China Medical University, Taichung 404, Taiwan. Tel.: +886 4 22057153; fax: +886 4 22060248.
E-mail addresses: jinx6609@yahoo.com.tw (M.-C. Lu), yachwu@mail.cmu.edu.tw (Y.-C. Wu).
[1] These authors contributed equally to this study.

0731-7085/$ – see front matter © 2011 Elsevier B.V. All rights reserved.
doi:10.1016/j.jpba.2011.09.007

acetyltransferase activities [9]. Moreover, after fractionation of EEAC and cytotoxicity evaluation of different fractions, we found that the ethyl acetate fraction (FEA), which showed characteristic ^{1}H NMR signals of triterpenoids, was the cytotoxic active fraction of EEAC. In this bio-guided fractionation procedure, the cytotoxic components of EEAC can be attributed to FEA. The aforementioned results encouraged us to carry out further chemical and cytotoxic analyses targeting the active fraction, FEA. In the current study, the chemical profile of FEA active components (the triterpenoid-rich fraction from *A. camphorata*) was illustrated by isolation, purification, and structural elucidation of the major ergostane and lanostane derivatives by NMR and HPLC-PDA/MS.

Chiral centers present in the skeleton of bioactive botanical secondary metabolites, which are generated by specific enzyme systems in biosynthesis, are always an important issues in drug discovery. The dramatic effect of chirality on the activity and/or toxicity of any therapeutic entity was always explored and monitored. Zhankuic acids, the most abundant triterpenoid of AC, were reported to be present in a mixture of a stereo-isomeric pairs with a chiral center at C-25 [10]. So far, only zhankuic acid A was successfully separated into two isolated peaks using capillary electrophoresis [11], however other zhankuic acids, such as antcin K, antcin C, zhankuic acid C, zhankuic acid A, etc., have never been obtained in a pure form utilizing the isolation procedures embedded by previous studies [4]. Separating chiral components of isomeric mixture is crucial for understanding the mechanism of action of each isomer and the adverse effect of the undesired isomer on human body [12,13]. The lack of studies on separating pure isomers of ergostane triterpenes from AC was the driving force to investigate the possibility of developing an efficient method for their separation. In this current study, purification and structural elucidation for a series of pure stereo-isomers of ergostane triterpenes (**1**–**8**) are described herein, and their chemical profiling and cytotoxic activities were also investigated.

2. Materials and methods

2.1. General experimental procedures

Melting points were determined using a Fisher-Johns melting point apparatus (Thermo Fisher Scientific Inc., Rockford, USA), and the values presented are uncorrected. Optical rotations were measured with a JASCO DIP-370 digital polarimeter (JASCO Inc., Tokyo, Japan). UV spectra were obtained on a JASCO V-530 UV-Vis spectrophotometer (JASCO Inc., Tokyo, Japan). The IR spectra were measured on a Mattson Genesis II spectrometer (Thermo Fisher Scientific Inc., Rockford, USA). ^{1}H and ^{13}C NMR spectra were recorded on VNMRS-600 (Varian Inc., Palo Alto, USA), Varian Unity plus-400 (Varian Inc., Palo Alto, USA) and Gemini 2000-200 (Varian Inc., Palo Alto, USA) NMR spectrometers. Chemical shifts were reported in parts per million (δ), and coupling constants (J) were expressed in Hertz. LRESIMS were measured on a VG Biotech Quattro 5022 mass spectrometer (VG Biotech, Altrincham, England). Silica gel 60 (230–400 mesh) (Merck KGaA, Darmstadt, Germany) and Sephadex LH-20 (Sigma–Aldrich Corp., St. Louis, USA) were used for column chromatography. TLC analysis was carried out on silica gel GF_{254} pre-coated plates (Merck KGaA, Darmstadt, Germany) and compounds were visualized using 50% H_2SO_4, followed by heating on a hot plate. HPLC isolation was performed with a Hitachi L-7100 series HPLC (Hitachi Inc., Tokyo, Japan), equipped with a Bischoff RI detector and a Shimadzu LC-10AT series HPLC (Shimadzu Inc., Tokyo, Japan) with a SPD-10A UV-Vis detector or photodiode array detector. The Hypersil ODS (250 mm × 10 mm I.D., 5 μm) (Thermo Fisher Scientific Inc., Rockford, USA) and Cosmosil 5C-18-MS-II (250 mm × 10 mm I.D., 5 μm) (Nacalai Tesque, Kyoto, Japan) columns were utilized for HPLC separation.

2.2. Preparation of the ethanol extracts from wild fruiting bodies (EEAC)

The ethanolic extract of AC wild fruiting bodies (EEAC) was prepared as reported previously [9]. In brief, the mushroom was refluxed with ethanol at 75 °C in a 1:10 (w/v) ratio for 2 h. The extract was cooled and allowed to precipitate at 4 °C overnight. The extract supernatant was further filtered to remove any precipitate, and then the filtrate was lyophilised and stored at −70 °C before use.

2.3. Fractionation of the ethanolic extract from wild fruiting bodies (EEAC)

We utilized four different methods for the efficient fractionation of AC wild fruiting bodies ethanolic extract (Fig. S1). In Type 1, EEAC (11.0 g) was extracted with *n*-hexane to obtain the *n*-hexane fraction (FNH, 1.4 g) and the first residue. The first residue was further extracted with EtOAc to obtain the ethyl acetate fraction (FEA, 6.8 g) and the second residue. The second residue was further extracted with EtOH to obtain the ethanol fraction (FET, 1.1 g) and the third residue (0.6 g). In Type 2, EEAC (101.9 mg) was fractionised by liquid–liquid partition between EtOAc and H_2O to obtain the ethyl acetate fraction (FEA-EEAC, 79.6 mg) and the water fraction (FW1-EEAC, 20.0 mg). In Type 3, EEAC (100.3 mg) was fractionised by liquid–liquid partition between $CHCl_3$ and H_2O to yield chloroform (FCl3-EEAC, 77.6 mg) and water (FW2-EEAC, 23.6 mg) fractions. In Type 4, EEAC (100.9 mg) was fractionised by liquid–liquid partition between CH_2Cl_2 and H_2O to obtain the dichloromethane fraction (FCl2-EEAC, 76.9 mg) and the water fraction (FW3-EEAC, 23.5 mg).

2.4. Isolation of major components from the ethyl acetate fraction (FEA) utilizing Type 1 process

FEA (6.8 g) was separated by silica gel column (5 cm × 20 cm) chromatography using gradient mixtures of *n*-hexane–EtOAc–MeOH (10:1:0, 5:1:0, 1:1:0, 0:1:0, 0:40:1, 0:30:1, 0:20:1 and 0:10:1, respectively) as eluents. According to TLC results, seventeen fractions were obtained. The fourth fraction (fraction 4, 588.4 mg) was chromatographed on Sephadex LH-20 (3.5 cm × 50 cm) using EtOAc–CH_2Cl_2–MeOH (1:1:6) as the eluent, yielding three fractions. Fraction 4-1 (568.6 mg) was further chromatographed on silica gel column (3 cm × 20 cm) using $CHCl_3$–MeOH (35:1) as eluent to yield three fractions. Fifty milligrams from fraction 4-1-2 (240.3 mg) were purified with reverse-phase HPLC (RI detector; Hypersil ODS, 250 mm × 10 mm; MeOH–H_2O, 90:10) to offer dehydroeburicoic acid (**10**) (10.3 mg; flow rate: 2 ml/min; R_t 26.9 min). The sixth fraction (fraction 6, 970.9 mg) was chromatographed with EtOAc–CH_2Cl_2–MeOH (1:1:6) on Sephadex LH-20 (3.5 cm × 50 cm) to render three fractions. Fraction 6-2 (901.0 mg) was separated by silica gel column (3.5 cm × 15 cm) with $CHCl_3$–MeOH (40:1) as eluent and further purified with reverse-phase HPLC (RI detector; Hypersil ODS, 250 mm × 10 mm; ACN–H_2O, 75:25) to obtain a mixture of zhankuic acid A epimers (77.5 mg; flow rate: 2 ml/min; R_t 12.4 min). The tenth fraction (fraction 10, 132.6 mg) was chromatographed using preparative TLC with CH_2Cl_2–MeOH (15:1) to afford five fractions. Fraction 10-2 (85.0 mg) was further purified with reverse-phase HPLC (RI detector; Hypersil ODS, 250 mm × 10 mm; ACN–H_2O, 70:30) to provide a mixture of antcin C epimers (40.9 mg; flow rate: 2 ml/min; R_t 10.8 min). The thirteenth fraction (fraction 13, 1.4 g) was divided on silica gel column (3.5 cm × 20 cm) with CH_2Cl_2–MeOH (15:1) to yield

seven fractions. Fraction 13-2 (307.3 mg) was chromatographed by preparative TLC which is eluted twice with CH_2Cl_2–MeOH (15:1) to yield five fractions. Fraction 13-2-2 (40.2 mg) was separated with reverse-phase HPLC (RI detector; Hypersil ODS, 250 mm × 10 mm; ACN–H_2O, 60:40) furnishing the isolation of dehydrosulphurenic acid (**9**) (7.0 mg; flow rate: 2 ml/min; R_t 22.1 min). Fraction 13-5 (107.5 mg) was purified using reverse-phase HPLC (RI detector; Hypersil ODS, 250 mm × 10 mm; ACN–H_2O, 70:30) yielding a mixture of zhankuic acid C epimers (26.0 mg; flow rate: 2 ml/min; R_t 10.6 min). The fifteenth fraction (fraction 15, 245.7 mg) was separated into four fractions using reverse-phase solid phase extraction column (Discovery DSC-18, 10 g) with a gradient solvent mixture of H_2O–MeOH (100:0, 70:30, 50:50, 0:100) obtaining four fractions. Fraction 15-2 (126.0 mg) was further chromatographed using reverse-phase HPLC (254 nm; Hypersil ODS, 250 mm × 10 mm; ACN–H_2O: 35:65 at 0 min, 45:55 at 20 min, 100:0 at 25 min) to obtain a mixture of antcin K epimers (10.3 mg; flow rate: 3 ml/min; R_t 14.2 min).

2.5. Purification of ergostane stereo-isomeric pairs

We developed a highly efficient reverse phase HPLC system to separate the major ergostane stereo-isomeric pairs. Antcin K was chromatographed with HPLC (254 nm; Hypersil ODS, 250 mm × 10 mm; ACN–H_2O: 35:65 at 0 min, 45:55 at 20 min, 100:0 at 25 min) to yield compounds **1** (flow rate: 4.7 ml/min; R_t 13.4 min) and **2** (flow rate: 4.7 ml/min; R_t 14.0 min), respectively. The separation of other ergostane stereo-isomeric pairs was achieved utilizing acidic mobile phase. In this mobile phase system, solvent A was acetonitrile and solvent B was water containing 0.05% acetic acid. Antcin C was divided using HPLC system (254 nm; Cosmosil 5C-18-MS-II, 250 mm × 10 mm; solvent A–B, 50:50) to offer compounds **3** (flow rate: 3 ml/min; R_t 26.8 min) and **4** (flow rate: 3 ml/min; R_t 29.3 min), respectively. Zhankuic acid C was separated with HPLC system (254 nm; Cosmosil 5C-18-MS-II, 250 mm × 10 mm; solvent A–B, 50:50) to yield compounds **5** (flow rate: 3 ml/min; R_t 31.1 min) and **6** (flow rate: 3 ml/min; R_t 32.7 min), respectively. Zhankuic acid A was chromatographed by HPLC system (254 nm; Cosmosil 5C-18-MS-II, 250 mm × 10 mm; solvent A–B, 50:50) to offer compounds **7** (flow rate: 3 ml/min; R_t 41.9 min) and **8** (flow rate: 3 ml/min; R_t 43.3 min), respectively.

2.6. Synthesis of (R)- and (S)-1-(9-anthryl)-2,2,2-trifluoroethanonyl [(R)- and (S)-AT] esters of compounds 2–8

The isolated compounds reacted with (*R*)- and (*S*)-1-(9-anthryl)-2,2,2-trifluoroethanonyl yielding chiral ester, and the absolute configuration of the isolated compounds was achieved through determining the configuration of the formed ester. The isolated quantity of compound **1** was insufficient for chemical modification and its configuration was achieved by comparing it with the configuration of its isomeric pair (compound **2**). The synthesis of chiral esters of the isolated compounds was done utilizing the same method and preparation of compound **7** chiral ester is presented here as an example (for the full synthetic procedures of other isolated compounds please see Supplementary data).

(*R*)-AT-ester of **7** was prepared as follows. Compound **7** (6.42 mg, 0.014 mmol) and (1*R*)-1-(9-anthryl)-2,2,2-trifluoroethanol (Sigma–Aldrich Corp., St. Louis, USA) (3.53 mg, 0.014 mmol) were dissolved in tetrahydrofuran (THF) (Sigma–Aldrich Corp., St. Louis, USA) and than were added to a solution of 1-ethyl-3-(3-dimethylaminopropyl)carbodiimide (EDCI) (TCI, Portland, USA) (7.61 mg, 0.042 mmol), triethylamine (Et_3N) (Sigma–Aldrich Corp., St. Louis, USA) (3.69 μl, 0.028 mmol) and 4-(dimethylamino)pyridine (DMAP) (Sigma–Aldrich Corp., St. Louis, USA) (2.43 mg, 0.021 mmol) in CH_2Cl_2. The mixture was stirred at room temperature for 12 h. The reaction mixture was concentrated under reduced pressure and then partitioned with CH_2Cl_2 and H_2O. The organic layer was then evaporated, and the residue was purified using preparative TLC (CH_2Cl_2) to yield (*R*)-AT-ester of **7** (3.43 mg, 33.75% yield). (*S*)-AT-ester of **7** was prepared as follows. The procedure was similar to that described for (*R*)-AT-ester of **7**. Starting from compound **7** (11.15 mg, 0.024 mmol), (1*S*)-1-(9-anthryl)-2,2,2-trifluoroethanol (Sigma–Aldrich Corp., St. Louis, USA) (6.57 mg, 0.024 mmol), EDCI (13.68 mg, 0.024 mmol), Et_3N (6.63 μl, 0.072 mmol), and DMAP (4.36 mg, 0.036 mmol), (*S*)-AT-ester of **7** (9.01 mg, 51.71% yield) was obtained.

2.7. HPLC analysis method for FEA

Sample analysis was carried out on a LC-10A VP HPLC system (Shimadzu Inc., Tokyo, Japan) consisting of a quaternary pump (LC-10AT), an on-line degasser (DGU-14A), an autosampler (SIL-10AD), a photodiode-array detector (SPD-M10A) and Class VP for data collection. Liquid chromatography was performed using a Cosmosil 5C-18-MS-II column (5 μm, 250 mm × 4.6 mm I.D.) supplied by Nacalai Tesque Inc., Kyoto, Japan. The sample injection volume was 20 μl. The mobile phase was a mixture of acetonitrile (ACN, A) and water (B) containing 0.1% (v/v) acetic acid. A gradient program was used as follows: the initial elution condition was A–B (45:55, v/v), linearly changed to A–B (50:50, v/v) at 30 min, A–B (55:45, v/v) at 35 min, A–B (60:40, v/v) at 45 min, A–B (70:30, v/v) from 45 min to 55 min, A–B (85:15, v/v) at 60 min. Over the next 40 min, the percentage of mobile phase A increased linearly to 100%. The mobile phase was filtered through a 0.22 μm Millipore filter and degassed before use. The flow rate was set at 1.0 ml/min, the column temperature was maintained at room temperature, and detection wavelengths were set at 254 nm and 270 nm. Ethyl acetate fraction (FEA) was obtained from EEAC using a Type 1 fractionation method. From the FEA dry extract, 1 mg was dissolved in 1 ml of methanol and filtered through a 0.45 μm membrane filter prior to loading into the HPLC column. HPLC samples of compounds **1**–**8** pure isolated isomers were prepared in a similar way.

2.8. LC–ESIMS method for FEA

The instrumentation and chromatographic conditions of HPLC for LC–MS were the same as the described in Section 2.7, except the injection volume was set at 10 μl. Identification of FEA was carried out using a Thermo Finnigan LC–MS system (Thermo Finnigan, San Jose, USA) consisting of a Spectra System P 4000 pump, a Spectra System AS 3000 autosampler with injection volume set to 10 μl and a Surveyor MSQ quadrupole mass spectrometer equipped with an electrospray ionization LC–MS interface (ESI). The LC effluent was introduced into the ESI source using a post-column splitting ratio of 2:1. Ultra high-purity nitrogen (N_2) was used as the nebulising gas. ESI was applied in the positive and negative ionization modes and the capillary was held at a potential of 3.0 kV. The cone voltage was set at 40 V and the ionization source was set to a temperature of 550 °C. We used dwell times of 1 s. For each analysis in the full scan mode, mass range was set at m/z 100–1000, enabling the identification purposes.

2.9. Cytotoxicity assays

Human acute lymphoblastic leukemia cells (CCRF-CEM and Molt 4) and human promyelocytic leukemia cells (HL 60) were obtained from the American Type Culture Collection. All cell lines were cultured on RPMI-1640 medium supplemented with 10% (v/v) FBS (fetal bovine serum), 100 U/ml penicillin and 100 μg/ml

streptomycin at 37 °C in a humidified atmosphere of 5% CO_2 and 95% air. Cell viability was measured by MTT (3-(4,5-dimethylthiazol-2-yl)-2,5-diphenyltetrazolium bromide) colorimetric method [9]. In brief, freshly trypsinized cell suspensions were seeded in 96-well microtiter plates at densities of 5000–10,000 cells per well and the test compounds were added from DMSO stock solutions (the final concentration of DMSO in culture medium was 0.2%). After 3 days in culture, the attached cells were incubated with MTT (0.5 μg/ml, 4 h) and subsequently solubilized in DMSO. The absorbance was measured at 550 nm using a microplate reader. The calculated IC_{50} was the concentration of the tested agent that reduced cell growth by 50% under the experimental conditions. The results represented the mean of three separate experiments, each performed in triplicate.

3. Results and discussion

3.1. Anti-proliferative effect of AC fractions obtained using a variety of sample preparation methods

Several preparation methods have been developed over the past few years by different research groups for offering AC extracts. We summarised the extraction and partition methods published in the previous papers [1,2,10,14–17]. It was stated in publications that these extraction methods were designed to yield the maximum possible amount of extracts for use in future applications. Developing a high yield process is especially desirable because of the high price of the raw materials (wild fruiting bodies of AC) [3]. In the current study we confirmed the reproducibility of our reported fractionation method to obtain FEA active fraction [9]. According to our previous preparation method, EEAC was sequentially extracted with *n*-hexane, ethyl acetate, and ethanol to obtain three different fractions, FNH, FEA, and FET (Type 1). Other partition methods reported by other research groups can be divided into three methods, labelled here as Types 2–4 (see Fig. S1; Section 2.3) [2,10,14,15]. In Type 2, EEAC was partitioned between EtOAc and H_2O according to the method published by Chen et al. and Hsu et al. [10,15], yielding both an ethyl acetate fraction (FEA-EEAC) and a water fraction (FW1-EEAC). In Type 3, EEAC was partitioned between $CHCl_3$ and H_2O, according to the report by Cherng et al. [14], to yield chloroform (FCl3-EEAC) and water (FW2-EEAC) fractions. In Type 4, CH_2Cl_2 (FCl2-EEAC) and H_2O (FW3-EEAC) fractions were obtained by liquid–liquid partition from EEAC according to method published by Shen et al. [2].

All fractions and EEAC were subjected to a cytotoxic assay against HL 60 cell line (Fig. S1). In all cases, the results showed that organic fractions with lower polarity (FNH, FEA, FEA-EEAC, FCl3-EEAC, and FCl2-EEAC) were active, whereas the highly polar fractions (FET, FW1-EEAC, FW2-EEAC, and FW3-EEAC) were inactive. In Type 1, FEA exhibited the best activity and demonstrated good repeatability for concentrating the cytotoxic components from EEAC. Interestingly the antiproliferative activity of the ethyl acetate active fraction (FEA) prepared by food science acceptable fraction method (Type 1) was more potent (104.10 μg/ml) than FEA-EEAC (156.47 μg/ml) prepared by Type 2. Although the anti-proliferative activity of fractions (FCl3-EEAC and FCl2-EEAC) was comparable to FEA, the use of chlorine-containing organic solvents, such as CH_2Cl_2 and $CHCl_3$, limits their application in pharmaceutical related products. Based on these findings, the previously established methods were not ideal preparation procedures [2,14,16]. Encouraged by the high antiproliferative activity of FEA and its benign fractionation procedures, we decided to shed light on the chemical composition and the pharmacological activity of FEA.

3.2. Chemical profile of FEA major components

HPLC analyses were applied to trace the complexity of the chemical profile of FEA and provided the guidance for further chemical isolation (Figs. S2 and S3). Based on our experience, the separation of FEA components using normal phase chromatography or reverse phase HPLC with MeOH:H_2O solvent system was not ideal. After testing several mobile phase systems with reverse phase HPLC, we found that the using gradient mobile phase of acetonitrile with acidic water (0.1% acetic acid in water) served to separate FEA constituents. The HPLC traces at 254 nm revealed the presence of ten major peaks, labelled numerically (Fig. S3). Upon shifting to a longer UV wave length (270 nm), peaks 9 and 10 did not appear (Fig. S3), suggesting a different conjugation pattern from peaks 1 to 8. Moreover, we observed that the retention times for peak pairs 1 and 2, 3 and 4, 5 and 6, as well as 7 and 8 are very close and single peak of each pair cannot be entirely separated using different chromatographic designs. This phenomenon suggests that each peak pair represents an isomeric-pair of compounds.

Triterpenoids and steroids from natural sources displayed no or weak UV absorption; however, ergostane and lanostane triterpenes from AC exhibited a UV absorption maxima within the range from 230 to 270 nm, due to the conjugated functionalities in their skeleton at C-7, C-8, C-9, and C-11 [1,16]. The major constituents of AC triterpenoid are zhankuic acids derivatives having chiral center at C-25. Zhankuic acids were isolated previously as a mixture of stereo-isomeric pairs [10]. According to literature findings and FEA HPLC fingerprint, it suggested that peaks 1–8 should be four pairs of zhankuic acid derivatives. In order to identify the components of FEA by HPLC, we attempted to isolate the compounds that corresponded to the major HPLC peaks (Figs. S2 and S3). The FEA was separated by normal phase fresh column chromatography using gradient mixtures of *n*-hexane–EtOAc–MeOH as eluents. According to the TLC results, seventeen fractions were obtained. The collected seventeen fractions were analyzed by analytical scale HPLC and the fractions containing constituents in the same polarity region corresponding to peaks 1–10 of FEA were further chromatographed (Fig. S3). Fraction 4, which was enriched with peak 10, was separated by Sephadex LH-20, silica gel columns and further purified by RP-HPLC, yielding compound **10**. After comparing its physical and spectroscopic data to those reported in literatures, compound **10** was identified as dehydroeburicoic acid [2]. Zhankuic acid A isomeric pair [10] was obtained by separation from fraction 6, enriched with peaks 7 and 8. The other three zhankuic acid derivatives, antcin C [10], zhankuic acid C [14], and antcin K [2] were obtained from fractions 10, 13, and 15, respectively, using similar methods. Dehydrosulphurenic acid (**9**) [2,16], corresponding to peak 9, was obtained from fraction 13 together with zhankuic acid C and then further purified with column chromatography.

In previous isolation processes [10,14,16,17], these ergostane and lanostane triterpenes were reported to be purified with a normal phase open column and/or preparative TLC. Based on our experience testing previously reported isolation methods, these methods could not lead to the isolation of pure isomers. For example, zhankuic acid A, one of the major ergostane constituents, showed only one spot on normal phase TLC, nevertheless, other impurities can be observed in reverse phase TLC and HPLC (Fig. S4). Similar findings were observed in the isolation of dehydroeburicoic acid, belonging to lanostane triterpenes (Fig. S5). To overcome these difficulties we used our developed reverse phase HPLC with acetonitrile–0.05% acetic acid in H_2O to separate the closely related isomeric pairs of steroidal AC triterpenes.

Identification of the ten peaks was achieved by comparing their retention time and ultraviolet absorption with isolated compounds (Fig. 1). The areas of these labelled peaks accounted for 78.57% and 85.07% of the total area of all the peaks at 254 nm and 270 nm,

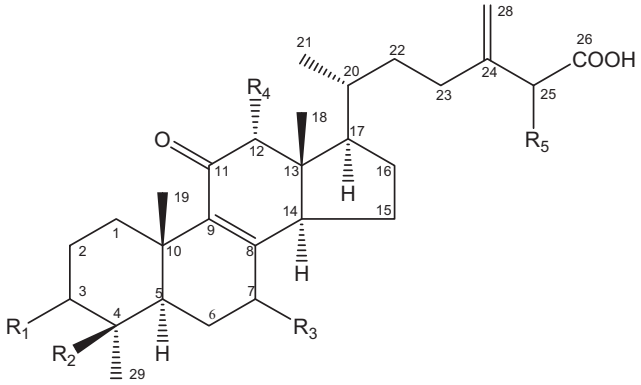

	R_1	R_2	R_3	R_4	R_5	peak no.	separation from
1	β-OH	OH	α-OH	H	α-CH_3	1	antcin K
2	β-OH	OH	α-OH	H	β-CH_3	2	
3	=O	H	α-OH	H	α-CH_3	3	antcin C
4	=O	H	α-OH	H	β-CH_3	4	
5	β-OH	H	=O	OH	β-CH_3	5	zhankuic acid C
6	β-OH	H	=O	OH	α-CH_3	6	
7	=O	H	=O	H	α-CH_3	7	zhankuic acid A
8	=O	H	=O	H	β-CH_3	8	

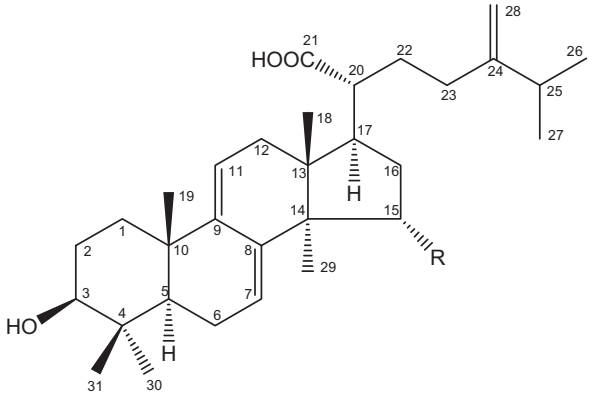

	R	peak no.
9	OH	9
10	H	10

Fig. 1. Chemical structures of compounds **1**–**10**.

respectively (Fig. S3). Under our HPLC optimized conditions (Fig. 2A and B), a series of peak pairs corresponded to zhankuic acid isomeric pairs were observed in the obtained chromatograms. Peak intensities of 1 and 2 (antcin K) as well as peaks 3 and 4 (antcin C) decreased at 270 nm due to less conjugation compared to peaks 5 and 6 (zhankuic acid C) as well as peaks 7 and 8 (zhankuic acid A). Peaks 9 and 10 were identified as dehydrosulphurenic acid (**9**) and dehydroeburicoic acid (**10**), respectively, which posses a single conjugated system in the lanostane skeleton showing no UV absorption at 270 nm. Comparing peak areas and heights of FEA respective constituents at 254 and 270 nm, indicated that FEA is mainly composed of the following major triterpenoids, antcin K, antcin C, zhankuic acid C, dehydrosulphurenic acid, zhankuic acid A, and dehydroeburicoic acid. Among the major triterpenoids, zhankuic acid A, corresponding to peaks 7 and 8, accounted the majority of peaks area and height.

3.3. Purification and structure elucidation of ergostane stereo-isomeric pairs

Analysing the separated peaks by NMR, pointed out that our developed HPLC system was able to separate zhankuic acids stereo-isomeric pairs for the first time. Purification and structural elucidation of zhankuic acid A isomeric pair, the major component in FEA, are illustrated here as an example. The recycle chromatography system in the reverse phase HPLC (254 nm; Hypersil ODS, 250 mm × 10 mm; ACN–H_2O, 55:45; flow rate: 4.3 ml/min) was used for purifying zhankuic acid A stereo-isomeric pair. Through

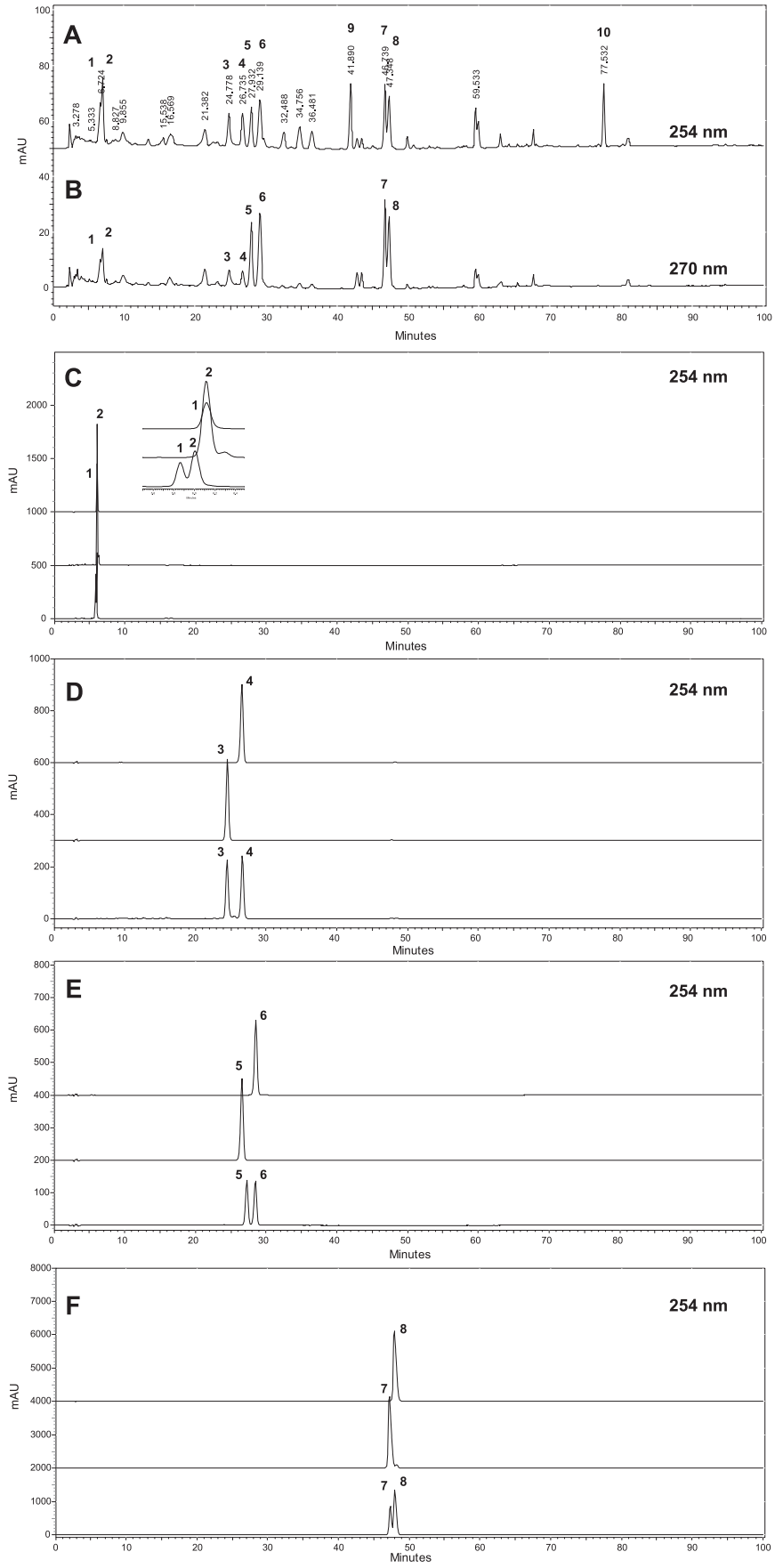

Fig. 2. HPLC chromatogram of the ethyl acetate fraction obtained using Type 1 process (FEA). Isolated compounds **1**–**8** are shown for comparison.

eight successive recycles, compounds **7** and **8** were separated and collected at the retention time of 416.2 and 446.5 min (Fig. S6). After several trials, we were able to separate compound **7** (R_t 41.9 min) and **8** (R_t 43.3 min) utilizing our developed HPLC system (254 nm; Cosmosil 5C-18-MS-II, 250 mm × 10 mm; 1:1 ACN:0.05% acetic acid in H_2O, flow rate: 3.0 ml/min) (see Fig. S7; Section 2.5). By comparing to the original recycle chromatography method, the application of the acidic solvent system decreased the retention time of the separated compounds ten folds. The other ergostane stereo-isomeric pairs were purified using similar HPLC system with slight modification of the mobile phase composition. Also antcin K, antcin C, and zhankuic acid C isomeric pairs were separated yielding compounds **1**–**6**, respectively (Figs. 1 and 2C–F).

The stereoconfiguration of the isolated compounds was determined based on NMR analysis and chemical modification through reacting the isolated compounds with chiral alcohol. Determination of the stereoconfiguration of the isomeric pair **7** and **8** is presented here as an example. The ^{1}H NMR spectrum of zhankuic acid A (in pyridine-D5, 600 MHz) exhibited two overlapped secondary methyl signals at δ_H 1.521 (3H-27, d, J = 7.2 Hz) and δ_H 1.528 (3H-27, d, J = 7.2 Hz), indicating the presence of two stereoisomers with different configuration at C-25 chiral center (Fig. S8A). The overlapped methyl signals cannot be clearly detected using lower frequencies NMR machine (e.g. 200 MHz and 400 MHz). Using 600 MHz NMR, two pairs of partially overlapped signals of the terminal olefinic protons (H_2-28) were also observed (Fig. S8A). The ^{13}C NMR spectrum of zhankuic acid A (in pyridine-D5, 150 MHz) clearly showed the isomeric pair patterns at δ_C 34.242 and 34.342 (CH_2-22), 31.575 and 31.766 (CH_2-23), 46.558 and 46.793 (CH-25), as well as 17.003 and 17.179 (CH_3-27), representing carbon signals close to C-25 on the 24-exo-methylene-26-oic acid side chain (Fig. S9A). On the other hand identical carbons of the isomeric pairs separated by more than 3 carbon atoms from C-25 showed slight difference in the chemical shift such as signals at δ_C 27.960 and 27.997 (CH_2-16), 53.937 and 53.986 (CH-17), 35.847 and 35.885 (CH-20), together with 18.519 and 18.564 (CH_3-21) (Fig. S9A). In an identical NMR experiment (pyridine-D5, 600 MHz), the ^{1}H and ^{13}C NMR spectra of the isomeric pair (**7** and **8**) showed only single signal pattern compared to the double signal pattern observed in zhankuic acid A spectra (Figs. S8B, S8C, S9B, and S9C). Assignments of the ^{1}H and ^{13}C signals of compounds **7** and **8** were performed by extended 2D NMR methods. Due to the high similarity of ^{1}H and ^{13}C signals of compounds **7** and **8**, the spectral data are presented in three significant figures after the decimal point (Tables 1 and 2). The NOE correlations in **7** and **8** were too similar to recognize the stereo chemical difference. To determine the absolute configuration of the chiral carbon at C-25 (α) to the carboxylic acid, chemical derivatization utilizing chiral pure alcohol was applied [18,19]. Compound **7** was treated separately with chiral derivatizing reagents, (1*R*)- and (1*S*)-1-(9-anthryl)-2,2,2-trifluoroethanol [(*R*)- and (*S*)-AT] to yield the (*R*)- and (*S*)-AT ester derivatives, respectively (Fig. S10A and S10B). The AT esters were formed successfully at C-26 as elucidated from the ^{13}C NMR signals of the ester carbonyl group at δ_C 172.774 [(*R*)-AT-ester of **7**] and δ_C 172.681 [(*S*)-AT-ester of **7**]. The calculated differences in chemical shifts [δ of protons in the (*R*)-AT-ester minus δ of the corresponding protons in the (*S*)-AT-ester] led to the assignment of the absolute configuration at C-25 in **7** as (*S*) (Fig. S10C and Table S1). Thus, compound **7** was named as 4α-methylergosta-8,24(28)-dien-3,7,11-trion-25*S*-26-oic acid. The absolute configuration of **8** at C-25 was assigned as *R* by using the same method (Table S1), and it was named 4α-methylergosta-8,24(28)-dien-3,7,11-trion-25*R*-26-oic acid.

After determining the absolute configuration, we tried to measure the optical rotation aiming to complete the spectral profile for the isolated compounds. In a previous report [2], the mixture form of zhankuic acid A was dissolved in methanol to measure its optical rotation. However, the solubility of **7** (25*S*) and **8** (25*R*) was not sufficient in single solvent (methanol or ethanol). The solubility of compounds **7** and **8** improved through using acetone-methanol mixture. Considering compounds solubility and the convenience of collecting physical and spectral data using single solvent, pyridine was used in optical rotation experiment. The optical rotation value of compounds **7** ($[\alpha]_D^{25}$ +32.1, *c* 0.70, pyridine) and **8** ($[\alpha]_D^{25}$ +9.0, *c* 0.84, pyridine) were determined.

The structures of compounds **1**–**6** were assigned by the 2D NMR methods (Tables 1 and 2) and the absolute configuration of the chiral center at C-25 was assigned as described for compounds **7** and **8** (Table S1). Compound **3** was assigned as 7β-hydroxy-4α-methylergosta-8,24(28)-dien-3,11-dion-25*S*-26-oic acid and its optical rotation was $[\alpha]_D^{25}$ +124.8 (*c* 0.81, pyridine). Compound **4** was assigned as 7β-hydroxy-4α-methylergosta-8,24(28)-dien-3,11-dion-25*R*-26-oic acid and its optical rotation was $[\alpha]_D^{25}$ +79.9 (*c* 0.47, pyridine). Compounds **5** and **6** were assigned as 3α,12α-dihydroxy-4α-methylergosta-8,24(28)-dien-7,11-dion-25*R*-26-oic acid and 3α,12α-dihydroxy-4α-methylergosta-8,24(28)-dien-7,11-dion-25*S*-26-oic acid, respectively. The optical rotation data of **5** and **6** were $[\alpha]_D^{25}$ +82.0 (*c* 0.64, pyridine) and $[\alpha]_D^{25}$ +110.6 (*c* 0.70, pyridine), respectively. Compounds **1** and **2** showed $[\alpha]_D^{25}$ +61.0 (*c* 0.42, pyridine) and $[\alpha]_D^{25}$ +71.8 (*c* 0.27, pyridine), respectively. From the results of chemical derivatization, **2** was assigned as 3α,4β,7β-trihydroxy-4α-methylergosta-8,24(28)-dien-11-on-25*R*-26-oic acid. Unfortunately, the separated quantity of compound **1** was insufficient for chemical modification. In order to assign compound **1** absolute configuration we depended on the general trend observed in determining the stereoconfiguration of the isolated isomeric pairs. It was noticed that in each isomeric pair, if the chiral center at C-25 is assigned as (*S*) the other isomer chiral center is assigned as (*R*). Based on this finding and by knowing the absolute configuration of the chiral center in compound **2** as (*R*), the chiral center at C-25 in compound **1** was estimated as (*S*). Compound **1** was assigned as 3α,4β,7β-trihydroxy-4α-methylergosta-8,24(28)-dien-11-on-25*S*-26-oic acid. It is clear that with respect to optical rotation values of the pure isomers, all (*S*) isomers possessed higher optical rotation values compared to the (*R*) isomers except for compounds **1** and **2**.

3.4. HPLC method optimization and relative percentage evaluation of FEA

The HPLC conditions for the active ethyl acetate fraction were further optimized after isolating the major triterpenes as standards from FEA (Fig. 2). Because the skeleton of these triterpenes contained a carboxylic acid moiety, symmetrical sharp peaks were easily obtained in the HPLC chromatogram using acidic mobile phase with a relatively low pH value. Due to the acidic properties of these AC triterpenes, three types of 0.1% organic acids, including trifluoroacetic acid (pH 2.2), acetic acid (pH 3.3) and formic acid (pH 2.8) were screened as additive to the mobile phase. The use of acidic additive in the separation of acidic constituents usually results in symmetrical well resolved peaks. We studied the relationship between peak area and retention time for the major peaks after adding organic acid into the aqueous phase. The results showed that retention times of the major peaks in these three different acidic systems were nearly identical. However, the best results in terms of maximum peak area of the major triterpenoids were obtained using the formic and acetic acidic systems. Although both 0.1% formic and acetic acids produced similar results, the latter was selected. The use of acetic acid provided more stable baseline and improved the shape of the desired peaks in the HPLC fingerprints. The maximum absorbance (λ_{max}) of ergostane and lanostane triterpenes was detected at 254 nm and 270 nm, respectively (Fig. 2A and B).

Table 1
^{1}H NMR data[a] for compounds **1**–**8** (C_5D_5N, δ in ppm, J in Hz).

Proton	1	2	3	4	5	6	7	8
1a	2.110 m	2.108 m	1.416 m	1.436 m	1.957 m	1.946 m	1.437 m	1.422 m
1b	3.148 dt (13.2, 3.0)	3.149 dt (13.2, 3.6)	3.232 qd (6.0, 2.4)	3.231 qd (6.6, 2.4)	2.737 dt (12.0, 3.6)	2.734 dt (13.2, 3.0)	3.178 qd (6.6, 3.0)	3.178 qd (6.6, 2.4)
2a	1.965 m	1.975 m	2.390 m	2.389 m	1.855 m	1.857 m	2.406 m	2.406 m
2b	2.771 m	2.778 m	2.548 m	2.537 m	1.855 m	1.857 m	2.588 m	2.570 m
3	β 4.092 s	β 4.094 s			β 3.877 s	β 3.874 br s		
4			β 2.374 m	β 2.373 m	β 1.692 m	β 1.699 m	β 2.464 m	β 2.458 m
5	α 2.202 m	α 2.201 m	α 1.416 m	α 1.414 m	α 2.596 m	α 2.592 m	α 1.886 m	α 1.880 m
6a	2.461 m	2.466 m	1.823 m	1.822 m	2.448 m	2.448 m	2.584 m	2.570 m
6b	2.749 m	2.750 m	2.374 m	2.373 m	2.611 m	2.613 m	2.584 m	2.570 m
7	α 4.650 t (8.4)	α 4.651 br t	α 4.524 t (7.8)	α 4.527 td (8.4, 1.2)				
12a	2.476 m	2.462 m	2.473 d (13.8)	2.477 d (13.8)	β 4.505 s	β 4.500 s	2.503 m	2.503 m
12b	3.000 d (13.2)	3.000 d (13.8)	3.000 d (13.8)	3.000 d (13.8)			3.019 d (13.8)	3.018 d (13.8)
14	α 2.666 m	α 2.674 m	α 2.755 ddd (12.0, 6.6, 1.2)	α 2.763 ddd (12.6, 7.2, 1.8)	α 3.567 dd (13.2, 7.8)	α 3.559 dd (13.2, 7.8)	α 2.742 m	α 2.745 m
15a	2.120 m	2.128 m	2.113 m	2.116 m	1.674 m	1.677 m	1.547 m	1.552 m
15b	2.546 m	2.541 m	2.548 m	2.537 m	2.858 m	2.854 m	2.753 m	2.734 m
16a	1.328 m	1.360 m	1.336 m	1.337 m	1.327 m	1.315 m	1.240 m	1.242 m
16b	1.965 m	1.952 m	1.947 m	1.924 m	1.978 m	1.982 m	1.915 m	1.906 m
17	α 1.441 m	α 1.436 m	α 1.416 m	α 1.424 m	α 2.302 m	α 2.300 m	α 1.390 m	α 1.382 m
18	0.929 s	0.925 s	0.893 s	0.891 s	0.821 s	0.819 s	0.707 s	0.703 s
19	2.099 s	2.098 s	1.604 s	1.602 s	1.547 s	1.547 s	1.611 s	1.609 s
20	β 1.405 m	β 1.417 m	β 1.336 m	β 1.335 m	β 1.490 m	β 1.478 m	β 1.381 m	β 1.390 m
21	0.908 d (6.0)	0.909 d (6.0)	0.911 d (6.0)	0.913 d (6.0)	1.077 d (6.6)	1.075 d (6.6)	0.895 d (5.4)	0.892 d (6.0)
22a	1.328 m	1.297 m	1.354 m	1.313 m	1.346 m	1.389 m	1.314 m	1.272 m
22b	1.740 m	1.789 m	1.737 td (12.0, 5.4)	1.775 m	1.806 m	1.767 m	1.697 td (11.4, 5.4)	1.738 td (12.0, 3.6)
23a	2.237 m	2.238 m	2.236 m	2.235 m	2.236 m	2.233 m	2.211 m	2.223 m
23b	2.498 m	2.439 m	2.484 m	2.431 m	2.423 m	2.474 m	2.448 m	2.406 m
25	3.485 br q	3.491 q (7.2)	3.487 br q (6.6)	3.483 q (6.6)	3.457 q (7.2)	3.452 q (7.2)	3.464 br q (7.2)	3.480 br q (6.6)
27	1.534 d (6.6)	1.530 d (7.2)	1.530 d (6.6)	1.522 d (7.2)	1.496 d (7.2)	1.504 d (6.6)	1.524 d (7.2)	1.529 d (6.6)
28a	5.076 s	5.083 s	5.089 s	5.085 s	5.059 s	5.073 s	5.069 s	5.060 s
28b	5.234 s	5.256 s	5.242 s	5.256 s	5.234 s	5.226 s	5.231 s	5.248 s
29	1.763 s	1.765 s	1.132 d (6.6)	1.132 d (6.6)	1.052 d (6.6)	1.050 d (7.2)	1.039 d (6.6)	1.039 d (6.6)

[a] Assignments were confirmed by coupling constants, ^{1}H–^{1}H COSY, NOESY, HMQC, and HMBC analysis.

Table 2
^{13}C NMR data[a] for compounds **1**–**8** (C_5D_5N, δ in ppm).

Carbon	1	2	3	4	5	6	7	8
1	29.687	29.687	36.163	36.160	28.583	28.575	34.947	34.936
2	26.786	26.785	38.123	38.121	30.155	30.148	37.771	37.767
3	74.711	74.711	211.368	211.359	69.308	69.301	209.898	209.909
4	73.957	73.957	44.069	44.074	35.324	35.316	43.925	43.918
5	43.498	43.498	48.629	48.634	41.605	41.602	48.914	48.896
6	30.199	30.199	33.504	33.509	38.685	38.677	39.208	39.201
7	70.805	70.805	69.311	69.319	202.004	201.993	200.778	200.789
8	154.299	154.292	155.860	155.856	144.406	144.395	145.504	145.504
9	143.939	143.939	140.862	140.873	153.160	153.145	151.957	151.953
10	38.755	38.751	37.391	37.396	38.980	38.976	38.630	38.618
11	201.504	201.504	201.318	201.317	203.938	203.927	202.679	202.701
12	58.817	58.817	58.454	58.470	80.956	80.941	57.474	57.470
13	47.942	47.938	47.882	47.891	50.240	50.225	47.238	47.234
14	53.768	53.772	53.577	53.597	42.707	42.692	49.471	49.463
15	25.486	25.490	25.362	25.371	24.617	24.598	25.297	25.301
16	28.298	28.234	28.227	28.183	27.351	27.377	28.027	27.979
17	54.855	54.877	54.645	54.699	46.079	46.027	54.001	54.016
18	12.493	12.493	12.470	12.480	11.815	11.796	12.092	12.092
19	20.956	20.956	17.643	17.648	16.457	16.449	16.249	16.241
20	36.242	36.271	36.114	36.160	35.974	35.891	35.881	35.959
21	18.614	18.655	18.603	18.657	18.141	18.070	18.549	18.601
22	34.419	34.509	34.359	34.472	34.640	34.491	34.253	34.383
23	31.999	31.764	31.860	31.675	31.843	32.052	31.855	31.657
24	150.833	150.707	150.601	150.616	150.830	150.490	150.642	150.116
25	47.068	47.005	46.720	46.923	47.095	46.602	47.006	47.518
26	177.842	177.237	177.371	177.154	177.479	177.113	177.770	178.124
27	17.165	17.255	17.086	17.234	17.290	17.058	17.138	17.425
28	110.003	110.186	110.280	110.302	110.145	110.291	110.127	109.888
29	28.059	28.059	11.888	11.893	16.394	16.393	11.558	11.551

[a] Assignments were confirmed by coupling constants, ^{1}H–^{1}H COSY, NOESY, HMQC, and HMBC analysis.

Considering the absorbance of these two type triterpenes, 254 nm was chosen as the detection wavelength. Accordingly, detection wavelength, acid concentration, and injection volume were set at 254 nm, 0.1% acetic acid, and 20 μl. The chromatogram was analyzed by using the software 'Class VP', and the percentage of all peaks with mean chromatogram were calculated by the same software based on the peak area. In addition, the relative peak area (RPA) of each characteristic peak (peaks 1–10) was calculated in comparison to the reference peak (peak 9) offering a semi-quantitative determination of the chemical composition of FEA.

In a simulative median chromatogram of FEA, it had ten well-resolved 'characteristic peaks', including eight ergostane triterpenes (peaks 1–8) and two lanostane triterpenes (peaks 9 and 10). Among them, peak 9, which appeared in the middle of the chromatogram with a maximum area, was considered as the internal reference peak. The RPA data of the ten characteristic peaks in FEA were 0.532 (compound **1**, peak 1, R_t 6.724), 0.781 (compound **2**, peak 2, R_t 7.004), 0.669 (compound **3**, peak 3, R_t 24.778), 0.623 (compound **4**, peak 4, R_t 26.735), 0.771 (compound **5**, peak 5, R_t 27.932), 0.996 (compound **6**, peak 6, R_t 29.139), 1.046 (compound **7**, peak 7, R_t 46.739), 0.862 (compound **8**, peak 8, R_t 47.348), 1.000 (compound **9**, peak 9, R_t 41.890), and 0.701 (compound **10**, peak 10, R_t 77.532), individually. The absolute stereoconfiguration at C-25 was not the decisive factor for the elution order in HPLC experiments. In the reverse phase HPLC analysis of antcin K and zhankuic acid C pure isomeric forms, peaks 1 and 5 corresponding to (*R*) isomers were eluted first followed by peaks 2 and 6 corresponding to (*S*) isomers. However an opposite trend was observed in the separating of pure isomeric forms of antcin C and zhankuic acid A. In both cases the (*S*) isomers were eluted first.

3.5. LC–ESI-MS analysis of FEA

In order to further identify the ergostane stereo-isomeric pairs in FEA, we employed HPLC-PDA/MS. Identification was accomplished by using on-line DAD, ESI-MS techniques, and co-elution with compounds **1**–**10**. At the beginning, both positive and negative ion modes were used in an attempt to ionize compounds **1**–**10**. It was found that the positive mode resulted in a larger number of ions compared to the negative mode. Therefore, ESI in the positive mode was selected for the follow-up analysis. Moreover, the MS peak intensity was compared at three different ionization source temperatures (350 °C, 450 °C and 550 °C). The MS results indicated that peak intensity obtained under ionization source temperature of 550 °C was over two fold higher than those at 450 °C or 350 °C. Therefore, 550 °C was selected as the suitable ionization source temperature. The total ion current (TIC) chromatogram in the positive mode is shown in Fig. S11. By comparing FEA and compounds **1**–**8** in the on-line ESI-MS spectra, the four major stereo-isomeric pairs of ergostane triterpenes (antcin K, antcin C, zhankuic acid C, and zhankuic acid A) were detected, corresponding to peak pairs of 1 and 2, 3 and 4, 5 and 6, as well as 7 and 8, respectively. The *m*/*z* data in the HPLC-ESI/MS spectra for these four major peak pairs (peaks 1–8) are shown in Table S2. The mass spectra of each isomer were similar to the mass spectra of the other isomer in the same pair as 1 and 2, 3 and 4, 5 and 6, 7 and 8. Fragments of these four major peak pairs were observed at $[M+H-18]^+$ or $[M+H-15]^+$, corresponding to the loss of hydroxyl or methyl groups. Furthermore, the fragment ion $[M+H-44]^+$, corresponding to the loss of $-COO^-$, was detected indicated the existence of carboxylic group in the structures. This is the first reported identification of these novel paired triterpene stereo-isomers in AC using HPLC and LC–MS. It was observed that lanostane triterpenes, dehydrosulphurenic acid and dehydroburicoic acid, corresponding to peaks 9 and 10, disappeared in the TIC chromatogram. The absence of peaks 9 and 10 indicated that the corresponding compounds cannot be easily ionized or their ions are unstable under the processes of electron spray ionization. To the best of our knowledge this is the first report showing differences in mass spectroscopic results between lanostane and ergostane triterpenes of AC.

3.6. Fractionation procedures for concentrating zhankuic acids from wild fruiting bodies of A. camphorata

We developed highly efficient fractionation procedures to concentrate zhankuic acids in FEA. On the basis of LC analysis, it was confirmed that zhankuic acid A and other zhankuic acid derivatives are the major components of FEA. The ^{1}H NMR spectrum of zhankuic acid A as a standard, proved also that the process developed in the current study was capable of concentrating zhankuic acids in FEA. The same result was observed in the isolation process of FEA (the ratio of zhankuic acid A weight to FEA was approximately 1:5). In order to study the difference in chemical composition between FEA and other fractions (FNH and FET) obtained using Type 1, ^{1}H NMR experiments were conducted. Several deuterated solvents such as $CDCl_3$, CD_3OD, D_2O, and pyridine-D5 were tested and considered for NMR measurements. After evaluating compounds solubility and analysing NMR data of the tested samples, pyridine-D5 was chosen as the deuterated solvent for our experiments. ^{1}H NMR spectra of EEAC, FNH, FEA, FET, and zhankuic acid A were measured under identical conditions (10 mg/0.75 ml, 400 MHz), and plotted for comparison (Fig. 3). The characteristic ^{1}H NMR signals of zhankuic acid A showed two tertiary methyl signals [δ_H 0.70 (H_3-18) and 1.61 (H_3-19) (each 3H, s)], three secondary methyl signals [δ_H 0.89 (3H-21, d, J = 5.6 Hz), 1.03 (3H-29, d, J = 6.4 Hz), and 1.52 (3H-27, d, J = 7.2 Hz)], and terminal olefinic protons (H_2-28) in a 24-exo-methylene-26-oic acid side-chain [δ_H 5.08 (1H, br s) and 5.24 (1H, br s)]. ^{1}H NMR spectra of EEAC and FEA clearly exhibited these distinguishable signals. Moreover, the signals of methine protons [δ_H 3.01 (1H-12, d, J = 13.6 Hz), 3.17 (1H-1, ddd, J = 13.3, 6.8, 2.4 Hz), and 3.48 (1H-25, q, J = 7.2 Hz)] of zhankuic acid A were also detected in ^{1}H-NMR spectra of EEAC and FEA. However, the specific signals mentioned above were not observed at all in the ^{1}H NMR spectra of FNH and FET. Therefore, it can be concluded that the major active component, zhankuic acid A, of the ethanolic extract of wild fruiting bodies of *A. camphorata* (EEAC) is concentrated in the ethyl acetate fraction (FEA) by the method presented in this study. On the basis HPLC and NMR analysis, FEA is unmistakably defined as the active triterpenoids-rich fraction.

3.7. Cytotoxic screening of ergostane stereo-isomeric pairs on leukemia cancer cell lines

Previous studies revealed that triterpenes from AC possessed anti-inflammatory activity in neutrophils [20] and cytotoxicity against leukemia, colon, liver, breast and lung cancer cells [21]. However, the relationship between the stereochemistry and bioactivity of 25-(*R*) and 25-(*S*) ergostane stereo-isomers has never been reported. In our continuing research for cytotoxic metabolites from FEA, compounds **1**–**8** and their mixture forms (antcin K, antcin C, zhankuic acid C, and zhankuic acid A) were subjected to an anti-proliferation assay against a panel of cancer cell lines, including two human acute lymphoblastic leukemia cells (CCRF-CEM and Molt 4) and one human promyelocytic leukemia cells (HL 60) (Table 3). Results showed that derivatives with the 3-carbonyl functional group (**3**, **4**, **7**, **8**, antcin C, and zhankuic acid A) exhibited better cytotoxicity with IC_{50} values ranging from 16.44 to 77.04 μg/ml. Comparatively, compounds with a hydroxyl group at C-3 were less active (IC_{50} > 80 μg/ml) suggesting the presence of carbonyl group is important for cytotoxic activity. Moreover the presence of other hydroxyl groups in rings A (C-4), B (C-7), C (C-12) did not have a

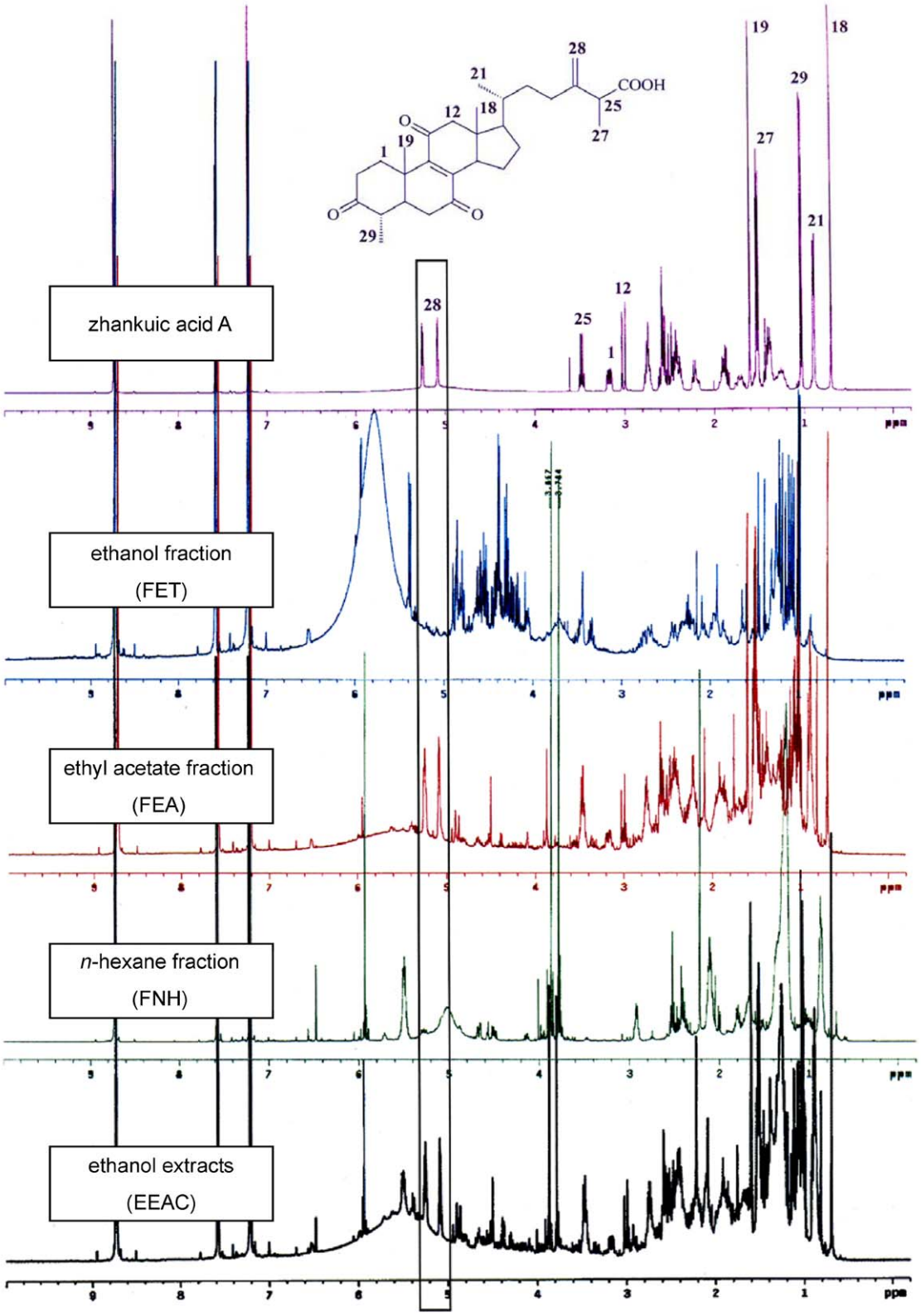

Fig. 3. ^{1}H NMR profiles of zhankuic acid A, FNH (*n*-hexane fraction), FEA (ethyl acetate fraction), FET (ethanol fraction), and EEAC (ethanol extract) separated using Type 1 process.

significant effect on cytotoxicity. To understand the effect of stereo-configuration of the isolated compounds on their cytotoxic activity, the activity of the isolated pure isomers and their mixture forms on leukemia cell lines was evaluated. Compounds **7** and **8** showed higher inhibitory potency than their mixture form, zhankuic acid A, in all cancer cell lines. On the other hand compounds **3** and **4** isolated from antcin C lost their cytotoxicity (IC_{50} > 80 μg/ml) against HL 60 cells. In the Molt 4 cell line, the 25*R* forms (**4** and **8**) were more active than the related 25*S* forms (**3** and **7**). Similar results in the HL 60 cell line were observed with compounds **7** and **8**. However,

Table 3
Cytotoxicity of zhankuic acids on leukemia cancer cell lines.

Compound	IC_{50} (μg/ml)[a]		
	CCRF-CEM[b]	Molt 4[b]	HL 60[c]
1	>80	>80	>80
2	>80	>80	>80
3	30.68 ± 5.30	77.04 ± 2.78	>80
4	27.94 ± 6.44	54.28 ± 1.96	>80
5	>80	>80	>80
6	>80	>80	>80
7	21.99 ± 7.91	42.16 ± 2.33	54.67 ± 8.14
8	22.90 ± 7.60	16.44 ± 3.77	23.32 ± 1.60
Antcin K	>80	>80	>80
Antcin C	28.82 ± 6.79	55.02 ± 3.34	47.02 ± 4.45
Zhankuic acid C	>80	>80	>80
Zhankuic acid A	47.04 ± 6.191	53.23 ± 3.88	69.98 ± 18.98

[a] Data are expressed as mean ± SD ($n = 3$).
[b] Human acute lymphoblastic leukemia cells.
[c] Human promyelocytic leukemia cells.

the 25*R* forms (**4** and **8**) and 25*S* forms (**3** and **7**) exhibited nearly equal potency against CCRF-CEM cells. Based on these findings, a clear correlation between the stereconfiguration of AC ergostane triterpenes and their cytotoxic activity cannot be defined.

4. Conclusions

We developed a convenient fractionation procedure for concentrating the anti-proliferative triterpenoids from AC fruiting bodies. The chemical profile of this triterpenoids-rich fraction was illustrated by HPLC, NMR, and HPLC-PDA/MS. Triterpenes (FEA) were the major constituents of AC fruiting bodies, accounting for about 22% of the original crude material total weight and nearly 20% of the total FEA weight was zhankuic acid A. Using a combination of extraction, fractionation, and HPLC, an effective analysis and preparation procedure of AC major triterpenes was established. The method we developed is feasible for comprehensive quality evaluation of AC fruiting bodies and its related products.

Since the first isolation of zhankuic acids in 1995 [10], the separation of their pure isomers has been always an unresolved issue. For the first time we report the separation of zhankuic acid derivatives in a pure isomeric form and the determination of their cytotoxic activity on different cancer cell lines.

In the current study we investigated also the effect of difference in stereoconfiguration at C-25 of the isolated triterpenes on the elution order in HPLC experiments, optical rotation values and cytotoxic activity. The biofunction and pharmacological mechanism of pure and individual zhankuic acid isomers are under investigation in our laboratory.

Acknowledgements

The authors would like to thank Dr. Hung-Liang Lay, the National Pingtung University of Science and Technology, Taiwan, for the identification of wild fruiting bodies of *Antrodia camphorata*. This work was supported by the National Science Council (NSC 98-2324-B-037-001 and 98-2321-B-037-060) and the Department of Health (DOH100-TD-C-111-002), Executive Yuan, Taiwan.

Appendix A. Supplementary data

Supplementary data associated with this article can be found, in the online version, at doi:10.1016/j.jpba.2011.09.007.

References

[1] Z.H. Ao, Z.H. Xu, Z.M. Lu, H.Y. Xu, X.M. Zhang, W.F. Dou, Niuchangchih (*Antrodia camphorata*) and its potential in treating liver diseases, J. Ethnopharmacol. 121 (2009) 194–212.
[2] C.C. Shen, Y.C. Kuo, R.L. Huang, L.C. Lin, M.J. Don, T.T. Chang, C.J. Chou, New ergostane and lanostane from *Antrodia camphorata*, J. Chin. Med. 14 (2003) 247–258.
[3] M.C. Lu, S.L. Hwang, F.R. Chang, Y.H. Chen, T.T. Chang, C.S. Hung, C.L. Wang, Y.H. Chu, S.H. Pan, Y.C. Wu, Immunostimulatory effect of *Antrodia camphorata* extract on functional maturation of dendritic cells, Food Chem. 113 (2009) 1049–1057.
[4] M. Geethangili, Y.M. Tzeng, Review of pharmacological effects of *Antrodia camphorata* and its bioactive compounds, Evid. Based Complement Altern. Med. 2011 (2009) 1–17.
[5] Y.C. Wu, M.C. Lu, F.R. Chang, Y.C. Du, T.Y. Wu, Ethanol extract of *Antrodia camphorata* for inducing apoptosis and preparation method thereof, United States Patent, US 2010/0210869 A1, August 19 (2010).
[6] Y.C. Chen, H.O. Ho, C.H. Su, M.T. Sheu, Anticancer effects of *Taiwanofungus camphoratus* extracts, isolated compounds and its combinational use, J. Exp. Clin. Med. 2 (2010) 274–281.
[7] Y.Y. Chan, C.S. Chang, L.H. Chien, T.F. Wu, Apoptotic effects of a high performance liquid chromatography (HPLC) fraction of *Antrodia camphorata* mycelia are mediated by down-regulation of the expressions of four tumor-related genes in human non-small cell lung carcinoma A549 cell, J. Ethnopharmacol. 127 (2010) 652–661.
[8] Y.H. Kuo, B.F. Lin, Compounds from *Antrodia camphorata*, United States Patent, US 7932285 B2, April 26 (2011).
[9] M.C. Lu, Y.C. Du, J.J. Chuu, S.L. Hwang, P.C. Hsieh, C.S. Hung, F.R. Chang, Y.C. Wu, Active extracts of wild fruiting bodies of *Antrodia camphorata* (EEAC) induce leukemia HL 60 cells apoptosis partially through histone hypoacetylation and synergistically promote anticancer effect of trichostatin A, Arch. Toxicol. 83 (2009) 121–129.
[10] C.H. Chen, S.W. Yang, Y.C. Shen, New steroid acids from *Antrodia cinnamomea*, a fungal parasite of *Cinnamomum micranthum*, J. Nat. Prod. 58 (1995) 1655–1661.
[11] E. Majid, K.B. Male, Y.M. Tzeng, J.O. Omamogho, J.D. Glennon, J.H. Luong, Cyclodextrin-modified capillary electrophoresis for achiral and chiral separation of ergostane and lanostane compounds extracted from the fruiting body of *Antrodia camphorata*, Electrophoresis 30 (2009) 1967–1975.
[12] J.B. Bartlett, K. Dredge, A.G. Dalgleish, The evolution of thalidomide and its IMiD derivatives as anticancer agents, Nat. Rev. Cancer 4 (2004) 314–322.
[13] C. Goosen, T.J. Laing, J.d. Plessis, T.C. Goosen, G.L. Flynn, Physicochemical characterization and solubility analysis of thalidomide and its *N*-alkyl analogs, Pharm. Res. 19 (2002) 13–19.
[14] I.H. Cherng, H.C. Chiang, M.C. Cheng, Y. Wang, Three new triterpenoids from *Antrodia cinnamomea*, J. Nat. Prod. 58 (1995) 365–371.
[15] Y.L. Hsu, Y.C. Kuo, P.L. Kuo, L.T. Ng, Y.H. Kuo, C.C. Lin, Apoptotic effects of extract from *Antrodia camphorata* fruiting bodies in human hepatocellular carcinoma cell lines, Cancer Lett. 221 (2005) 77–89.
[16] K.B. Male, Y.K. Rao, Y.M. Tzeng, J. Montes, A. Kamen, J.H. Luong, Probing inhibitory effects of *Antrodia camphorata* isolates using insect cell-based impedance spectroscopy: inhibition vs chemical structure, Chem. Res. Toxicol. 21 (2008) 2127–2133.
[17] S.W. Yang, Y.C. Shen, C.H. Chen, Steroids and triterpenoids of *Antrodia cinnamomea* – a fungus parasitic on *Cinnamomum micranthum*, Phytochemistry 41 (1996) 1389–1392.
[18] J.M. Seco, E. Quiñoá, R. Riguera, The assignment of absolute configuration by NMR, Chem. Rev. 104 (2004) 17–117.
[19] L. Muñoz, M.P. Bosch, G. Rosell, A. Guerrero, Asymmetric synthesis of (*R*)- and (*S*)-4-methyloctanoic acids. A new route to chiral fatty acids with remote stereocenters, Tetrahedron: Asymmetr. 20 (2009) 420–424.
[20] Y.C. Shen, Y.H. Wang, Y.C. Chou, C.F. Chen, L.C. Lin, T.T. Chang, J.H. Tien, C.J. Chou, Evaluation of the anti-inflammatory activity of zhankuic acids isolated from the fruiting bodies of *Antrodia camphorata*, Planta Med. 70 (2004) 310–314.
[21] C.T. Yeh, Y.K. Rao, C.J. Yao, C.F. Yeh, C.H. Li, S.E. Chuang, J.H. Luong, G.M. Lai, Y.M. Tzeng, Cytotoxic triterpenes from *Antrodia camphorata* and their mode of action in HT-29 human colon cancer cells, Cancer Lett. 285 (2009) 73–79.

Hindawi Publishing Corporation
Evidence-Based Complementary and Alternative Medicine
Volume 2011, Article ID 212641, 17 pages
doi:10.1093/ecam/nep108

Review Article

Review of Pharmacological Effects of *Antrodia camphorata* and Its Bioactive Compounds

Madamanchi Geethangili and Yew-Min Tzeng

Institute of Biochemical Sciences and Technology, Chaoyang University of Technology, Wufeng, Taiwan

Correspondence should be addressed to Yew-Min Tzeng, ymtzeng@cyut.edu.tw

Received 22 May 2009; Accepted 21 July 2009

Antrodia camphorata is a unique mushroom of Taiwan, which has been used as a traditional medicine for protection of diverse health-related conditions. In an effort to translate this Eastern medicine into Western-accepted therapy, a great deal of work has been carried out on *A. camphorata*. This review discusses the biological activities of the crude extracts and the main bioactive compounds of *A. camphorata*. The list of bioactivities of crude extracts is huge, ranging from anti-cancer to vasorelaxation and others. Over 78 compounds consisting of terpenoids, benzenoids, lignans, benzoquinone derivatives, succinic and maleic derivatives, in addition to polysaccharides have been identified. Many of these compounds were evaluated for biological activity. Many activities of crude extracts and pure compounds of *A. camphorata* against some major diseases of our time, and thus, a current review is of great importance. It is concluded that *A. camphorata* can be considered as an efficient alternative phytotherapeutic agent or a synergizer in the treatment of cancer and other immune-related diseases. However, clinical trails of human on *A. camphorata* extracts are limited and those of pure compounds are absent. The next step is to produce some medicines from *A. camphorata*, however, the production may be hampered by problems related to mass production.

1. Introduction

About 80% of the world population currently relies on indigenous or traditional medicines for their primary health needs, and most of these therapies involve the use of herbal extracts, often in aqueous solutions [1–3]. *Antrodia camphorata* (Syn. *Antrodia cinnamomea*) is a fungal parasite on the inner cavity of the endemic species *Cinnamomum kanehirae* (Bull camphor tree) Hayata (Lauraceae) (Figure 1). The host plant is a large evergreen broad-leaved tree, which only grows in Taiwan, and is distributed over broad-leaved forests at an altitude of 200–2000 m [4]. *Cinnamomum kanehirai* is a high quality material used to manufacture valuable furniture. The government has recently protected this endemic tree species from forest-denudation since this species in nature is relatively rare [5]. In Taiwan, *A. camphorata* is called as "*Niu-chang-chih*" or "*Chang-chih*" or "*Niu-chang-ku*" or "*Chang-ku*" [5]. Locally, it is believed that *A. camphorata* is a present from heaven for Taiwanese and, is a well-known Chinese folk medicine and claimed "ruby in mushroom" in Taiwan [5]. It grows in the mountain ranges of Taoyuan, Miaoli, Nantou, Kaohsiung, Taitung and Hualien of Taiwan [3]. The trophophase of *A. camphorata* occurs from June to October [6]. Being a local species, *A. camphorata* was historically used in Taiwan by the aborigines as a traditional prescription for the discomforts caused by alcohol drinking or exhaustion [5]. Furthermore, the regular consumption is believed to preserve human vitality and promote longevity. The preparations from fruiting bodies have been used for the prevention, or treatment, of numerous diseases including liver diseases, food and drug intoxication, diarrhea, abdominal pain, hypertension, itchy skin and tumorigenic diseases [7, 8]. The aim of this contribution is to review the literature covering pharmacological and phytochemical aspects of *A. camphorata*.

2. Taxonomical Description

Ku is a Chinese common name meaning mushroom; *chih* means a famous *Ganoderma*-like fungus. *Antrodia camphorata* was first published and identified as new *ganoderma* species, *Ganoderma camphoratum*, by Zang and Su in 1990 [9]. However, according to fruiting-body morphology and

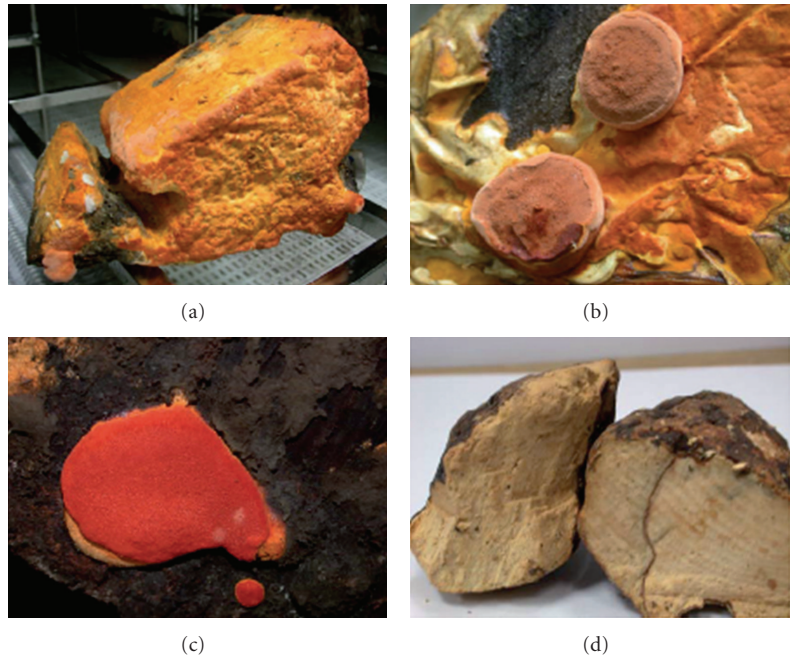

Figure 1: *Antrodia camphorata* from solid-state cultivation of wood. (a) Mycelium from 12-month-old sample. (b) Fruiting bodies from 18-month-old sample. (c) Fruiting bodies from 24-month-old sample. (d) Fruiting bodies from multiple years grown sample.

cultural characteristics, this fungus has been proposed the name as *A. camphorata* [5, 10]. In 2004, a phylogenetic analysis based on sequence data derived from large ribosomal subunit sequences of ribosomal RNA genes indicated that *A. camphorata* is distantly related to other species in *Antrodia* and, consequently, the fungus was transferred to the new genus *Taiwanofungus* [11]. However, using polymorphism analysis of internal transcribed spacer regions of the ribosomal RNA gene, *A. camphorata* was reconsidered as an *Antrodia* species [12]. The current taxonomic position of *A. camphorata* is as follows [13]: Fungi, Basidiomycota, Homobasidiomycetes, Aphyllophorales, Polyporaceae. Clearly, however, the nomenclature and exact taxonomy (genus and species) of *A. camphorata* is still the subject of debate and needs further research. In this article, we have chosen the name as *A. camphorata* to describe this unique Formosan fungus. The fruiting bodies of *A. camphorata* assume different plate-like, bell-like, hoof-like or tower-like shapes. They are flat on the surface of wood at the beginning of growth. Then the brim of the front edge rises to roll into plate-shaped or stalactites. The top surfaces of *A. camphorata* are lustrous, brown to dark brown in color, with unobvious wrinkles, flat and blunt edges. The bottom sides are orange red or partially yellow with ostioles all over [12]. In addition, *A. camphorata* exhales strong smell of sassafras (camphor aroma), becomes pale yellowish brown when sun-dried and has a strong bitter taste. The red to light cinnamon fruiting bodies of *A. camphorata* are bitter and have a mild camphor scent like the host woods [5]. The mycelia isolated from the fruiting bodies of *A. camphorata* form orange red and orange brown to light cinnamon-colored colonies [5]. The hyphae of *A. camphorata* possess generative hyphae 2–3.5 μm with clamp connections, and hyaline to light brown skeletal hyphae up to 4.5 μm wide with weakly amyloid. Basidia, 12–14 $\times$ 3.0–5.0 μm, is clavate and 4-sterigmate with a basal clamp. Basidiospores, 3.5–5.0 $\times$ 1.5–2 μm, are cylindrical, hyaline, smooth and sometimes slightly bent [14].

3. Ethnomedicine

Antrodia camphorata has long been used in traditional medicines of Taiwan for the treatment of twisted tendons and muscle damage, terrified mental state, influenza, cold, headache, fever and many internally affiliated diseases [14]. In 1773, a traditional Chinese medical doctor Wu-Sha found that Taiwan aborigines have often chewed the fruiting bodies and/or decoction of *A. camphorata* for the discomfort caused by excess alcohol or exhaustion because of lifestyle [14]. After that Dr Wu studied the usage of *A. camphorata* based on the locals' experiences, and began to use it to treat diarrhea, abdominal pain, hypertension, itchy skin, viral infection, stomachitis, diabetes mellitus, nephritis, proteinuria, liver cirrhosis, hepatoma, influenza, car sickness, calenture and motion-sickness [7, 15]. After being used for years in Taiwan, the mushroom is now believed to be a potential protecting agent for metabolic syndrome. Recently, many studies have indicated that its medicinal applications go far beyond the original usage. Therefore, demand for the fruiting bodies of *A. camphorata* has far exceeded the supply. Thus, artificial cultivation was developed as a substitute. Currently, *A. camphorata* is available in three ways, gathering in the wild fruiting bodies, wood or solid-state cultivation, and submerged cultivations. Particularly, fruiting bodies and mycelium produced by *A. camphorata* wood or solid-state

cultivation instead of gathering in the wilds may solve market's demand. In Taiwan *A. camphorata* is commercially available in the form of fermented wine or pure cultures in powdered, tablet and capsule form [16].

4. Chemical Constituents

A total of 78 compounds have been identified and structurally elucidated. Predominant in fruiting bodies are generally terpenoids in a large number (39 compounds) [17–25], though there are a few publications on the constituents of the solid-state cultivated mycelium and, mycelium from submerged cultivations [26–36]. A large number of triterpenoid compounds (31 structures) with similar or even the same structures were described within the last few years. A common feature of these structures is ergostane or lanostane skeleton. Due to the high amount of 63% of terpenoids in the fruiting bodies of *A. camphorata*, this group of natural compounds has been in the focus of many phytochemical studies. Interestingly, no distinct terpenoid glycosides have ever been isolated from this species; in contrast to polysaccharides that have been elucidated. Furthermore, several other constituents were described from *A. camphorata* comprising benzenoids, lignans, benzoquinones and maleic/succinic acid derivatives, in addition to polysaccharides. Finally, sterols, nucleotides and fatty acids were detected in this species [37–40]. Typical structures and their activities of isolated constituents from *A. camphorata* are depicted in Figure 2 and Table 1, respectively.

5. Pharmacological Effects of Crude Extracts

The scientific world's particular interest in *A. camphorata* and its curative properties originated from the realm of traditional medicine. Ethnic medicine has come to be an irreplaceable source of knowledge of medicinal mushrooms and their curative qualities, as well as creating clues for scientific research, which usually confirms the legitimacy of their usage [41, 42]. This part of review will deal with the pharmacological effects of crude extracts of the *A. camphorata* in different models of *in vivo* and *in vitro* studies.

5.1. Anti-Cancer Activities. Both the fruiting bodies and mycelium of *A. camphorata* have potent anti-proliferative activity against various cancers *in vitro* and *in vivo*. It was indicated that there were multiple potent mechanisms underlying the anti-cancerous effects of *A. camphorata*. The crude $CHCl_3$/MeOH extract from fruiting bodies of *A. camphorata* exhibited significant cytotoxic activity with an IC_{50} value of 4.1 μg ml^{-1} against P-388 murine leukemia cells [18]. The ethylacetate extract from fruiting bodies of *A. camphorata* (EAC) exhibited apoptotic effects in two human liver cancer cell lines, Hep G2 and PLC/PRF/5 in a dose-dependent manner [43]. In addition, EAC also initiated mitochondrial apoptotic pathway through regulation of B-cell lymphoma (Bcl)-2 family proteins expression, release of cytochrome c, and activation of caspase-9 both in Hep G2 and PLC/PRF/5 cells [43]. Furthermore, EAC also inhibited the cell survival signaling by enhancing the amount of Iκ-α in cytoplasm and reducing the level and activity of nuclear factor (NF)-κB in the nucleus, and subsequently attenuated the expression of Bcl-X_L in Hep G2 and PLC/PRF/5 cells [43]. Treatment with EAC also caused another human liver cancer cell line Hep 3B to undergo apoptotic cell death by way of calcium-calpain-mitochondria signaling pathway [44]. Another study reported that EAC could inhibit the invasiveness and metastasis of liver cancer cell line PLC/PRF/5 cells through the inhibition of angiogenesis [45]. We previously reported that the $CHCl_3$ extract from fruiting bodies of *A. camphorata* (FBAC) showed cytotoxic activity with an IC_{50} value of 22, 150, 65 and 95 μg ml^{-1}, against cancer cell lines Jurkat, Hep G2, Colon 205 and MCF 7, respectively. Furthermore, MeOH extract from FBAC also cytotoxic (IC_{50} = 40 μg ml^{-1}) to Jurkat cells [46]. *Antrodia camphorata* solid-state cultured mycelium (AC-SS, 1 μg ml^{-1}) showed adjuvant anti-proliferative effects with cisplatin (10 μM) or mitomycin (10 μM) in hepatoma cell lines C3A and PLC/PRF/5 cells (*in vitro*) and, on xenografted cells in tumor implanted nude mice (*in vivo*). Furthermore, AC-SS showed its adjuvant effects through the inhibition of MDR gene expressions and the pathway of COX-2-dependent inhibition of AKT phosphorylation [47]. In terms of the very recent literature, Lu et al. [48] noted that ethanol extract from wild fruiting bodies of *A. camphorata* (EEAC) dose-dependently induced human premyelocytic leukemia HL 60 cells apoptosis via histone hypoacetylation, upregulation of histone deacetyltransferase 1 (HDAC 1), and downregulation of histone acetyltransferase activities including GCN 5, CBP and PCAF. Furthermore, combined treatment with 100 nM of trichostatin A (histone deacetylase inhibitor) and 100 μg ml^{-1} EEAC caused synergistic inhibition of cell growth and increase of apoptotic induction through the upregulation of DR5 and NF-κB activation [48].

There are relatively fewer studies on extracts from the solid-state or submerged cultivated mycelium or culture filtrates. Aqueous extract from submerged cultivation mycelium (SCM) of *A. camphorata* exhibited significant cytotoxicity against HL-60 cells but not against cultured human endothelial cells [49]. The SCM resulted dose (25–150 μg ml^{-1}) and time-dependent apoptosis, as shown by loss of cell viability, chromatin condensation and internucleosomal DNA fragmentation in HL-60 cells [50]. Furthermore, apoptosis in these cells was accompanied by the release of cytochrome c, activation of caspase-3, specific proteolytic cleavage of poly (ADP-ribose) polymerase (PARP), and also with a reduction in the levels of Bcl-2 [50]. In an another study, the ethanolic extract (0.2–2%, v/v) from solid-state cultivated mycelia of *A. camphorata* showed potent anti-proliferation effect in human non-small cell lung carcinoma A549 cells but not primary human fetal lung fibroblast MRC-5 cells [51]. In addition, this extract triggered the apoptosis in the A549 cells by downregulated human galectin-1, human eukaryotic translation initiation factor 5A, human Rho GDP dissociation inhibitor α, human calcium-dependent protease small subunit and human annexin V [51]. To continue, the effects of *A. camphorata* on cancer cells was investigated,

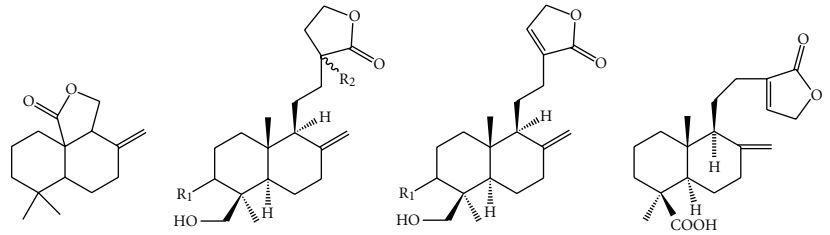

1.

2. $R_1 = H_2$, $R_2 = H$
3. $R_1 = OH$, $R_2 = H$
4. $R_1 = OH$, $R_2 = H$

5. $R_1 = H_2$
6. $R_1 = OH$
7. $R_1 = OH$

8.

(a)

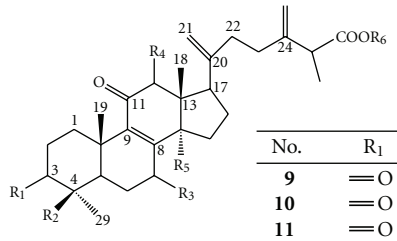

No.	R_1	R_2	R_3	R_4	R_5	R_6
9	=O	H	H_2	H_2	H	H
10	=O	H	=O	H_2	H	H
11	=O	H	β-OH	H_2	H	H
12	=O	H	=O	H_2	OH	H
13	=O	H	H_2	H_2	H	HΔ^{14}
14	=O	H	β-OH	H_2	–	HΔ^{14}
15	=O	H	α-OAc	H_2	–	H
16	α-OH	H	=O	α-OH	H	H
17	α-OH	H	=O	H_2	H	H
18	α-OH	β-OH	β-OH	H_2	H	H
19	=O	H	H_2	H_2	H	CH_3
20	=O	H	=O	H_2	H	CH_3
21	=O	H	=O	H_2	H	C_2H_5
22	=O	H	α-OAc	H_2	H	CH_3
23	α-OH	H	=O	α-OH	H	CH_3
24	α-OH	H	=O	α-OH	H	C_2H_5

(b)

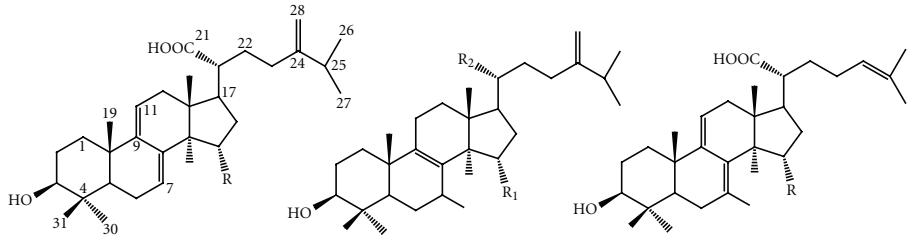

25. R = H
26. R = OH
27. R = OAc

28. $R_1 = H_2$, $R_2 = COOH$
29. $R_1 = OH$, $R_2 = COOH$
30. $R_1 = OAc$, $R_2 = COOH$
31. $R_1 = H_2$, $R_2 = CH_3$

32. R = OH
33. R = H

(c)

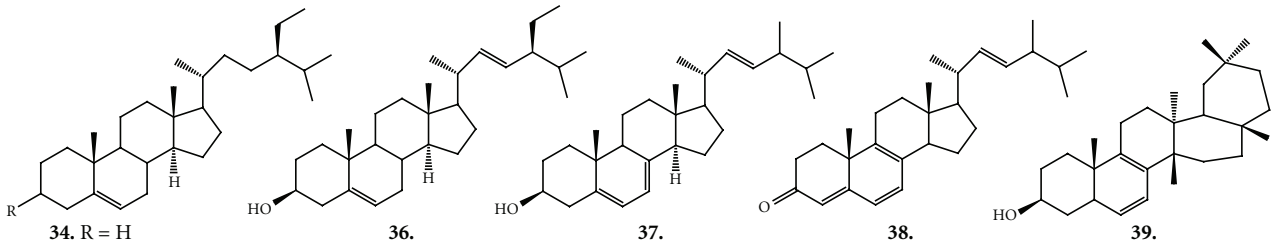

34. R = H
35. R = (=O)

36.

37.

38.

39.

(d)

Figure 2: Continued.

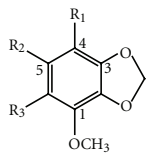

40. $R_1 = OCH_3$, $R_2 = CH_3$, $R_3 = H$
41. $R_1 = OCH_3$, $R_2 = CO_2$, $R_3 = H$
42. $R_1 = COOH$, $R_2 = H$, $R_3 = OCH_3$

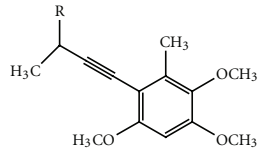

43. R = (═CH_2)
44. R = (═O)

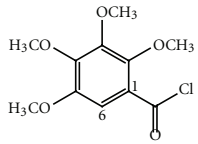

45.

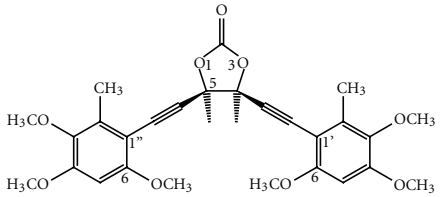

46.

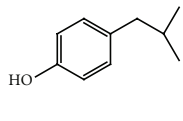

47.

(e)

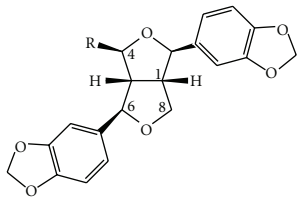

48. R = H
49. R = OH

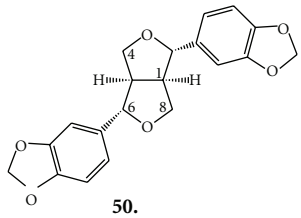

50.

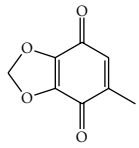

51.

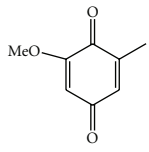

52.

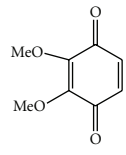

53.

(f)

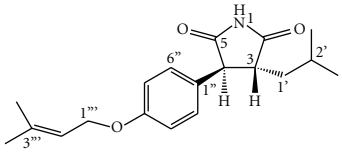

54.

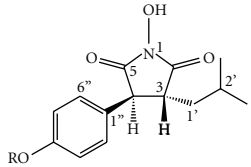

55. R = H
56. R =

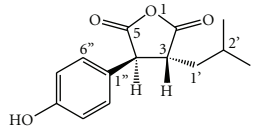

57.

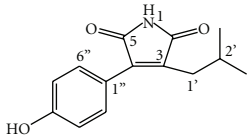

58.

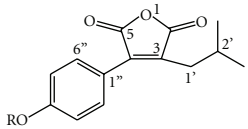

59. R = H
60. R =

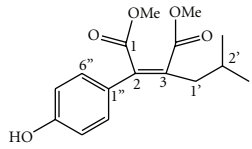

61.

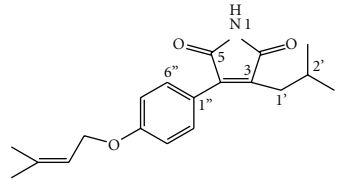

62.

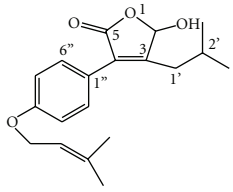

63.

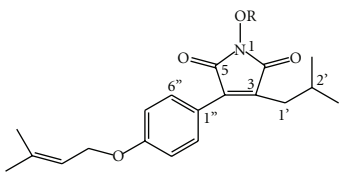

64. R = H
65. R =

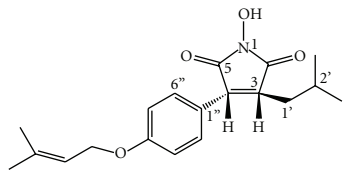

66.

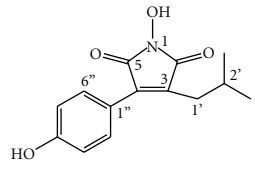

67.

(g)

Figure 2: Continued.

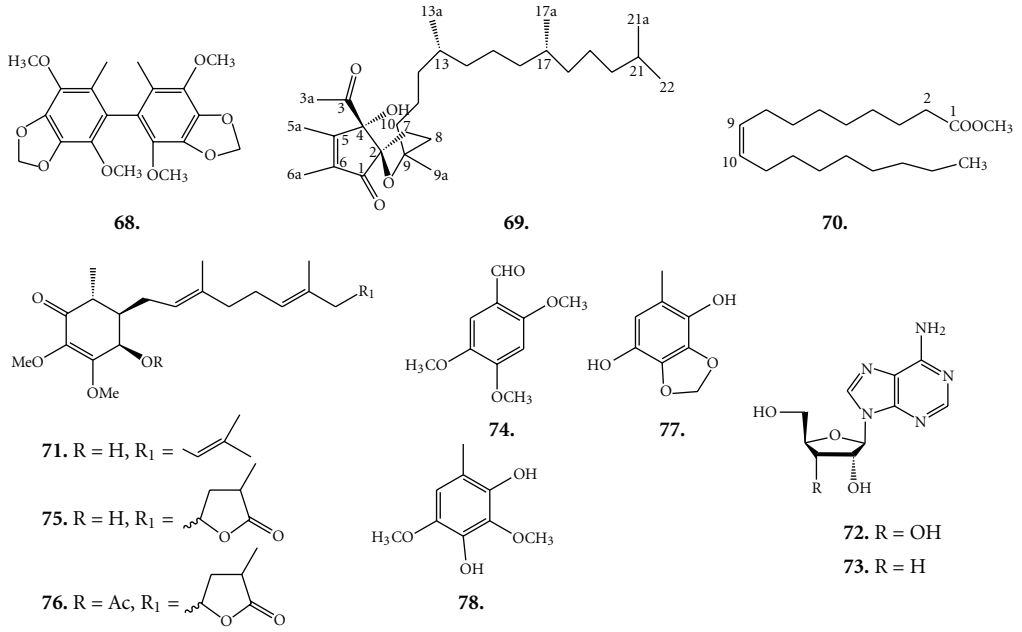

Figure 2: Isolated constituents from A. camphorata. (a) Sesqui- and diterpenoids. (b) Ergostane type triterpenoids. (c) Lanostane-type triterpenoids. (d) Triterpenoid related compounds. (e) Benzenoids. (f) Lignans and benzoquinone derivatives. (g) Succinic and maleic derivatives. (h) Miscellaneous compounds.

methanol extract of SCM exhibited the cytotoxicity in Hep G2 (wild-type p53) and Hep 3B (delete p53) cells with IC_{50} values of 49.5 and 62.7 $\mu g\,ml^{-1}$, respectively, after 48 h of incubation. Cell-cycle analysis revealed that the above SCM extract treatment induced apoptosis on Hep G2 via G0/G1 cell-cycle arrest followed by the apoptosis through activation of the caspase-3 and -8 cascades [52]. Furthermore, these authors also reported that the mechanism of MEM-mediated apoptosis in Hep G2 cells through the Fas/Fas ligand (FasL) death receptor pathway [53]. In parallel, Chen et al. [54] noted that the ethanolic extract from SCM has anti-proliferation against Hep G2 and Hep G3 cells with 54.2 and 82.9 $\mu g\,ml^{-1}$, respectively. On the other hand, Yang et al. [55] reported that fermented culture broth of *A. camphorata* (FCBAC) exhibits dose (25–150 $\mu g\,ml^{-1}$) and time-dependent anti-proliferative effect by induction of apoptosis in breast cancer cell line MCF-7. In addition, this apoptic effect is associated with cytochrome *c* translocation, caspase-3 activation, PARP degradation and dysregulation of Bcl-2 and Bax in MCF-7 cells [55]. These authors also reported that FCBAC has the dose (40–240 $\mu g\,ml^{-1}$) and time-dependent apoptotic effect in estrogen-nonresponsive human breast cancer cell line MDA-MB-231 with a similar kind of mechanism as mentioned above [56]. In addition, FCBAC treatment also inhibited the cyclooxygenase (COX)-2 protein expression and prostaglandin E_2 (PGE_2) production in MDA-MB-231 cells [56]. Furthermore, FCBAC treatment induced cell-cycle arrest and apoptosis in MDA-MB-231 both *in vitro* and *in vivo* [57]. The *A. camphorata* crude extract (ACCE) at 50 $\mu g\,ml^{-1}$ acts as an anti-metastatic agent, by anti-proliferative through induces G2/M cell-cycle arrest followed by suppress the active form of matrix metalloproteinase (MMP)-9 in bladder cancer cell T24 cells [58]. In addition, ACCE (100 $\mu g\,ml^{-1}$) showed significant anti-proliferation effect in transitional cell carcinomas (TCC) cell lines RT4, TSGH-8301 and T24 [59]. In RT4 cells, 100 $\mu g\,ml^{-1}$ of ACCE showed the p53-independent over expression of p21 followed by downregulation of pRb. On the contrary, treatment with ACCE at 50 $\mu g\,ml^{-1}$ resulted in downregulations of Cdc2 and Cyclin B1 in the cell lines TSGH-8301 and T24 [59]. In another study, the ACCE extract at 150 $\mu g\,ml^{-1}$ concentration showed anti-cancer effect in androgen responsive prostate cancer cell line LNCaP through pathway Akt → p53 → p21 → CDK4/cyclin D1 → G1/S-phase arrest → apoptosis [60]. In addition, ACCE also inhibited the androgen independent prostate cancer cell line PC-3 through G2/M-phase arrest mediated through pathway p21 → cyclin B1/Cdc2 with limited degree of apoptosis [60]. Recently, Lu et al. [61] noted that submerged cultivated *A. camphorata* extract prevents serum-deprived PC-12 cell apoptosis through a PKA-dependent pathway and by suppression of JNK and p38 activities. Ho et al. [62] reported that crude extract of *A. camphorata* (AC) at concentrations of 5–50 $\mu g\,ml^{-1}$ did not affect tumor cells PC-3 viability, but at 100–200 $\mu g\,ml^{-1}$ decreased viability and induced apoptosis in a concentration-dependent manner. In addition, 25–200 $\mu g\,ml^{-1}$ did not alter basal $[Ca^{2+}]_i$, however at 25 $\mu g\,ml^{-1}$ decreased the $[Ca^{2+}]_i$ induced by ATP, bradykinin, histamine and thapsigargin [62]. The mycelia powder of *A. camphorata* (MAC) at 25–50 $\mu g\,ml^{-1}$, did not affect the cell viability in MG63 human osteosarcoma cells, however, at 100–200 $\mu g\,ml^{-1}$ decreased viability and induced

apoptosis via inhibition of ERK MAPK phosphorylation [63].

In summary, extracts of *A. camphorata* inhibited markedly intracellular signaling and invasive behavior of cancer cells. This complexity can also bring significant advantages. For example, certain components in the natural products can reduce the cytotoxicity of the whole product (and vice versa). Also, the interaction between different biologically active components can be responsible for their effects *in vivo*. Different compounds can modulate unrelated signaling and therefore, can possess synergistic effects [73]. However, the molecular mechanism(s) has not been fully elucidated. Further studies are needed to explore the benefits and safety to cancer patients.

5.2. Anti-Inflammatory/Immunomodulatory Effects. Compounds that are capable of interacting with the immune system to up regulate or down regulate specific aspects of the host response can be classified as immunomodulators or biologic response modifiers [74–76]. In peripheral human neutrophils, extracts from SCM of *A. camphorata* displayed anti-inflammatory effects by inhibiting reactive oxygen species (ROS) production with an IC_{50} ranging from 2–20 $\mu g\,ml^{-1}$ [77]. The aqueous extract from SCM dose-dependently (25–100 $\mu g\,ml^{-1}$) inhibited the lipopolysaccharide (LPS)-induced nitric oxide (NO), tumor necrosis factor (TNF-α), interleukin (IL)-1β and PGE_2 production, and inducible nitric oxide synthase (iNOS) and COX-2 protein expression via NF-κB pathway, in macrophages [78]. These results are in parallel to our previous report that $CHCl_3$ (3–25 $\mu g\,ml^{-1}$) and MeOH (6–50 $\mu g\,ml^{-1}$) extracts from fruiting bodies of *A. camphorata* significantly inhibited the enhanced production NO through reducing iNOS expression and, TNF-α and IL-12 productions from macrophages [46]. Liu et al. [79] reported that the methanol extract (50 $\mu g\ ml^{-1}$) from wild fruiting bodies have more potency than water extracts on the anti-inflammatory activity through inhibiting iNOS, COX-2 and TNF-α expression in mouse microglia cell line EOC13.31. In addition, the extracts from solid-state culture were similar to wild-fruiting body in anti-inflammatory activity, but liquid-state fermentation was less effective [79]. To continue, a hot water extracts (fraction MII from mycelium, fractions EII and EIII from culture filtrate) of submerged cultured *A. camphorata* show dose-dependent (5–60 $\mu g\ ml^{-1}$) induction of TNF-α and IL-6 in peripheral blood culture. Furthermore, these fractions at 20 $\mu g\ ml^{-1}$ also showed marked activity in enhancing phagocytosis in human polymorphonuclear neutrophils (PMN), in addition to CD11b upregulation, and monocytes [80]. According to Chang et al. [72] *in vivo* data, hexane extract (100, 200 and 400 mg kg^{-1}) from SCM of *A. camphorata* has protection from nephritis by suppression of urine protein and serum blood urea nitrogen levels and decreased the thickness of the kidney glomerular basement membrane in SLE-prone NZB/W F1 mice [72].

5.3. Anti-Hepatitis B Virus Replication. It was reported that extracts from the mycelium of *A. camphorata* have *in vivo* anti-hepatitis B virus (HBV) activity in a dose-dependent manner without cytotoxicity [81]. The ethanol extract displayed anti-HBV effects on both wild-type and lamivudine-resistant HBV mutants [71]. The ability of *A. camphorata* to inhibit the replication of HBV *in vivo* and *in vitro* may be one additional reason for considering this fungus as a potential therapeutic for HBV infection.

5.4. Anti-Oxidant Activities. Accumulating data have shown that *A. camphorata* is a potent direct free radical scavenger [82–85]. The stable free radical 1,1-diphenyl-2-picrylhydrazyl (DPPH) is scavenged by the extracts of *A. camphorata* [83, 84]. Aqueous extracts of *A. camphorata* inhibited nonenzymatic iron-induced lipid peroxidation in rat brain homogenates with an IC_{50} value of 3.1 mg ml^{-1} [83]. It has been reported that, compared to other *A. camphorata* extracts, the fermented culture broth of *A. camphorata* (FCBA) and aqueous extracts of the mycelia from *A. camphorata* (AEMA) harvested from submerged cultures are the most potent inhibitors of lipid peroxidation, possessing marked free-radical-scavenging activity [82]. The aqueous extract from SCM of *A. camphorata* is possessing anti-oxidant property with respect to oxidative modification of human low-density lipoproteins (LDL) in a time- and concentration-dependent manner [86]. A recent study reported that FCBA and AEMA at 25–100 $\mu g\ ml^{-1}$ and 50–200 $\mu g\ ml^{-1}$, respectively, possess antioxidant properties in human umbilical vein endothelial cell (EC) culture system [87]. In addition, both FCBA and AEMA treatment significantly inhibited apoptotic cell death in the ECs, as evidenced by reduced DNA fragmentation, cytochrome *c* release, caspase-3 activation and dysregulation of Bcl-2 and Bax [87]. Shu and Lung [85] observed the antioxidant activity (lipid peroxidation, scavenging effect on DPPH radical, hydroxyl free radicals, superoxide anion, reducing power activity and chelating effect on ferrous ions) of methanolic extracts from mycelia and filtrates of *A. camphorata* at two different concentrations (0.2 and 0.6 mg ml^{-1}). To continue, 2.5 mg ml^{-1} of methanolic extract irradiated with 20 kGy γ-rays showed potent anti-oxidant property by scavenging abilities of 92.3–103% on DPPH radicals [88].

5.5. Hepatoprotective Activity. Ao et al. [89] reviewed the potential of *A. camphorata* in treating liver diseases, which provided the major biologically active constituents and their effect or mode of action. The fruiting bodies and mycelium of *A. camphorata* are shown to have protective activity against liver hepatitis and fatty liver induced by acute hepatotoxicity of alcohol [90]. The methanolic extract from wild and solid-state cultures of *A. camphorata* exhibited angiotensin-converting enzyme (ACE) inhibitory activities in spontaneously hypertensive rats [91]. The dry matter of submerged cultivation (DMC) filtrate and aqueous extracts from fruiting bodies have been reported to possess hepatoprotective activity against liver damage induced by CCl_4 [83, 92]. Both of the extracts reduce glutathione (GSH)-dependent enzymes such as glutathione peroxidase, glutathione reductase and glutathione S-transferase. Histopathological evaluation of the rat liver revealed that the DMC reduced the incidence of liver lesions, including neutrophil infiltration,

Table 1: Chemical constituents and their reported activities of *A. camphorata*.

No.	Compound name	Source	Biological activity	Ref.
	Terpenoids			
1	Antrocin	F		[19]
2	19-Hydroxylabda-8(17)-en-16,15-olide	F	*In vitro* neuroprotective	[28]
3	3β,19-Dihydroxylabda-8(17),11E-dien-16,15-olide	F	*In vitro* neuroprotective	[28]
4	13-*epi*-3β,19-Dihydroxylabda-8(17),11E-dien-16,15-olide	F	*In vitro* neuroprotective	[28]
5	19-Hydroxylabda-8(17),13-dien-16,15-olide	F	*In vitro* neuroprotective	[28]
6	14-Deoxy-11,12-didehydroandrographolide	F	*In vitro* neuroprotective	[28]
7	14-Deoxyandrographolide	F		[28]
8	Pinusolidic acid	F		[28]
9	Antcin A	F	*In vitro* anti-inflammatory, anti-insecticidal and cytotoxic	[30, 64, 65]
10	Antcin B (Zhankuic acid A)	F	*In vitro* anti-inflammatory, anti-insecticidal and cytotoxic	[18, 30, 64–66]
11	Antcin C	F	*In vitro* anti-inflammatory and cytotoxic	[65, 67]
12	Antcin D (Zhankuic acid F)	F		[23]
13	Antcin E	F		[21]
14	Antcin F	F		[21]
15	Antcin G	F		[21]
16	Antcin H (Zhankuic acid C)	F	*In vitro* anti-inflammatory, anti-insecticidal and cytotoxic	[18, 64–66]
17	Antcin I (Zhankuic acid B)	F	*In vitro* anti-inflammatory	[66]
18	Antcin K	F	*In vitro* anti-inflammatory	[66]
19	Methyl antcinate A	F		[25]
20	Methyl antcinate B	F	*In vitro* anti-insecticidal and cytotoxic	[64, 65]
21	Zhankuic acid D	F		[25]
22	Methyl antcinate G	F		[21]
23	Methyl antcinate H	F		[21]
24	Zhankuic acid E	F		
25	Dehydroeburicoic acid	F	*In vitro* anti-inflammatory, anti-insecticidal	[64, 65, 67]
26	Dehydrosulphurenic acid	F	*In vitro* anti-insecticidal and cytotoxic	[64, 65]
27	15α-Acetyl-dehydrosulphurenic acid	F	*In vitro* anti-insecticidal and cytotoxic	[64, 65]
28	Eburicoic acid	F	*In vitro* anti-insecticidal and cytotoxic	[64, 65]
29	Sulphurenic acid	F	*In vitro* anti-insecticidal and cytotoxic	[64, 65]
30	Versisponic acid D	F		
31	Eburicol (24-methylenedihydrolanosterol)	F	*In vitro* anti-inflammatory	[30]
32	3β, 15α-Dihydroxy lanosta-7,9(11),24-triene-21-oic acid	F	*In vitro* anti-insecticidal and cytotoxic	[64, 65]
33	3β-Hydroxy lanosta-	F		[17]
34	β-Sitosterol	F		[28]

Table 1: Continued.

No.	Compound name	Source	Biological activity	Ref.
35	*β*-Sitostenone	F		[28]
36	Stigmasterol	F		[28]
37	Ergosterol	F		[28]
38	Ergosta-4,6,8(14)22-tetraen-3-on3	F		[30]
39	*epi*-Friedelinol	F		[30]
	Benzenoids			
40	1,4-Dimethoxy-2,3-methylenedioxy-5-methylbenzene	F	*In vitro* cytotoxic	[68]
41	1,4-Dimethoxy-2,3-methylenedioxy-5-benzoate	F		[24]
42	1,6-Dimethoxy-2,3-methylenedioxy-4-benzoic acid	F		[24]
43	Antrocamphin A	F	*In vitro* anti-inflammatory	[30]
44	Antrocamphin B	F		[30]
45	2,3,4,5-Tetramethoxybenzoyl chloride	F		[30]
46	Antrodioxolanone	F		[30]
47	Isobutylphenol			[34]
	Lignans			
48	(+) Sesamin	F		[20]
49	4-Hydroxy sesamin	F		[20]
50	(−) Sesamin	F		[20]
	Benzoquinone derivatives			
51	5-Methyl-benzo(1,3)-dioxole-4,7-dione	M		[20]
52	2-Methoxy-5-methyl(1,4)benzoquinone	M	*In vitro* anti-oxidant	[20]
53	2,3-Dimethoxy-5-methyl(1,4)benzoquinone	M	*In vitro* anti-inflammatory	[20, 30]
	Succinic and Maleic derivatives			
54	*trans*-3-Isobutyl-4-[4-(3-methyl-2-butenyloxy)phenyl]pyrrolidine-2,5-dione	F	*In vitro* anti-inflammatory	[33]
55	*trans*-1-Hydroxy-3-(4-hydoxyphenyl)-4-isobutylpyrrolidine-2,5-dione	F	*In vitro* anti-inflammatory	[33]
56	3*R**,4*S**-1-Hydroxy-3-isobutyl-4-[4-(3-methyl-2-butenyloxy)phenyl]pyrrolidine-2,5-dione (antrodin D or Camphorataimide E)	F, M	*In vitro* anti-inflammatory, anti-HBV and anti-HCV	[29, 33, 69]
57	*cis*-3-(4-Hydroxyphenyl)-4-isobutyldihydrofuran-2,5-dione	F	*In vitro* anti-inflammatory	[33]
58	3-(4-Hydroxyphenyl)-4-isobutyl-1*H*-pyrrole-2,5-dione	F	*In vitro* anti-inflammatory	[33]
59	3-(4-Hydroxyphenyl)-4-isobutylfuran-2,5-dione (Antrocinnamomin C)	F	*In vitro* anti-inflammatory	[33, 35]
60	3-Isobutyl-4-[4-(3-methyl-2-butenyloxy)phenyl]furan-2,5-dione (antrodin A or Camphorataanhydride A)	M	*In vitro* anti-HBV and anti-HCV	[29, 69]
61	Dimethyl 2-(4-hydroxyphenyl)-3-isobutylmaleate	F	*In vitro* anti-inflammatory	[33]
62	3-Isobutyl-4-[4-(3-methyl-2-butenyloxy)phenyl]-1*H*-pyrrole-2,5-dione (Antrodin B or Camphorataimide B)	M, B	*In vitro* anti-inflammatory, anti-HBV and anti-HCV	[26, 29, 69]

Table 1: Continued.

No.	Compound name	Source	Biological activity	Ref.
63	Antrocinnamomin D	M		[35]
64	3-Isobutyl-4-[4-(3-methyl-2-nyloxy)phenyl]-1*H*-pyrrol-1-ol-2,5-dione (antrodin C or) Camphorataimide C)	M	*In vitro* anti-inflammatory, anti-HBV and anti-HCV	[28, 31, 70]
65	Antrocinnamomins A	M	*In vitro* anti-inflammatory	[37]
66	3*R**,4*R**-1-Hydroxy-3-isobutyl-4-[4-(3-methyl-2-butenyloxy)phenyl]pyrrolidine-2,5-dione (Antrodin E or Camphorataimide D)	M	*In vitro* anti-HBV and anti-HCV	[31, 70]
67	Antrocinnamomins B	M	*In vitro* anti-inflammatory	[37]
	Miscellaneous compounds			
68	2,2′,5,5′-Tetramethoxy-3,4,3′,4′-bi-methylenedioxy-6,6′-dimethylbiphenyl	F	*In vitro* anti-HBV	[71]
69	α-Tocospiro B	F		[30]
70	Methyl oleate	F		[20]
71	Antroquinonol	M, F	*In vitro* cytotoxic, anti-inflammatory, anti-HBV	[12, 32, 72]
72	Adenosine	M	Prevention of PC 12 cells apoptosis	[37]
73	Cordycepin	M		[37]
74	2,4,5-trimethoxybenzaldehyde	M	Prevention of PC 12 cells apoptosis	[31]
75	Antroquinonol B	M	*In vitro* anti-inflammatory	[36]
76	4-acetyl-antroquinonol B	M	*In vitro* anti-inflammatory	[36]
77	2,3-(methylenedioxy)-6-methylbenzene-1,4-diol	M	*In vitro* anti-inflammatory	[36]
78	2,4-dimethoxy-6-methylbenzene-1,3-diol	M	*In vitro* anti-inflammatory	[36]

F: Fruiting bodies; M: Mycelium; B: Culture broth.

hydropic swelling and necrosis induced by CCl_4 [92]. A new formulation comprising the filtrate of *A. camphorata* and extracts from *Astragalus membranaceus*, *Salvia miltiorrhiza* and *Lycimm chinense* found to have significant inhibitory activity against the elevated ALT level in CCl_4-treated animals to an extent that was even better than when the filtrate was used alone [93].

In conclusion, the reported data showed that *A. camphorata* may exert its hepatoprotective effects, though different mechanisms such as scavenging free radicals responsible for cell damage, enhancing the enzymes responsible for antioxidant activity, inhibiting the inflammatory mediators and/or induction of the regeneration of the liver cells. Previously reported data revealed that *A. camphorata* is a potent free radical scavenger [82–85]. It is therefore possible that hepatoprotective action of *A. camphorata* is partially due to its antioxidant activity. The antioxidant activities of the filtrate and mycelium extracts were correlated with the presence of total polyphenols, crude triterpenoids and the protein/polysaccharide ratio of the crude polysaccharides [82]. Aqueous extracts of *A. camphorata* inhibited non-enzymatic iron-induced lipid peroxidation in rat brain homogenates with an IC_{50} value of about 3.1 mg ml^{-1} [83]. These results suggest that *A. camphorata* exerts effective protection against chemical-induced hepatic injury *in vivo* by free radical scavenging activities.

5.6. Prevention of Liver Fibrosis. Using CCl_4-treated rats as an experimental model, it is found that the filtrate of fermented mycelium from *A. camphorata* has the preventive and curative properties of liver fibrosis [94]. Post treatment with mycelium to CCl_4-administered rats clearly accelerated the reversal of fibrosis and lowered the elevated mRNA levels of hepatic collagen I, transforming growth factor (TGF)-β1 and tissue inhibitors of matrix metalloproteinase (TIMP)-1. Furthermore, it is confirmed that hepatic lipid peroxidation is increased during fibrogenesis where hepatic malondialdehyde (MDA) and hydroxyproline (HP) contents in curative groups were remarkably restored [94]. Another study reported that fermented mycelium is effective in reversing liver fibrosis induced by dimethylnitrosamine (DMN), while the lowered activities of antioxidative enzymes (SOD, catalase and GSH-Px) in the liver were not restored [95]. Therefore, more *in vivo* studies and randomized controlled clinical studies should be performed to further elucidate the mechanisms of action of *A. camphorata*.

5.7. Neuroprotective Effect. It is reported that mycelium extract from submerged cultivation of *A. camphorata* prevents serum-deprived PC-12 cell apoptosis through PKA-dependent pathway and by suppression of JNK and p38 activities [61, 96].

5.8. Antihypertensive Effect. The extracts of wild and solid-state cultures *A. camphorata* were obtained by sequential extraction with cold water (CWS), methanol (MS) and hot water (HWS), respectively. Among these three, only extract MS (10 mg kg^{-1} BW) showed potent antihypertensive effects in spontaneously hypertensive rats by decreased systolic blood pressure and diastolic blood pressure, however these effects were absent in Wistar Kyoto rats [97]. These results might have a scope to develop *A. camphorata* to be a healthy (or functional) food to regulate blood pressure.

5.9. Vasorelaxation Effect. The SCM extract of strain B85 shown to have concentration-dependent vasorelaxation with maximal relaxation of 40.34 ± 7.53% through an endothelium-dependent mechanism, whereas strains 35 398, 35 396 and B71 had mild effects in isolated rat aortic rings [98]. In conclusion, preclinical and clinical studies are necessary for the validation of this natural product in the prevention and/or therapy of above mentioned applications. Also, the effects of isolated compounds require to be tested further as discussed subsequently.

6. Bioactivities of Isolated Compounds

6.1. Terpenoids. The bitter components of *A. camphorata* are triterpenoids and have known pharmacological activities (Table 1). Triterpenes are considered to be potential anti-cancer agents due to activity against growing tumors, they have direct cytotoxicity against tumor cells rather than to normal cells. Cultivated mycelium has been reported to contain similar compounds with wild fruiting bodies [8]. Biological study revealed that zhankuic acids A (**10**) and C (**16**) exhibited cytotoxic activity against P-388 murine leukemia cells with an IC_{50} value of 1.8 and 5.4 μg ml^{-1}, respectively [18]. However, the molecular mechanism(s) responsible for the inhibitory effects have not been fully elucidated. We reported that the isolates (**10**, **16**, **20**, **25–27**, **29** and **32**) from fruiting bodies of *A. camphorata* showed inhibitory effects on *Spodoptera frugiperda Sf*9 insect cells where zhankuic acids A (**10**) and C (**16**) and methyl antcinate B (**20**) being most potent [64]. In continuation of our studies on the activities of pure compounds from fruiting bodies of *A. camphorata*, these eight compounds together with antcins A (**9**) and C (**11**) were examined for their cytotoxic data against various cancer cell types. The three zhankuic acids, **10**, **16** and **20** displayed the tumor-specific cytotoxicity with an IC_{50} range from 22.3 to 75.0 μM against the colon, breast, liver and lung cancer cell lines [65]. One of the most potent triterpene was methyl antcinate B (**20**). Furthermore, compounds **10**, **16** and **20** demonstrated to induce apoptosis in HT-29 cells, as confirmed by sub-G1 cell-cycle arrest as well as DNA fragmentation. Furthermore, the expression of poly-(ADP-ribose) polymerase cleavage, Bcl-2 and procaspase-3 were also suppressed, in addition to their synergistic cytotoxic effect (4 μM each) in HT-29 cells [65]. Our previous results state that the chloroform extract of *A. camphorata* demonstrated inhibitory activity on colon cancer cells (see previously). Analysis suggested that the active principles *in vivo* were triterpenoids. These results indicate that the triterpenoids fraction of *A. camphorata* may be a useful ingredient in the treatment of colon cancer. To continue, our results also reveal that compounds **9**, **18** and **20** displayed potential anti-*Helicobacter pylori* activity and its associated inflammation in human gastric epithelial AGS cells, by inhibition of adhesion and invasion, NF-κB activation and the subsequent release of IL-8 in AGS cells [99].

Antcins A (**9**), B (**10**) and eburicol (**31**) have anti-inflammatory activity by inhibition of *N*-formylmethionyl-leucyl-phenylalanine (fMLP)-induced superoxide generation in human neutrophils with an IC_{50} value of 8.5, 9.8 and 50.5 μM, respectively [30]. To continue, antcin C (**11**), dehydroeburicoic acid (**25**) and eburicoic acid (**28**) also noted for their immuno-modulating activity by reduced ROS in the above mentioned system with IC_{50} values of 16.9, 144.8 and 43.9, respectively [67]. The compounds **10**, **17** and **16** and, antcin K (**18**) isolated from ethanol extracts of wild fruiting body has shown concentration-dependent (1–25 μM) anti-inflammatory effects (by modulation of leukocyte activity and inhibition of ROS) induced by fMLP and TPA in human neutrophils [66]. The diterpenoid compounds **2**, **3**, **4**, **5** and **6** isolated from the fruiting bodies of *A. camphorata* have neuroprotective activity in cortical neurons from the cerebral cortex of Harlan Sprague-Dawley rat pups by 39.2, 35.0, 36.7, 30.6 and 27.0%, respectively, at concentrations between 5 and 20 μM [28].

6.2. Maleic and Succinic Acid Derivatives. Nakamura et al. [24] noted the cytotoxic data of five new maleic and succinic acid derivatives from the mycelium of *A. camphorata* in LLC tumor cells. The compounds antrodins A (**60**) and D (**56**) had no activity whereas antrodins B (**62**) and C (**64**) had cytotoxic activity with ED_{50} values of 7.5 and 3.6 μg ml^{-1}, respectively [24]. Furthermore, the compounds antrodins A–E (**56**, **60**, **62**, **64** and **66**) from mycelium noted to have anti-hepatitis activity [27]. The succinic derivative **54** isolated from fruiting bodies exert both immunostimulatory and anti-inflammatory effects by increased spontaneous TNF-α secretion from unstimulated RAW264.7 cells, in addition to suppressed IL-6 production (IC_{50} = 10 μg ml^{-1}) in LPS-stimulated cells. Furthermore, the compounds, **57**, **58** and **61** suppressed IL-6 production in LPS-stimulated cells with IC_{50} values of 17, 18 and 25 μg ml^{-1}, respectively [31]. Antrocinnamomins A (**65**) isolated from mycelium of *A. camphorata* noted to have inhibition of NO production of macrophages [33]. To continue, the tested maleic and succinic-acid derivatives **60**, **62**, **64, 56** and **66** (antrodins A–E) showed HCV protease inhibitory activity with IC_{50} values of 0.9, >100, 2.9, 20.0 and 20.1 μg ml^{-1}, respectively [98].

6.3. Polysaccharides. Polysaccharides represent a structurally diverse class of biological macromolecules with a wide-range of physicochemical properties. Polysaccharides of *A. camphorata* have been reported to be composed of a variety of monosaccharides, galactose, glucose, mannose, glucosamine and galactosamine [38]. The majority of anti-tumor β-D-glucans isolated from *A. camphorata* are β-(1 → 3)-D-glucopyranans and characteristic β-(1 → 6)-D-glucosyl branches [38].

Scientific investigations concerning the inhibition of anti-HBV activity by polysaccharides from fruiting bodies and cultured mycelia of *A. camphorata* were reported in 2002 [38]. Polysaccharides from strain B86 at a dosage 50 μg ml^{-1} exhibited the highest anti-hepatitis B surface antigen effect, which was higher than that of α-interferon at a concentration of 1000 U/ml [38]. It is interesting to note that the anti-HBV activity has not been reported for polysaccharides from any other mushroom. Thus, further studies on the relationship between specific polysaccharide fraction and their biological activities are required. Recently, extensive studies on the immunomodulatory and anti-tumor effects polysaccharides from different sources have been reported [100]. For example, a partially purified polysaccharide inhibited the proliferation of human leukemic U937 cells via activation of human mononuclear cells [101]. In addition, these *in vitro* anti-tumor activity was substantiated by the *in vivo* study in sarcoma 180-bearing mice where the intraperitoneal and oral administration of 100 and 200 mg kg^{-1} significantly suppressed the tumor growth with the inhibition rate of 69.1% and 58.8%, respectively [101]. Polysaccharides isolated from *A. cinnamomea* reported to have anti-angiogenic activities in endothelial cells, by dose-dependent inhibition of cyclin D1 expression through vascular endothelial growth factor receptor signal pathway [102]. To continue, Han et al. [103] reported that a neutral polysaccharide named *ACN2a* from the hot water extract of the mycelium of *A. camphorata* to have *in vivo* hepatoprotective activity in mouse model of liver injury that was induced by *Propionibacterium acnes*-LPS [103]. Another study reported that the polysaccharide fractions (from SCM), AC-1, AC-2, AC-3, AC-4 and AC-5 belonged to the category of glycoprotein with mean molecular mass in the range of 394–940 kDa showed anti-inflammatory activity in macrophages [40]. At a concentration of 1 μm, polysaccharides AC-1 and AC-2 showed DPPH radical scavenging activity by 74.5 and 50.5%, respectively. In addition, AC-2 dose-dependently (50–200 μg ml^{-1}) inhibit the LPS-induced NO production and iNOS protein expression in macrophages [40]. Polysaccharides from SCM possess immunomodulatory activity by modulating the pro-inflammatory cytokines [104], through inducing Th1-type cytokines such as IFN-γ and TNF-α in a time-dependent manner but not of Th2 cytokines [70]. A recent study reported that 3–6 weeks oral administration with 2.5 mg of polysaccharides derived from *A. camphorata* (AC-PS) modulate the expression of Th1 cytokines in splenocytes as well as the type1 differentiation of T and B lymphocytes, in addition to reduce the infection rate of *Schistosoma mansoni* in mice [105]. Furthermore, water-soluble polysaccharides (200 μg ml^{-1}) from the fermented filtrate and mycelia of *A. cinnamomea* significantly reduced the oxidative DNA damage and ROS induced by hydrogen peroxide in Chang liver cells [106]. A recent study for the first time reported the sulfated polysaccharides (SPSs) from submerged cultivation medium of *A. cinnamomea*. These SPSs dose-dependently inhibited *in vitro* Matrigel tube formation in an angiogenesis model, in addition to their prevention of serum-deprived apoptosis in neuronal-like PC-12 cells [107].

6.4. Compounds with Miscellaneous Biological Activities. Among the 10 pure compounds (in concentration range of 5–50 μM) which included one biphenyl, four ergostane- and five lanostane derivatives tested for anti-viral activity against wild-type (HBsAg) and lamivudine-mutant (HBeAg) HBV, the only one biphenyl compound (**68**) at a 50 μM suppressed HBsAg and HBeAg levels by 54.2 and 32.2%, respectively [71]. The compound adenosine isolated from ethanolic extract of SCM, noted it acts through adenosine A_{2A} receptors to prevent rat PC-12 cells from serum deprivation-induced apoptosis [37]. A benzenoid 2,4,5-trimethoxybenzaldehyde (**74**) produced by submerged cultivation of *A. camphorata* reported to has COX-2 inhibitory activity [31]. The compounds antrocamphin A (**43**) and 2,3-dimethoxy-5-methyl[1, 4]benzoquinone (**53**) inhibit the fMLP-induced superoxide generation in human neutrophils with an IC_{50} value of 9.3 and 26.1 μM, respectively [30]. Antroquinonol (**71**), a ubiquinone derivative isolated from mycelia and the fruiting bodies of *A. camphorata* reported to has cytotoxic activities against cancer cell lines MCF-7, MDA-MB-231, Hep 3B, Hep G2 and DU-145, LNCaP with the IC_{50} values ranged from 0.13 to 6.09 μM [32]. In addition, **71** at 256 μM significantly inhibited the production of TNF-α and IL-1β by 75 and 78%, respectively, in RAW 264.7 cells [72]. Furthermore, compound **71** also noted as potent inhibitor in the synthesis of HBsAg and HBeAg [108]. The compounds antroquinonol B (**75**), 4-acetyl-antroquinonol B (**76**), 2,3-(methylenedioxy)-6-methylbenzene-1,4-diol (**77**) and 2,4-dimethoxy-6-methylbenzene-1,3-diol (**78**) and antrodin D (**56**) from mycelium of *A. camphorata* inhibit NO production in LPS-activated macrophages with an IC_{50} values of 16.2, 14.7, ∼18, 32.2 and 26.3 μg ml^{-1}, respectively [36]. A benzenoid compound **40** has dose-dependent (50–150 μM) anti-proliferation activity in human colon cancer cell line COLO 205 through G0/G1 cell-cycle arrest and induction of apoptosis (>150 μM). In addition, cell-cycle arrest is associated with a significant increase in levels of p53, p21/Cip1 and p27/Kip1, and a decrease in cyclins D1, D3 and A [68].

7. Summary and Outlook

This review summarized important areas of investigation being performed on *A. camphorata* with particular emphasis on crude extracts and isolated compounds. Some correlation between the ethnomedical employment and the pharmacological activities has been duly observed in the present review. *Antrodia camphorata* extracts from its fruiting bodies,

mycelium and cultivation filtrate showed multiple cancer preventive and anti-inflammatory activities. In addition, these extracts provide a variety of anti-cancer and anti-inflammatory active secondary metabolites and polysaccharides. Of particular promise, due to their potent cytotoxic activity against a number of cancer cell lines, are the triterpenoids with ketonic functional groups. In fact, these triterpenoids, which have also been found in a small number of other mushrooms, are currently under active investigation as potential therapeutic leads [109]. Because the antioxidant action is also a means of lowering chronic anti-inflammatory action, *A. camphorata* hold potential in functional food approaches aimed at normalizing metabolic syndrome.

In the search for active compounds from *A. camphorata*, the majority of research has been performed on extracts from the fruiting bodies and mycelium and, there have been fewer studies on extracts from the submerged cultivated medium. Further studies would be desirable to isolate useful new secondary metabolites by varying cultivation conditions. The pharmacological studies so far have mostly been performed *in vitro* and *in vivo* with animals. Therefore, clinical studies are needed in order to confirm traditional wisdom in the light of a rational phytotherapy. Nevertheless, the former reports could be considered as providing leads for more scientific research. The biological activities of the pure compound administrated or consumed alone were found to be lower than those obtained from the original mixture of active ingredients present in natural medicines including *A. camphorata*. Thus, the combined, synergistic effects of a mixture of active components that are present in *A. camphorata* on biological activities need to be thoroughly assessed. Finally, though we recently developed a cyclodextrin-modified capillary electrophoresis method for the separation and analysis of achiral and chiral triterpenoids from fruiting bodies of *A. camphorata* [110], there however, is a need to establish suitable quality parameters and analytical methods to determine active compounds.

Acknowledgment

The first author would like to thank the Ministry of Education, Taiwan for supporting her to conduct research in Taiwan.

References

[1] X. Zhang, *WHO Traditional Medicine Strategy 2002–2005*, World Health Organization, Geneva, Switzerland, 2002.

[2] J. C. I. Tsao and L. K. Zeltzer, "Complementary and alternative medicine approaches for pediatric pain: a review of the state-of-the-science," *Evidence-Based Complementary and Alternative Medicine*, vol. 2, no. 2, pp. 149–159, 2005.

[3] B. Patwardhan, D. Warude, P. Pushpangadan, and N. Bhatt, "Ayurveda and traditional Chinese medicine: a comparative overview," *Evidence-Based Complementary and Alternative Medicine*, vol. 2, no. 4, pp. 465–473, 2005.

[4] T. T. Chang and W. N. Chou, "*Antrodia cinnamomea* sp. nov. on *Cinnamomum kanehirai* in Taiwan," *Mycological Research*, vol. 99, no. 6, pp. 756–758, 1995.

[5] S.-H. Wu, L. Ryvarden, and T.-T. Chang, "*Antrodia camphorata* ('niu-chang-chih'), new combination of a medicinal fungus in Taiwan," *Botanical Bulletin of Academia Sinica*, vol. 38, no. 4, pp. 273–275, 1997.

[6] J. C. Chen, W. H. Lin, C. N. Chen, S. J. Sheu, S. J. Huang, and Y. L. Chen, "Development of *Antrodia camphorata* mycelium with submerged culture," *Fungal Sciences*, vol. 16, pp. 7–22, 2001.

[7] Z. T. Tsai and S. L. Liaw, *The Use and the Effect of Ganoderma*, San Yun Press, Taichung, Taiwan, 1985.

[8] C. J. Chen, C. H. Su, and M. H. Lan, "Study on solid cultivation and bioactivity of *Antrodia camphorata*," *Fungal Sciences*, vol. 16, pp. 65–72, 2001.

[9] M. Zang and Q. H. Su, "*Ganoderma comphoratum*, a new taxon in genus *Ganoderma* from Taiwan, China," *Acta Botanica Yunnanica*, vol. 12, pp. 395–396, 1990.

[10] T.-T. Chang and W.-N. Chou, "*Antrodia cinnamomea* reconsidered and *A. salmonea* sp. nov. on *Cunninghamia konishii* in Taiwan," *Botanical Bulletin of Academia Sinica*, vol. 45, no. 4, pp. 347–352, 2004.

[11] S. H. Wu, Z. H. Yu, Y. C. Dai et al., "*Taiwanofungus*, a polypore new genus," *Fungal Sciences*, vol. 19, pp. 109–116, 2004.

[12] H.-H. Chiu, "Phylogenetic analysis of *Antrodia* species and *Antrodia camphorata* inferred from internal transcribed spacer region," *Antonie van Leeuwenhoek*, vol. 91, no. 3, pp. 267–276, 2007.

[13] D. L. Hawksworth, P. M. Kirk, B. C. Sutton, and D. N. Pegler, *Ainsworth and Bisby's Dictionary of the Fungi*, International Mycological Institute, Egham, UK, 8th edition, 1995.

[14] C. H. Su, *Health Guardian Angel: Antrodia camphorata*, EKS Book Publishing, Taipei, Taiwan, 1st edition, 2002.

[15] J. C. Chen, *King of Ganoderma: Antrodia camphorata in Taiwan*, Yuen Chi Jai Book Publishing, Taipei, Taiwan, 2nd edition, 2008.

[16] J.-J. Cheng, C.-J. Yang, C.-H. Cheng, Y.-T. Wang, N.-K. Huang, and M.-K. Lu, "Characterization and functional study of *Antrodia camphorata* lipopolysaccharide," *Journal of Agricultural and Food Chemistry*, vol. 53, no. 2, pp. 469–474, 2005.

[17] I.-H. Cherng, H.-C. Chiang, M.-C. Cheng, and Y. U. Wang, "Three new triterpenoids from *Antrodia cinnamomea*," *Journal of Natural Products*, vol. 58, no. 3, pp. 365–371, 1995.

[18] C.-H. Chen, S.-W. Yang, and Y.-C. Shen, "New steroid acids from *Antrodia cinnamomea*, a fungal parasite of *Cinnamomum micranthum*," *Journal of Natural Products*, vol. 58, no. 11, pp. 1655–1661, 1995.

[19] C. H. Chiang, D. P. Wu, I. W. Cherng, and U. C. Ueng, "A sesquiterpene lactone, phenyl and biphenyl compounds from *Antrodia cinnamomea*," *Phytochemistry*, vol. 39, no. 3, pp. 613–616, 1995.

[20] D. P. Wu and C. H. Chiang, "Constituents of *Antrodia cinnamomea*," *Journal of the Chinese Chemical Society*, vol. 42, pp. 797–800, 1995.

[21] I.-H. Cherng, D.-P. Wu, and H.-C. Chiang, "Triterpenoids from *Antrodia cinnamomea*," *Phytochemistry*, vol. 41, no. 1, pp. 263–267, 1996.

[22] S.-W. Yang, Y.-C. Shen, and C.-H. Chen, "Steroids and triterpenoids of *Antrodia cinnamomea*—a fungus parasitic on *Cinnamomum micranthum*," *Phytochemistry*, vol. 41, no. 5, pp. 1389–1392, 1996.

[23] Y.-C. Shen, S.-W. Yang, C.-S. Lin, C.-H. Chen, Y.-H. Kuo, and C.-F. Chen, "Zhankuic acid F: a new metabolite from

a formosan fungus *Antrodia cinnamomea*," *Planta Medica*, vol. 63, no. 1, pp. 86–88, 1997.

[24] K.-F. Huang, W.-M. Huang, and H.-C. Chiang, "Phenyl compounds from *Antrodia cinnamomea*," *Chinese Pharmaceutical Journal*, vol. 53, no. 6, pp. 327–331, 2001.

[25] C. C. Shen, Y. C. Kuo, R. L. Huang et al., "New ergostane and lanostane from *Antrodia camphorata*," *The Journal of Chinese Medicine*, vol. 14, pp. 247–58, 2003.

[26] N. Nakamura, A. Hirakawa, J.-J. Gao et al., "Five new maleic and succinic acid derivatives from the mycelium of *Antrodia camphorata* and their cytotoxic effects on LLC tumor cell line," *Journal of Natural Products*, vol. 67, no. 1, pp. 46–48, 2004.

[27] C. C. Shen, H. C. Yang, R. L. Huang, J. C. Chen, and C. C. Chen, "Anti-HBV principle from the culture broth of *Antrodia camphorata* (strain # CCRC-35396)," *The Journal of Chinese Medicine*, vol. 16, pp. 57–61, 2005.

[28] C.-C. Chen, Y.-J. Shiao, R.-D. Lin et al., "Neuroprotective diterpenes from the fruiting body of *Antrodia camphorata*," *Journal of Natural Products*, vol. 69, no. 4, pp. 689–691, 2006.

[29] M. Hattori and C. C. Sheu, "Compounds from *Antrodia camphorata* having anti-inflammatory and anti-tumor activity," *US 7109232-2006-9-19*, 2006.

[30] J.-J. Chen, W.-J. Lin, C.-H. Liao, and P.-C. Shieh, "Anti-inflammatory benzenoids from *Antrodia camphorata*," *Journal of Natural Products*, vol. 70, no. 6, pp. 989–992, 2007.

[31] C.-C. Chen, C.-C. Chyau, and T.-H. Hseu, "Production of a COX-2 inhibitor, 2,4,5-trimethoxybenzaldehyde, with submerged cultured *Antrodia camphorata*," *Letters in Applied Microbiology*, vol. 44, no. 4, pp. 387–392, 2007.

[32] T.-H. Lee, C.-K. Lee, W.-L. Tsou, S.-Y. Liu, M.-T. Kuo, and W.-C. Wen, "A new cytotoxic agent from solid-state fermented mycelium of *Antrodia camphorata*," *Planta Medica*, vol. 73, no. 13, pp. 1412–1415, 2007.

[33] S.-C. Chien, M.-L. Chen, H.-T. Kuo, Y.-C. Tsai, B.-F. Lin, and Y.-H. Kuo, "Anti-inflammatory activities of new succinic and maleic derivatives from the fruiting body of *Antrodia camphorata*," *Journal of Agricultural and Food Chemistry*, vol. 56, no. 16, pp. 7017–7022, 2008.

[34] M.-D. Wu, M.-J. Cheng, B.-C. Wang, W.-Y. Wang, J.-T. Lai, and G.-F. Yuan, "Chemical constituents from the mycelia of *Antrodia cinnamomea*," *Journal of the Chilean Chemical Society*, vol. 52, no. 4, pp. 1338–1340, 2007.

[35] M.-D. Wu, M.-J. Cheng, B.-C. Wang et al., "Maleimide and maleic anhydride derivatives from the mycelia of *Antrodia cinnamomea* and their nitric oxide inhibitory activities in macrophages," *Journal of Natural Products*, vol. 71, no. 7, pp. 1258–1261, 2008.

[36] S.-S. Yang, G.-J. Wang, S.-Y. Wang, Y.-Y. Lin, Y.-H. Kuo, and T.-H. Lee, "New constituents with iNOS inhibitory activity from mycelium of *Antrodia camphorata*," *Planta Medica*, vol. 75, no. 5, pp. 512–516, 2009.

[37] M.-K. Lu, J.-J. Cheng, W.-L. Lai, Y.-R. Lin, and N.-K. Huang, "Adenosine as an active component of *Antrodia cinnamomea* that prevents rat PC12 cells from serum deprivation-induced apoptosis through the activation of adenosine A2A receptors," *Life Sciences*, vol. 79, no. 3, pp. 252–258, 2006.

[38] I.-H. Lee, R.-L. Huang, C.-T. Chen, H.-C. Chen, W.-C. Hsu, and M.-K. Lu, "*Antrodia camphorata* polysaccharides exhibit anti-hepatitis B virus effects," *FEMS Microbiology Letters*, vol. 209, no. 1, pp. 63–67, 2002.

[39] S. C. Chen, M. K. Lu, J. J. Cheng, and D. L. Wang, "Antiangiogenic activities of polysaccharides isolated from medicinal fungi," *FEMS Microbiology Letters*, vol. 249, no. 2, pp. 247–254, 2005.

[40] C.-C. Chen, Y.-W. Liu, Y.-B. Ker et al., "Chemical characterization and anti-inflammatory effect of polysaccharides fractionated from submerge-cultured *Antrodia camphorata* mycelia," *Journal of Agricultural and Food Chemistry*, vol. 55, no. 13, pp. 5007–5012, 2007.

[41] J. Mahajna, N. Dotan, B.-Z. Zaidman, R. D. Petrova, and S. P. Wasser, "Pharmacological values of medicinal mushrooms for prostate cancer therapy: the case of *Ganoderma lucidum*," *Nutrition and Cancer*, vol. 61, no. 1, pp. 16–26, 2009.

[42] U. Lindequist, T. H. J. Niedermeyer, and W.-D. Jülich, "The pharmacological potential of mushrooms," *Evidence-Based Complementary and Alternative Medicine*, vol. 2, no. 3, pp. 285–299, 2005.

[43] Y.-L. Hsu, Y.-C. Kuo, P.-L. Kuo, L.-T. Ng, Y.-H. Kuo, and C.-C. Lin, "Apoptotic effects of extract from *Antrodia camphorata* fruiting bodies in human hepatocellular carcinoma cell lines," *Cancer Letters*, vol. 221, no. 1, pp. 77–89, 2005.

[44] P.-L. Kuo, Y.-L. Hsu, C.-Y. Cho, L.-T. Ng, Y.-H. Kuo, and C.-C. Lin, "Apoptotic effects of *Antrodia cinnamomea* fruiting bodies extract are mediated through calcium and calpain-dependent pathways in Hep 3B cells," *Food and Chemical Toxicology*, vol. 44, no. 8, pp. 1316–1326, 2006.

[45] Y.-L. Hsu, P.-L. Kuo, C.-Y. Cho et al., "*Antrodia cinnamomea* fruiting bodies extract suppresses the invasive potential of human liver cancer cell line PLC/PRF/5 through inhibition of nuclear factor κB pathway," *Food and Chemical Toxicology*, vol. 45, no. 7, pp. 1249–1257, 2007.

[46] Y. K. Rao, S.-H. Fang, and Y.-M. Tzeng, "Evaluation of the anti-inflammatory and anti-proliferation tumoral cells activities of *Antrodia camphorata*, *Cordyceps sinensis*, and *Cinnamomum osmophloeum* bark extracts," *Journal of Ethnopharmacology*, vol. 114, no. 1, pp. 78–85, 2007.

[47] C.-Y. Chang, Z.-N. Huang, H.-H. Yu et al., "The adjuvant effects of *Antrodia camphorata* extracts combined with anti-tumor agents on multidrug resistant human hepatoma cells," *Journal of Ethnopharmacology*, vol. 118, no. 3, pp. 387–395, 2008.

[48] M.-C. Lu, Y.-C. Du, J.-J. Chuu et al., "Active extracts of wild fruiting bodies of *Antrodia camphorata* (EEAC) induce leukemia HL 60 cells apoptosis partially through histone hypoacetylation and synergistically promote anticancer effect of trichostatin A," *Archives of Toxicology*, vol. 83, no. 2, pp. 121–129, 2009.

[49] Y.-C. Hseu, W.-C. Chang, Y.-T. Hseu et al., "Protection of oxidative damage by aqueous extract from *Antrodia camphorata* mycelia in normal human erythrocytes," *Life Sciences*, vol. 71, no. 4, pp. 469–482, 2002.

[50] Y.-C. Hseu, H.-L. Yang, Y.-C. Lai, J.-G. Lin, G.-W. Chen, and Y.-H. Chang, "Induction of apoptosis by *Antrodia camphorata* in human premyelocytic leukemia HL-60 cells," *Nutrition and Cancer*, vol. 48, no. 2, pp. 189–197, 2004.

[51] H. Wu, C.-L. Pan, Y.-C. Yao, S.-S. Chang, S.-L. Li, and T.-F. Wu, "Proteomic analysis of the effect of *Antrodia camphorata* extract on human lung cancer A549 cell," *Proteomics*, vol. 6, no. 3, pp. 826–835, 2006.

[52] T.-Y. Song, S.-L. Hsu, and G.-C. Yen, "Induction of apoptosis in human hepatoma cells by mycelia of *Antrodia camphorata* in submerged culture," *Journal of Ethnopharmacology*, vol. 100, no. 1-2, pp. 158–167, 2005.

[53] T. Y. Song, S. L. Hsu, C. T. Yeh, and G. C. Yen, "Mycelia from *Antrodia camphorata* in submerged culture induced

apoptosis of human heptoma Hep G2 cells possibility through regulation of Fas pathway," *Journal of Agricultural and Food Chemistry*, vol. 53, pp. 5559–5564, 2005.

[54] Y.-S. Chen, J.-H. Pan, B.-H. Chiang, F.-J. Lu, and L.-Y. Sheen, "Ethanolic extracts of *Antrodia cinnamomea* mycelia fermented at varied times and scales have differential effects on hepatoma cells and normal primary hepatocytes," *Journal of Food Science*, vol. 73, no. 7, pp. H179–H185, 2008.

[55] H.-L. Yang, C.-S. Chen, W.-H. Chang et al., "Growth inhibition and induction of apoptosis in MCF-7 breast cancer cells by *Antrodia camphorata*," *Cancer Letters*, vol. 231, no. 2, pp. 215–227, 2006.

[56] Y.-C. Hseu, S.-C. Chen, P.-C. Tsai et al., "Inhibition of cyclooxygenase-2 and induction of apoptosis in estrogen-nonresponsive breast cancer cells by *Antrodia camphorata*," *Food and Chemical Toxicology*, vol. 45, no. 7, pp. 1107–1115, 2007.

[57] Y.-C. Hseu, S.-C. Chen, H.-C. Chen, J.-W. Liao, and H.-L. Yang, "*Antrodia camphorata* inhibits proliferation of human breast cancer cells in vitro and in vivo," *Food and Chemical Toxicology*, vol. 46, no. 8, pp. 2680–2688, 2008.

[58] C.-C. Peng, K.-C. Chen, R. Y. Peng, C.-H. Su, and H. M. Hsieh-Li, "Human urinary bladder cancer T24 cells are susceptible to the *Antrodia camphorata* extracts," *Cancer Letters*, vol. 243, no. 1, pp. 109–119, 2006.

[59] C.-C. Peng, K.-C. Chen, R. Y. Peng, C.-C. Chyau, C.-H. Su, and H. M. Hsieh-Li, "*Antrodia camphorata* extract induces replicative senescence in superficial TCC, and inhibits the absolute migration capability in invasive bladder carcinoma cells," *Journal of Ethnopharmacology*, vol. 109, no. 1, pp. 93–103, 2007.

[60] K.-C. Chen, C.-C. Peng, R. Y. Peng et al., "Unique formosan mushroom *Antrodia camphorata* differentially inhibits androgen-responsive LNCaP and -independent PC-3 prostate cancer cells," *Nutrition and Cancer*, vol. 57, no. 1, pp. 111–121, 2007.

[61] M.-K. Lu, J.-J. Cheng, W.-L. Lai, Y.-J. Lin, and N.-K. Huang, "Fermented *Antrodia cinnamomea* extract protects rat PC12 cells from serum deprivation-induced apoptosis: the role of the MAPK family," *Journal of Agricultural and Food Chemistry*, vol. 56, no. 3, pp. 865–874, 2008.

[62] C.-M. Ho, C.-C. Huang, C.-J. Huang et al., "Effects of *Antrodia camphorata* on viability, apoptosis, and $[Ca^{2+}]i$ in PC3 human prostate cancer cells," *Chinese Journal of Physiology*, vol. 51, no. 2, pp. 78–84, 2008.

[63] Y.-C. Lu, C.-C. Huang, C.-J. Huang et al., "Effects of *Antrodia camphorata* on viability, apoptosis, $[Ca^{2+}]i$, and MAPKs phosphorylation in MG63 human osteosarcoma cells," *Drug Development Research*, vol. 68, no. 2, pp. 71–78, 2007.

[64] K. B. Male, Y. K. Rao, Y.-M. Tzeng, J. Montes, A. Kamen, and J. H. T. Luong, "Probing inhibitory effects of *Antrodia camphorata* isolates using insect cell-based impedance spectroscopy: inhibition vs chemical structure," *Chemical Research in Toxicology*, vol. 21, no. 11, pp. 2127–2133, 2008.

[65] C. T. Yeh, Y. K. Rao, C. F. Yeh et al., "Cytotoxic triterpenes from *Antrodia camphorata* and their mode of action in HT-29 human colon cancer cells," *Cancer Letters*, vol. 285, no. 1, pp. 73–79, 2009.

[66] Y.-C. Shen, Y.-H. Wang, Y.-C. Chou et al., "Evaluation of the anti-inflammatory activity of zhankuic acids isolated from the fruiting bodies of *Antrodia camphorata*," *Planta Medica*, vol. 70, no. 4, pp. 310–314, 2004.

[67] Y.-C. Shen, C.-F. Chen, Y.-H. Wang, T.-T. Chang, and C.-J. Chou, "Evaluation of the immuno-modulating activity of some active principles isolated from the fruiting bodies of *Antrodia camphorata*," *Chinese Pharmaceutical Journal*, vol. 55, no. 5, pp. 313–318, 2003.

[68] H. M. Lien, H. W. Lin, Y. J. Wang et al., "Inhibition of anchorage-independent proliferation and G0/G1 cell-cycle regulation in human colorectal carcinoma cells by 4,7-dimethoxy-5-methyl-l,3-benzodioxole isolated from the fruiting body of *Antrodia camphorata*," *Evidence-Based Complementary and Alternative Medicine*, 2009.

[69] D. T. Phuong, C.-M. Ma, M. Hattori, and J. S. Jin, "Short communication: inhibitory effects of antrodins A-E from *Antrodia cinnamomea* and their metabolites on hepatitis c virus protease," *Phytotherapy Research*, vol. 23, no. 4, pp. 582–584, 2009.

[70] Y.-J. Chen, P.-C. Cheng, C.-N. Lin et al., "Polysaccharides from *Antrodia camphorata* mycelia extracts possess immunomodulatory activity and inhibits infection of *Schistosoma mansoni*," *International Immunopharmacology*, vol. 8, no. 3, pp. 458–467, 2008.

[71] R.-L. Huang, Q. Huang, C.-F. Chen, T.-T. Chang, and C.-J. Chou, "Anti-viral effects of active compounds from *Antrodia camphorata* on wild-type and lamivudine-resistant mutant HBV," *Chinese Pharmaceutical Journal*, vol. 55, no. 5, pp. 371–379, 2003.

[72] J. M. Chang, Y. R. Lee, L. M. Hung et al., "An extract of *Antrodia camphorata* mycelia attenuates the progression of nephritis in systemic lupus erythematosus-prone NZB/W F1 mice," *Evidence-Based Complementary and Alternative Medicine*, 2008.

[73] G. Aydemir, "Research on nutrition and cancer: the importance of the standardized dietary assessments," *Asian Pacific Journal of Cancer Prevention*, vol. 3, pp. 177–180, 2002.

[74] P. S. Haddad, G. A. Azar, S. Groom, and M. Boivin, "Natural health products, modulation of immune function and prevention of chronic diseases," *Evidence-Based Complementary and Alternative Medicine*, vol. 2, no. 4, pp. 513–520, 2005.

[75] A. Vojdani and J. Erde, "Regulatory T cells, a potent immunoregulatory target for CAM researchers: modulating tumor immunity, autoimmunity and alloreactive immunity (III)," *Evidence-Based Complementary and Alternative Medicine*, vol. 3, no. 3, pp. 309–316, 2006.

[76] S. Kaminogawa and M. Nanno, "Modulation of immune functions by foods," *Evidence-Based Complementary and Alternative Medicine*, vol. 1, pp. 241–250, 2005.

[77] Y.-C. Shen, C.-J. Chou, Y.-H. Wang, C.-F. Chen, Y.-C. Chou, and M.-K. Lu, "Anti-inflammatory activity of the extracts from mycelia of *Antrodia camphorata* cultured with water-soluble fractions from five different *Cinnamomum* species," *FEMS Microbiology Letters*, vol. 231, no. 1, pp. 137–143, 2004.

[78] Y.-C. Hseu, F.-Y. Wu, J.-J. Wu et al., "Anti-inflammatory potential of *Antrodia camphorata* through inhibition of iNOS, COX-2 and cytokines via the NF-κB pathway," *International Immunopharmacology*, vol. 5, no. 13-14, pp. 1914–1925, 2005.

[79] D.-Z. Liu, H.-J. Liang, C.-H. Chen et al., "Comparative anti-inflammatory characterization of wild fruiting body, liquid-state fermentation, and solid-state culture of *Taiwanofungus camphoratus* in microglia and the mechanism of its action," *Journal of Ethnopharmacology*, vol. 113, no. 1, pp. 45–53, 2007.

[80] M.-C. Kuo, C.-Y. Chang, T.-L. Cheng, and M.-J. Wu, "Immunomodulatory effect of *Antrodia camphorata* mycelia and culture filtrate," *Journal of Ethnopharmacology*, vol. 120, no. 2, pp. 196–203, 2008.

[81] J. C. Chen, C. N. Chen, S. J. Sheu et al., "Liver-caring medicine containing *Antrodia camphorate*," US 0113297-2003-6-19, 2003.

[82] T.-Y. Song and G.-C. Yen, "Antioxidant properties of *Antrodia camphorata* in submerged culture," *Journal of Agricultural and Food Chemistry*, vol. 50, no. 11, pp. 3322–3327, 2002.

[83] G. Hsiao, M.-Y. Shen, K.-H. Lin et al., "Antioxidative and hepatoprotective effects of *Antrodia camphorata* extract," *Journal of Agricultural and Food Chemistry*, vol. 51, no. 11, pp. 3302–3308, 2003.

[84] J.-L. Mau, P.-N. Huang, S.-J. Huang, and C.-C. Chen, "Antioxidant properties of methanolic extracts from two kinds of *Antrodia camphorata* mycelia," *Food Chemistry*, vol. 86, no. 1, pp. 25–31, 2004.

[85] C.-H. Shu and M.-Y. Lung, "Effect of culture pH on the antioxidant properties of *Antrodia camphorata* in submerged culture," *Journal of the Chinese Institute of Chemical Engineers*, vol. 39, no. 1, pp. 1–8, 2008.

[86] H.-L. Yang, Y.-C. Hseu, J.-Y. Chen et al., "*Antrodia camphorata* in submerged culture protects low density lipoproteins against oxidative modification," *American Journal of Chinese Medicine*, vol. 34, no. 2, pp. 217–231, 2006.

[87] Y.-C. Hseu, S.-C. Chen, Y.-J. Yech, L. Wang, and H.-L. Yang, "Antioxidant activity of *Antrodia camphorata* on free radical-induced endothelial cell damage," *Journal of Ethnopharmacology*, vol. 118, no. 2, pp. 237–245, 2008.

[88] S.-J. Huang and J.-L. Mau, "Antioxidant properties of methanolic extracts from *Antrodia camphorata* with various doses of γ-irradiation," *Food Chemistry*, vol. 105, no. 4, pp. 1702–1710, 2007.

[89] Z.-H. Ao, Z.-H. Xu, Z.-M. Lu, H.-Y. Xu, X.-M. Zhang, and W.-F. Dou, "Niuchangchih (*Antrodia camphorata*) and its potential in treating liver diseases," *Journal of Ethnopharmacology*, vol. 121, no. 2, pp. 194–212, 2009.

[90] Y.-Y. Dai, C.-H. Chuang, C.-C. Tsai et al., "The protection of Anthrodia camphorata against acute hepatotoxicity of alcohol in rats," *Journal of Food and Drug Analysis*, vol. 11, no. 3, pp. 177–185, 2003.

[91] Z.-M. Lu, W.-Y. Tao, X.-L. Zou, H.-Z. Fu, and Z.-H. Ao, "Protective effects of mycelia of *Antrodia camphorata* and *Armillariella tabescens* in submerged culture against ethanol-induced hepatic toxicity in rats," *Journal of Ethnopharmacology*, vol. 110, no. 1, pp. 160–164, 2007.

[92] T.-Y. Song and G.-C. Yen, "Protective effects of fermented filtrate from *Antrodia camphorata* in submerged culture against CCl4-induced hepatic toxicity in rats," *Journal of Agricultural and Food Chemistry*, vol. 51, no. 6, pp. 1571–1577, 2003.

[93] J. S. Huang, H. C. Chang, E. I. C. Li, T. M. Huang, Y. H. Su, and K. C. Wang, "Enhancement of hepatoprotective efficacy of *Antrodia camphorata* by Chinese tradition medicine," *Journal of Gastroenterology and Hepatology*, vol. 21, supplement 2, p. A234, 2006.

[94] W.-C. Lin, S.-C. Kuo, W.-L. Lin, H.-L. Fang, and B.-C. Wang, "Filtrate of fermented mycelia from *Antrodia camphorata* reduces liver fibrosis induced by carbon tetrachloride in rats," *World Journal of Gastroenterology*, vol. 12, no. 15, pp. 2369–2374, 2006.

[95] S. Q. Guo, *Ameliorative effects of Antrodia camphorata on liver fibrosis and gastrointestinal functions in rats*, M.S. thesis, China Medical College, Taiwan, 2002.

[96] N.-K. Huang, J.-J. Cheng, W.-L. Lai, and M.-K. Lu, "*Antrodia camphorata* prevents rat pheochromocytoma cells from serum deprivation-induced apoptosis," *FEMS Microbiology Letters*, vol. 244, no. 1, pp. 213–219, 2005.

[97] D.-Z. Liu, Y.-C. Liang, S.-Y. Lin et al., "Antihypertensive activities of a solid-state culture of *Taiwanofungus camphoratus* (Chang-Chih) in spontaneously hypertensive rats," *Bioscience, Biotechnology and Biochemistry*, vol. 71, no. 1, pp. 23–30, 2007.

[98] G.-J. Wang, H.-W. Tseng, C.-J. Chou, T.-H. Tsai, C.-T. Chen, and M.-K. Lu, "The vasorelaxation of *Antrodia camphorata* mycelia: involvement of endothelial Ca^{2+}-NO-cGMP pathway," *Life Sciences*, vol. 73, no. 21, pp. 2769–2783, 2003.

[99] M. Geethangili, S. H. Fang, C. H. Lai, Y. K. Rao, H. M. Lien, and Y. M. Tzeng, "Inhibitory effect of *Antrodia camphorata* constituents on the *Helicobacter pylori*-associated gastric inflammation," *Food Chemistry*, vol. 119, no. 1, pp. 149–153, 2010.

[100] I. A. Schepetkin and M. T. Quinn, "Botanical polysaccharides: macrophage immunomodulation and therapeutic potential," *International Immunopharmacology*, vol. 6, no. 3, pp. 317–333, 2006.

[101] J.-J. Liu, T.-S. Huang, M.-L. Hsu et al., "Antitumor effects of the partially purified polysaccharides from *Antrodia camphorata* and the mechanism of its action," *Toxicology and Applied Pharmacology*, vol. 201, no. 2, pp. 186–193, 2004.

[102] J.-J. Cheng, N.-K. Huang, T.-T. Chang, D. L. Wang, and M.-K. Lu, "Study for anti-angiogenic activities of polysaccharides isolated from *Antrodia cinnamomea* in endothelial cells," *Life Sciences*, vol. 76, no. 26, pp. 3029–3042, 2005.

[103] H.-F. Han, N. Nakamura, F. Zuo, A. Hirakawa, T. Yokozawa, and M. Hattori, "Protective effects of a neutral polysaccharide isolated from the mycelium of *Antrodia cinnamomea* on *Propionibacterium acnes* and lipopolysaccharide induced hepatic injury in mice," *Chemical and Pharmaceutical Bulletin*, vol. 54, no. 4, pp. 496–500, 2006.

[104] Y.-Y. Wu, C.-C. Chen, C.-C. Chyau, S.-Y. Chung, and Y.-W. Liu, "Modulation of inflammation-related genes of polysaccharides fractionated from mycelia of medicinal basidiomycete *Antrodia camphorata*," *Acta Pharmacologica Sinica*, vol. 28, no. 2, pp. 258–267, 2007.

[105] P.-C. Cheng, C.-Y. Hsu, C.-C. Chen, and K.-M. Lee, "*In vivo* immunomodulatory effects of *Antrodia camphorata* polysaccharides in a T1/T2 doubly transgenic mouse model for inhibiting infection of *Schistosoma mansoni*," *Toxicology and Applied Pharmacology*, vol. 227, no. 2, pp. 291–298, 2008.

[106] M.-C. Tsai, T.-Y. Song, P.-H. Shih, and G.-C. Yen, "Antioxidant properties of water-soluble polysaccharides from *Antrodia cinnamomea* in submerged culture," *Food Chemistry*, vol. 104, no. 3, pp. 1115–1122, 2007.

[107] J.-J. Cheng, N.-K. Huang, H.-S. Lur, C.-I. Kuo, and M.-K. Lu, "Characterization and biological functions of sulfated polysaccharides from sulfated-salt treatment of *Antrodia cinnamomea*," *Process Biochemistry*, vol. 44, no. 4, pp. 453–459, 2009.

[108] S. Y. Liu, M. T. Kuo, and W. C. Wen, "Inhibition of hepatitis B virus by cyclohexenone compounds from *Antrodia camphorata*," US US 7411003, 2009.

[109] R. R. M. Paterson, "Ganoderma—a therapeutic fungal biofactory," *Phytochemistry*, vol. 67, no. 18, pp. 1985–2001, 2006.

[110] E. Majid, K. B. Male, Y.-M. Tzeng, J. O. Omamogho, J. D. Glennon, and J. H. T. Luong, "Cyclodextrin-modified capillary electrophoresis for achiral and chiral separation of ergostane and lanostane compounds extracted from the fruiting body of *Antrodia camphorata*," *Electrophoresis*, vol. 30, no. 11, pp. 1967–1975, 2009.

Food and Chemical Toxicology xxx (2010) xxx–xxx

Contents lists available at ScienceDirect

Food and Chemical Toxicology

journal homepage: www.elsevier.com/locate/foodchemtox

A 90-day subchronic toxicological assessment of *Antrodia cinnamomea* in Sprague–Dawley rats

Tai-I Chen [a], Chin-Chu Chen [a,*], Ting-Wei Lin [a], Yueh-Ting Tsai [b], Mun-Kit Nam [b]

[a] *Grape King Biotechnology Inc., Chungli, Taiwan*
[b] *Testing Center, Super Laboratory Inc., Taipei, Taiwan*

ARTICLE INFO

Article history:
Received 7 July 2010
Accepted 13 November 2010
Available online xxxx

Keywords:
Antrodia cinnamomea
90-Day subchronic toxicity
NOAEL
Safety assessment

ABSTRACT

Antrodia cinnamomea (Ac) is a medicinal mushroom widely used for the treatment of abdominal pain, hypertension and hepatocellular carcinoma, but subchronic toxicity of this material has not yet been investigated. This present study was conducted to assess the 90-day oral toxicity of *A. cinnamomea* from submerged culture in male and female Sprague–Dawley (SD) rats. Eighty rats were divided into four groups, each consisting of ten male and ten female rats. Test articles were administered by oral gavage to rats at 3000, 2200 and 1500 mg/kg BW/day for 90 consecutive days and reverse osmosis water was used as control. All animals survived to the end of the study. During the experiment period, no abnormal changes were observed in clinical signs, body weight and ophthalmological examinations. No significant differences were found in urinalysis, hematology and serum biochemistry parameters between the treatment and control groups. Necropsy and histopathological examination indicated no treatment-related changes. According to the above results, the no-observed-adverse-effect level (NOAEL) of *Antrodia cinnamomea* is identified to be greater than 3000 mg/kg BW/day in Sprague–Dawley rats.

1. Introduction

Antrodia cinnamomea (Ac) in the Polyporaceae, Basidiomycotine family, is a native mushroom parasitic on the endemic perennial tree, *Cinnamomum kanehirai* Hay in Taiwan (Chang and Chou, 1995). Ac is considered highly expensive due to its rareness and cultivation difficulties of fruit bodies, but has been commonly used as traditional herb material for treatment against abdominal pain, hypertension and hepatocellular carcinoma (Tsai and Liaw, 1985). Many studies have been shown its exclusive biological activity as both supplementary medicines and functional foods (Hseu et al., 2006; Liu et al., 2007; Lu et al., 2007; Yang et al., 2006). In Taiwan, matured fermentation techniques have promoted mass production of Ac and its products have been marketed in the form of mycelium from submerged culture as functional foods for over 10 years. Currently the dried mycelia powder of Ac is considered officially as a dietary supplementation in Taiwan. The mycelia of Ac powder contain 8% polysaccharides with molecular weight 10^6 Da. Its neutral monosaccharides are mannose, glucose and xylose linked by a β-D-glucan chain (Huang and Mau, 2000), which naturally possess a variety of pharmaceutical functions (Chen et al., 2001). Ac has been found with antioxidant properties (Song and Yen, 2002) which may act as a possible chemopreventing agent, while it could also provide protection against CCl_4-induced hepatic toxicity in rats (Song and Yen, 2003). Partially-purified polysaccharides from Ac showed antitumor effects against human leukemic U937 cells by promoting a Th-1 state and killer activities (Liu et al., 2004). Other biological active ingredients include an anti-HBV pyrrolidione (Shen et al., 2005), and the most recent finding of ergostatrien-3β-ol, which possesses anti-inflammatory activity and analgesic effects in formalin-induced mice (Huang et al., 2010). Although several in vitro and in vivo studies regarding the biological functions of Ac has been published, very few toxicological studies were reported. Toxicological evaluation of Ac performed so far included Ames mutagenicity tests, in vitro and in vivo chromosomal aberration tests, the latter in pneumonocytes of CHL mice and a 28 day gavage toxicity test in SD rats have been evaluated (Chen et al., 2001). The results of the chromosomal aberration test showed no dose-dependent cytotoxicity and no significant correlation in numerical aberrations compared to the control group. Results from the 28 day toxicity study suggested that daily treatment with Ac at 2 g/kg BW/day for 28 days did not induce observable toxicopathologic lesions in male and female rats. However, a 90-day subchronic toxicity study has not yet been conducted for a comprehensive safety profile of this potential mushroom. The objective of the present study was to investigate its toxicity in a 90 day subchronic toxicity study to further support its safety upon its possible use as a functional food ingredient.

* Corresponding author. Address: 60 Sec. 3, Lung-Kang Rd., Chungli, Taiwan. Tel.: +886 034572121; fax: +886 034287807.
E-mail address: gkbioeng@mars.seed.net.tw (C.-C. Chen).

0278-6915/$ - see front matter © 2010 Published by Elsevier Ltd.
doi:10.1016/j.fct.2010.11.018

2. Materials and methods

2.1. Material preparation

A. cinnamomea (BCRC 35398) was purchased from Bioresources Collection and Research Center in Food Industry Research and Development Institute (Hsinchu, Taiwan). A small square of mycelium was cut and transferred onto a potato dextrose agar plate and incubated at 28 °C for 15 days. The strain was cut and inoculated into a 2 l Hinton flask with 1 l medium consisting of glucose 1.0%; soya bean powder 0.5%; peptone 0.5%; $MgSO_4$ 0.01%, and pH was adjusted to 4.0 with 1 mol^{-1} HCl. The whole medium was cultivated at 28 °C on a 100 rev min^{-1} rotary shaker for 7 days and then scaled up to 500 l fermenter with agitation for another 7 days as seed culture. The seed trough was then inoculated into a 50-ton fermenter and cultured for 14 days under the same conditions. The red-brown broth was then freeze-dried under vacuum, ground to powder and stored at room temperature. The proximate composition analysis, including crude protein, total crude lipids, ash, fiber, and moisture contents of the freeze-dried mycelia were determined according to the AOAC official procedures [methods 984.13, 43.275, 968.08, 991.43, and 950.46 B, respectively] (AOAC, 1995). Pyrroledione and ergostatrien-3β-ol were assayed with HPLC following the conditions described by Shen et al. (2005) and Huang et al., 2010.

2.2. Animals

Eighty seven-week-old Sprague–Dawley (SD) rats (BioLASCO, Taiwan) were quarantined for 2 weeks and acclimated in polyethylene cages for at least 5 days prior to being randomly assigned to the control and treatment groups of 10 rats per sex in each group by stratified randomization. The rats were identified by ear punch and housed in pairs. The animals had free access to standard rodent diet (Laboratory Autoclavable Rodent Diet® #5010, PMI Nutrition International, USA) and reverse osmosis water ad libitum, and were maintained at controlled temperature (20–23 °C), relative humidity (40–70%) and light cycle (12 h light/12 h dark). Frequency of ventilation was 10–15 times/h. Body weights of all rats were measured prior to the administration of the test article.

2.3. Study design

This study was performed based on the Organization for Economic Co-operation and Development (OECD) Guideline 408 and was conducted in accordance with Good Laboratory Practices (GLP). The protocol was approved by the Institutional Animal Care and Use Committee (IACUC No. 98-14a) before the beginning of the study. Body weight of all rats was measured before the experiment and then weekly until scheduled necropsy 90 days later. Average measurement of feed and water consumption was conducted weekly during the study period for both male and female rats. *Antrodia cinnamomea* were given daily by gavage to rats at different dosage: 3000 mg/kg (high), 2200 mg/kg (medium), 1500 mg/kg (low), and 0 mg/kg (control). To prevent the adverse effect of gavage, the volume of test sample administered was calculated as 20 mL/kg. Ac was prepared freshly everyday and administered to each rat via a stainless steel ball-tipped gavage needle. The test animals were not first fasted before gavage. Clinical observations were made daily during the experiment period for mortality, morbidity and possible signs of toxicity. At the end of the experiment, all surviving animals were anesthetized with carbon dioxide and euthanized after blood collection.

2.4. Urinalysis

One day before the gross necropsy examination, each rat was placed in metabolic cages for 16 h to collect urine. Immediately after each urine sample is obtained, specific gravity (SG), color, protein, urobilinogen, pH, ketone, bilirubin, glucose, nitrite, and occult blood were analyzed by using a semiquantitative urinalysis system (Urisys 2400, Roche, Basel, Switzerland). Sediments of each urine sample were observed for white blood cell (WBC), red blood cell (RBC), epithelial cell (EP), crystals, and microbes by using a microscope.

2.5. Ophthalmology

An ophthalmological examination was conducted for all rats on the first day of the experiment prior to the administration of Ac and on the 90th day after the experiment. The peripheral and internal structure of both eyes in each rat were examined then evaluated with naked eyes and indirect ophthalmoscopy, respectively.

2.6. Hematology and serum biochemistry

After overnight fasting, all rats were anesthetized with inhalation of carbon dioxide. Each blood sample was collected by heart puncture and collected in an EDTA blood collecting tube and mixed well. An automatic blood analyzer (Gen. S™, Beckman, California, USA) was applied to the following detection: hematocrit, hemoglobin, RBC, WBC, platelet count, mean corpuscular volume (MCV), mean corpuscular hemoglobin (MCH), mean corpuscular hemoglobin concentration (MCHC), lymphocyte, neutrophil, monocyte, eosinophil and basophil. Anticoagulated blood samples were analyzed by Blood Coagulation Analyzer (CA-1500, Sysmex, Kobe, Japan) for prothrombin time and activated partial thromboplastin time. The following clinical chemistry parameters were evaluated: alkaline phosphatase (ALP), aspartate aminotransferase (AST), alanine aminotransferase (ALT), γ-glutamyltranspeptidase (γ-GT), albumin, total protein, total bilirubin, creatinine, blood urea nitrogen (BUN), glucose, cholesterol, triglyceride, phosphorus, calcium, chloride, potassium and sodium (by using an automated analyzer (Beckman LX®-20, California, USA)).

2.7. Pathology

All surviving animals at the end of the study were subjected to a complete necropsy. The weights of major organs such as the brain, heart, kidney, liver, spleen, adrenal gland, testes or ovaries were recorded after the removal of peripheral fat tissue. In addition, relative organ weights were calculated according to the formula: Relative organ weight (%) = organ weight (g)/body weight (g) × 100. The peripheral oral cavity, cranial cavity and all tissues and organs in the thoracic and abdominal cavity were examined visually for any abnormality and recorded. Histopathological examinations were performed for the brain, heart, kidney, liver, spleen, adrenals, testes, ovary, aorta, bone marrow, duodenum, jejunum, ileum, caecum, colon, rectum, eyes, esophagus, mammary gland, Harderian gland, trachea, lung, lymph node, pancreas, sciatic nerve, pituitary, prostate gland, salivary gland, skin, spinal cord, stomach, thigh muscle, thymus, thyroid/parathyroid gland, urinary bladder, and the uterus. All the collected tissues mentioned above were fixed in 10% neutral buffered formalin. Preserved organs and tissues were dehydrated, clarified, infiltrated with paraffin and embedded after trimming, forming paraffin tissue blocks and sliced into 5 μm thick sections using a microtome (Leica RM 2145, Nussloch, Germany), then stained with Hematoxylin & Eosin (H&E). Histopathology was conducted using an optical microscope (Opticphot-2, Nikon, Tokyo, Japan). If treatment-related changes were observed in a particular organ or tissue in the high dose group, extended examination was conducted on the corresponding organs of other dose-treated groups.

2.8. Statistical analysis

All data were expressed as mean and standard deviation (SD). Body weight, feed consumption, organ weight, hematology and serum biochemistry analysis were tested by conducting One-Way ANOVA using the SPSS statistical software. Duncan's test was used to determine statistical significance ($P < 0.05$) between the control and treatment groups. Male and female rats were evaluated separately.

3. Results

3.1. Proximate composition

The composition analysis of *Antrodia cinnamomea* submerged culture contains approximately 4% moisture and 96% dry matter, both based on air dry weight; 53% carbohydrate, 24% crude protein, 6% crude fat, 7% crude fiber and 10% ash (Chen et al., 2007). The total carbohydrate content in freeze-dried powder of Ac fermented broth was consistent with the fundamental composition usually found in most of the cultivated mushrooms (Mattila et al., 2002). The active ingredients pyrroledione and ergostatrien-3β-ol were determined at 1168 ppm (w/w) and 2750 ppm (w/w), respectively.

3.2. Body weight and feed intake

No mortalities occurred during the study. Physical and behavioral examinations did not reveal any treatment-related adverse effects after dosing. Lower average body weights were noted for the low dose and high dose group of male rats and for all the treated groups of female rats. However, these differences were not significant compared to their respective control groups ($P > 0.05$) (Fig. 1). The overall feed consumption of animals receiving Ac was similar to that of the control groups and was not statistically significant (data not shown).

Please cite this article in press as: Chen, T.-I., et al. A 90-day subchronic toxicological assessment of *Antrodia cinnamomea* in Sprague–Dawley rats. Food Chem. Toxicol. (2010), doi:10.1016/j.fct.2010.11.018

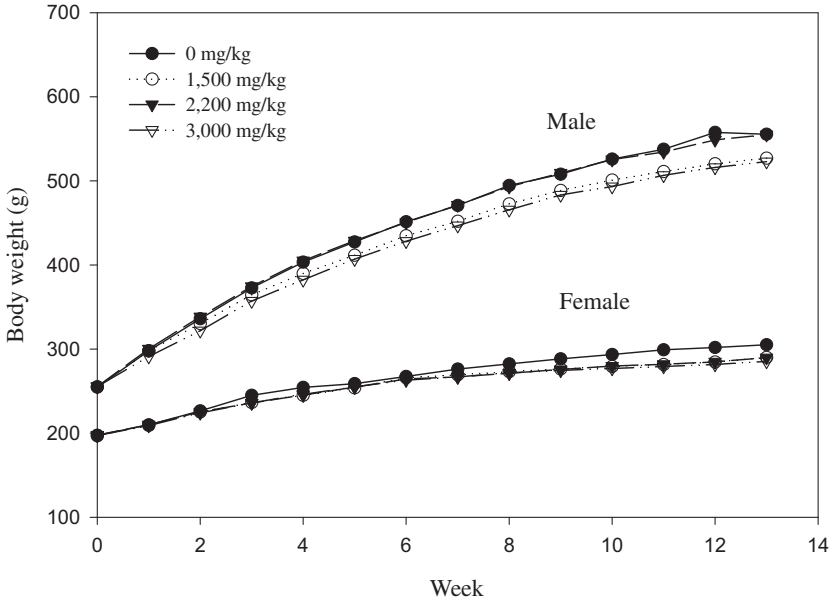

Fig. 1. Body weight changes of male and female SD rats during the 90-day safety assessment.

3.3. Urinalysis

No significant differences in urine sediments or urinalysis response variables were observed between the treatment and control groups of both sexes (data not shown).

3.4. Opthalmology

Opthalmoscopic examinations revealed no abnormality in the treated or control groups during the test period (data not shown).

3.5. Hematology

Only one parameter in each sex was noted to be statistically significant during hematological analysis. Mean corpuscular hemoglobin (MCH) in the high dose of Ac-treated males (18.5 ± 0.3) was significantly higher than in the control (17.9 ± 0.6). In female rats, platelet counts significantly increased in the low (897.5 ± 109.1) and medium dose group (907.9 ± 107.7) compared to the control group (788.9 ± 84.5), Except for the above two significant differences, all other parameters were comparable to the control (data not shown). Results showed the statistical differences observed in one sex were not observed in the other and were found to be non dose-dependent. No significant differences were noticed in other parameters for both sexes.

3.6. Serum biochemistry

In male rats, BUN of the high dose group was significantly lower (11.2 ± 1.4) than the control group (12.3 ± 1.1) (Table 1), and the creatinine level showed a significant increase in both the low dose (0.48 ± 0.04) and medium dose group (0.48 ± 0.03) compared to the control group (0.44 ± 0.04). The cholesterol level showed a significant decrease in the low dose group (52.6 ± 7.0) compared to

Table 1
Serum biochemistry findings in male Sprague–Dawley rats after 90 days of Ac administration.

Items	Dose (mg/kg BW/day)			
	0	1500	2200	3000
AST (U/L)	116.5 ± 18.4[a]	116.1 ± 17.6	131.6 ± 57.5	122.9 ± 12.7
ALT (U/L)	50.4 ± 8.8	52.2 ± 14.2	48.7 ± 8.6	48.4 ± 5.7
ALP (U/L)	90.4 ± 13.3	102.5 ± 22.1	93.2 ± 15.2	102.8 ± 25.1
T. bilirubin (mg/dL)	0.10 ± 0.00	0.14 ± 0.13	0.10 ± 0.00	0.10 ± 0.00
γ-GT (U/L)	3.0 ± 0.0	3.1 ± 0.3	3.0 ± 0.0	3.0 ± 0.0
T. protein (g/dL)	7.2 ± 0.2	7.1 ± 0.4	7.2 ± 0.3	7.0 ± 0.5
Albumin (g/dL)	4.3 ± 0.1	4.3 ± 0.2	4.3 ± 0.1	4.2 ± 0.2
Globulin (g/dL)	2.9 ± 0.2	2.8 ± 0.3	2.9 ± 0.2	2.8 ± 0.3
BUN (mg/dL)	12.3 ± 1.1	12.4 ± 1.4	13.4 ± 1.2	11.2 ± 1.4*
Creatinine (mg/dL)	0.44 ± 0.04	0.48 ± 0.04*	0.48 ± 0.03*	0.43 ± 0.04
Glucose (mg/dL)	156.1 ± 23.5	179.7 ± 44.3	150.7 ± 30.7	150.3 ± 32.8
Triglyceride (mg/dL)	71.3 ± 29.4	58.3 ± 20.7	56.2 ± 28.4	53.1 ± 17.3
Cholesterol (mg/dL)	66.3 ± 12.2	52.6 ± 7.0*	64.5 ± 16.4	55.6 ± 9.9
Sodium (meq/L)	151.1 ± 1.5	150.8 ± 1.9	151.3 ± 1.8	150.1 ± 1.2
Potassium (meq/L)	6.0 ± 0.6	6.2 ± 0.7	6.0 ± 0.3	6.2 ± 1.0
Calcium (meq/L)	11.6 ± 0.3	11.2 ± 0.5	11.3 ± 0.3	11.2 ± 0.5
Chloride (meq/L)	100.0 ± 1.9	100.5 ± 1.3	100.4 ± 2.2	100.2 ± 2.3
Phosphorus (mg/dL)	9.4 ± 0.7	9.0 ± 0.8	9.7 ± 2.1	9.4 ± 1.1

[a] Data expressed as mean ± S.D., $n = 10$.
* Significant different from control group ($P < 0.05$).

Please cite this article in press as: Chen, T.-I., et al. A 90-day subchronic toxicological assessment of *Antrodia cinnamomea* in Sprague–Dawley rats. Food Chem. Toxicol. (2010), doi:10.1016/j.fct.2010.11.018

Table 2
Serum biochemistry findings in female Sprague–Dawley rats after 90 days of Ac administration.

Items	Dose (mg/kg BW/day)			
	0	1500	2200	3000
AST (U/L)	115.7 ± 40.7[a]	107.8 ± 23.6	95.3 ± 13.8	113.0 ± 31.5
ALT (U/L)	38.5 ± 8.5	37.9 ± 8.4	32.8 ± 4.7	45.0 ± 22.6
ALP (U/L)	45.9 ± 12.5	51.5 ± 16.6	44.3 ± 6.2	50.0 ± 15.3
T. bilirubin (mg/dL)	0.09 ± 0.03	0.08 ± 0.04	0.08 ± 0.04	0.09 ± 0.03
γ-GT (U/L)	2.6 ± 0.8	2.6 ± 0.8	2.6 ± 0.8	2.6 ± 0.8
T. protein (g/dL)	7.7 ± 0.3	7.4 ± 0.4	7.8 ± 0.2	7.7 ± 0.4
Albumin (g/dL)	4.7 ± 0.2	4.6 ± 0.3	4.7 ± 0.2	4.8 ± 0.3
Globulin (g/dL)	3.0 ± 0.1	2.8 ± 0.2	3.0 ± 0.1	2.9 ± 0.2
BUN (mg/dL)	14.6 ± 2.5	13.9 ± 2.5	14.2 ± 1.4	13.8 ± 1.6
Creatinine (mg/dL)	0.55 ± 0.09	0.52 ± 0.07	0.54 ± 0.07	0.51 ± 0.06
Glucose (mg/dL)	195.3 ± 33.5	179.4 ± 38.0	198.6 ± 41.5	175.3 ± 42.8
Triglyceride (mg/dL)	47.3 ± 12.3	47.1 ± 8.5	49.5 ± 7.6	46.7 ± 11.2
Cholesterol (mg/dL)	60.4 ± 10.8	69.2 ± 17.1	75.0 ± 14.4*	57.4 ± 9.6
Sodium (meq/L)	147.4 ± 1.4	146.6 ± 1.2	146.3 ± 1.0	147.3 ± 1.3
Potassium (meq/L)	6.4 ± 0.5	6.4 ± 0.8	6.6 ± 0.6	6.5 ± 0.4
Calcium (meq/L)	11.5 ± 0.4	11.2 ± 0.5	11.5 ± 0.6	11.6 ± 0.4
Chloride (meq/L)	101.5 ± 2.2	100.9 ± 1.4	101.6 ± 1.4	101.5 ± 2.6
Phosphorus (mg/dL)	8.0 ± 1.1	7.7 ± 1.2	7.7 ± 0.8	7.8 ± 0.9

[a] Data expressed as mean ± S.D., $n = 10$.
* Significant different from control group ($P < 0.05$).

the control group (66.3 ± 12.2) for males, while a significant increase was observed in the medium dose group (75.0 ± 14.4) compared to the control group (60.4 ± 10.8) for females (Table 2). Results showed the statistical differences observed in one sex were not observed in the other and were found to be non dose-dependent. No significant differences were found in other parameters.

3.7. Pathology

No treatment-related changes were observed for tissues of the peripheral cavity, thymus, heart, lung, liver, kidney, gastrointestinal tract, spleen, brain and the reproductive system in the treated and control groups (data not shown). During the postmortem organ examination, no significant difference was observed in male rats for absolute organ weight, but as for the females, the weight of the heart in the medium dose group significantly decreased (0.93 ± 0.04) compared to the control group (1.04 ± 0.10), however, no significant differences were found in either sex for the relative organ weight compared to the control group (data not shown). Histopathological examination was performed on 40 rats (ten rats per sex from the control and high dose group). No significant treatment-related changes were observed for both Ac-treated and control groups for females. In males, mononuclear cell infiltration (focal) was found in the heart, incidence rate of the control and high dose group were 3/10 and 2/10, respectively. Minimal to mild tubular regeneration was found in the kidney of the male control group (incidence rate of 2/10). Only one male rat in the control group presented focal and mild seminiferous tubular atrophy in the testes, but the above results were not considered relevant to the test article treatment (Table 3).

4. Discussion

The results from the 90-day subchronic toxicity study did not show any changing trends of dose dependency on individual body weight or individual organ weight after 90 days of Ac administration, which correlates to the Ac toxicology study results of Chen et al. (2001). Opthalmoscopic results showed no abnormality. No particular lesions were found during the gross necropsy for major organs and tissues. The absolute heart weight in females from the medium dose group was significantly lower compared with the control, but no significant changes in heart-to-body weight ratio was found. This finding was not associated with other clinical data, and no indication of pathological abnormality was noted. Therefore, this change is considered to be of no toxicological significance. Hematology results showed no changes from the Ac administration in all parameters, except for a significant increase of MCH in the high dose for male rats, and a significant increase of platelet counts in the low and medium dose group for female rats compared to

Table 3
Result of histopathological examination.

Organ	Lesion	Group			
		Control		High dose	
		Male	Female	Male	Female
Heart	Infiltration, mononuclear cell, focal, minimal[a]	3/10[b]	–	2/10	–
Kidney	Regeneration, tubule, focal, minimal to slight	2/10	–	–	–
Testes	Atrophy, seminiferous tubule, focal, slight	1/10	N	–	N

(–) No effect. N: No tissue.
[a] Degree of lesions was graded from one to five depending on severity: 1 = minimal (<1%); 2 = slight (1–25%); 3 = moderate (26–50%); 4 = moderate/severe (51–75%); 5 = severe/high (76–100%).
[b] Incidence: affected rats/total examined rats ($n = 8$–10).

Please cite this article in press as: Chen, T.-I., et al. A 90-day subchronic toxicological assessment of *Antrodia cinnamomea* in Sprague–Dawley rats. Food Chem. Toxicol. (2010), doi:10.1016/j.fct.2010.11.018

their respective control groups. Clinical chemistry findings showed significant decrease of BUN in the high dose group and a significant increase of creatinine in the low and medium dose group. Total cholesterol level was also found to be significantly lower in the low dose group for male rats, while significantly higher level of cholesterol was found in the medium dose for female rats. The above findings are changes within the range observed in normal SD rats (OECD, 1998), and the changes were not found to be dose-dependent. Therefore, it is concluded that the results are not due to Ac administration. Histopathological examination showed mononuclear cell infiltration and tubular regeneration in the treated group, and one male rat in the control group presented mild seminiferous tubular atrophy. No positive correlations of the degree and incidence rate of the changes between the treated and control groups were noted, and histopathological changes were non-specific.

5. Conclusion

In this present study, the 90-day subchronic toxicity test showed no systemic toxicity attributable to Ac administration, and Ac from submerged culture showed no significant toxicity even at the highest dose of 3000 mg/kg BW/day in SD rats. In conclusion, the toxicity in a 90 day subchronic toxicity study of *Antrodia cinnamomea* does not raise concern with respect to possible use as a functional food ingredient, provided that the margin of safety between the NOAEL now established and the estimated intake resulting from the proposed uses and use levels would be adequate.

Conflict of Interest

The authors declare that there are no conflicts of interest.

References

AOAC, Official Methods of Analysis, 16th ed., Association of Official Analytical Chemists, Washington, DC, 1995.

Chang, T.T., Chou, W.N., 1995. *Antrodia cinnamomea* sp. nov. on *Cinnamomum kanehirai* in Taiwan. Mycology Research 99, 756–758.

Chen, C.C. 2007. Functional activities and safety of *Antrodia camphorate*. Ph.D. thesis, National Tsing Hua University, Hsinchu, Taiwan.

Chen, C.C., Lin, W.H., Chen, C.N., Hsu, S.J., Huang, S.C., Chen, Y.L., 2001. Development of *Antrodia camphorata* mycelium with submerge culture. Fungi Science 16, 7–22.

Hseu, Y.C., Chen, S.C., Tsai, P.C., Chen, C.S., Lu, F.J., Chang, N.W., Yang, H.L., 2006. Inhibition of cyclooxygenase-2 and induction of apoptosis in estrogen-nonresponsive breast cancer cells by *Antrodia camphorata*. Food and Chemical Toxicology 45, 1107–1115.

Huang, G.J., Huang, S.S., Lin, S.S., Shao, Y.Y., Chen, C.C., Hou, W.C., Kuo, Y.H., 2010. Analgesic effects and the mechanisms of anti-inflammation of ergostatrien-3β-ol from *Antrodia camphorate* submerged whole broth in mice. Journal of Agricultural and Food Chemistry 58, 7445–7452.

Huang, L.C., Mau, J.L., 2000. Antioxidant properties and polysaccharide composition analysis of *Antrodia camphorate* and *Agaricus blazei*. M.Sc. thesis, National Chung Hsing University, Taichung, Taiwan.

Liu, D.Z., Liang, Y.C., Lin, S.Y., Lin, Y.S., Wu, W.C., Hou, W.C., Su, C.H., 2007. Antihypertensive activities of a solid-state culture of *Taiwanofungus camphorates* (Chang-Chih) in spontaneously hypertensive rats. Bioscience Biotechnology Biochemistry 71, 23–30.

Liu, J.J., Huang, T.S., Hsu, M.L., Chen, C.C., Lin, W.S., Lu, F.J., Chang, W.H., 2004. Antitumor effects of the partially purified polysaccharides from *Antrodia camphorata* and the mechanism of its action. Toxicology and Applied Pharmacology 201, 186–193.

Lu, Y.C., Huang, C.C., Huang, C.J., Chu, S.T., Chi, C.C., Su, H.H., Hsu, S.S., Wang, J.L., Chen, I.S., Liu, S.I., Huang, J.K., Ho, C.M., Kuo, S.J., Jan, C.R., 2007. Effects of *Antrodia camphorate* on viability, apoptosis, $[Ca2^{+}]I$, and MAPKs phosphorylation in MG63 human osteosarcoma cells. Drug Development Research 68, 71–78.

Mattila, P., Salo-Vaananen, P., Konko, K., 2002. Basic composition and amino acid content of mushrooms cultivated in Finland. Journal of Agricultural and Food Chemistry 50, 6419–6422.

OECD, 1998. 90-Day Oral Toxicity Studies in Rodents. OECD 408.

Shen, C.C., Yang, H.C., Huang, R.L., Chen, C.C., Chen, C.C., 2005. Anti-HBV principle from the culture broth of *Antrodia camphorate* (Strain CCRC-35396). Journal of Chinese Medicine 16, 57–61.

Song, T.Y., Yen, G.C., 2002. Antioxidant properties of *Antrodia camphorate* in submerged culture. Journal of Agricultural and Food Chemistry 50, 3322–3327.

Song, T.Y., Yen, G.C., 2003. Protective effects of fermented filtrate from *Antrodia camphorate* in submerged culture against CCl_4-induced hepatic toxicity in rats. Journal of Agriculture and Food Chemistry 51, 1571–1577.

Tsai, Z.T., Liaw, S.L., 1985. The Use and the Effect of Ganoderma. San Yun Press, Taichung, Taiwan. p. 116.

Yang, H.L., Chen, C., Chang, W.H., Lu, F.J., Lai, Y.C., Chen, C.C., Hseu, T.H., Kuo, C.T., Hseu, Y.C., 2006. Growth inhibition and induction of apoptosis in MCF-7 breast cancer cells by *Antrodia camphorate*. Cancer Letters 231, 215–227.

Please cite this article in press as: Chen, T.-I., et al. A 90-day subchronic toxicological assessment of *Antrodia cinnamomea* in Sprague–Dawley rats. Food Chem. Toxicol. (2010), doi:10.1016/j.fct.2010.11.018

Journal of the American Association for Laboratory Animal Science
Copyright 2009
by the American Association for Laboratory Animal Science

Vol 48, No 4
July 2009
Pages 387–390

Reference Values for Serum Proteins of Common Laboratory Rodent Strains

Julia Zaias,[1,2,*] Martha Mineau,[1] Carolyn Cray,[2] David Yoon,[2,3] and Norman H Altman[2]

Protein electrophoresis is a common proven technique to determine the protein components of plasma or serum in human, veterinary, and laboratory animal medicine. Changes in albumin and globulin protein levels can provide early and valuable diagnostic and prognostic information. Here we describe a preliminary analysis of the distribution of serum protein fractions in adult BALB/c, C57BL/6, and CD1 mice and Sprague-Dawley rats and describe the changes in protein values from birth to maturity in BALB/c mice and Sprague-Dawley rats. Quantifiable changes in the electrophoretic profile were apparent in mice with chronic-active dermatitis.

Protein electrophoresis is a common tool to determine the protein components of plasma or serum. This technique involves overlaying plasma or serum on a thin agarose gel. Electric current applied to the gel causes the proteins to migrate according to the charge and size of the proteins, intensity of the electric field, and characteristics of the support medium through which the protein particles migrate. The movement of the proteins creates bands in the gel which can be quantified. The gel is fixed and stained, and the protein bands are analyzed and quantified by using laser tracings from a densitometer.[12] Specific proteins within these bands can be identified through immunologic staining; however, in many animal species, such identification is limited by the availability of species-specific sera. Historically, several substrates (for example, cellulose acetate, starch gel, polyacrylamide gel, and paper) have been used for protein electrophoresis, thus complicating comparison of results because protein migration is related to the substrate medium. More modern techniques (for example, agarose gel electrophoresis and capillary electrophoresis) using commercial electrophoretic systems provide increased resolution and precision.

Serum protein bands or peaks visualized by electrophoresis include albumin and α1, α2, β, and γ globulins. Collectively, the proteins in these bands or fractions serve various functions, including maintaining colloid osmotic pressure and acting as enzymes, hormones, and antibodies. Albumin is the primary and most homogenous fraction, comprising 35% to 50% of total serum protein in animals.[12] A key metabolic function of albumin is its role as a general binding and transport protein. Among the globulins, α1 and α2 globulins include many of the diagnostically important acute-phase proteins (for example, α2 macroglobulin, haptoglobin), whereas β globulins include other acute-phase proteins in addition to complement and various proteins important in coagulation. The γ globulins include the immunoglobulins (IgA, IgM, IgE, and IgG), but some immunoglobulins migrate in the β region. Protein fractions can change with factors such as age, nutritional status, stress, and disease state. Albumin is a negative acute-phase protein (that is, its quantity decreases during the acute-phase response), whereas α, β, and γ globulins are positive acute-phase proteins and increase in quantity during the acute-phase response.[12]

Protein electrophoresis has been a proven diagnostic technique to examine proteins in plasma or serum in human, veterinary, and laboratory animal medicine for more than 40 y.[8,12-15] In domestic species, diseases such as multiple myeloma and Aleutian's disease in ferrets are characterized by a gammaglobulinopathy. In mice, protein electrophoresis was used as a tool to investigate protein changes in tumor-bearing compared with normal animals,[2] and increases in β and γ globulins were noted in mice carrying transplantable plasma cell leukemias.[3] Another study[4] used protein electrophoresis to compare the serum proteins of female mice in different stages of estrus and pregnancy.

The aims of the current study study were to (1) perform a preliminary analysis of serum protein fractions in common strains of laboratory mice and rats by using a commercially available agarose gel electrophoresis system, (2) monitor age-associated changes in protein fractions, and (3) document that this technique could be used to define protein changes in B6.129P2-*Apoe*^{tm1Unc}/Crl (apoE) mice with dermatitis. These results will help lay the foundations for the use of protein electrophoresis as a diagnostic and prognostic tool for use in health monitoring of small laboratory animals including *Mus musculus* and *Rattus norvegicus*.

Materials and Methods

Animals and housing. All animals were maintained in accordance with recommendations regarding housing, temperature, and humidity in the *Guide for the Care and Use of Laboratory Animals*[10] at AAALAC-accredited facilities. All experimental procedures were approved by the University of Miami Animal Care and Use Committee. Sprague–Dawley rats (Crl:SD, Charles River Laboratories, Wilmington, MA) and mice [BALB/cAnNCrl, C57BL/6NCrl, and Crl:CD1(ICR); Charles River Laboratories] of various ages were housed conventionally in standard polycarbonate cages (Ancare, Bellmore, NY) with shredded aspen bedding (Harlan Teklad, Madison, WI) and microisolation lids. Room conditions included a 12:12-h light:dark cycle, temperature range of 20.6 to 23.3 °C (69 to 74 °F), and 30% to 70% humidity. The rats and mice were provided ad libitum access to

Received: 29 Dec 2008. Revision requested: 26 Jan 2009. Accepted: 13 Mar 2009.
Divisions of [1]Veterinary Resources and [2]Comparative Pathology, University of Miami Miller School of Medicine, Miami, Florida, and [3]College of Health Sciences, Barry University, Miami Shores, Florida.
[*]Corresponding author. Email: jzaias@med.miami.edu

rodent chow (diet 5001, Purina, St Louis, MO) and municipal water by bottle. A group of 11 female B6.129P2-*Apoe*^{tm1Unc}/Crl (apoE) mice (age, 10 wk) that were housed similarly and had moderate chronic-active dermatitis were sampled as part of a diagnostic workup for an investigator.

Rodent colony health was monitored by using a sentinel system. Sentinel mice maintained on dirty bedding were screened quarterly for the following agents: mouse hepatitis virus, Sendai virus, *Mycoplasma pulmonis*, pneumonia virus of mice, minute virus of mice, Thieler murine encephalomyelitis virus, mouse parvovirus, mouse rotavirus, lymphocytic choriomeningitis virus, and parasitic infections. Once each year, the panel was extended to include the following agents: mouse norovirus, *Ectromelia* virus, K virus, *Encephalitozoon cuniculi*, polyoma virus, mouse adenovirus, reovirus, murine cytomegalovirus, Hantaan virus, mouse thymic virus, *Clostridium piliforme*, and cilia-associated respiratory bacillus. During this study, all samples were negative for the tested agents.

Blood was collected from the submandibular vein or by cardiocentesis under anesthesia (isoflorane by mask) from rats and mice of various ages (and approximately equal numbers of both sexes). No animal underwent multiple sampling to avoid possible interference from repeated handling and technique stimulation. Blood was collected into tubes without anticoagulant, allowed to clot, and centrifuged, and serum was separated and frozen (–20 °C) before analysis. The sample sizes for each age and time point are presented in the tables.

Protein electrophoresis. Serum samples were analyzed by using an agarose gel electrophoresis system (Paragon SPEP-II, Beckman, Fullerton, CA). Briefly, a 2-µL sample of serum was diluted 1:4 in running buffer and applied to the gel, which was exposed to 100 V for 37 min. After a wash in water, the gel was fixed, dried, and stained (Beckman Blue Stain, Beckman). Bands were scanned and quantified by densitometer at 600 µm (Figure 1). Percentages and absolute values (g/dL) for the protein fractions were determined on the basis of the total protein concentration obtained by refractometry. The albumin:globulin ratio was calculated as albumin/(α1 + α2 + β + γ globulins).

Statistical analyses. All data were checked for normality and statistical analyses performed (Sigma Stat, version 3.11, SYSTAT, Chicago, IL). If data were normally distributed, 1-way ANOVA and *t* tests were used. If data were not normally distributed, Kruskal–Wallis 1-way ANOVA or Mann–Whitney *U* tests were used.

Results

In mice (Table 1), both albumin and total protein values increased dramatically within the first several weeks of neonatal life. Albumin comprised between 46% and 58% of total serum protein. The albumin:globulin ratio increased with age in mice. In addition, α1 globulins comprised approximately 6% to 10% of serum proteins, increased with age, and appeared to reach stable adult levels by 6 wk of age. In comparison, α2 globulins comprised approximately 12% to 17% of serum proteins, appeared to increase more rapidly than α1 globulins, and maintained increases at 6 wk. In mice, β globulins comprised approximately 16% to 28% of serum protein. These globulins were increased at 2 wk of age but then decreased as the mice neared adulthood. In contrast, γ globulins remained at low concentration, approximately 2% to 3% of total serum protein.

In rats (Table 2), both albumin and total protein values increased dramatically within the first several weeks of neonatal life. Albumin comprised between 47% and 57% of serum proteins throughout the neonatal period. Albumin absolute values

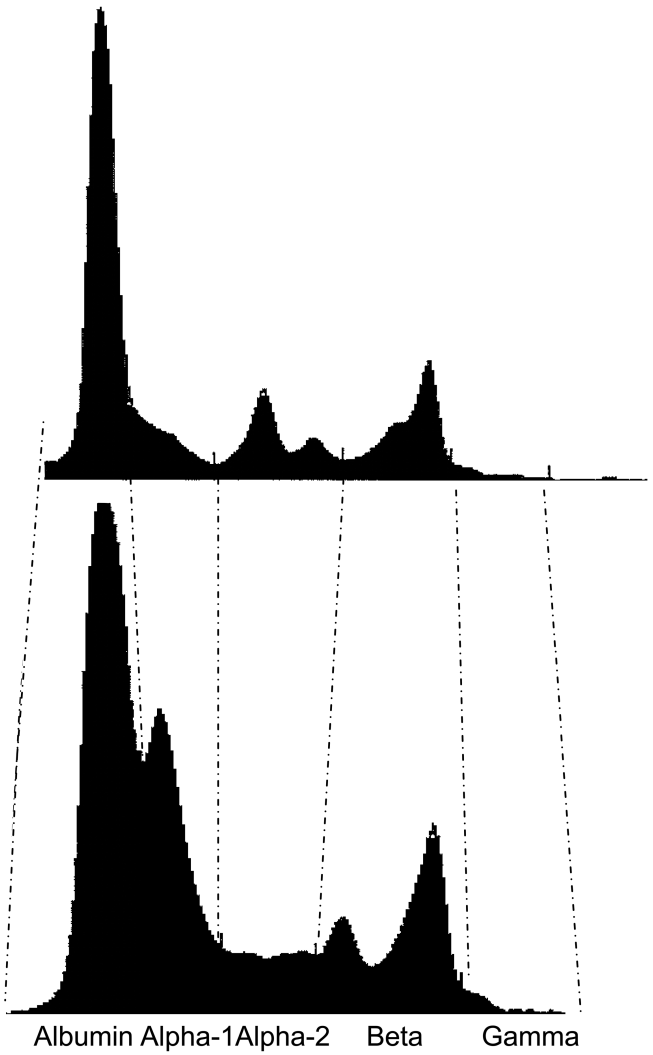

Figure 1. Representative typical electrophoretograms for a clinically healthy (A) adult BALB/c mouse and (B) adult Sprague–Dawley rat.

increased, whereas the albumin percentage decreased as the total protein increased. The albumin:globulin ratio decreased with age in rats, apparently plateauing at about 45 d of age. Quantities of α1 (8% to 20% of serum protein) and α2 (7% to 9%) globulins increased steadily and reached adult values at 45 d of age. Whereas β globulins comprised between 19% and 27% of the total protein and increased in concentration into adulthood, γ globulins comprised only 2% to 5.5% of serum proteins in rats, and their absolute value and percentage was variable over the time period examined.

We compared the results of serum protein electrophoresis for 2 commonly used laboratory inbred strains, BALB/c and C57BL/6, and 1 outbred stock (CD1; Table 3). All data were from mice 8 to 10 wk of age. Differences in protein values were apparent. C57BL/6 and CD1 mice had higher concentrations of total protein, albumin, α2 globulins, and γ globulins than did BALB/c mice. Compared with CD1 mice, C57BL/6 mice had lower albumin values and higher γ globulin values.

Relative to that of an average healthy adult C57BL/6 mouse, the electrophoretograms of samples from B6.129P2-*Apoe*^{tm1Unc}/Crl mice with clinical chronic–active dermatitis demonstrated significant increases in total protein (apoE mice, 5.7 ± 0.16 g/dL; C57 mice, 5.0 ± 0.06 g/dL; Mann–Whitney test: T = 67, P = 0.003), α2 globulins (apoE, 1.45 ± 0.06 g/dL; C57, 0.82 ± 0.02 g/

Table 1. Electrophoretic reference values for BALB/c mice

	7 d (n = 6)	14 d (n = 11)	21 d (n = 6)	28 d (n = 6)	42 d (n = 15)	56 d (n = 8)
Total protein (g/dL)*	2.5 ± 0.20[a,b]	4.0 ± 0.10[b]	3.8 ± 0.07[c]	4.0 ± 0.10	4.7 ± 0.10[a,c]	4.0 ± 0.10
Albumin (g/dL)*	1.2 ± 0.08[a,b]	2.0 ± 0.1	2.1 ± 0.08	2.3 ± 0.05[b]	2.7 ± 0.10[a,c]	2.0 ± 0.10[c]
Albumin (%)*	46.1 ± 0.5[a,b]	49.8 ± 0.6[c,d]	52.7 ± 2.4	57.8 ± 0.5[a,c]	57.0 ± 1.4[b,d]	50.7 ± 2.5
α1 Globulin (g/dL)*	0.22 ± 0.03[a,b]	0.28 ± 0.02[c]	0.30 ± 0.02	0.23 ± 0.03[d,e]	0.45 ± 0.03[a,c,d]	0.41 + 0.03[b,e]
α1 Globulin (%)*	8.4 ± 0.4	6.8 ± 0.5[a,b]	7.8 ± 0.5	5.7 ± 0.6[c,d]	9.5 ± 0.6[a,c]	10.3 ± 0.3[b,d]
α2 Globulin (g/dL)*	0.35 ± 0.03[a,c,d]	0.50 ± 0.02[b]	0.63 ± 0.05[c]	0.57 ± 0.02	0.71 ± 0.03[a,b]	0.62 + 0.03[d]
α2 Globulin (%)*	14.0 ± 0.4[a]	11.9 ± 0.3[ab,c,d,e]	16.7 ± 1.2[a,b]	14.2 ± 0.4[c]	15.1 ± 0.5[d]	15.7 ± 0.5[e]
β Globulin (g/dL)*	0.67 ± 0.09[a]	1.21 ± 0.07[a,b,c]	0.81 ± 0.02	0.80 ± 0.03	0.75 ± 0.04[b]	0.84 + 0.13[c]
β Globulin (%)*	25.9 ± 1.7[a]	28.8 ± 0.8[b]	21.4 ± 0.6	19.8 ± 1.0	16.1 ± 1.0[a,b]	20.6 ± 2.3
γ Globulin (g/dL)*	0.08 ± 0.01	0.11 ± 0.01	0.08 ± 0.01[a]	0.10 ± 0.02	0.12 ± 0.01[a]	0.11 + 0.01
γ Globulin (%)	3.1 ± 0.4	2.7 ± 0.1	2.0 ± 0.2	2.6 ± 0.4	2.5 ± 0.2	2.9 ± 0.3
Albumin:globulin ratio*	0.90 ± 0.05[a,b]	1.0 ± 0.02[c,d]	1.1 ± 0.09	1.4 ± 0.03[a,c]	1.4 ± 0.08[b,d]	1.1 ± 0.10

Data are presented as mean ± 1 SE. Asterisks indicate significant (Kruskal–Wallis 1-way ANOVA, $P < 0.05$) differences with age. For each parameter, values indicated with the same superscript letters are significantly different (Dunn pairwise multiple comparisons, $P < 0.05$).

Table 2. Electrophoretic reference values (g/dl and %) for Spraque Dawley rats

	7 d (n = 10)	14 d (n = 10)	21 d (n = 10)	28 d (n = 9)	45 d (n = 8)	53 d (n = 18)	60 d (n = 11)
Total protein (g/dL)*	3.0 ± 0[a,e,h]	4.1 ± 0.04[b,f,i]	4.1 ± 0.06[c,g,j]	4.6 ± 0.07[d]	5.5 ± 0.20[e,f,g]	5.4 ± 0.10[h,i,j]	6.5 ± 0.20[a,b,c,d]
Albumin (g/dL)*	1.6 ± 0.03[a,b,c,d]	2.2 ± 0.03[e]	2.2 ± 0.05[f]	2.6 ± 0.04[a]	2.6 ± 0.10[b]	2.6 ± 0.0[c]	3.0 ± 0.10[d,e,f]
Albumin (%)*	52.2 ± 1.0[a,b,c,j]	54.7 ± 0.6[d,e,f]	53.4 ± 1.2[g,h,i]	56.9 ± 0.5[j,k,l,m]	46.6 ± 0.9[a,d,g,k]	48.6 ± 0.8[b,e,h,l]	47.0 ± 0.9[c,f,i, m]
α1 Globulin (g/dL)*	0.31 ± 0.01[a,b,c]	0.38 ± 0.01[d,e,f]	0.35 ± 0.02[g,h,i]	0.71 ± 0.02	1.10 ± 0.05[a,d,g]	1.1 ± 0.04[b,e,h]	1.01 ± 0.08[c,f,i]
α1 Globulin (%)*	10.2 ± 0.4[a,d]	9.4 ± 0.3[b,e,i]	8.4 ± 0.5[c,f,j]	15.5 ± 0.4	19.8 ± 0.5[a,b,c]	20.4 ± 0.4[d,e,f]	16.6 ± 1.4[i,j]
α2 Globulin (g/dL)*	0.24 ± 0.004[a,b,c]	0.32 ± 0.01[d,e,f]	0.31 ± 0.01[h,i,j]	0.30 ± 0.02[k,l,m]	0.50 ± 0.02[a,d,h,k]	0.50 ± 0.02[b,e,i,l]	0.51 ± 0.03 [c,f,j,m]
α2 Globulin (%)*	8.1 ± 0.1[a]	7.9 ± 0.3[d]	7.4 ± 0.2[b,c]	6.6 ± 0.4[a,e,f]	9.1 ± 0.3[b,e,g]	9.0 ± 0.2[c,d,f]	7.8 ± 0.3[g]
β Globulin (g/dL)*	0.72 ± 0.02[a,b,c,d]	0.97 ± 0.02[e]	1.10 ± 0.04[a]	0.89 ± 0.05[f]	1.20 ± 0.04[b]	1.10 ± 0.03[c,g]	1.65 ± 0.11[c,e,f,g]
β Globulin (%)	24.1 ± 0.6[a,b]	23.8 ± 0.5[c]	26.5 ± 0.6[d,e,f]	19.3 ± 1.0[a,d,h]	21.4 ± 0.8[e]	19.9 ± 0.3[b,c,f,i]	25.3 ± 1.1[h,i]
γ Globulin (g/dL)*	0.17 ± 0.01[a]	0.22 ± 0.02[b,d]	0.18 ± 0.02[c]	0.08 ± 0.01[a,b,c,e]	0.20 ± 0.04	0.10 ± 0.01[d,f]	0.25 ± 0.03[e,f]
γ Globulin (%)*	5.5 ± 0.3[a,b]	5.3 ± 0.3[c,d]	4.4 ± 0.4[e,f]	1.7 ± 0.1[a,c,e,h]	3.2 ± 0.7	2.1 ± 0.1[b,d,f]	3.8 ± 0.4[h]
Albumin: globulin ratio*	1.1 ± 0.04[a,b,c,d]	1.2 ± 0.03[e,f,g,h]	1.2 ± 0.06[i,j,k,l]	1.3 ± 0.03[a,e,i,m,n,o]	0.90 ± 0.03[b,f,j,m]	1.0 ± 0.03[c,g,k,n]	0.88 ± 0.03[d,h,l,o]

Data are presented as mean ± 1 SE. Asterisks indicate significant (Kruskal–Wallis 1-way ANOVA, $P < 0.05$) differences with age. For each parameter, values indicated with the same superscript letters are significantly different (Dunn pairwise multiple comparisons, $P < 0.05$).

dL; Mann–Whitney test: T = 55, $P < 0.001$), and β globulins (apoE, 1.51 ± 0.06 g/dL; C57, 0.81 ± 0.03 g/dL; Mann–Whitney test: T = 55, $P < 0.001$) and a significant decrease in the albumin:globulin ratio (apoE, 0.52 ± 0.03; C57, 1.18 ± 0.04; t test: t = –14.03, df = 19, $P < 0.001$).

Discussion

This study is the first to document the baseline electrophoretic pattern and preliminary reference values of albumin and α1, α2, β, and γ globulin proteins from birth to 60 d of age in BALB/c mice and Sprague–Dawley rats. These values reflect the developing profile of proteins integral in maintenance of homeostasis and metabolism in typical healthy mice and rats. The globulins comprise the positive acute-phase proteins involved in the response to injury, inflammation, and stress. Significant changes in the absolute value of the globulin fractions occur with growth to maturity. Neonatal mice and rats show the typical pattern of hypoalbuminemia seen in mammals.[12] Adult levels of albumin are attained by 4 wk of age.

Previously published electrophoretograms, regardless of medium, clearly identify albumin and α1, α2, β, and γ globulin fractions in rodents.[8,12] By using paper-based electrophoretic separation with samples from white Swiss mice, 1 study[2] documented percentages of albumin and β and γ globulins that were lower than those of the outbred stock in the present study and α1 and α2 globulin percentages that were higher than those we found. Similar findings were noted in other strains of Swiss mice in which the protein electrophoresis was run by using cellulose acetate as the substrate.[14] In the current study, we document differences between the outbred CD1 stock and inbred BALB/c and C57BL/6 strains as visualized by using a commercial agarose gel electrophoresis system. Because these mice are used widely in laboratory animal research, the availability of specific reference values for the protein fractions (like strain-specific reference values for hematologic and biochemical parameters) provides an additional level of diagnostic capability.

Dermatitis is a common clinical problem in C57BL/6 strains.[1] In apoE knockout mice with dermatitis, α2 and β globulin fractions were increased relative to those in normal control C57BL/6 mice, suggesting that an acute-phase response was activated in apoE mice. With appropriate treatment of and subsequent recovery from dermatitis, the acute-phase response in mice

Table 3. Comparison of electrophoretic reference values of various strains of laboratory mice

	Total protein	Albumin	α1 Globulin	α2 Globulin	β Globulin	γ Globulin	Albumin:globulin rato
BALB/C (n = 8)							
g/dL	3.98 ± 0.14[a,c]	2.0 ± 0.07[a,c]	0.41 ± 0.02	0.62 ± 0.02[a,c]	0.84 ± 0.13	0.11 ± 0.01[a,c]	1.06 ± 0.1
%	not applicable	50.7 ± 2.5	10.3 ± 0.3[c]	15.7 ± 0.5	20.6 ± 2.3	2.9 ± 0.3	
C57BL/6 (n = 10)							
g/dL	5.0 ± 0.06[a]	2.7 ± 0.04[a,b]	0.38 ± 0.02	0.82 ± 0.02 [a]	0.81 ± 0.03	0.30 ± 0.02[a,b]	1.18 ± 0.04
%	not applicable	54.0 ± 0.8	7.5 ± 0.4	16.3 ± 0.3	16.1 ± 0.6	6.1 ± 0.4[b]	
CD1 (n = 6)							
g/dL	5.1 ± 0.07[c]	2.9 ± 0.07[b,c]	0.34 ± 0.04	0.84 ± 0.02[c]	0.85 ± 0.03	0.20 ± 0.01[b,c]	1.30 ± 0.07
%	not applicable	56.4 ± 1.3	6.5 ± 0.7[c]	16.5 ± 0.6	16.7 ± 0.6	4.0 ± 0.3[b,c]	

Data are presented as mean ± 1 SE. Values with the same superscript letters are significantly different ($P < 0.05$) between the strains indicated.

should diminish and be visible by serum protein electrophoresis as decreases in the α2 and β globulin fractions. These readily apparent changes in globulin levels and electrophoretic pattern can be used to identify and monitor progress of inflammatory (and other) processes. An alternative explanation is that the differences are due in part to the mixed genetic background of ApoE mice (for example, C57BL6 and 129 backgrounds). Further studies are underway in our lab to evaluate the use of serum protein electrophoresis in common rodent inflammatory or pathologic conditions.

The benefits of using serum protein electrophoresis as an ancillary diagnostic and prognostic tool have been described previously for companion animals, large animals, birds, and exotic species.[5,6,8,9,12,19] In birds, serum protein electrophoresis is a documented technique in the diagnosis of aspergillosis and sarcocystosis.[6,7,11] Monitoring of acute-phase proteins has become a more prominent tool recently in farm animal herd health management.[8,14,17,18] This technique would be most valuable for use in small species or subjects from which only a small amount of blood (that is, yielding <10 µL of serum) can be obtained safely. In addition, the small volumes of blood necessary render serial serum protein electrophoresis feasible and humane. A recent study[8] has begun to apply capillary electrophoresis methodology to animals.

Increases in the levels of serum cytokines and acute-phase proteins occur early in disease processes, often preceding clinically observable behavioral and physiologic changes in animals.[16] These biochemical changes are correlated with more subjective assessments of pain and distress.[16] Numerous acute-phase proteins migrate in the α, β, and γ fractions generated on agarose gels.[12] Therefore progressive changes in albumin and globulin levels (and the albumin:globulin ratio) may provide early and valuable diagnostic and prognostic information when managing clinical conditions in animals. Characterization of the serum protein profile in select populations of laboratory animals may greatly benefit toxicologic studies. In addition, these parameters may also be sensitive in defining humane endpoints for experimental studies, an area of marked concern in laboratory animal medicine.[16] Further studies addressing the utility of serum protein electrophoresis as a diagnostic and prognostic tool and as an objective marker of pain and distress are ongoing in our laboratory.

References

1. **Brayton C.** 2007. Spontaneous diseases in commonly used mouse strains. In: Fox JG, Davisson MT, Quimby FW, Barthold SW, Newcomer CE, Smith AL, editors. The mouse in biomedical research, 2nd ed. Amsterdam (Netherlands): Academic Press.
2. **Brenneman M, Rigby P.** 1968. Protein electrophoretic patterns of serum and peritoneal fluid in normal, tumor-bearing and immune mice. Cancer Res **28:**1138–1142.
3. **Clausen J, Heremans J, Heremans M, Rask-Nielsen R.** 1959. Immunoelectrophoretic studies of serums from mice carrying two transplantable plasma cell leukemias. J Natl Cancer Inst **22:**57–81.
4. **Cons JM, Glass LE.** 1963. Electrophoresis of serum proteins and selected enzymes in males, non-pregnant, pregnant, and lactating female mice. Proc Soc Exp Biol Med **113:**893–897.
5. **Cray C, Rodríguez M, Zaias J.** 2007. Protein electrophoresis of psittacine plasma. Vet Clin Pathol **36:**64–72.
6. **Cray C, Tatum LM.** 1998. Application of protein electrophoresis in avian diagnostics. J Avian Med Surg **12:**4–10.
7. **Cray C, Zielzienzki-Roberts K, Bonda M, Stevenson R, Ness R, Clubb S, Marsh A.** 2005. Serologic diagnosis of sarcocystosis in psittacine birds: 16 cases. J Avian Med Surg **19:**208–215.
8. **Crivellente F, Bonato M, Cristofori P.** 2008. Analysis of mouse, rat, dog, marmoset, and human serum proteins by capillary electrophoresis: comparison with agarose gel electrophoresis. Vet Clin Pathol **37:**73–78.
9. **Ganheim C, Alenius S, Waller KP.** 2007. Acute phase proteins as indicators of calf herd health. Vet J **173:**645–651.
10. **Institute of Laboratory Animal Resources.** 1996. Guide for the care and use of laboratory animals. Washington (DC): National Academy Press.
11. **Ivey ES.** 2000. Serological and plasma protein electrophoresis findings in 7 psittacine birds with aspergillosis. J Avian Med Surg **14:**103–106.
12. **Kaneko JJ.** 1997. Serum proteins and the dysproteinemias. In: Kaneko JJ, editor. Clinical biochemistry of domestic animals. San Diego (CA): Academic Press. p 117-138
13. **Kozma CK, Pelas A, Salvador RA.** 1967. Electrophoretic determination of serum proteins of laboratory animals. J Am Vet Med Assoc **151:**865–869.
14. **Murata H, Shimada N, Yoshioka M.** 2004. Current research on acute phase proteins in veterinary diagnosis: an overview. Vet J **168:**28–40.
15. **Ngure RM, Eckersall PD, Jennings FW, Mburu J, Burke J, Mungatana N, Murray M.** 2008. Acute phase response in mice experimentally infected with *Trypanosoma congolense*: a molecular gauge of parasite host interaction. Vet Parasitol **151:**14–20.
16. **Olfert ED, Godson DL.** 2000. Humane endpoints for infectious disease animal models. ILAR J **41:** 99-104.
17. **Orro T, Jacobsen S, LePage JP, Niewold T, Alasuutari S, Soveri T.** 2008. Temporal changes in serum concentrations of acute phase proteins in newborn dairy calves. Vet J **176:**182–187.
18. **Petersen HH, Nielsen JP, Heegaard PMH.** 2004. Application of acute phase protein measurements in veterinary clinical chemistry. Vet Res **35:**163–187.
19. **Zaias J, Cray C.** 2002. Protein electrophoresis: a tool for the reptilian and amphibian practitioner. Journal of Herpetological Medicine and Surgery **12:**30–32.